Mitochondrial signaling pathway in Alzheimer´s disease: disclosure of new therapeutic targets
Diana Filipa Ferreira da Silva
Universidade de Coimbra
2014

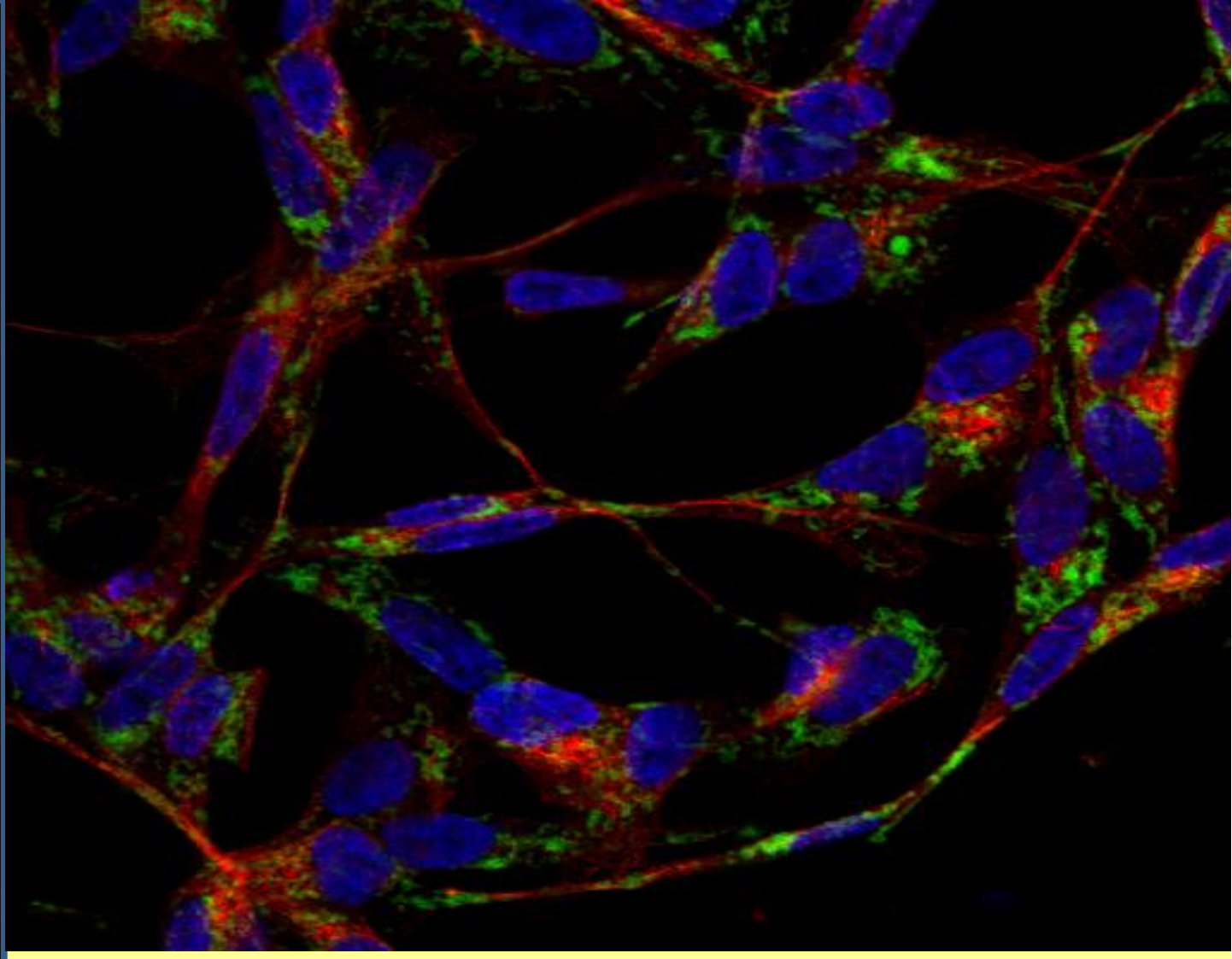

Diana Filipa Ferreira da Silva

Mitochondrial signaling pathway in Alzheimer´s disease: disclosure of new therapeutic targets

Tese de Doutoramento em Biociências na especialidade de Neurociências, orientada por Doutora Sandra Morais Cardoso e Doutor António Matos Moreno e apresentada ao Departamento de Ciências da Vida da Universidade de Coimbra

2014

UNIVERSIDADE DE COIMBRA

Diana Filipa Ferreira da Silva

Mitochondrial signaling pathway in Alzheimer´s disease: disclosure of new therapeutic targets

Via de sinalização mitochondrial na Doença de Alzheimer: descoberta de novos alvos terapêuticos

Tese de Doutoramento em Biociências, orientada por Doutora Sandra Morais Cardoso e Doutor António de Matos Moreno e apresentada ao Departamento de Ciências da Vida da Faculdade de Ciências e Tecnologia da Universidade de Coimbra

2014

· U C ·

UNIVERSIDADE DE COIMBRA

Dissertação apresentada ao Departamento de Ciências da Vida da Faculdade de Ciências e Tecnologia da Universidade de Coimbra para prestação de provas de Doutoramento em Biociências, na especialidade de Neurociências

(…)

O sonho é ver as formas invisíveis
Da distância imprecisa, e, com sensíveis
Movimentos da esp´rança e da vontade
Buscar na linha fria do horizonte
A árvore, a praia, a flor, a ave, a fonte –
Os beijos merecidos da Verdade.

[Fernando Pessoa, in Mensagem]

Agradecimentos

Um obrigado muito especial à minha orientadora Sandra Morais Cardoso. Obrigada pela presença, pelos ensinamentos, pela motivação. Obrigada por tudo. Foi e continuará a ser um grande privilégio trabalhar consigo.

Obrigada ao Dr António Moreno, meu co-orientador, pela disponibilidade, prontidão e pelo gosto com que partilha tão grande sabedoria.

Obrigada à Raquel e à Daniela, elas que foram as minhas mentoras no início desta caminhada e que estiveram sempre prontas a ajudar. Muito obrigada em especial à Raquel pela ajuda e amizade.

Agradeço aos colegas do laboratório a amizade e entre ajuda. A união sempre fez a força, e a vossa amizade faz do laboratório um local ideal para trabalhar. Obrigada Ana Plácido, Sónia, Cristina, Emanuel, Inês, Ana Duarte e Renato.

Thank you Dr Russell Swerdlow for the opportunity to work with you and for the teaching and scientific discussions. Thank you for enjoying Science so much and share that passion with me. I felt so welcome in your laboratory that I cannot forget the great people I met there: Eva, Jane, Lezi and Narita.

Obrigada ao Centro de Neurociências e Biologia Celular pela oportunidade e aos técnicos e funcionários do centro por todo o auxílio prestado no desenvolvimento do trabalho experimental.

Obrigada aos meus amigos, os de sempre, pela força que me dão só por acreditarem que faço tudo com "uma perna às costas"! Merci beaucoup à Liliana, Marilyn, Sandrina e Marta.

Obrigada à minha família por fazerem da minha casa um lugar à parte do mundo: obrigada mãe, pai, Bruno, Filipe e Carla.

Fundação para a Ciência e a Tecnologia e Fundo Europeu para o Desenvolvimento Regional o financiamento da minha bolsa (SFRH/BD/72644).

À minha famíla.

Table of Contents

SUMMARY

The etiology of sporadic Alzheimer´s disease remains largely unknown. Data from literature show that a bioenergetics failure, especially due to mitochondrial dysfunction, is a common event in Alzheimer's disease and mild cognitive impairment, a clinical syndrome that frequently precedes symptomatic Alzheimer´s disease. Mitochondria play a pivotal role in cellular metabolism since they regulate key aspects of cellular metabolism by ATP production, also have important functions in intracellular calcium homeostasis, endogenous reactive oxygen species production and decide cellular fate by regulating programmed cell death.

The use of cytoplasmic hybrid cell lines that contain mitochondria from Alzheimer´s disease and mild cognitive impairment subjects allow to infer that mitochondrial dysfunction, through complex IV decreased activity, are an upstream event in the pathology of Alzheimer´s disease. Further, the transfer of mitochondria from Alzheimer´s disease subjects, mild cognitive impairment and control subjects to mtDNA depleted cells enable to study downstream events driven by mitochondrial dysfunction. Previous studies using Alzheimer´s disease cybrids showed decreased complex IV, we extended these results by showing that in mild cognitive impairment cybrids complex IV dysfunction is also present. Besides decreased complex IV activity, Alzheimer´s disease and mild cognitive impairment cybrids also exhibit decreased mitochondrial membrane potential which favors the release of cytochrome c, an initiator of programmed cell death. Mitochondrial network is disrupted and more susceptible to stress in both groups. Also, oxidative stress markers are increased in Alzheimer´s disease cybrids while mild cognitive impairment cybrids did not reach the same damaged state.

Since we have established that mitochondrial dysfunction is present in both groups of study we moved to evaluate its downstream effects. We found that mitochondrial respiration is decreased and mitochondrial oxidative phosphorylation is less coupled in Alzheimer´s disease and mild cognitive impairment cybrids. This drives a decrease in ATP/ADP ratio and activates a number of compensatory response pathways like AMPK. This is accompanied by a shift of Sirtuin1 from the nucleus to the cytosol and a decrease in its phosphorylation as well as a decrease in PGC1α levels. Nevertheless mitochondrial copy number as well as other markers for mitochondrial mass are increased.

Our next goal was to access macroautophagy state in both goups. Macroautophagy is responsible for the degradation of protein aggregates and dysfunctional mitochondria, in a process called mitophagy. If this process is compromised in Alzheimer´s disease that may be explanation for the conflicting results on mitochondrial content stated above. Cytoplasmic hybrid cell lines were differentiated into neurons to have better understanding of the pathogenic processes on the brain. We found that mitochondrial network in Alzheimer´s disease and mild cognitive impairment groups is less interconnected and fragmented. This is in accordance with increased levels of proteins that orchestrate mitochondrial fission such as DRP1 and Fis1 and unchanged proteins responsible for mitochondria fusion, OPA1, MFN1 and 2. Further, the rise in the levels of Sirtuin2 in AD cybrids, a tubulin deacetylase that we found to be located only in the cytosol of differentiated cybrids, cause the breakdown of microtubules, which does not allow the completion of macroautophagic process since the transport of autophagosomes along microtubules to lysosomes is impeded in Alzheimer´s disease cybrids. Surprisingly, mild cognitive impairment cybrids are able to mount compensatory responses by increasing macroautophagy and microtubule stability.

Because macroautophagy and, consequently mitophagy is impaired in Alzheimer´s disease, Abeta oligomers and other protein aggregates will accumulate and cause further toxicity. The exposure of Alzheimer´s disease cybrids to Sirtuin2 specific inhibitor AK1, prevented the loss of acetylated tubulin and consequently ameliorated macroautophagy process and the clearance of Abeta oligomers.

In this thesis we show that mitochondrial dysfunction present in Alzheimer´s disease and mild cognitive impairment cybrids, triggers several pathways of the cellular metabolism including Sirtuin2 activation, which damages microtubules and compromises macroautophagy. We provide insights that mitochondrial regulation of microtubule-dependent cellular traffic compromises the degradation of aberrant protein aggregates and dysfunctional mitochondria. This innovate viewpoint of Alzheimer´s disease may pave the path for new therapeutic strategies targeting Sirtuin2, aiming to restore microtubule network proper function.

SUMÁRIO

A etiologia da doença de Alzheimer permanece amplamente desconhecida. Várias evidências têm mostrado que a disfunção bioenergética, especialmente a disfunção mitocondrial, ocorre na doença de Alzheimer e em défice cognitivo ligeiro, uma síndrome que frequentemente precede a sintomatologia da doença de Alzheimer. As mitocôndrias têm um papel primordial no metabolismo celular pois regulam aspetos chave do metabolismo celular sendo responsáveis pela produção de ATP, têm funções importantes na homeostasia do cálcio intracelular, na produção de espécies reativas de oxigénio e decidem o destino celular regulando a morte celular programada. O uso de linhas celulares de híbridos citoplasmáticos, que contêm mitocôndrias de sujeitos portadores de doença de Alzheimer e défice cognitivo ligeiro, permite inferir que a disfunção mitocondrial, através do decréscimo da atividade do complexo IV é um evento precoce na patologia da doença de Alzheimer. Ademais a transferência de mitocôndrias de pacientes da doença de Alzheimer, defeito cognitivo ligeiro e controlos para células depletadas do seu ADN mitocondrial, permite o estudo de eventos devidos e posteriores à disfunção mitocondrial. Estudos já efetuados recorrendo aos cíbridos da doença de Alzheimer mostraram um decréscimo na atividade do completo IV. Nós mostramos que também os cíbridos de défice cognitivo ligeiro têm um compromisso na actividade do complexo IV. Para além desta alteração no complexo IV, os cíbridos da doença de Alzheimer e défice cognitivo ligeiro também exibem um decréscimo no potencial de membrana mitocondrial o que favorece a libertação de citocromo c, um iniciador da morte celular programada. A rede mitocondrial está interrompida e mais susceptível a stress em ambos os grupos. Os marcadores de stress oxidativo estão aumentados nos cíbridos da doença de Alzheimer enquanto os cíbridos de défice cognitivo ligeiro ainda não atingem o mesmo nível de dano. Como estabelecemos que a

disfunção mitocondrial está presente em ambos os grupos de estudo avaliamos os seus efeitos posteriores. Descobrimos que a respiração mitocondrial está decrescida e a fosforilação oxidativa mitocondrial está menos acoplada nos cíbridos da doença de Alzheimer e de défice cognitivo ligeiro. Tal conduz a um decréscimo no rácio ATP/ADP e ativa um número de respostas compensatórias como a via da AMPK. Tal é acompanhado por uma mudança na compartimentação da Sirtuina1 do núcleo para os citosol e uma diminuição da sua fosforilação tal como uma diminuição nos níveis de PGC1α. No entanto o número de cópias de DNA mitocondrial, tal como outros marcadores de massa mitocondrial estão aumentados.

O nosso próximo objetivo foi determinar a via da macroautofagia em ambos os grupos. A macroautoafagia é responsável pela degradação de agregados proteicos e mitocôndrias disfuncionais, por um processo denominado mitofagia. Se este processo se encontrar comprometido na doença de Alzheimer então os resultados acima descritos sobre o aumento do conteúdo mitocondrial pode ser explicado. As linhas de híbridos citoplasmáticos foram diferenciadas em neurónios para obter um melhor entendimento dos processos patogénicos no cérebro. Descobrimos que a rede mitocondrial nos grupos de doença de Alzheimer e défice cognitivo ligeiro está menos interconectada e fragmentada. Esta observação está de acordo com os níveis elevados de proteínas que orquestram a fissão mitocondrial, tal como DRP1 e Fis1, e os níveis inalterados de proteínas responsáveis pela fusão mitocondrial, OPA1, MFN1 e 2.

O aumento nos níveis proteicos da Sirtuina2, uma deacetilase da tubulina que encontrámos localizada apenas no citosol dos cíbridos diferenciados, causa o colapso dos microtúbulos o que não permite a completação do processo macroautofágico pois o transporte de autofagossomas, ao longo dos microtúbulos, está impedido nos cíbridos de doença de Alzheimer. Surpreendentemente os cíbridos de défice cognitivo ligeiro

conseguem orquestrar respostas compensatórias aumentando a macroautofagia e a estabilidade dos microtúbulos. Devido ao comprometimento da macroautofagia e, consequentemente da mitofagia, os oligómeros de Abeta e outros agregados proteicos vão acumular agravando a toxicidade celular. A exposição dos cíbridos de Alzheimer a um inibidor específico da Sirtuina2, AK1, preveniu a perda de tubulina acetilada e, consequentemente melhorou o processo autofágico e a degradação dos oligómeros de Abeta.

Nesta tese mostramos que a disfunção mitocondrial, amplamente presente nos cíbridos da doença de Alzheimer e défice cognitivo ligeiro, está envolvida em várias vias do metabolismo celular promovendo alterações do estado redox, activação da Sirtuina2 o que causa danos nos microtúbulos e compromete a macroautofagia. Nós mostramos que a regulação do tráfego dependente dos microtúbulos pela mitocôndria compromete a degradação de agregados proteicos aberrantes bem como mitocôndrias disfuncionais. Este inovador ponto de vista da doença de Alzheimer pode favorecer o aparecimento de novas estratégias terapêuticas visando a Sirtuina2, tendo como objetivo restaurar a função da rede microtubular.

LIST OF ABBREVIATIONS

α ketoglutarate dehydrogenase complex (KDHC)

2-deoxyglucose (2-DG)

4-(2-hydroxyethyl)-1-piperazineethanesulfonic acid (HEPES)

8-hydroxy-2-deoxyguanosine (2DG)

Activity-dependent neuroprotective protein (ADNP)

Adenosine diphosphate (ADP)

Adenosine monophosphate (AMP)

Adensine triphosphate (ATP)

Alzheimer's disease (AD)

AMP-activated protein kinase (AMPK)

Amyloid precursor protein (APP)

Amyotrophic lateral sclerosis (ALS)

Apolipoprotein E gene (APOE)

Autophagic lysosomal pathway (ALP)

Autophagic vacuole (AV)

Beta amyloid (Aβ)

Bovine serum albumin (BSA)

Carbonyl cyanide-p-trifluoromethoxyphenylhydrazone (FCCP)

Central nervous system (CNS)

Citrate synthase (CS)

Clinical Dementia Rating Sale (CDR)

Coenzyme Q (CoQ)

Complementary DNA (cDNA)

Cyclin-dependent protein kinase 5 (cdk5)

Cytochrome oxidase (COX)

Cytoplasmic hybrid (Cybrid)

Davunetide (NAP)

Dihydroehidium (DHE)

Dimethyl sulfoxide (DMSO)

Dinitrophenylhydrazine (DNPH)

Ditiotreitol (DTT)

Dulbecco's modified Eagle's medium (DMEM)

Dynamin related protein (Drp)

Electron microscopy (EM)

Electron transport chain (ETC)

Ethylene glycol tetraacetic acid (EGTA)

Ethylenediamine tetraacetic acid (EDTA)

Fetal Bovine Serum (FBS)

Fission 1 (Fis1)

Glutathione peroxidase (GPx)

Glutathione reductase (GR)

High Performance Liquid Chromatography (HPLC)

Histone deacetylases (HDAC)

Huntinton's disease (HD)

Hydrogen peroxide (H_2O_2)

Hypoxia-inducible factor 1-alpha (HIF1α)

Knock-out (KO)

Lipoic acid (LA)

Lysosomal Storage Diseases (LSD)

Malondialdehyde (MDA)

Mammalian target of rapamycin (mTOR)

Microtubule associated protein (MAP)

Microtubule-associated protein light chain 3 (LC3)

Mild cognitive impairment (MCI)

Mini Mental State Examination (MMSE)

Mitochondrial DNA (mtDNA)

Mitofusin (Mfn)

Mitogen-activated protein kinase (P38)

Neurofibrillary tangle (NFT)

Nicotinamide adenine dinucleotide (NAD)

Nicotinamide mononucleotide adenylyltransferase (NMNAT)

Nicotinamide phosphoribosiyltransferase (NAMPT)

Nitric oxide (NO)

Non-glycolysis extracellular acidification rate (ECAR)

Optic atrophy 1 (Opa1)

Oxygen consumption rate (OCR)

Parkin-interacting substrate (PARIS)

Peroxisome proliferator activated receptor gamma coactivator 1α (PGC1α)

PGC-1-related coactivator (PRC)

Phenylmethanesulfonyl Fluoride (PMSF)

Phosphate buffered saline (PBS)

Polythylene glycol (PEG)

Polyvinylidene difluoride (PVDF)

Presenilin (PS1)

Pyruvate dehydrogenase complex (PDHC)

Quantitative real-time PCR (qPCR)

Reactive oxygen species (ROS)

Reduced Nicotinamide adenine dinucleotide (NADH)

Retinoic acid (RA)

Sirtuin (SIRT)

S-nitrosocysteine (SNOC)

S-nitrosylation (SNO)

Sodium dodecyl sulfate (SDS)

Superoxide dismutase (SOD)

Terminal deoxynucleotidyl transferase dUTP nick end labeling (TUNEL)

Tetramethylrhodamine, methyl ester (TMRM)

Thiobarbituric acid reactive substances (TBARS)

Transcription factor A of the mitochondria (TFAM)

Translocase of outer membrane (TOM)

Tris-beffered saline (TBS)

Wild-type (WT)

CHAPTER 1

General introduction

1.1 INTRODUCTION

Alzheimer's Disease (AD) is a progressive and chronic condition, accounting for 65-70% of all dementia cases and, consequently, is a major health and socioeconomic problem (Rosa et al., 2014). Since Alois Alzheimer's first reports were presented and published at the begining of the 20th century (Alzheimer, 1907, 1911; Alzheimer et al., 1995), a boost in AD research occurred, nevertheless, successful therapies that can cure, or even alleviate the disease are still out of reach (Hunter and Brayne, 2013). The identification of a major mitochondrial metabolic deficiency in AD patient's brains and or peripheral cell models opened new windows for the identification of new therapeutic targets. The recognition that mitochondrial function decays with age places ageing has a pivotal risk factor for the development of AD (Lin and Beal, 2006; Swerdlow et al., 2010, 2013; Swerdlow and Khan, 2009). It is believed that genetic and environmental factors may act synergistically in the onset of the sporadic AD (Bicalho et al., 2013; Meng and D'Arcy, 2013). Mitochondrial dysfunction likely starts a cascade of events that spread across specific neurons and culminate with neuronal loss across the brain.

1.2 Ageing as a risk factor for AD

Mutations dominantly inherited in presenilin-1 (PS-1), presenilin-2 (PS-2) and amyloid precursor protein (APP) allow to explain the early-onset familial forms of AD although only a small percentage, about 13% of patients, exhibit this familial trait (Bettens et al., 2013; Campion et al., 1999). The vast majority of AD patients develop this condition later in life where mutations are rarely found (Shepherd et al., 2009). Characterized to be multi-factorial and heterogeneous, sporadic AD may be the result of stochastic

driven ageing process. Ageing exerts a deleterious effect on neuronal activity and there have been some clues stating environmental and epigenetic variations that contribute to AD pathology (Cacabelos, 2007; Cacabelos et al., 2005). Genetic analyses suggest that several genes exert influence in the susceptibility of an individual to develop AD (Mattson, 2004). The ε4 allele of the apolipoprotein E (apoE) gene was identified as a major risk factor for late-onset AD across populations (Belinson and Michaelson, 2009; Chang et al., 2013; Raber et al., 2004). APOE plays an important role in the metabolism of lipoproteins and cholesterol and has been associated with increased deposition of Aβ, brain inflammation, impaired neuronal plasticity and repair (Belinson and Michaelson, 2009; Rhinn et al., 2013). Even though the correlation between the presence of APOE alleles and the emergence of AD sporadic cases is well documented, their products, even present in homozygoty, are not determinants for AD development (Laws et al., 2003). Besides, in the vast majority of AD sporadic cases the referred alleles are absent. The etiology of sporadic AD remains elusive and, in the last years, the first steps have been taken in order to find therapeutic targets that allow a true beneficial outcome, which is mandatory since this disease represents a major health problem in developed societies, and is predicted to increase disproportionately as the global elderly population increases (Da et al., 2013).

1.3 Mitochondrial function in AD

Proposed by Swerdlow and Khan (Swerdlow and Khan, 2004), the 'mitochondrial cascade hypothesis' enabled to compass some handicaps of another proposed theory for AD etiology, the 'Aβ cascade hypothesis' first proposed by Hardy and Selkoe in 2002 (Hardy and Selkoe, 2002). These authors stated that the primordial event in AD etiopathology is the production of Aβ derived from APP processing and that its brain

accumulation culminates in generalized neurodegeneration. More recently, it was suggested that this theory should only be applied to familial early-onset AD cases (Castello and Soriano, 2013; Swerdlow, 2007b). Mitochondrial cascade hypothesis relies on the central idea that similar mechanisms underlie brain ageing and AD (Swerdlow, 2012b). Mitochondrial dysfunction is believed to occupy an upstream position in the pathogenesis of the disease, giving rise to the histopathological and pathophysiological features of AD (Swerdlow et al., 2010, 2013; Swerdlow and Khan, 2009). Supporting Swerdlow and Khan point of view is the systemic mitochondrial dysfunction in AD, which cannot simply represent a consequence of neurodegeneration (Swerdlow, 2007b; Swerdlow et al., 2013).

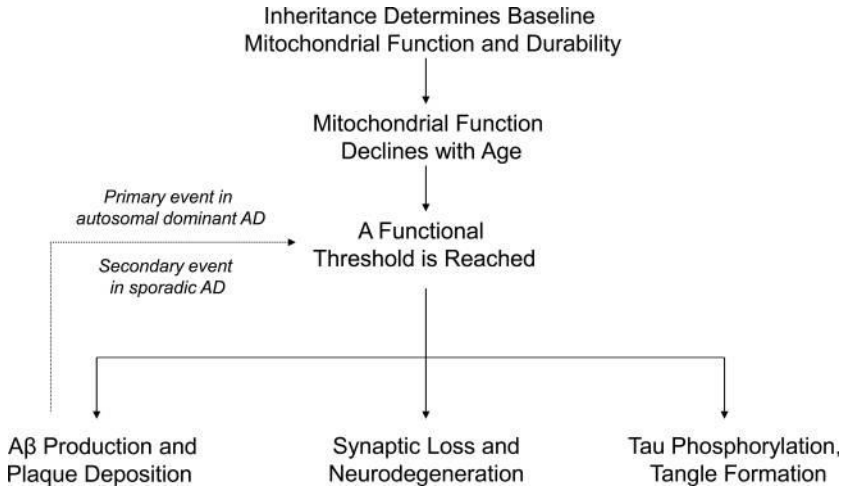

Figure 1. Mitochondrial Cascade Hypothesis for sporadic Alzheimer´s disease (Adapted from Swerdlow, 2012).

In addition, inherited polymorphic variations of mtDNA (mitochondrial DNA), together with the age-related mitochondrial changes, determine a functional threshold that when is reached triggers AD-characteristic histopathology (Swerdlow et al., 2010, 2013; Swerdlow and Khan, 2009). The mitochondrial dysfunction and consequent superoxide

anion overproduction seems to be the bridge between 'mitochondrial cascade hypothesis' and 'Aβ cascade hypothesis'. Over the years many evidences have been presented in order to unify the cellular processes responsible for ageing, mitochondrial dysfunction and, consequently, neurodegenerative diseases, such as late onset AD. A number of studies have demonstrated that mitochondrial integrity declines with age (Breitenbach et al., 2013; Gomes et al., 2013; Shigenaga et al., 1994), affecting multiple brain functions such as memory, learning and sensory processes (Aliev et al., 2009; Boumezbeur et al., 2010). Age dependent mitochondrial abnormalities leads to the decline of mitochondrial function, namely decreased oxidative phosphorylation and ATP synthesis mainly due to an increase in superoxide anion production and accumulation of mtDNA mutations (Beal, 2005; Shi et al., 2008; Wang et al., 2013). Experiments performed with platelets from AD patients, age-matched controls and young control subjects showed that mitochondrial membrane potential was higher in young controls than in AD patients and aged control subjects (Shi et al., 2008). These observations point to mitochondrial dysfunction occurring during ageing that can predispose elderly individuals to age related disorders. To further support the rational of mitochondrial dysfunction as an early event in AD etiology, subjects with Mild Cognitive Impairment (MCI), considered a nosological entity or a translational state between normal ageing and AD (Morris et al., 2001; Padurariu et al., 2010), have been studied. The early markers of metabolic dysfunction observed in AD have also been found in MCI subjects, such as mtDNA oxidative damage, reported as a major risk for AD development and progression (Manczak et al., 2004; Migliore et al., 2005). Studies made in lymphocytes showed significantly higher levels of primary oxidative mtDNA damage in AD and MCI subjects compared with control subjects (Migliore et al., 2005).

In the AD brain, particular enzymes that mediate glucose metabolism may have either altered amounts or altered Vmax activities. For example, the neuron enolase is highly expressed, and also shows a high degree of oxidative modification (Butterfield and Lange, 2009). Within the mitochondria themselves, the measured activities of pyruvate dehydrogenase complex (PDHC) and the Krebs cycle enzyme α-ketoglutarate dehydrogenase complex (KDHC), are reduced (Gibson et al., 1998). The KDHC activity reduction is likely a consequence of post-translational modification due to oxidative stress (Shi et al., 2011). The activity of isocitrate dehydrogenase, another proximal Krebs cycle enzyme, is reduced. Activities of enzymes in the distal Krebs cycle, including succinate dehydrogenase and malate dehydrogenase, are increased (Gibson et al., 2010).

Regarding the electron transport chain (ETC), COX activity has consistently been observed to be lower in AD subject brains than it is in control subject brains (Swerdlow, 2011a; Swerdlow and Kish, 2002). Histochemical approaches reveal that AD brain hippocampi contained higher numbers of COX-activity deficient neurons (Cottrell et al., 2001). Some studies have suggested neuroanatomically limited reductions, which are consistent with the possibility that the COX activity deficit is due to reduced synaptic activity (Simonian and Hyman, 1993). Other studies have utilized spectrophotometric Vmax measurements from brain homogenates (Swerdlow and Kish, 2002). In one study, dividing the COX Vmax to the density of a COX protein subunit on a Western blot rendered the activity comparable to that of the corrected control group activity (Kish et al., 1999). The authors concluded reduced COX in AD brains is a consequence of reduced COX enzyme. Another study, though, found that COX activity, when divided by the amount of spectrally determined COX was still low (Parker and Parks, 1995). It was further demonstrated that COX kinetics were altered, and that the

holoenzyme's low K_M binding site was absent. These data argue that COX is structurally altered in the AD brain. Peripherally, COX activity was found to be decreased in platelets from AD subjects whereas the protein subunits are normally present (Cardoso et al., 2004a) and this fact is not a consequence of tissue degeneration, ROS (reactive oxygen species)-induced membrane damage, deficient antioxidant defenses neither decreased synthesis rates. This data supports the idea that mitochondrial dysfunction is a primary or at least a non-amyloid dependent process (Cardoso et al., 2004a). Fibroblasts from sporadic AD patients revealed a greater amount of abnormal mitochondrial morphology and distribution when compared to age-matched normal human fibroblasts (Wang et al., 2008a). AD cybrid cell lines (cytoplasmic hybrids) have shown to correlate in many ways to AD pathophysiology, for instance, decreased COX activity (Cardoso et al., 2004a; Silva et al., 2013a; Silva et al., 2013b; Swerdlow et al., 1997), decline in bioenergetics over time in culture (Trimmer et al., 2004) and decrease viability in comparison to control cybrids (Onyango et al., 2005). It is well accepted that changes observed in AD cybrids recapitulate the early events of the disease (Trimmer et al., 2000). Cybrid technique was first described by King and Attardi (King and Attardi, 1989) and is based on the central idea that cybrid cells lines result from the repopulation of a host mtDNA depleted cell (ρ0) with different mtDNA, having the same nuclear background.

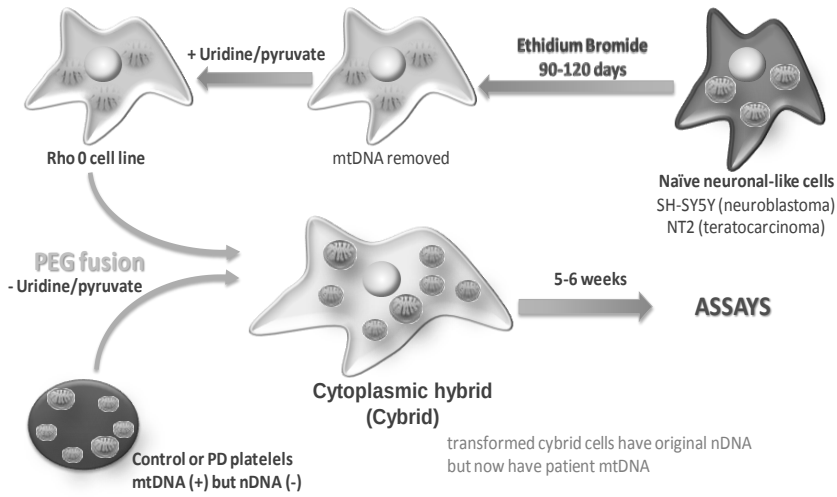

Figure 2. Cytoplasmic hybrids. ρ0 cell lines are generated by chronically treating an established cell line with ethidium bromide (EtBr). This blocks mtDNA replication and leads to its total depletion from the EtBr-treated cells. Due to a lack of mtDNA-encoded oxidative phosphorylation complex subunits, the resultant cell lines are unable to complete electron transport chain transport and oxidative phosphorylation. The ρ0 cells can then be fused with platelets isolated from patient blood samples to generate cytoplasmic hybrid (cybrid) cell lines. Cybrid lines contain mtDNA from the platelet donors, and nuclear DNA from the ρ0 cell line. This relationship lets investigators study how specific mtDNA sequences affect cell bioenergetics, and how these effects infl uence downstream cell biochemical, molecular, and physiologic parameters. (Adpated from Silva, 2012).

1.4 AD: a disorder of protein misfolding

Independent of its etiology, AD is characterized clinically by chronic and progressive dementia, including severe memory loss, profound changes in behavior and personality, incapacitating patients even in their daily tasks (Mattson, 2004). Histopathological hallmarks are intracellular NFT (neurofribrillary tangles) of abnormally phosphorylated tau, neuropil threads, dystrophic neurites and extracellular senile plaques composed of Aβ (Iqbal and Grundke-Iqbal, 2008). The presence of the referred hallmarks in AD brains is a necessary prerequisite for the definitive *postmortem* diagnosis of AD. Anatomically, AD brains are characterized by a severe atrophy, which correlates with a reduction of cell density in brain regions involved in learning and memory, as a

consequence of generalized degeneration of synapses and death of neurons (Mattson, 2004). The course of AD neurodegeneration is initiated in the entorhinal cortex and spreads to the hippocampus, temporal cortex, frontoparietal cortex and, finally, to subcortical nuclei causing severe dementia (Reddy and McWeeney, 2006). Since the first description of an AD patient by Alois Alzheimer, some decades were required to finally isolate and identify AD-related brain areas and histopathological hallmarks (Small and Duff, 2008). This isolation allowed inferring that senile or neuritic plaques are mainly composed of deposits of amyloid fibrils surrounded by dystrophic neuritis, activated microglia and reactive astrocytes (Sorrentino and Bonavita, 2007). In AD brains, Aβ is concentrated around meningeal and cerebral vessels and in the gray matter as Aβ plaques (Gotz et al., 2004).

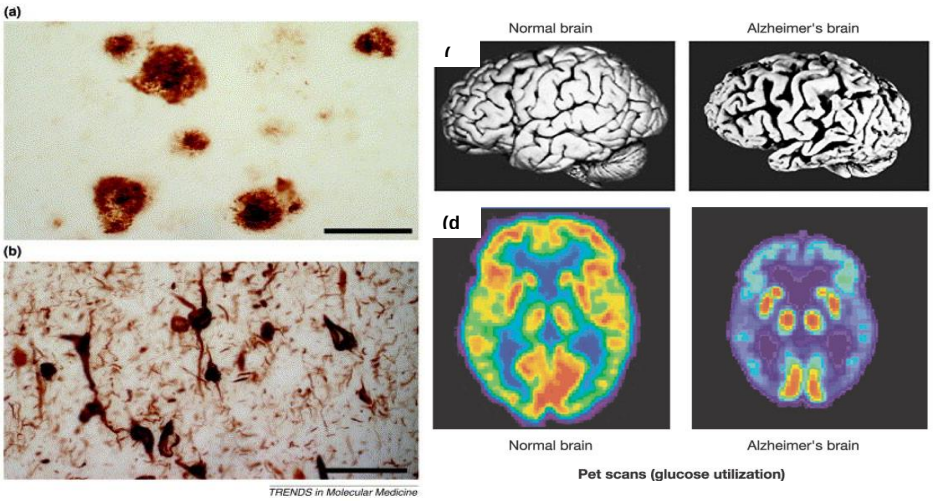

Figure 3. Histopatological hallmarks of Alzheimer´s disease brain: a) amyloid plaques, b) neurofibrillary tangles. c) Neuronal death results in severe brain shrinkage and d) decreased glucose utilization by neuronal cells. (Adapted from LaFerla and Oddo, 2005 and Mattson 2004)

Aβ is a 4 kDa proteolytic fragment that presents more often two carboxyl-terminal variants of Aβ: $A\beta_{1\text{-}40}$ mainly secreted from cultured cells and found in cerebrospinal fluid and $A\beta_{1\text{-}42}$, which is the main component of amyloid deposits in the brain (Neve et al., 2000), resulting from cleavage of amyloid-β precursor protein (βAPP) (Reddy and McWeeney, 2006; Selkoe, 2001). APP is a type I integral membrane glycoprotein through a single transmembrane domain (Evin et al., 2003), which possesses a large extracellular glycosylated N-terminus and a shorter cytoplasmic C-terminus (Marlow et al., 2003). Aβ region is located at the cell surface or in the luminal side of endoplasmic reticulum and Golgi membranes where part of the peptide is anchored. Along the secretory pathway APP is cleaved sequentially by β-secretase (BACE1 a β-site of APP cleaving enzyme) at the N-terminal end (Marlow et al., 2003) originating a soluble βAPP fragment and a membrane-associated C-terminal fragment, βCTF (Sambamurti et al., 2002; Yu et al., 2004). This fragment then suffers cleavage by gamma secretase, a proteolytic complex composed of presenilin, nicastrin, APH-1 (anterior pharynx-defective 1) and PEN-2 (presenilin enhancer 2) (Gotz et al., 2008) at the C-terminal, in

the amyloidogenic pathway (Mattson, 2004) originating a series of beta-sheet containing peptides, the Aβ peptides. The second classical neuropathological lesion present in AD brains is NFT which consist in intracellular bundles of abnormal fibers aggregated into paired helical filaments (Sorrentino and Bonavita, 2007). NFT were found to be mainly composed of an abnormally hyperphosphorylated form of the microtubule-associated protein, tau. Its physiological functions inside the cell include the assembly and stabilization of microtubules (Gotz et al., 2004; Zhang et al., 2009). Other roles have been attributed to tau, such as signal transduction, organization of neuronal cytoskeleton, intracellular axonal transport, generation of cell polarity and shape and anchoring of phosphatases and kinases (Maas et al., 2000; Noble et al., 2013; Sorrentino and Bonavita, 2007). NFTs are found in cell bodies, apical and distal dendrites and in dystrophic neurites associated with amyloid plaques (Gotz et al., 2008). In an AD context, it was shown that tau is 3 to 4 fold more phosphorylated due to the activity of some groups of kinases like, glycogen-synthase kinase-3β, cyclin-dependent protein kinase 5 (cdk5), c-AMP protein dependent and stress-activated protein kinases (Gong and Iqbal, 2008). The consequence of an augmented tau phosphorylation is a change in its conformation, its dissociation from microtubules, and a potential increase in cell toxicity (Zhang et al., 2009). Ultimately, these changes in microtubule conformation affect morphology and biological functions of neurons, such as axonal transport deficits (Schwalbe et al., 2013).

1.5 Mitochondrial DNA

The consensus on the role of mtDNA in sporadic AD development has not been reached, namely the discrepant data concerning mtDNA content. These findings are not as diametrically opposed as it may seem. The amount of mtDNA may vary from neuron

to neuron, and may further associate with the health of the neuron. Healthier neurons may have an increased amount of mtDNA, while more affected neurons may have decreased amounts. Certainly, in AD brain hippocampi the number of neurons that show succinate dehydrogenase activity but which lack COX activity is increased (Cottrell et al., 2001). Because succinate dehydrogenase is entirely encoded by nuclear genes while COX contains mtDNA-encoded subunits, this suggests AD neurons have abnormally high levels of mutated mtDNA, or else a severe state of mtDNA depletion.

In addition to changes in the content of mtDNA, differences in the quality of mtDNA have been reported. A probe specific to mtDNA that detect the 5 kD common deletion found in AD brain hippocampal neurons showed a marked increase in the amounts of this deletion (Hirai et al., 2001). Other studies using different approaches have also found that relative to controls, AD brains contain increased amounts of the 5 kD mtDNA deletion (Corral-Debrinski et al., 1994; Hamblet and Castora, 1997).

Oxidative modifications of the mtDNA are increased in AD brains, as evidenced by higher levels of 8-hydroxy-2-deoxyguanosine (2DG) (Mecocci et al., 1994). Oxidation-related nucleotide modifications can induce replication errors and an accumulation of somatic mutations. Some AD brain studies that surveyed mtDNA protein coding genes have reported a quantitative increase in the number of these mutations, although others have not (Chang et al., 2000; Lin et al., 2002). Another study determined levels of low-abundance heteroplasmic mutations in the mtDNA D-loop control region. Specific mutations were found in AD brains that were not present in control brains, and the overall burden of control region mutations was markedly increased in the AD brains (Coskun et al., 2004). This study also reported reductions in an mtDNA-derived transcript, as well as a decreased mtDNA to nuclear DNA ratio.

While some have focused on characterizing presumably somatic, acquired mutations, others have probed whether inherited mtDNA sequences and mutations are present. To date, particular homoplasmic mtDNA mutations have been reported in AD subjects, but the causality of these mutations has been virtually impossible to prove (Swerdlow, 2011a). In any scenario, inherited homoplasmic mtDNA mutations are at most an extremely rare cause of AD.

Excess deletion mutations have not been demonstrated in AD subject peripheral tissues, but it is important to note that in general, deletions are uncommon in some peripheral tissues, such as blood, probably because these cells are not post-mitotic. An increase in control region point mutations was reported in AD subject lymphocytes (Coskun et al., 2010). Of course, mtDNA haplogroup association studies have utilized mtDNA from blood samples, and a number of these association studies have reported associations (Swerdlow, 2011a).

Studies using cybrid cell lines consistently suggest that if mtDNA does in fact differ between AD and control subjects, then these differences are not brain-limited (Swerdlow, 2011a). These mtDNA-depleted cell lines, referred to as ρ0 cell lines, do not have a functional oxidative phosphorylation apparatus because they lack 13 crucial mtDNA-encoded proteins (7 from complex I, 1 from complex III, 3 from complex IV, and 2 from complex V). mtDNA contained within the transferred mitochondria populates the cell lines and restores their aerobic competence. The resulting unique cell lines are true cytoplasmic hybrids because they contain cytosolic components from two sources, the original ρ0 cell line and the cells that provided their functional mitochondria. Biochemical differences, although often subtle, are demonstrable between cybrid cell lines whose mtDNA is reconstituted from different sources. Because different cybrid cell lines prepared using the same parent ρ0 line have identical

nuclear DNA genes, and because cell lines are expanded and maintained under identical conditions, these biochemical differences presumably reflect and arise from differences in their mtDNA.

Additional indirect support for systemic mtDNA differences between AD and non-AD individuals comes from AD endophenotype studies. An endophenotype is a partial or limited manifestation of a condition that is not sufficient to render a diagnosis of that condition. The presence of an endophenotype state does not necessarily indicate the affected individual will acquire the condition, although it does infer the individual has an increased risk of developing the condition.

In recent years numerous studies have reported AD-consistent endophenotypes can be demonstrated in the asymptomatic, middle-aged offspring of AD subjects. Interestingly, these endophenotypes are more profound in the children of AD mothers than they are in the children of AD fathers (Swerdlow, 2011a). This suggests that although both parents contribute to AD risk, AD mothers contribute to a greater extent. This, in turn, implies that a maternally-inherited genetic factor influences the development of AD (Mosconi et al., 2010a).

These AD endophenotype studies have been conducted using metabolic, structural, and biochemical approaches. Fluorodeoxyglucose positron emission tomography (FDG PET) studies show the children of AD mothers, but not the children of AD fathers, have patterns of reduced glucose utilization that resembles patterns observed in AD subjects themselves (Mosconi et al., 2007; Mosconi et al., 2009). MRI studies show increased atrophy and rates of brain atrophy in the middle-aged offspring of AD mothers as compared to the middle-aged offspring of AD fathers (Berti et al., 2011; Honea et al., 2011; Honea et al., 2010). Oxidative stress and Aβ changes can be observed in the children of AD mothers (Mosconi et al., 2010b). As they age, the children of AD

mothers accumulate greater amounts of Aβ in their brain parenchyma than do the children of AD fathers (Mosconi et al., 2010c). Collectively, these findings suggest that a maternally-inherited genetic factor influences AD risk, and that this is more likely to be mtDNA than an epigenetic or sex-linked factor.

1.6 Mitochondrial driven oxidative stress

ROS are a frequent by-product of electron leakage from the inner mitochondrial membrane during mitochondrial oxidative phosphorylation. It is estimated that up to 4% of O_2 used by mitochondria is converted to superoxide radical (Hansford et al., 1997; Inoue et al., 2003; Markesbery and Lovell, 1998; Morten et al., 2006; Turrens and Boveris, 1980), and that approximately 10^9 to 10^{11} ROS are produced per cell per day (Bonda et al., 2010; Feinendegen, 2002; Ji, 1999; Petersen et al., 2007). Under normal conditions, ROS are rapidly cleared by enzymes such as SOD (superoxide dismutase) 1, SOD2, catalase, and glutathione peroxidase (GPx). When mitochondria are perturbed, however, ROS production may exceed the cell's ability to neutralize them, resulting in oxidative damage to the cell (Smith et al., 2000). Aging itself is associated with elevated ROS production by mitochondria (Ames et al., 1995; Shigenaga et al., 1994), and accumulation of oxidative damage over time may contribute to the noted association between advancing age and AD. Oxidative stress is thought to be one early manifestation of AD (Nunomura et al., 2001). Studies in post-mortem AD brains indicate widespread oxidative damage. Four-hydroxynonenal and acrolein, which are aldehydes produced by lipid peroxidation, and isoprostanes, which are pro-inflammatory products of arachidonic acid peroxidation, are significantly elevated in hippocampi from AD brains (Markesbery and Lovell, 1998; Pratico et al., 1998; Sayre

et al., 1997; Singh et al., 2010). This indicates that excessive lipid oxidation occurs in the AD brains. Additionally, both nuclear and mitochondrial DNA and RNA also display evidence of oxidative damage (Gabbita et al., 1998; Mecocci et al., 1994; Nunomura et al., 1999). Brains from individuals affected with AD further display increased protein oxidation, as evidenced by carbonyl-alterations of specific proteins (Castegna et al., 2002a; Castegna et al., 2002b; Smith et al., 1991; Sultana et al., 2010).

Many studies suggest that oxidative damage is also present in individuals with MCI, (Aluise et al., 2011; Butterfield et al., 2006b; Butterfield et al., 2007; Keller et al., 2005; Lovell and Markesbery, 2008; Markesbery and Lovell, 2007; Pratico et al., 2002). In fact, data from the literature suggest that levels of oxidative markers directly correlate with severity of cognitive impairment as well as symptomatic progression from MCI to AD (Ansari and Scheff, 2010; Keller et al., 2005).

Extensive oxidative damage likely has significant consequences for neurons, as oxidative modification of proteins and other molecular components can alter cell function (Butterfield et al., 1997; Lauderback et al., 2001; Subramaniam et al., 1997; Sultana and Butterfield, 2009). As a major source for ROS production, mitochondria are themselves at risk of acquiring oxidative damage. The activities of certain mitochondrial enzymes including isocitrate dehydrogenase, PDHC, KDHC, and COX are significantly reduced in the AD brain (Aksenov et al., 1999; Bubber et al., 2005; Butterfield et al., 2006a; Gibson et al., 1998; Manczak et al., 2004; Yates et al., 1990). These enzyme impairments may represent a consequence or cause of ROS production, or both. For instance, COX dysfunction might further elevate ROS production by stalling electron transfer (Barrett et al., 2004; Skulachev, 1996; Sullivan and Brown, 2005; Sullivan et al., 2004). Thus, dysfunctional mitochondria in AD may give rise to and perpetuate a vicious cycle of oxidant production in which impairment of one mitochondrial enzyme

elevates ROS production that in turn impairs the function of other mitochondrial enzymes, further increasing ROS production (Bonda et al., 2010; Zhu et al., 2004).

As discussed before, AD features are not brain limited, and that is also valid for oxidative stress damage. One study evaluated the presence of oxidative stress in platelets and erythrocytes from controls and AD patients. This study found elevated oxidative stress markers in AD patients in the form of thiobarbituric acid-reactive substances, nitric oxide synthase activity, and Na,K-ATPase activity, suggesting that oxidative stress is present systemically in AD (Kawamoto et al., 2005). Another study found that ROS are elevated in circulating neutrophils from AD patients (Vitte et al., 2004). Plasma from AD subjects shows significantly decreased levels of the antioxidants lycopene, lutein, and carotene when compared to plasma from control subjects, and leukocytes from AD patients display elevated levels of oxidized DNA (Mecocci et al., 2002; Mecocci et al., 1998; Migliore et al., 2005; Morocz et al., 2002).

Oxidative stress is also ubiquitous in patients with MCI, suggesting that the oxidative damage progresses. Interestingly, many studies further suggest that between MCI and AD subjects, no major differences in oxidative stress markers, such as malondialdehyde and oxidized glutathione, exist (Baldeiras et al., 2008; Bermejo et al., 2008; Padurariu et al., 2010). These studies propose that the primary biochemical differences between MCI and AD lie in the levels and activity of antioxidants such as superoxide dismutase, glutathione peroxidase, and vitamin E. This suggests that a loss of one's ability to compensate for oxidative stress may underlie or else serve as a marker of MCI-to-AD progression.

Additional evidence suggests that oxidative stress markers may correlate with disease progression and severity in AD patients. Torres and colleagues recently found that plasma levels of malondialdehyde, a lipid peroxidation product, directly associate with

impaired cognitive function in AD patients. The authors also found that the ratio of GR (glutathione reductase) activity to GPx activity, which provides an indication of a cell's antioxidant capacity, associates with cognitive function (Torres et al., 2011). It has also been reported that in AD subjects, serum levels of vitamin E, a dietary antioxidant, relate to cognitive status (Baldeiras et al., 2008; Panza et al., 2010).

Data such as these have encouraged investigators to attempt to develop peripheral AD diagnostic and biomarker tests (Burns et al., 2009; Pratico, 2005). While a definitive biomarker with adequate sensitivity and specificity remains to be identified, a plethora of data suggests that at least on a biochemical and molecular level, AD is a systemic disorder.

1.7 Mitochondrial Dynamics in AD

1.7.1 Mitochondrial morphology

Mitochondria in AD brains show a cristae disruption and intra-mitochondrial accumulations of osmiophilic material (Baloyannis, 2006, 2011; Saraiva et al., 1985). There is an increased range of mitochondrial size, with more enlarged mitochondria but also elevated numbers of exceptionally small mitochondria (Hirai et al., 2001). Overall, the average size of AD neuron mitochondria is smaller than it is in control brain neurons (Baloyannis, 2006; Hirai et al., 2001). Altogether these data show that mitochondrial network is altered in AD.

1.7.2 Mitochondrial content and Biogenesis

How mitochondrial mass changes in AD brains is not straightforward. Using PCR-based approaches to quantify mtDNA reveals genomic DNA samples prepared from AD subject brain cortices contains lesser amounts of amplifiable mtDNA (Brown et al.,

2001; de la Monte et al., 2000). The simplest explanation for this is that AD brains have reduced amounts of mtDNA, and by extension a reduced mitochondrial mass. However, in a study in which a labeled oligonucleotide probe was used to detect mtDNA in hippocampal neurons, an intricate picture emerged (Hirai et al., 2001). mtDNA levels were reduced when only mtDNA within normal-appearing mitochondria was considered. Nevertheless, a large number of mitochondria were also found within phagosomes, and these mitochondria also hybridized with mtDNA oligonucleotide probe. When this additional mtDNA was taken into account, the AD hippocampal neurons actually contained more mtDNA.

Mitochondrial mass has been assessed using alternative approaches, including an immunochemical quantification of mitochondrial-localized proteins. In one study an antibody against an mtDNA-encoded cytochrome oxidase (COX) subunit, COX1, was found to be increased in AD brain hippocampal neurons (Hirai et al., 2001). In a different study, tangle-free hippocampal neurons showed more COX1 and COX4 staining, while staining was markedly reduced in tangle-bearing neurons (Nagy et al., 1999). Other authors reported cytochrome COX protein in general was reduced in AD brain homogenates (Kish et al., 1999). Since immunobloting for mtDNA-encoded proteins is a very indirect index of mitochondrial mass, mtDNA expression in the form of mitochondrial RNA has also been evaluated. Northern blot-based studies found some, but not all, mitochondrial RNA transcripts were reduced (Chandrasekaran et al., 1994), and nuclear-encoded oxidative phosphorylation subunit expression was also reduced (Liang et al., 2008). Findings from other studies suggest a more complex picture. For example, Manczak and colleagues reported COX subunit expression was actually increased in at least some AD brain neurons (Manczak et al., 2004). The

authors concluded this up-regulation might represent a compensatory response to perturbed COX function.

Electron microscopy (EM) has been used to quantify AD neuron mitochondria. Several studies have reported the number of normal appearing mitochondria was decreased (Baloyannis, 2006; Hirai et al., 2001). In one study there was a concomitant increase in mitochondria located within phagosomes (Hirai et al., 2001).

Collectively these studies suggest that within the AD brain the total number of mitochondria is increased despite the normal-appearing mitochondria are diminished. Whether this reflects decreased turnover, decreased synthesis, or both is not entirely clear. Potentially pertinent to this question, two relatively recent studies measured protein levels of peroxisome-proliferator activated receptor gamma coactivator 1α (PGC1a), a transcriptional co-activator that serves as a master regulator of mitochondrial mass (Qin et al., 2009; Sheng et al., 2012). Both these studies found PGC1a levels were reduced in AD brains.

1.7.3 Mitochondrial Fusion and Fission

Mitochondrial dynamics impairment has been widely implicated in neurodegenerative disorders such as AD (Chan, 2006a; Su et al., 2010). Mitochondria can undergo consecutives cycles of fusion – two mitochondria fuse giving origin to only one organelle; and fission - where occurs a breakdown of a mitochondrion in other smaller parts (Detmer and Chan, 2007), relying on a large group of conserved proteins, the dynamin-related GTPasesA balance between these two events is crucial to maintain mitochondrial functional integrity, especially in neurons where mitochondrial fission and fusion are mandatory for the formation of synapses and dendritic spines (Arduino et al., 2011). Mitochondrial fission enables the isolation of deficient mitochondria and

allows their removal by autophagy, specifically, mitophagy, whereas mitochondrial fusion is required for mtDNA complementation and precedes the isolation of healthier mitochondrial pools.

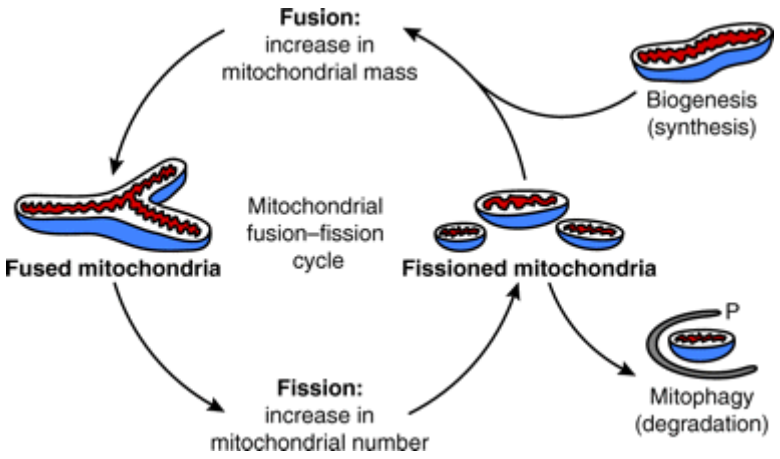

Figure 4. Mitochondrial life cycle. The mitochondrial life cycle starts with growth and division of pre-existing organelles (biogenesis) and ends with degradation of impaired or surplus organelles by mitophagy (turnover). In-between, mitochondria undergo frequent cycles of fusion and fission that allow the cell to generate multiple heterogeneous mitochondria or interconnected mitochondrial networks, depending on the physiological conditions. (Adapted from Seo et al., 2010).

Fusion is orchestrated by mitofusins, Mfn1 and Mfn2, which are responsible for outer membrane fusion and Opa1 (Optic atrophy 1), involved in fusion of outer and intermembranes. On the other hand fission requires Drp1 (Dynamin related protein) to start the formation of a ring-like complex within mitochondrial surface that constricts the organelle initiating fission. Then, complete constriction of the membranes takes place via hFis (Fission 1) (Chan, 2006b; Yoon et al., 2003). Analyses of AD brains show down regulation of the Mnf1, Mnf2, and Opa1 fusion genes and increased expression of the Fis1 fission gene (Manczak et al., 2011b; Wang et al., 2009). The variation in the levels of fission-mediating protein, Drp1, are less clear since it has been

reported a reduction and an increase (Manczak et al., 2011a; Wang et al., 2009). Regardless, Drp1 activity is inactivated by S-nitrosylation (SNO-Drp1), and Cho and colleagues reported high levels of SNO-Drp1 in brain biopsies from AD subjects (Cho et al., 2009). Increased Drp1 activity could lead to perturbed mitochondrial fission, which would result in an accumulation of fragmented and bioenergetically impaired mitochondria, and ultimately reduce synapse energy supplies (Barsoum et al., 2006).

Drp1, Opa1, Mfn1, Mfn2, and Fis1 proteins re-distribute so that they accumulate in the cell soma. Neuronal processes are therefore depleted of these fission-fusion proteins (Wang et al., 2009). The authors of this study also manipulated mitochondrial fission-fusion proteins in M17 cells and hippocampal primary neurons, and found this affected intracellular mitochondrial distributions. They concluded altered mitochondrial fission-fusion protein dynamics may play an important role in mitochondrial distribution and, consequently, synaptic dysfunction in AD neurons.

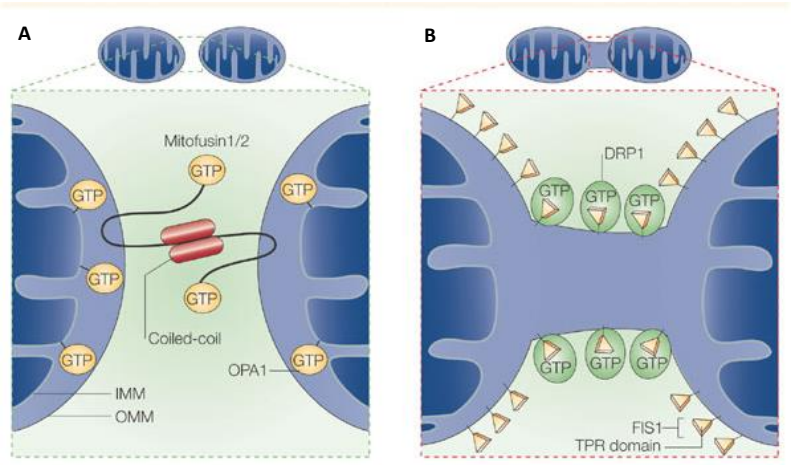

Figure 5. Dynamics of the mitochondrial network in mammalian cells. During fusion, two mitochondria dock through coiled-coil-domain interactions between mitofusins that are anchored into the outer mitochondrial membrane (OMM; their GTPase domains face the cytosol), whereupon optic atrophy protein 1 (OPA1), which is anchored partially on the inner mitochondrial membrane (IMM), participates in the membrane fusion process **b)**. During fission, fission protein 1 (Fis1) circumscribing the outer

mitochondrial membrane recruits the large GTPase and dynamin-like protein 1 (DRP1) through its tetratricopeptide repeats (TPR), which subsequently coalesces into foci at mitochondrial scission sites **c)**. (Adapted from Youle and Karbowski, 2005).

In primary cortical neuronal cultures exposed to S-nitrosocysteine (SNOC), a nitric oxide (NO) donor, uncontrolled fission occurs and this appears to represent an upstream and early event in SNOC-induced neuronal death (Barsoum et al., 2006). Further, when mitochondrial fission is blocked by expression of the dominant negative Drp1K38A, cell death is reduced. Accordingly, when cultured cerebrocortical neurons were exposed to Aβ, S-nitrosylation of Drp1 occurred and resulted in the formation of SNO-Drp1 dimers (Westermann, 2009). This pattern is similar to what is found in the brains of human AD patients (Cho et al., 2009).

Along with changes in brain metabolism a great number of studies performed in peripheral tissues allow us to suggest that AD can constitute a systemic disease affecting several tissues. Similarly, M17 cells that over-express wild type APP or APP carrying the Swedish mutation show mitochondrial fragmentation and redistribution of their mitochondria (Wang et al., 2008b). In both sporadic AD fibroblasts and M17 cells over-expressing APP, mitochondria cluster in the perinuclear region while the number of mitochondria in the cell periphery falls. Whether perturbed mitochondrial fission and fusion in sporadic AD subject fibroblasts is truly caused by Aβ overproduction is unclear, but the simple fact that mitochondrial dynamics are altered outside the brains of sporadic AD subjects contributes to the increasing realization that at biochemical and molecular levels, AD is not a brain-limited disease (Wang et al., 2008a).

1.7.4 Mitochondrial metabolic control of intracellular cargo transport

Neurons are highly differentiated cells with widespread synapses, branched dendritic arbors, and axons that can achieve a considerable size. The delivery of mitochondria to regions of the neuron with high bioenergetics demand is required for proper neuron function (Hollenbeck and Saxton, 2005; Li et al., 2004; MacAskill et al., 2010; Mattson et al., 2008). This mitochondrial transport is impaired in a number of neurodegenerative disorders. For example, it has been reported that mutant huntingtin protein in Huntington's disease enhances mitochondrial Drp1 activity, disrupts mitochondrial trafficking, and induces mitochondrial fission (Reddy and Shirendeb, 2011). Anterograde mitochondrial transport is significantly reduced in neuronal cultures of SOD1-mutant mice, suggesting that impaired mitochondrial trafficking is an early event in amyotrophic lateral sclerosis (ALS) (De Vos et al., 2007). Additionally, mitochondrial transport is impaired in dopaminergic neurons from a Parkinson's disease (PD) mouse model (Sterky et al., 2011). Given the prevalence of altered mitochondrial transport in other neurodegenerative diseases, it is likely that this critical phenomenon is also impaired in AD. Indeed, mitochondrial distribution is abnormal in AD brains (Wang et al., 2009). One study showed that mitochondrial transport in AD patient brains is significantly decreased compared to control brains (Dai et al., 2002). In an elegant study by Trimmer and Borland, fluorescently-labeled mitochondria in differentiated cybrid cell lines generated from AD patients displayed reduced trafficking to neurite-like processes compared to control cybrid lines (Trimmer and Borland, 2005). This study provides further evidence that mitochondrial transport may be impaired in AD. Additionally, this study suggests that impaired mitochondrial transport in AD is mediated by mitochondrial function itself and ultimately by mtDNA. Other studies suggest that mitochondrial transport is altered in cell cultures treated with Aβ (Calkins

and Reddy, 2011; Wang et al., 2009) and in mouse models of AD (Calkins et al., 2011; Massaad et al., 2010; Pigino et al., 2003). In general, it appears that Drp1 changes of expression may impair mitochondrial transport by perturbing a functional relationship that exists between Drp1 and the dynein-dynactin transport complex (Ishihara et al., 2009; Varadi et al., 2004; Wang et al., 2009). Therefore, although mitochondrial transport is certainly difficult to study in the autopsy brain, data suggest that in AD perturbed mitochondrial fission-fusion dynamics may contribute to the apparent presence of impaired mitochondrial transport. Intracellular transport relies on microtubules that wire neuronal cell body to the synapse. It has been widely documented that AD neurons have changes at cytoskeleton level being a reduction of assembled microtubules evident when compared with control cases (Cash et al., 2003; Santa-Maria et al., 2005). Disruption in microtubule dynamics results in incapacity of many subcellular processes to go on, which conducts to retrograde degeneration accompanied by synaptic loss and neuronal cell death (Li et al., 2007a). Evidence points to a mitochondrial dysfunction and an increase in superoxide anion production to be the cause of redox equilibrium changes, which have a straight influence on microtubule disassembly (Santa-Maria et al., 2005). Causative influence of microtubule dysruption on tau phosphorylation was studied by Miyasaka and colleagues (Miyasaka et al., 2010). Authors concluded that microtubule network disruption induces Tau to dissociate from microtubules, which leads to a subsequent phosphorylation. Cash and co-workers (Cash et al., 2003) found, in brain biopsies of AD patients, alterations in the microtubules of pyramidal neurons, mitochondrial abnormalities and increase oxidative damage, before detectable changes in Tau. Further, it was demonstrated that in SHSY5Y treated with $A\beta_{1-42}$, mitochondrial dysfunction, microtubule network dysruption, results in Tau increased phosphorylation and impairment of the autophagic

pathway. Restoring microtubule network assembly with Taxol, a known microtubule stabilizer, induced the degradation, by macroautophagy, of $A\beta_{1-42}$- mediated mitochondrial damaged and cell demise is avoided (Silva et al., 2011a). Additionally to tau detachment from microtubules, posttranslational modification of tubulin may also have a role on microtubule disassemble in AD. Mammalian sirtuins (SIRTs) are homologues of the silent information regulator factor 2, first described in *Saccharomyces cerevisiae* (Denu, 2005; Michan and Sinclair, 2007). These proteins have been found in organisms from all domains of life, ranging from prokaryotes to humans (Moniot et al., 2012). The SIRT family is composed of seven members (SIRT1-SIRT7) who are characterized by the presence of an approximately 275-amino-acid core that require nicotinamide adenine dinucleotide (NAD^+) for their enzymatic activity (Moniot et al., 2012). These proteins catalyze mainly deacetylation reactions in a variety of substrates including histones, transcription factors and apoptotic modulators (Michan and Sinclair, 2007; Yu and Auwerx, 2009). Although the molecular mechanisms underlying the ageing process are not fully understood, in the last years a body of evidence emerged pointing to SIRTs as mediators of life extension, described in a wide range of organisms including yeast, insects and rodents (Han, 2009; Outeiro et al., 2008). It is consensual that SIRTs differ in their sub-cellular localization, where SIRT1, SIRT6 and SIRT7 are predominantly in the nucleus, SIRT3, SIRT4 and SIRT5 in the mitochondria, whether SIRT2 resides mostly in the cytoplasm (Michan and Sinclair, 2007). SIRT2 can be found associated with the microtubule network showing affinity to acetylated tubulin as a substrate, in comparison to acetylated histone (North et al., 2003). North and colleagues (North et al., 2003) demonstrated using GFP-SIRT2 that SIRT2 deacetylated Lys40 of α-tubulin, and colocalize with the microtubule network. In the same experiments, using SIRT2 knockout mice it was shown that tubulin was

hyperacetylated. Even though SIRTs have been related with some potential protective effects, not everything is perfect in the SIRT world. In fact, SIRT2 activation has been reported to promote cell death (Han, 2009). Chong and collaborators (Chong et al., 2005) demonstrated that nicotinamide, a known inhibitor of SIRTs activity could reduce anoxia-induced neuronal injury in primary rat hippocampal neuronal cultures. Nicotinamide increased cell viability, prevented caspase activation, reduced DNA fragmentation and increased phosphorylation of proteins like Akt (serine/threonine protein kinase) and Bad (Bcl-2-associated death promoter), preventing apoptosis. Only indirectly we can infer that, at least part of these results is due to SIRT2 inhibition. Studies made in a triple-transgenic model of AD (3xTg-AD) expressing APPSwe, PS1M146V, and tauP301L transgenes showed that nicotinamide was able to prevent cognitive deficits through the inhibition of brain SIRTs associated with increased levels of deacetylated tubulin (Green et al., 2008). Further, 3xTg-AD mice at 8 months of age have high levels of tau phosphorylation in serine and threonine residues. Remarkably, treatment with nicotinamide significantly reduced Thr231-phosphotau (Green et al., 2008). Since acetylation of tubulin, a primary substrate of SIRT2, was implicated in nicotinamide-dependent results, is tempting to infer that SIRT2 inhibition by nicotinamide results in neuroprotection in this AD model. But, Wu and co-workers recently showed that an analog inhibitor of SIRT2 directly inhibits gamma-secretase (Wu et al., 2010). More recently results from cells overexpressing SIRT2 showed that inhibits lysosome-mediated autophagic turnover, impairing autopahgic flux (Gal et al., 2012).

1.7.5 Mitochondrial metabolic control of the autophagic-lysosomal pathway

In age-related diseases like AD, protein oligomerization and aggregation are prominent features that trigger neuronal disturbances including over-activation of macroautophagy (Cardoso et al., 2010). Macroautophagy, herein referred as autophagy, is a degradative pathway of the lysosomal system that allows the removal of cellular organelles and long-lived proteins (Boland et al., 2008). Autophagy is a tightly regulated process that begins with the formation of a cytosolic membrane under the control of multiple proteins, including microtubule-associated light chain 3. This complex controls the membrane elongation that sequestrates a region of the cytoplasm into a double-membrane, the autophagosome (Levine and Kroemer, 2008). The degradation of sequestered materials is completed when autophasosomes fuse with lysosomes (autolysosomes), a process that allows the acidification and acquisition of proteolytic enzymes (Klionsky et al., 2008; Levine and Kroemer, 2008; Nixon, 2007). First described as a mainly starvation-inducible process, the constitutive role of autophagy as a quality control mechanism in the brain it is now recognized (Nixon, 2007).

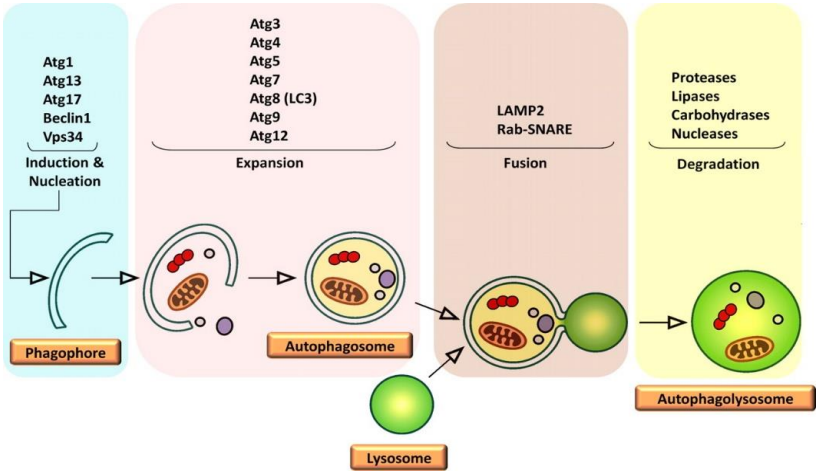

Figure 6. Schematic representation of the macroautophagy machinery. Macroautophagy begins with the formation of a double-layered isolation membrane (phagophore) around the moledcules and/or organelles to be degraded. The phagophore groes in size and completely engulfs the cargo, forming an

autophagosome. The autophagosome subsequently fuses with a lysosome, evolving into an autolysosome, wherein the cargo is digested. LC3 indicates light chain-3; LAMP2, lysosomal membrane-associated protein-2; and SNARE, Soluble N-ethylmaleimide-sensitive factor Attachment protein Receptor; Vps, vacuolar protein sorting. (Afapted from Dutta et al, 2012)

This "self-eating" process is crucial for cellular maintenance providing essential elements for cellular metabolism (Cuervo, 2004). Further, it is well documented that the "autophagic-lysosomal pathway" (ALP) is simultaneously impaired and induced in AD brains (Nixon, 2007). Autophagic vacuoles accumulate within dystrophic neurites in the brain of AD patients and animal models, suggesting a progressive dysfunction of ALP process (Ghavami et al., 2014; Nixon et al., 2005) and, consequently, protein aggregates turnover is blocked.

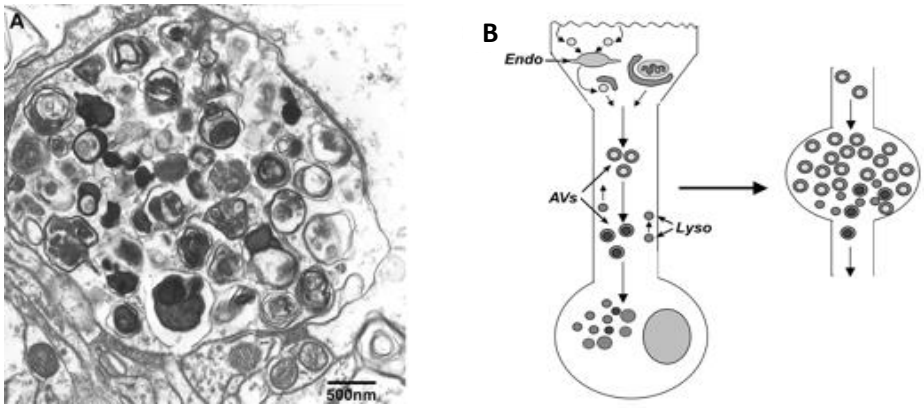

Figure 7. Dystrophic neurites in AD brains. A) Autophagosomes within dystrophic neurites, B) schematic representation of dystrophic neurites development in AD brains. Pathological accumulation of AVs is associated with impaired retrograde AVs transport or impaired auphagosome-lysosome fusion. (Adapted from Nixon 2005).

Low levels of mRNA of beclin 1, a protein required for induction of autophagy *in vivo*, have been documented in MCI subjects and AD patients (Lee and Gao, 2008; Pickford

et al., 2008). In the APP mice model, low levels of beclin 1 were also detected and are associated with enhanced Aβ pathology, and impaired autophagy (Pickford et al., 2008). Likewise, mitochondrial dynamics impairment has been widely implicated in neurodegenerative disorders such as AD (Chan, 2006a; Zhu et al., 2013). Mitochondria are degraded by the autophagic process, herein referred as mitophagy (Moreira et al., 2007). It was observed an increase in mitochondrial degradation products in vulnerable AD neurons, suggesting an augmented mitochondrial turn-over by mitophagy (Moreira et al., 2007). Electron microscopy analyses of AD brain samples stained for lipoic acid (LA) and COX-1 revealed that LA becomes associated with autophagic vacuoles in opposition to control cases. These observations demonstrated that mitochondria are key targets of autophagy in AD. A close interaction between autophagic vacuoles accumulation and Aβ deposition has been demonstrated. Endosomes and autophagic vacuoles, isolated from a variety of tissues, were shown to be enriched in APP and APP-cleaving secretases, namely in the gamma-secretase components PS-1 and nicastrin, which are required to generate Aβ (Mizushima, 2005; Vieira et al., 2010). This impairment in ALP leads to an exacerbation of Aβ production known to exert cytotoxicity (Boland et al., 2008). Yang and coworkers (Yang et al., 2008) reported that activated caspase-3 was found within dystrophic neurites, most exactly in autophagic vacuoles associated with amyloid plaques in PS/APP mice.

Under these conditions, pro-apoptotic proteins accumulate and apoptotic cell death take place, culminating in the neurodegenerative process observed in AD brains. Valid proofs have been presented pointing to the link between Aβ-mediated toxicity and mitochondrial dysfunction. Aβ species have been found associated with mitochondria in human AD brains (Caspersen et al., 2005; Devi et al., 2006; Hirai et al., 2001; Manczak et al., 2006). Many studies showed that Aβ added extracellularly can act intracellularly

promoting mitochondrial dysfunction (Devi et al., 2006) by lowering enzymatic activities. Aβ treatments in isolated rat brain mitochondria induced deficits in energy metabolism (Casley et al., 2002). Data obtained using PC12 and NT2 cells showed that Aβ decreases the activity of mitochondrial respiratory chain complexes (Cardoso et al., 2001; Pereira et al., 1999). PC12 cell line bearing APP Swedish mutation (APPSwe PC12) showed a decrease in COX activity and failure in other mitochondrial respiratory chain enzymes, when compared with wild-type APP-bearing cells or empty vector-transfected cells (Keil et al., 2004). Furthermore, it was demonstrated that Aβ is targeted to mitochondria by TOM-40, one of the mitochondrial translocase proteins, and transported towards the matriz by the translocase of the inner membrane (TIM) (Hansson Petersen et al., 2008). As discussed before, mitochondrial dysfunction triggers abnormalities along microtubule cytoskeleton that can be responsible for the impairment of autophagic vacuoles retrograde transport towards the cell body where lysosomes are located. In support of this hypothesis, it has been shown that microtubule depolymerizing agents disrupt vesicular transport inducing rapid accumulation of autophagosomes (Arduino et al., 2012; Kochl et al., 2006). In opposition, microtubule polymerizing agents prevent cognitive deficits in AD mice model (Matsuoka et al., 2008). Directly affecting mitochondria, some uncouplers were shown to disturb mitochondrial dynamics (Cappelletti et al., 2005; Silva et al., 2013a). In post-mitotic cells, the continuous accumulation of oxidative damage triggers the accumulation of non-functional mitochondria, a process that induces autophagy. Besides, damaged oxidative-modified proteins potentiate lipofuscin accumulation into the lysosome (Zheng et al., 2006). Lipofuscin is a polymeric material composed of oxidatively modified protein and lipid residues, which decreases lysosomal capacity and sensitizes cells to oxidative stress (Terman et al., 2006). Such evidence points to an interplay

between mitochondrial dysfunction, impaired microtubule network, and activation of the autophagic process, which creates a positive feedback loop where autophagic vacuoles are being continuously produced and accumulated due to lack of degradation within lysosomes (Cardoso et al., 2010; Cataldo et al., 1996; Silva et al., 2011b).

1.8 Apoptosis

AD brains experience significant neuron loss, which likely contributes to cognitive decline (Shimohama, 2000; Terry et al., 1991). While some neuronal loss could be due to necrosis, the vast majority is caused by apoptosis, a tightly-regulated form of programmed cell death (Barinaga, 1998).

DNA fragmentation, as assessed by TUNEL staining, is a common hallmark of apoptosis. Neurons in AD brains display increased DNA fragmentation compared to control brains (Anderson et al., 1996; Broe et al., 2001; Colurso et al., 2003; Lassmann et al., 1995; Li et al., 1997; Smale et al., 1995; Su et al., 1994; Troncoso et al., 1996). Many of these studies also reveal morphologic changes associated with apoptosis including abnormal chromatin, an absence of nucleoli, and shrunken or irregular cell shapes (Shimohama, 2000). Other studies note an increased proportion of apoptotic to normal neurons (Broe et al., 2001). Correspondingly, AD brains express significantly higher levels of the pro-apoptotic proteins Bak and Bad (Kitamura et al., 1998; Shimohama, 2000). Other studies suggest that AD brains display elevated pro-apoptotic Bax (Su et al., 1997). Caspases 3 and 6 activities/levels, which are apoptosis "executioner" caspases, are increased in AD brains (Avila, 2010; Guo et al., 2004; Masliah et al., 1998; Rohn et al., 2001b; Selznick et al., 1999; Stadelmann et al., 1999), as are the initiator caspases 8 and 9 (Albrecht et al., 2007; Rohn and Head, 2009; Rohn et al., 2001a; Rohn et al., 2002).

Further evidence that apoptotic events are more frequent in AD brains than in age-matched controls comes from experiments evaluating the presence of the cytoskeletal spectrin protein fodrin, which is cleaved early in the apoptotic cascade by caspases (Cribbs et al., 2004). Brains from AD patients display increased amounts of fodrin cleavage products (Ayala-Grosso et al., 2006; Masliah et al., 1991; Masliah et al., 1990).

Interestingly, evidence suggests that the pro-apoptotic shifts seen in AD subjects are not brain-limited. One study found that lymphocytes from AD patients were pre-disposed to apoptosis (Eckert et al., 2001). Another study reported increased fodrin cleavage in fibroblasts from AD patients (Peterson et al., 1991).

In summary, substantial data suggest that apoptosis is elevated in AD. This is not surprising given the other molecular and biochemical perturbations observed in this disease. For example, oxidative stress can predispose cells to apoptosis (Buttke and Sandstrom, 1994; Ray et al., 2012; Sandstrom et al., 1994). The prolific oxidative damage present in AD may, therefore, contribute to increased apoptosis.

1.9 New therapeutic strategies in AD

1.9.1 Mitochondrial mass manipulation

Increasing mitochondrial mass for the treatment of AD was first proposed in 2007 (Ghosh et al., 2007; Swerdlow, 2007c). A rudimentary attempt to increase mitochondrial mass was previously attempted using the thiazolidinedione drugs rosiglitazone and pioglitazone. Although these drugs were originally considered for AD treatment based largely on their demonstrated anti-inflammatory effects, these drugs, which are used to treat type II diabetes, were subsequently shown to activate mitochondrial biogenesis signaling under pre-clinical testing paradigms. However, it is

doubtful that can reach levels within the brain that are high enough to activate mitochondrial biogenesis. Although the thiazolidinedione clinical trial data to date have not been uniformly negative, the overall impression these data give is that pioglitazone and rosiglitazone will provide no measurable benefit or, at best, an extremely small benefit (Geldmacher et al., 2011; Gold et al., 2010; Risner et al., 2006). In the meantime, other ways to manipulate mitochondrial mass are in various stages of development.

1.9.2 Redox state manipulation

Redox state refers to a cell's electron balance as defined by ratios of electron donor and acceptor molecule pairs. In this respect, an important indicator of a cell's bioenergetic state is the ratio defined by amounts of nicotinamide adenine dinucleotide's oxidized (NAD^+) and reduced (NADH) derivatives.

While bioenergetics help determine a cell's redox state, a cell's redox state can also influence its bioenergetic function. Data demonstrating this latter point comes from multiple lines of investigation. Caloric restriction shifts the liver's redox balance towards a more oxidized state, and this is associated with mitochondrial biogenesis at least in the liver (Civitarese et al., 2007; Lambert et al., 2004; Lopez-Lluch et al., 2006) and also perhaps in the brain (Nisoli et al., 2005). Physical exercise, which should shift the muscle redox balance towards a more oxidized state, induces muscle mitochondrial biogenesis (Baar et al., 2002; Holloszy and Coyle, 1984; Hood, 2009).

Theoretically, enzymes that depend on NAD^+ levels, such as SIRT1, should activate in the setting of increased NAD^+ (Guarente, 2007; Haigis and Guarente, 2006). SIRT1 activation has been advocated for the treatment of several diseases, including AD (Anekonda and Reddy, 2006; Guarente, 2007; Haigis and Guarente, 2006). Polyphenol

compounds are believed to work as sirtuin activators (Baur, 2010; Lagouge et al., 2006). An AD clinical that will evaluate the effects of resveratrol, a polyphenol, on AD clinical status is scheduled to be performed.

1.9.3 Cytoskeletal manipulation

Mitochondrial dysfunction can induce cytoskeletal perturbations (Cardoso et al., 2010; Moreira et al., 2006). In the AD brain, reduced ATP levels may deregulate cytoskeleton homeostasis and microtubule integrity. Because features of neuron morphology, which include extended axons, branched dendritic arbors, and synaptic connections, both communication and continuity between a neuron's cell body and its distal regions must be adequately maintained. In this regard it is well known that neurons are highly sensitive to disturbances in microtubule-dependent transport (Trimmer and Borland, 2005).

AD neurons show cytoskeletal changes. Compared to brains from control subjects microtubule assemblies are reduced (Cash et al., 2003; Santa-Maria et al., 2005). Surveys of AD brain pyramidal neurons suggest changes in microtubule homeostasis precede neurofibrillary tangle formation (Cash et al., 2003). NFT consist of the microtubule-associated protein (MAP) tau, which plays a role in microtubule function, neurite growth, and cytokeleton maintenance (Stamer et al., 2002). Although a number of tau residues are phosphorylated under physiological conditions, in AD tau phosphorylation increases 3 to 4-fold. Other studies show that tau over-expression alters cell shape, leads to a loss of polarization, and slows cell growth. This is accompanied by a change in mitochondrial distribution; this change is characterized by organelle clustering (Ebneth et al., 1998). The associated microtubule perturbations are accompanied by changes in autophagy.

It ensures adequate levels of essential cell intermediates are maintained (Cuervo, 2004). APP, which is a transmembrane protein, can be processed by the endosomal-lysosomal pathway which initiates when material internalized by endocytosis or pinocytosis is sorted into endosomes (Nixon, 2007). Data suggest that a change in the rate of autophagy or the factors which cause autophagic vacuoles to accumulate may contribute to Aβ overproduction in AD brains (Levine and Kroemer, 2008; Yu et al., 2004). Indeed, evidence from AD brains shows massive AV accumulation within dystrophic neurites occurs (Nixon et al., 2005; Yu et al., 2005). Autophagy may therefore be simultaneously impaired and induced in AD. One potential explanation for this is that mitochondrial dysfunction may disrupt the microtubule cytoskeleton, and lead to impaired AV retrograde transport towards the cell body where lysosomes are located. In support of this, it has been shown that microtubule depolymerizing agents disrupt vesicular transport and induce rapid AV accumulation (Kochl et al., 2006). Vinblastine, which inhibits microtubule assembly, leads to microtubule depolymerization and prevents AV-lysosome fusion (Boland et al., 2008; Xie et al., 2010).

Recently, Miyasaka and colleagues (Miyasaka et al., 2010) reported that tau hyperphosphorylation is more likely a consequence, as opposed to a cause, of microtubule disruption. This is consistent with the view that when the microtubule network is disrupted, tau dissociates from microtubules and becomes accessible to the kinases that promote its hyperphosphorylation (Silva et al., 2011a). For this reason, it was postulated that microtubule stabilizing agents could potentially reduce neuronal dystrophy (Lee et al., 1994; Silva et al., 2011b). Data consistent with this view come from experiments using taxol (paclitaxel), a microtubule polymerizing agent that has been shown to mitigate AD-associated pathology in AD model systems. In rats, taxol was found to protect cortical neurons from $A\beta_{25-35}$ toxicity, decrease calpain activation,

and decrease cdk5/p25 complex formation (Li et al., 2003). In other models taxol pretreatment prevents tau hyperphosphorylation and reduces Aβ-induced apoptosis (Michaelis et al., 2002). In a hippocampal slice model of lysosomal dysfunction it was found that pretreatment with TX67, an analogue of taxol, restored pre and post synaptic proteins levels and reduced synapse damage (Butler et al., 2007).

Recently, we demonstrated that in SH-SY5Y cells exposed to $A\beta_{1-42}$, the resultant mitochondrial dysfunction perturbs AV transport via a microtubule dependent mechanism (Silva et al., 2011a). Taxol prevents $A\beta_{1-42}$ induced disorganization of the tubulin cytoskeleton, which secondarily reduces both cytosolic and mitochondrial Aβ content by enhancing ALP function.

Taxol, though, does not robustly access to the central nervous system (CNS) (Liu et al., 2002). A drug with taxol-like properties, NAP (davunetide), an eight amino acid peptide derived from the activity-dependent neuroprotective protein (ADNP), was recently shown to cross the blood brain barrier after systemic or intranasal administration (Gozes et al., 2005). Although NAP was first described as an antioxidant, it is now recognized that following cell internalization NAP interacts with the microtubule cytoskeleton (Divinski et al., 2004; Gozes and Divinski, 2007). NAP has been shown to reduce tau hyperphosphorylation and Aβ accumulation in both *in vitro* and in *vivo* AD models, and also benefit cognitive test performance in some of these models (Gozes and Divinski, 2004; Matsuoka et al., 2007; Matsuoka et al., 2008; Shiryaev et al., 2009; Vulih-Shultzman et al., 2007). Although its biological effects remain to be fully investigated (Shiryaev et al., 2011), based on encouraging preclinical data and an apparent lack of toxicity NAP is now being tested in persons with AD and other disorders of the CNS (Greggio et al., 2011; Idan-Feldman et al., 2011; Javitt et al., 2011). A recent phase IIa clinical study reported that intranasal NAP improved memory performance in patients

with an amnestic MCI syndrome, which is frequently an AD precursor state (Gozes et al., 2009).

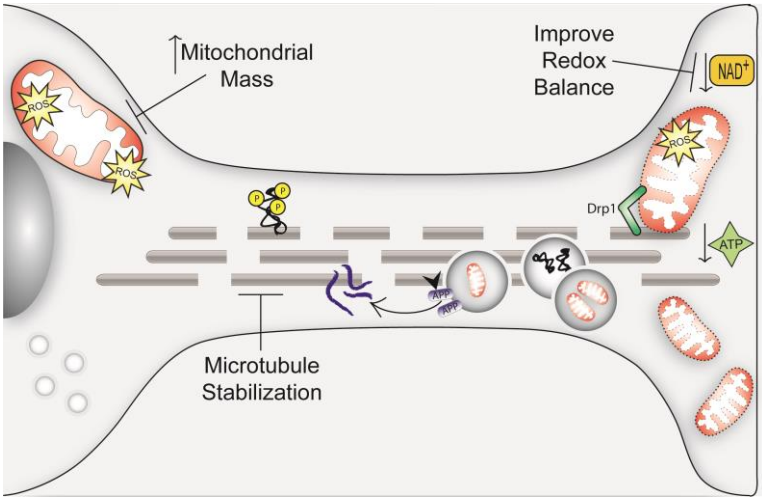

Figure 8. Current and anticipated mitochondrial medicine strategies. Dysfunctional mitochondria in AD result in reduced ATP availability (A), which promotes microtubule network breakdown (B), jeopardizing the transport of molecules and organelles along the cell. Further, it promotes tau dissociation from microtubules and its consequent hyperphosphorylation (C). These events compromise synapse energy supplies (D), and the transport of AVs toward the cell body (where lysosomes are located) is impeded (E). This promotes accumulation of Aβ aggregates, which may be formed by APP cleavage at AV membranes (F). Microtubule network stabilization may improve ALP function, promote transport along axons, and reduce Aβ production. Increasing mitochondrial mass may compensate for declines in mitochondrial function and their overall functional capacity. Shifting the cell redox balance to a more oxidized state may cause the cell bioenergetic infrastructure to function more efficiently, promote mitochondrial biogenesis, and activate pathways that allow cells to tolerate stress conditions (Adapted from Silva et al, 2012).

Objectives

AD and other neurodegenerative disorders are expected to constitute a major health problem as life expectancy increase. Efforts have been taken in order to tackle innovate therapies namely, addressing mitochondrial dysfunction, a striking feature in AD that

has great influence in the etiology of the disease, nevertheless the idea that mitochondrial dysfunction is the leading cause of AD is still a matter for debate within scientific community. Taking this into account, the major goal of this thesis was to prove that mitochondrial dysfunction-dependent events are responsible for intracellular trafficking failure, impairing ALP pathway and consequent Aβ peptides formation, which will cause further cellular damage. For this purpose we used AD, MCI and age-matched control (CTR) cybrids, an *ex-vivo* cellular model, in order to evaluate mitochondrial contribution to sporadic AD pathology. We evaluated mitochondrial function in these cells and several pathways governed by mitochondrial function such as: oxidative stress, microtubule network disruption, and macroautophagy/mitophagy. Using several experimental approaches we attempt to elucidate the involvement of mitochondrial dysfunction-driven events in sporadic AD pathology development.

Chapter 2

Materials and Methods

MATERIALS AND METHODS

2.1 Chemicals

Table 1. Chemicals

Compound	Company
FCCP	Sigma
Oligomycin	Sigma
Rotenone	Sigma
NH_4Cl	Calbiochem
Leupeptin	Sigma
Retinoic acid	Sigma
Aβ 1-42	American Peptide
AK1	Sigma
Tubastatin	BioVision
2-DG	Seahorse Bioscience

2.2 Human Subjects

For experiments regarding Chapter 3, subject participation was approved by the Ethics Board of Coimbra University Hospital, and all subjects or responsible caregivers,

whenever appropriate, gave their informed consent. The study sample was recruited at the Dementia Clinic, Neurology Department of Coimbra University Hospital and included 5 patients with mild late onset AD with the age of 81±2,6; 5 MCI patients with the age of 76±3,4; and 3 age-matched controls - 81±3,6 with no subjective or objective evidence of cognitive impairment. As this study was focused on mitochondrial role in sporadic AD, we wanted to exclude other genetic risk factors associated with nuclear DNA, so we selected only female subjects over 65 years and ApoE-ε4 non-carrier patients. Patients underwent a methodical biochemical, neurological and imaging evaluation, and were in a stable condition, without acute co-morbidities. Cognitive and functional status was assessed by the Mini Mental State Examination (MMSE)(Folstein et al., 1975), Portuguese version (Guerreiro, 1998), Alzheimer's Disease Assessment Scale – Cognitive (ADAS-Cog) (Mohs et al., 1983; Rosen et al., 1984), Portuguese version (Guerreiro M, 2003b), the Clinical Dementia Rating Sale (CDR) (Berg, 1988) and a comprehensive neuropsychological battery tests with normative data for the portuguese population (BLAD) (Guerreiro M, 2003a) exploring memory (Wechsler Memory Scale sub-tests) and other cognitive domains (including language, praxis, executive functions and visuo-construtive tests). Based on these instruments, patients were classified as probable AD or amnestic MCI. The diagnosis of probable AD was based on the guidelines of the Diagnostic and Statistical Manual of Mental Disorders – fourth edition (DSM-IV-TR) (1994) and the criteria of the National Institute of Neurological and Communicative Disorders and Stroke-Alzheimer's Disease and Related Disorders Association (NINCDS-ADRDA) (McKhann et al., 1984). MCI diagnosis was made in accordance with the criteria defined by Petersen et al. (Petersen et al., 2001), and the patients were classified as 0.5 in CDR.

For experiments regarding Chapter 4 and 5, subject participation was approved by the Kansas University Medical Center's Institutional Review Board. Subjects for this study were recruited from the University of Kansas Alzheimer's Disease Center (KU ADC). Each subject was determined, based on cognitive testing and by a memory disorders subspecialist clinician, to meet criteria for normal cognition (control status), mild cognitive impairment (MCI), or sporadic Alzheimer's disease (AD). After providing informed consent, sporadic AD (n = 8), MCI (n = 7), and age-matched control (n = 7) subjects underwent a 10 ml phlebotomy using tubes containing acid-citrate-dextrose as an anticoagulant. The age of the AD subject platelet donors was 71.5 ± 9.7 years, the age of the MCI platelet donors was 72.3 ± 6.6, and the age of the control subject platelet donors was 73.9 ± 7.7.

2.2.1 Creation of cybrid cell lines

Experiments regarding Chapter 3, NT2 ρ0 cells were briefly agitated in polyethylene glycol with platelets from the human subjects (Cardoso et al., 2004b). Seven days after plating the ρ0 growth medium, consisting of Optimem (Gibco-Invitrogen) supplemented with 10% non-dialysed FBS, 200 µg/ml sodium piruvate (Sigma), 100 µg/ml uridine (Sigma) and 1% penicilina-streptomycin, was changed to cybrid selection medium. NT2 ρ0 cells lack intact mtDNA, do not possess a functional electron transport chain (ETC), and are auxotrophic for pyruvate and uridine (Cardoso et al., 2004b; Swerdlow et al., 1997). Maintaining cells in selection medium, consisting of Optimem supplemented with 10% dialized, heat inactivated fetal calf serum (Gibco-Invitrogen), penicilin (Sigma) (50U/ml), and streptomycin (Sigma) (50 µg/ml), removes ρ0 cells that have not been repopulated with platelet mtDNA.

Concerning experiments of Chapter 4 and 5, cybrid cell lines were created on an SH-SY5Y cell nuclear background (Miller et al., 1996) by the KU ADC Mitochondrial Genomics and Metabolism Core. To generate the cybrid lines used in these studies, platelets from human subjects were mixed with SH-SY5Y cells previously depleted of endogenous mtDNA (ρ0 cells) as previously described (Swerdlow et al., 1996).

During the overall cybrid generation procedure several different types of media were used. For each medium, Dulbecco's modified Eagle's medium (DMEM) was obtained from Gibco-Invitrogen, while non-dialyzed or dialyzed fetal bovine serum (FBS) was obtained from Sigma. SH-SY5Y ρ0 cell growth medium consisted of DMEM supplemented with 10% non-dialyzed FBS, 200 ug/ml sodium pyruvate, 150 ug/ml uridine, and 1% penicillin–streptomycin solution. SH-SY5Y cybrid selection medium consisted of DMEM supplemented with 10% dialyzed FBS and 1% penicillin–streptomycin solution. The selection process lasted 6 weeks. After cell line selection was completed, each line was continuously maintained in a cybrid growth medium containing DMEM supplemented with 10% non-dialyzed FBS and 1% penicillin-streptomycin solution for over 2 months prior to biochemical and molecular assays.

2.3 Cybrid and parental SHSY5Y neuronal differentiation

Control, MCI, AD cybrids and SH-SY5Y cell line (ATCC-CRL-2266) where plated at a confluence of about 70%. After 24h medium was renewed to DMEM containing 1% of FBS, 200 ug/ml sodium pyruvate, 150 ug/ml uridine, 1% penicillin–streptomycin solution and freshly supplemented with 10 μM of Retinoic Acid (RA). Medium containing RA was refreshed every 2 days. Cells were harvested and experiments were made 14-17 days after the beginning of the differentiation.

2.4 Mitochondrial function and structural evaluation

2.4.1 Cytochrome oxidase Vmax assays

Complex IV activity was measured according to the method of Wharton and Tzagoloff (Wharton DC, 1967) by measuring the decrease in absorbance at 550 nm that occurs as reduced cytochrome c is oxidized. Cytochrome c reduction was initially performed by adding ascorbate crystals to cytochrome c and placing the mixture in a dialysis membrane for 18–24 h against 0.01 M phosphate buffer, pH 7.0, at 4ºC. Reduced-cytochrome c concentration was then determined with 0.1 M ferricyanide. The reaction mixture contained 0.01 M potassium phosphate, pH 7.0, and 50 µM reduced cytochrome c. The reaction was initiated by the addition of the mitochondrial sample at 30ºC. The pseudo first order rate constant (K) was calculated, because the reaction is of first order with respect to cytochrome c. Results were obtained in K/min/mg of protein.

Concerning Chapter 4, whole cell cytochrome oxidase (COX) Vmax activities were determined as previously described (Swerdlow et al., 1997). The total protein contained in each assayed cuvette was estimated using the DC Protein assay (BioRad, Hercules, California, USA). The relative amount of a COX protein subunit, COX4I1, was determined for each cell line by Western blot. COX activities in sec^{-1}/mg protein values were calculated. The sec^{-1}/mg protein Vmax activity for each line was also normalized to the amount of COX4I1 protein in the line.

2.4.2 Citrate synthase assay

Citrate synthase activity was determined by the method of Coore and team (Coore et al., 1971) which follows, spectrophotometrically, the formation of 5-thio-2-nitrobenzoate at 412 nm. The assay was initiated by the addition of 100 µM oxaloacetate at 30ºC. Results were obtained in nanomoles per minute per mg of protein.

2.4.3 Analysis of Adenine nucleotides

ADP/ATP ratios were determined using the EnzyLight^{TM} ADP/ATP Ratio Assay Kit (Bioassay Systems, CA, USA). Briefly, $1x10^5$ cells per well were plated in 96 well plates. In the first step, cells were lysed to release ATP and ADP. ATP reacts with the kit substrate in an initial fluorescence reaction, which provided a direct indication of the ATP concentration. Next, we followed the change in fluorescence that occurred when ADP was converted to ATP. The difference between the initial and final fluorescences indicated the ADP concentration.

2.4.4 Analysis of mitochondrial membrane potential ($\Delta\Psi_m$)

Changes in mitochondrial membrane potential were detected using the fluorescent cationic dye rhodamine 123 (Rh123) or TMRM, as indicated. Cells were loaded with 0.5 μM Rh123 or 300nM of TMRM (in the dark, at 37 ºC) and the fluorescence (λexc = 505 nm and λem = 525 nm) was recorded during 45 min before, and 10 min after mitochondrial depolarization, using a Spectramax Plus 384 spectrofluoremeter (Molecular Devices) for Rh123. For TMRM the fluorescence (λexc = 540 nm and λem = 590 nm) was recorded during 5 min before and 3 min after mitochondrial depolarization, using the same device described above. Maximal mitochondrial depolarization (Δψm collapse) was performed in every individual experiment by adding 1 μM FCCP (proton ionophore), which was always preceded by oligomycin (2 μg/ml) to prevent ATP synthase reversal. Either dye retention was determined by the difference between total fluorescence (after depolarization) and the initial value of fluorescence. Since positively charged dyes are retained by functional mitochondria with a high Δψm, a decrease of cellular retention of these dyes has been associated with a decrease in Δψm.

2.4.5 Respiration and glycolysis analysis

Approximately 80,000 cells from each cybrid line were used to seed the wells of Seahorse XF cell culture microplates (Seahorse Bioscience, Billerica, MA). A standard manufacturer-recommended two-step seeding procedure was utilized. After achieving cell adherence, microplates were placed overnight in a 37^{o}, 5% CO2 incubator.

For respiratory analyses, on the assay day shortly before placing culture microplates in the Seahorse Analyzer the cells were washed in buffered DMEM and the medium was then changed to the actual assay medium, which consisted of buffered DMEM containing no pyruvate and no BSA. Oxygen consumption rate (OCR) respiration measurements were made using a 3 minute mix, 2 minute wait, and 3 minute read cycling protocol. During the first 4 reading periods total cell OCRs were determined, with the fourth reading providing the value used for the analysis. After the fourth reading wells were injected with 500 nM oligomycin and the resulting OCR was measured over 3 reading cycles. The third post-oligomycin reading cycle provided the post-oligomycin OCR. After this, we injected a mixture of rotenone (1 uM) and antimycin A (200 nM) and measured the resultant OCR over 3 reading cycles. The third post-rotenone/antimycin reading cycle provided the non-mitochondrial OCR. The non-mitochondrial OCR was subtracted from the total OCR to yield the mitochondrial OCR, and from the post-oligomycin OCR to yield the mitochondrial proton leak OCR. After OCR measurements were completed, the cell mass in each well was estimated by measuring the total protein in each well (DC Protein Assay, BioRad). OCR values from each well were normalized to the amount of protein in that well to yield a final corrected OCR in pmol O_2/minute/mg protein.

For glycolysis analyses, on the assay day the cells were washed in unbuffered DMEM and following this the cells were placed in unbuffered DMEM containing no pyruvate,

no bovine serum albumin (BSA), and no glucose. The microculture plates were then de-gassed in a non-CO2 incubator at 37^{o}C for 1 hour before being placed into the Seahorse Analyzer. The wells were analyzed according to the procedure described in the Seahorse Glycolysis Stress Test kit. Briefly, initial measurements taken in the absence of glucose, and again after an injection of 2-deoxyglucose (to a final concentration of 100 mM), provide a non-glycolysis extracellular acidification rate (ECAR). In between these two baseline ECAR measurements, glucose was added to each well at a concentration of 10 mM. The resulting ECAR minus the non-glycolysis ECAR (in these experiments, we specifically subtracted the post-2-deoxyglucose non-glycolysis ECAR) provided the glycolysis ECAR. Next, oligomycin was added to each well (in this case, at a 1 uM concentration). The resulting ECAR minus the non-glycolysis ECAR provided the glycolysis capacity ECAR. Subtracting the glycolysis ECAR from the glycolysis capacity ECAR yielded the glycolysis spare reserve capacity.

2.4.6 Electron microscopy

Cell suspensions were fixed with 3% glutaraldehyde in 0.1 M phosphate-buffered pH 7.3 overnight at 4 °C. The fixed pellets were washed in 0.1 M phosphate-buffered. Pellets were then post-fixed with 1% osmium tetroxide during 2 h, dehydrated in grade ethanol and embedded in Spurr. The ultrathin sections were cut with an LKB ultra-microtome ULTRATOME III, and then contrasted with uranyl acetate and with lead citrate for transmission electron microscopy. Electron microphotographs were taken with JEOL JEM-100 SX electron microscope operated at 80 kV.

2.4.7 Immunocytochemistry and confocal visualization of mitochondrial network

Experiments presented in Chapter 3 consisted in 4h treatment with 5µM of FCCP AD, MCI and control (CT) cybrids that were then washed twice with PBS and fixed for 30 min at room temperature using 4% paraformaldehyde. For experiments of Chapter 5, after the differentiation process described above, cells were fixed for 30 min at room temperature using 4% paraformaldehyde. Both sets of fixed cells were washed again with PBS, permeabilized with 0.2% Triton X-100, and blocked with 3% BSA. The permeabilized cells were incubated with primary antibody (1:100 anti-TOM20 from Santa Cruz, CA, USA) overnight in a wet chamber, at 4ºC. Afterward, cells were incubated 1h with appropriate secondary antibody (1:250 AlexaFluor 488 from Molecular Probes, Eugene, OR, USA). Finally, cells were washed in PBS, incubated for 5 minutes with Hoechst 33342 (15mg/L in PBS, pH 7.4) in the dark and visualized by confocal microscopy. Images were acquired on a Zeiss LSM 510 meta-confocal microscope (63 × 1.4NA plan-apochromat oil immersion lens) by using the Zeiss LSM510 v3.2 software (Carl Zeiss, Inc., Thornwood, NY, USA) and analyzed using Zeiss LSM Image Examiner.

To quantify two parameters of mitochondrial morphology, a custom-written ImageJ macro containing plug-ins (Dagda et al., 2009) was used, as described by Arduino and colleagues (Arduino et al., 2012). Cells stained with TOM20 antibody were extracted to grayscale, inverted to show mitochondria-specific fluorescence as black pixels and thresholded to optimally resolve individual mitochondria. This macro traces mitochondrial outlines, using the ‘analyze particles’ function. The area/perimeter ratio was employed as an index of mitochondrial interconnectivity, and inverse roundness was used as a measure of mitochondrial elongation.

2.4.8 Western blot analysis of Flux modifying proteins

Cells were harvested with trypsin, centrifuged at 500 g for 5 minutes, re-suspended PBS, and centrifuged again. To prepare whole cell lysates, the washed cell pellet was suspended in M-PER Mammalian Protein Extraction Reagent (Pierce, Rockford, IL, USA) supplemented with Halt Protease Inhibitor Cocktail (Pierce) and gently shaken for 5 minutes as directed. To prepare pure nuclear and cytosolic lysates, the washed cell pellet was processed using an N-PER Nuclear and Cytoplasmic Extraction Reagent Kit (Pierce) as directed. Protein concentrations for all lysates were determined using a DC Protein Assay Kit (BioRad).

For Western blot analyses, samples were boiled, diluted 1:5 in sample buffer, resolved by electrophoresis in pre-cast 4–12% gels (BioRad), and transferred to polyvinylidene difluoride (PVDF) membranes. Non-specific binding was blocked by gently agitating the membranes in 5% non-fat milk or 5% BSA, as recommended, and 0.1% Tween in PBS for 1 hour at room temperature. Blots were subsequently incubated in buffer containing a designated primary antibody. Primary antibodies purchased from Cell Signaling Technology (Beverly, MA, USA) included antibodies to phospho-sirtuin-1 (Ser47), sirtuin 1, tubulin, HIF1α, phospho-P38, total P38, phospho-AMPK (Thr172), and total AMPK; these antibodies were each used at a 1:1000 dilution. Primary antibodies purchased from Santa Cruz Biotechnology (Santa Cruz, CA, USA) included PGC1α antibody (used at a 1:500 dilution). An antibody to HDAC1 was purchased from Thermo Scientific (Pierce, Rockford, IL, USA) and used at a 1:1000 dilution. An antibody to PARIS (ZNF746) was obtained from the UC Davis/NIH NeuroMab Facility (Antibodies Inc., PO Box 1560, Davis, CA) and used at a 1:1000 dilution.

After addition of a primary antibody membranes were incubated overnight at 4°C with gentle agitation. Blots were washed with PBS containing 0.1% Tween three times (each

time for 10 minutes), and incubated with the appropriate horseradish peroxidase-conjugated secondary antibody for 1 hour at room temperature with gentle agitation. After three washes, the blots were incubated with SuperSignal West Femto Maximum Sensitivity Substrate (Pierce). Chemiluminescence signals were detected using a Bio-Rad ChemiDoc Imager and band densities determined using Quantity One Software.

2.4.9 Western blot analysis of mitochondrial mass and dynamics proteins

Regarding experiments from Chapter 4, cells were harvested with trypsin, centrifuged at 500 g for 5 minutes, re-suspended PBS, and centrifuged again. Mitochondrial fractions were prepared as follows: cells were harvested and the pellet processed using a Mitochondrial Isolation Kit for Cultured Cells (MitoSciences, Abcam, MA, USA). To prepare whole cell lysates, the washed cell pellet was suspended in M-PER Mammalian Protein Extraction Reagent (Pierce, Rockford, IL, USA) supplemented with Halt Protease Inhibitor Cocktail (Pierce) and gently shaken for 5 minutes as directed. Protein concentrations for all lysates were determined using a DC Protein Assay Kit (BioRad). For Western blot analyses, samples were boiled, diluted 1:5 in sample buffer, resolved by electrophoresis in pre-cast 4–12% gels (BioRad), and transferred to polyvinylidene difluoride (PVDF) membranes. Non-specific binding was blocked by gently agitating the membranes in 5% non-fat milk or 5% BSA, as recommended, and 0.1% Tween in PBS for 1 hour at room temperature. Blots were subsequently incubated in buffer containing a designated primary antibody: α-tubulin, Drp1, total Drp1, mTOR, and COX4; these antibodies were each used at a 1:1000 dilution and were obtained from Cell Signaling Technology (Beverly, MA, USA). An antibody to COX2 was purchased from Molecular Probes (Molecular Probes, Eugene, OR, USA) and used at a 1:500 dilution. An antibody to TFAM was purchased from Aviva Systems Biology (San

Diego, CA, USA) and used at a 1:1000 dilution. An antibody to Opa1 was purchased from BD Biosciences (San Jose, CA, USA) and used at a 1:1000 dilution. After addition of a primary antibody membranes were incubated overnight at 4°C with gentle agitation. Blots were washed with PBS containing 0.1% Tween three times (each time for 10 minutes), and incubated with the appropriate horseradish peroxidase-conjugated secondary antibody for 1 hour at room temperature with gentle agitation. After three washes, the blots were incubated with SuperSignal West Femto Maximum Sensitivity Substrate (Pierce). Chemiluminescence signals were detected using a Bio-Rad ChemiDoc Imager and band densities determined using Quantity One Software.

In experiments from Chapter 5, cells were washed with PBS, scraped and homogenized in a buffer containing 250 mM sucrose, 20 mM Hepes, 1 mM EDTA, 1 mM EGTA, and protease inhibitors (0.1 M PMSF, 0.2 M DTT, and 1:1000 dilution of a protease inhibitor cocktail), and disrupted by homogenization. This suspension was centrifuged at 500 g for 12 min at 4ºC. The resulting supernatant was centrifuged at 9,500 g for 20 min at 4ºC. Pellets resulting from this step constitute a crude mitochondrial fraction. Mitochondrial pellets were resuspended in sucrose buffer and freeze-thawed three times. The total amount of resulting mitochondrial fractions obtained were removed and stored at −80 °C. Protein content was determined using Bradford protein assay (Bio-Rad, Hercules, CA, USA). Mitochondrial fractions containing the same amounts of protein were diluted (1:6) with sample buffer and were separated by electrophoresis in 10% SDS polyacrylamide gels. Both were transferred to PVDF membranes (Millipore, Billerica, MA, USA). Non-specific binding was blocked by gently agitating the membranes in 3% BSA and 0.1% Tween in TBS for 1h at room temperature. The blots were subsequently incubated with the respective primary antibodies overnight at 4°C with gentle agitation: 1:1000 anti-DRP1and p-DRP1 from Cell Signaling Technology

(Beverly, MA, USA); 1:1000 anti-OPA1 from BD Biosciences (San Jose, CA, USA); 1:1000 anti-FIS1 from Imagenex (Port Coquitlam, BC, Canada); 1:1000 anti-Mitofusin 1 and Mitofusion 2 from Abnova (Taipei City, Taiwan). Membranes were further washed three times with TBS, 0.1% Tween and then incubated with the corresponding alkaline phosphatase - conjugated secondary antibody (1:20,000, GE Healthcare UK Limited, Buckinghamshire, UK) for 1h at room temperature. The membranes were washed again three times and bound antibodies detected using the enhanced chemifluorescence reagent ECF (Amersham Biosciences UK Limited, Buckinghamshire, UK) according to the manufacturer's instructions. Blots were visualized using a VersaDoc imaging system (Bio-Rad, Hercules, CA, USA) and quantified using Quantity-One software (Bio-Rad, Hercules, CA, USA).

2.5 Apoptotic cell death evaluation

2.5.1 Western blot analysis of mitochondrial cytochrome c and Beta-amyloid content

For the analysis of mitochondrial cytochrome c and Aβ content, cells were washed with PBS, scraped and homogenized in a buffer containing 250 mM sucrose, 20 mM Hepes, 1 mM EDTA, 1 mM EGTA, and protease inhibitors (0.1 M PMSF, 0.2 M DTT, and 1:1000 dilution of a protease inhibitor cocktail), and disrupted by homogenization. This suspension was centrifuged at 500 g for 12 min at 4ºC. The resulting supernatant was centrifuged at 9,500 g for 20 min at 4ºC. Pellets resulting from this step constitute a crude mitochondrial fraction. Mitochondrial pellets were resuspended in sucrose buffer and freeze-thawed three times. The total amount of resulting mitochondrial fractions obtained were removed and stored at −80 °C. Protein content was determined using Bradford protein assay (Bio- Rad, Hercules, CA, USA). Mitochondrial fractions

containing the same amounts of protein were diluted (1:2) with sample buffer and were separated by electrophoresis on a 4–16% Tris–Tricine SDS gel to determine Aβ oligomeric content. For mitochondrial cytochrome c equal amount of protein were resolved by electrophoresis in SDS polyacrylamide on 15% gels. Both were transferred to PVDF membranes (Millipore, Billerica, MA, USA). Non-specific binding was blocked by gently agitating the membranes in 3% BSA and 0.1% Tween in TBS for 1h at room temperature. The blots were subsequently incubated with the respective primary antibodies overnight at 4°C with gentle agitation (1:500 anti-cytochrome c and 1:1000 6E10 mouse monoclonal anti-Aβ or anti-Abeta from Cell Signaling). Membranes were further washed three times with TBS, 0.1% Tween and then incubated with the corresponding alkaline phosphatase - conjugated secondary antibody (1:20,000, GE Healthcare UK Limited, Buckinghamshire, UK) for 1h at room temperature. The membranes were washed again three times and bound antibodies detected using the enhanced chemifluorescence reagent ECF (Amersham Biosciences UK Limited, Buckinghamshire, UK) according to the manufacturer's instructions. Blots were visualized using a VersaDoc imaging system (Bio-Rad, Hercules, CA, USA) and quantified using Quantity-One software (Bio-Rad, Hercules, CA, USA).

2.6 NAD metabolism

2.6.1 NAD^+/NADH assay

Cells were harvested and assayed for NAD^+/NADH levels using the Fluorescent NAD/NADH Detection Kit (Cell Technology, Inc, CA, USA). Briefly, $2x10^6$ cells were harvested and divided into two different vials, one for NAD^+ and another for NADH. Cells were then re-suspended in the appropriate extraction and lysis buffers. After vortexing, the lysates were incubated at 60ºC for 15 minutes. Immediately following

this the lysates were cooled and reaction buffer was added. Samples were centrifuged at 8000 g for 5 minutes to clarify the supernatants. After this, centrifugation samples were assayed for NAD^+/NADH with fluorescence measurements taken at excitation 530 nm and emission 590 nm.

2.6.2 Evaluation of SIRT2 protein levels and NAD^+ savage pathway enzyme

For cellular fractionation for the detection of NAD^+ enzymes of the Savage Pathway, cybrid cell lines were differentiated and cellular fractionation was performed, after 14 to 17 days, as directed in Subcellular Proteome Extraction Kit, from Calbiochem (Billerica, MA, USA), in order to obtain cytosolic and nuclear fractions. All fractions containing the same amounts of protein were diluted (1:6) with sample buffer and were separated by electrophoresis in 10% SDS polyacrylamide gels. Proteins were transferred to PVDF membranes (Millipore, Billerica, MA, USA). Non-specific binding was blocked by gently agitating the membranes in 3% BSA and 0.1% Tween in TBS for 1h at room temperature. The blots were subsequently incubated with the respective primary antibodies overnight at 4°C with gentle agitation: 1:100 anti-NAMPT from Santa Cruz (CA, USA); 1:1000 anti HDAC1 and anti SIRT2 from Cell Signaling Technology (Beverly, MA, USA), and 1:5000 anti-actin (Sigma). Membranes were further washed three times with TBS, 0.1% Tween and then incubated with the corresponding alkaline phosphatase - conjugated secondary antibody (1:20,000, GE Healthcare UK Limited, Buckinghamshire, UK) for 1h at room temperature. The membranes were washed again three times and bound antibodies detected using the enhanced chemifluorescence reagent ECF (Amersham Biosciences UK Limited, Buckinghamshire, UK) according to the manufacturer's instructions. Blots were visualized using a VersaDoc imaging

system (Bio-Rad, Hercules, CA, USA) and quantified using Quantity-One software (Bio-Rad, Hercules, CA, USA).

2.7 DNA and RNA isolation and quantification

2.7.1 Purification of genomic DNA

Genomic DNA was extracted using a QIAamp DNA Mini Kit (QIAGEN, Valencia, CA, USA). Briefly, $2x10^6$ cells were harvested with trypsin. The cell pellets were resuspended in PBS and Proteinase K was added. Cells were lysed using AL Buffer and purification was performed as directed in the QIAamp DNA Handbook. At the end of the purification process DNA was eluted from the columns using nuclease-free water. The resulting DNA was stored at -80ºC prior to use.

2.7.2 Purification of total RNA

Total RNA was extracted using a QIAamp RNA Blood Mini Kit (QIAGEN). Briefly, $2x10^6$ cells were harvested with trypsin. RTL buffer was added to help lyse the cells and then cell lysates were homogenized in QIAshredder spin columns. The resultant flow-through was placed in QIAamp spin columns and the purification procedure was performed according to the QIAamp RNA Handbook. RNA was eluted from columns using nuclease-free water and the resulting RNA was stored at -80ºC prior to use.

2.7.3 cDNA reaction

cDNA was obtained using the High Capacity cDNA Reverse Transcription Kit (Applied Biosystems, Foster City, CA). cDNA reverse transcription reactions were prepared with 10 ul of 2x RT master mix to which we added 1 µg of total RNA and sufficient nuclease-free water to bring the total reaction volume to 20 ul.

2.7.4 Quantitative real time PCR

Quantitative real-time PCR (qPCR) was performed using the TaqMan Universal PCR Master Mix (Applied Biosystems, Foster City, CA) and ready-to-use TaqMan Gene Expression Assays (Applied Biosystems). We quantified mRNA levels deriving from the following genes: HIF1, PGC1α, PGC1b, PRC, TFAM, COX4, cytochrome c, sirtuin1, and Bax. GAPDH was used as an internal loading control. qPCR amplification was determined utilizing an Applied Biosystems StepOnePlus Real-Time PCR System (Applied Biosystems).

To quantify mtDNA, we used the TaqMan Gene Expression Assay Kit (Applied Biosystems) and primers towards two mtDNA-encoded genes, NADH dehydrogenase subunit 1 (ND1) and the 16S RNA gene, as well as to the nuclear 18s rRNA gene. The relative mtDNA to nuclear DNA copy number ratio was determined using the comparative ΔΔCT method, in which ND1/18S and 16S/18S ratios were calculated.

2.8 Oxidative stress evaluation

2.8.1 Superoxide anion ($O_2^{\bullet-}$) formation

Superoxide anion ($O_2^{\bullet-}$) formation was determined by using the fluorescence probe dihydroehidium (DHE) (Molecular Probes, Invitrogen). DHE is permeable to cell membrane and in cytoplasm is converted to ethidium by $O_2^{\bullet-}$ emitting fluorescence (Bindokas et al., 1996). Briefly, 5 μM DHE dissolved in Krebs medium was incubated in cells during 1 h at 37ºC. Fluorescence measurements were taken during 1 h (518 nm excitation; 605 nm emission). Mitochondrial contribution to $O_2^{\bullet-}$ production was determined by challenging cells with 5uM of rotenone (complex I inhibitor) and fluorescence measurements were taken for 1h (518nm excitation; 605 nm emission). In order to correct the DHE fluorescence values for variations in total protein content in

the wells, cell protein in each well was quantified by the BioRad protein assay. The values were obtained as slope per mg protein for each condition and then expressed in relation to control in absolute values.

2.8.2 Determination of protein carbonyls groups

Protein carbonyl content was determined as described by Levine et al. (Levine et al., 1994), with slight modifications in plasma and CT, MCI and cybrids cellular extracts under basal conditions. Cellular and plasma proteins were precipitated with 10% TCA (trichloroacetic acid) and then incubated with 10 mM DNPH (dinitrophenylhydrazine) in 2 M HCl (or 2M HCl alone for the blanks), for 1 h at room temperature. The protein hydrazone derivatives were precipitated with 20% trichloroacetic acid and the precipitates were washed three times with 1 mL ethanol:ethylacetate (1:1). During each washing, the homogenized pellet was vortexed and left in the washing solution for 10 min at room temperature before centrifugation. The final pellet was resuspended in 6 M guanidine HCl, and incubated during 15 min at 37ºC. The carbonyl content was determined spectrophotometrically, using a microplate reader, at 360 nm on the basis of molar absorbance coefficient of 22,000 M-1 cm-1.

2.8.3 Measurement of TBARS levels

Cells where harvested in ice-cold PBS and equal amounts of protein was used to determine TBARS. TBARS levels were determined by using the thiobarbituric acid assay (TBA), according to a modified procedure described by Ernster and Nordenbrand (Ernster L, 1967). The amount of TBARS formed was calculated using a molar coefficient of $1.56x10^5$ mol-1 cm-1 and expressed as nmol TBARS/mg protein. Levels of lipid peroxidation in plasma were measured by the formation of a thiobarbituric acid

(TBA) adduct of malondialdehyde (MDA), separated by High Performance Liquid Chromatography (HPLC) (Draper and Hadley, 1990) using an analytical column Spherisorb ODS2 5 μm (250 × 4.6 mm), eluted with 60% (v/v) potassium phosphate buffer 50 mM, pH 6.8, and 40% (v/v) methanol at a flow rate of 1 mL/min. Spectrophotometric detection of the TBA-MDA adducts occurred at 532 nm.

2.8.4 Vitamin E measurements

Plasma levels of vitamins E were quantified after lipid extraction by HPLC using an analytic column Spherisorb ODS1-5 μm (250 × 4.6 mm), eluted at 2.5 mL/minute with a water solution of methanol (90%), at 45◦C, with spectrophotometric detection (Gilson, Lewis Center, Ohio, USA) at 295 nm (De Leenheer et al., 1979; Vatassery, 1978).

2.9 Microtubule network evaluation

2.9.1 Confocal microscopy analysis of α-tubulin and acetylated tubulin

Cells were fixed for 10 min at room temperature using 4% paraformaldehyde. Both sets of fixed cells were washed again with PBS, permeabilized with 0.2% Triton X-100, and blocked with 3% BSA. The permeabilized cells were incubated with primary antibody (1:2,000 anti-alpha-tubulin; 1:2,000 anti-acetylated-tubulin both from Sigma) overnight in a wet chamber, at 4ºC. Afterward, cells were incubated 1h with appropriate secondary antibody (1:250 AlexaFluor 488 from Molecular Probes, Eugene, OR, USA). Finally, cells were washed in PBS, incubated for 5 minutes with Hoechst 33342 (15mg/L in PBS, pH 7.4) in the dark and visualized by confocal microscopy. The cells stained with Acetylated Tubulin (Ac-Tub) were extracted to grayscale, inverted to show Ac Tub-specific fluorescence as black pixels and thresholded to optimally resolve Ac Tub staining. Background fluorescence and specific Ac Tub fluorescence were

determined. The final value for fluorescence intensity results from the subtraction of background fluorescence to specific fluorescence and the result is further divided by the number of cells from each image acquired.

2.9.2 Preparation of cell extracts containing soluble α-tubulin

To prepare soluble fractions of cell α-tubulin, cells were washed twice, very gently, with a microtubule stabilizing buffer (0.1M N-morpholinoethanesulfonic acid, pH 6.75, 1mM $MgSO_4$, 2mM EGTA, 0.1mM EDTA, 4M glycerol). Soluble proteins were extracted at 37ºC for 4-6 min in 100ul of microtubule stabilizing buffer containing 0.1% Triton X-100. Protein was quantified by the Bradford method. Samples were resolved by electrophoresis in SDS, 10% polyacrylamide gels and transferred to PVDF membranes (Millipore, Billerica, MA, USA). Non-specific binding was blocked by gently agitating the membranes in 3% BSA and 0.1% Tween in TBS for 1h at room temperature. The blots were subsequently incubated with the respective primary antibodies overnight at 4°C with gentle agitation- 1:10,000 anti-alpha tubulin and, 1:5000 anti-actin, both from Sigma. Fluorescence signals were detected using a Biorad Versa-Doc Imager, and band densities were determined using Quantity One Software.

2.9.3 Western blot analysis of acetylated tubulin and Tau phosphorylation

Individual cell lines were washed in ice-cold phosphate-buffered saline (PBS) and lysed in hypotonic lysis buffer (25 mM HEPES, pH 7.5, 2 mM MgCl2, 1 mM EDTA and 1 mM EGTA supplemented with 2 mM DTT, 0.1 mM PMSF and a 1:1000 dilution of a protease inhibitor cocktail) supplemented with 2 mM ortovanadate and 50 mM sodium fluoride. Protein content was determined using Bradford protein assay (Bio- Rad, Hercules, CA, USA) and equal amounts of protein were resolved by electrophoresis in

SDS, 10% polyacrylamide gels and transferred to PVDF membranes (Millipore, Billerica, MA, USA). Non-specific binding was blocked by gently agitating the membranes in 3% BSA and 0.1% Tween in TBS for 1h at room temperature. The blots were subsequently incubated with the respective primary antibodies overnight at 4°C with gentle agitation- 1:750 anti phospho-Tau Thr181 and 1:750 anti phospho-Tau Ser396, both from Santa Cruz Biotechnology (Santa Cruz, CA, USA); 1:1000 anti-acetylated tubulin and 1:5,000 anti-actin, both from Sigma.

2.10 Autophagy assessment

2.10.1 Cell treatment

Where indicated, autophagy modulation consisted of the treatment of differentiated cybrids with 15 mM ammonium chloride and 100 μM leupeptine for 4h, after 14-17 days of differentiation. In differentiated SH-SY5Y cells, the ammonium chloride and leupeptin were added, in the above described concentrations, during 12h. The former combination efficiently blocks all types of autophagy, as it reduces the activity of all lysosomal proteases by increasing the lumenal lysosomal pH without affecting the activity of other intracellular proteolysis systems.

2.10.2. Western blot analysis of proteins involved in autophagic pathway

Individual cell lines were washed in ice-cold PBS and lysed in 1% Triton X-100 containing hypotonic lysis buffer (25 mM HEPES, pH 7.5, 2 mM MgCl2, 1 mM EDTA and 1 mM EGTA supplemented with 2 mM DTT, 0.1 mM PMSF and a 1:1000 dilution of a protease inhibitor cocktail). Cell suspensions were frozen three times in liquid nitrogen and centrifuged at 20,000×g for 10 min. The total amount of resulting cell lysates obtained were removed and stored at −80 °C. Protein content was determined

using Bradford protein assay (Bio- Rad, Hercules, CA, USA). Samples containing the similar amount of protein were resolved by electrophoresis in SDS, 15% polyacrylamide gels and transferred to PVDF membranes (Millipore, Billerica, MA, USA). Non-specific binding was blocked by gently agitating the membranes in 3% BSA and 0.1% Tween in TBS for 1h at room temperature. The blots were subsequently incubated with the respective primary antibodies overnight at 4°C with gentle agitation –1:1000 anti LC3B, 1:100 anti Beclin 1; 1:1000 anti BCL2; 1:1000 anti PINK1; 1:1000 anti Parkin (Cell Signaling Technology, Inc., Danvers, MA, USA); anti-SQSTM1/p62 (1:1000); anti-actin (1:5000) both from Sigma; 1:500 anti-Ubiquitin (Santa Cruz, CA, USA). Membranes were washed with TBS containing 0.1% Tween three times (each time for 10 min), and then incubated with the appropriate horseradish peroxidase-conjugated secondary antibody for 1h at room temperature with gentle agitation. After three washes specific bands of interest were detected by developing with an alkaline phosphatase enhanced chemical fluorescence reagent (ECF from GE Healthcare). Fluorescence signals were detected using a Biorad Versa-Doc Imager, and band densities were determined using Quantity One Software.

2.10.3 Immunocytochemistry of LC3 and Lamp1

Cybrid cells were differentiated into neurons on ibidiTreat µ-Slide eight-well plates. Following 14-17 days of differentiation, cells were washed twice with with serum-free medium and fixed with 4% paraformaldehyde for 20 min at room temperature. The fixed cells were washed again with PBS, permeabilized with 0.2% Triton X-100 or Methanol at -20ºC during 20 min (for LC3B staining), and incubated with 3% BSA, to prevent nonspecific binding, for 30 min. Then, cells were incubated with primary antibodies: 1:400 rabbit monoclonal anti-LC3 XP® from Cell Signaling (Danvers, MA,

USA and 1:100 anti-LAMP-1 clone H4A3 from the Developmental Studies Hybridoma Bank (University of Iowa, Iowa City, IA, USA); overnight followed by washing with PBS and secondary antibody incubation for 1 h (1:250 alexa fluor 594 or 1:250 alexa fluor 488 from Molecular Probes (Eugene, OR, USA). After washing twice in PBS, nuclei were counterstained with Hoechst 33342. After a final wash, the coverslips were immobilized on a glass slide with mounting medium (DakoCytomation, Dako, Glostrup, Denmark). Images were acquired on a Zeiss LSM 510 meta-confocal microscope (63 × 1.4NA plan-apochromat oil immersion lens) by using the Zeiss LSM510 v3.2 software (Carl Zeiss, Inc., Thornwood, NY, USA) and analyzed using Zeiss LSM Image Examiner. The number of LC3 puncta per cell were quantified using the 'analyze particles' function of the ImageJ v1.39k (NIH, Bethesda, MD, USA) program after thresholding of images with size settings from 0.2–10 pixel^2 and a circularity of 0–1. The cells stained with Lamp1 were extracted to grayscale, inverted to show Lamp1-specific fluorescence as black pixels and thresholded to optimally resolve Lamp1 staining. Background fluorescence and specific Lamp1 fluorescence were determined. The final value for fluorescence intensity results from the subtraction of background fluorescence to specific fluorescence and the result is further divided by the number of cells from each image acquired.

2.10.4 Live imaging on AVs movements

Cybrid cells were differentiated into neurons on ibidiTreat µ-Slide eight-well plates. Following 14-17 days of differentiation, cells were washed twice with differentiation-DMEM without phenol red and FBS and mitochondria were labeled with Cyto-ID™ Green Detection Reagent provided in the Cyto-ID™ Autophagy Detection Kit (Enzo, Lausen, Switzerland), according to the manufacturer's instructions. After a gentle wash,

cells were kept in differentiation-DMEM without phenol red and FBS and were imaged autophagic vacuole movements. Time-lapse images were captured under a Zeiss LSM 510 meta-confocal microscope with a stage-based chamber (5% CO_2, 37°C). The inverted microscope was driven by the LSM software and images were taken every 2 s for a total of 4 min under 63× magnification (Zeiss Plan-ApoChromat 63×, 1.4NA). For transport analysis, mitochondria or autophagosomes were considered not mobile if they remained stationary for the entire recording period. Movement was counted only if the displacement was more than the length of the autophagosome (~500 nm). For each time-lapse movie, autophagic vacuoles were manually tracked and transport parameters were generated using the ImageJ software plug-in Multiple Kymograph, submitted by J. Rietdorf and A. Seitz (European Molecular Biology Laboratory, Heidelberg, Germany). Movement velocity data were determined from the kymographic images and were calculated based on the slope ($v = dx/dt$) obtained for each profile along the recording time. Each series of images was recorded for at least three randomly selected Cyto-ID™ Green-labeled cells per culture and three independent cultures per condition.

2.11 Sirtuin2 modulation

2.11.1 Sirtuin2 inhibition with AK1

After 14 to 17 days of differentiation, cybrid cell lines were incubated for 24h with 10µM of AK1 (Sigma, a SIRT2 inhibitor, 5 µm of Tubastatin (BioVision South Milpitas Blvd., CA), HDAC6 inhibitor, as a control. After 4h of exposure to N/L, cells were washed with ice-cold PBS and lysed in 1% Triton X-100 containing hypotonic lysis buffer (25 mM HEPES, pH 7.5, 2 mM MgCl2, 1 mM EDTA and 1 mM EGTA

supplemented with 2 mM DTT, 0.1 mM PMSF and a 1:1000 dilution of a protease inhibitor cocktail) for LC3B analysis.

Cell suspensions were frozen three times in liquid nitrogen and centrifuged at 20,000×g for 10 min. The total amount of resulting cell lysates obtained were removed and stored at −80 °C. Protein content was determined using Bradford protein assay (Bio- Rad, Hercules, CA, USA). Samples containing the similar amount of protein were resolved by electrophoresis in SDS, 10 or 15% polyacrylamide gels and transferred to PVDF membranes (Millipore, Billerica, MA, USA). Non-specific binding was blocked by gently agitating the membranes in 3% BSA and 0.1% Tween in TBS for 1h at room temperature. The blots were subsequently incubated with the respective primary antibodies overnight at 4°C with gentle agitation – 1:1000 anti-LC3B (Cell Signaling Technology, Inc., Danvers, MA, USA); 1:1000 anti-acetylated tubulin and 1:5000 anti-actin (Sigma). Membranes were washed with TBS and 0.1% Tween three times (each time for 10 min), and then incubated with the appropriate horseradish peroxidase-conjugated secondary antibody for 1h at room temperature with gentle agitation. After three washes specific bands of interest were detected by developing with an alkaline phosphatase enhanced chemical fluorescence reagent (ECF from GE Healthcare). Fluorescence signals were detected using a Biorad Versa-Doc Imager, and band densities were determined using Quantity One Software.

2.12 Animals

Sirtuin2 knockout mice (B6129) were obtained from The Jackson Laboratory (Bar Harbur, Maine, USA). Experiments involving animals were approved by and performed

in accordance with the University of Coimbra Institutional Animal Care and Use Committee guidelines and European Community Council Directive for the Care and Use of Laboratory Animals (86/609/ECC).

2.12.1 Isolation and treatment of primary cortical neurons

Primary neuronal cultures were obtained as described in (Agostinho and Oliveira, 2003), with minor modifications. Frontal cortices were removed from embryonic day 15-16 of C57BL/6 mice and Sirtuin2 knockout mice (B6129) and were aseptically dissected and combined in Ca^{2+} and Mg^{2+} free Krebs buffer [120 mM NaCl, 4.8 mM KCl, 1.2 mM KH2PO4, 13mM glucose, 10 mM HEPES (pH 7.4)] and then incubated in Krebs solution supplemented with BSA (0.3 g/l) containing trypsin (0.5 g/l) and DNase I (0.04 g/l) for 10 min at 378C. Tissue digestion was stopped by the addition of trypsin inhibitor (type II-S; 0.75 g/l) in Krebs buffer containing DNase I (0.04 g/l), followed by a centrifugation at 140 g for 5 min. After washing the pellet once with Krebs buffer, the cells were dissociated mechanically and resuspended in fresh Neurobasal medium supplemented with 2 mM L-glutamine, 2% B-27 supplement, penicillin (100 000 U/l) and streptomycin (100 mg/l). The cells were seeded on poly-L lysine (0.1 g/l)-coated dishes at a density of 0.33×10^6 cells/cm2 for western blotting and mitochondrial membrane potential assays. For immunofluorescence studies, neurons were mounted on poly-L-lysine-coated glass coverslips at a density of 0.75×10^6 cells/cm2. The cultures were maintained in serum-free Neurobasal medium supplemented with B-27 at 37ºC in a humidified atmosphere of 5% CO2, 95% air for 6 days before treatment in order to allow neuronal differentiation. After 6 days in vitro, cultured neurons were treated with 5 µM $A\beta_{1-42}$, 24 h before fixation or harvesting. Where indicated, 20 mM ammonium chloride and 20 mM leupeptin were added in the culture medium in the last 4 h of $A\beta_{1-42}$

treatment. The composition of the cultures was determined by immunolabeling in addition to physiological characterization. The majority of cells (90–95%) were positive for neuronal markers (Map2, βIII Tubulin) whereas, 10% of cells showed immunolabeling for the astrocytic marker glial fibrillary acidic protein.

2.12.2 Primary cortical neurons mitochondrial membrane potential ($\Delta\Psi_m$)

After 6 days of plating to allow neuronal differentiation, cells were treated with 5μM of $Abeta_{1-42}$ and changes in mitochondrial membrane potential were detected using the fluorescent cationic dye or TMRM. Cells were loaded with 300nM of TMRM (in the dark, at 37 ºC) and the fluorescence (λexc = 540 nm and λem = 590 nm) was recorded during 5 min before, and 3 min after mitochondrial depolarization, using a Spectramax Plus 384 spectrofluoremeter (Molecular Devices). Maximal mitochondrial depolarization (Δψm collapse) was performed in every individual experiment by adding 1 μM FCCP (proton ionophore), which was always preceded by oligomycin (2 μg/ml) to prevent ATP synthase reversal. TMRM retention was determined by the difference between total fluorescence (after depolarization) and the initial value of fluorescence.

2.12.3 Primary cortical neurons immunobloting

After 24h treatment with $Abeta_{1-42}$ with or without N/L in the last 4h of the treatment, as indicated, cells were harvested and lysed in lysis buffer (25 mM HEPES, pH 7.5, 2 mM MgCl2, 1 mM EDTA and 1 mM EGTA supplemented with 2 mM DTT, 0.1 mM PMSF and a 1:1000 dilution of a protease inhibitor cocktail), supplemented with 1% Triton X-100 for LC3 flux analysis. Cell suspensions were frozen three times in liquid nitrogen and centrifuged at 20,000×g for 10 min. The total amount of resulting cell lysates

obtained were removed and stored at −80 °C. Protein content was determined using Bradford protein assay (Bio- Rad, Hercules, CA, USA). Samples containing the similar amount of protein were resolved by electrophoresis in SDS, 10 or 15% polyacrylamide gels and transferred to PVDF membranes (Millipore, Billerica, MA, USA). Non-specific binding was blocked by gently agitating the membranes in 3% BSA and 0.1% Tween in TBS for 1h at room temperature. The blots were subsequently incubated with the respective primary antibodies overnight at 4°C with gentle agitation – 1:1000 anti-LC3B (Cell Signaling Technology, Inc., Danvers, MA, USA); 1:1000 anti-acetylated tubulin and 1:5000 anti-actin (Sigma). Membranes were washed with TBS and 0.1% Tween three times (each time for 10 min), and then incubated with the appropriate horseradish peroxidase-conjugated secondary antibody for 1h at room temperature with gentle agitation. After three washes specific bands of interest were detected by developing with an alkaline phosphatase enhanced chemical fluorescence reagent (ECF from GE Healthcare). Fluorescence signals were detected using a Biorad Versa-Doc Imager, and band densities were determined using Quantity One Software.

2.13 Data analysis

Data are expressed as means ± standard error of the means (SEM). To compare means between three groups we used one-way analysis of variance (ANOVA) followed by Fisher's least significant difference (LSD) post-hoc testing. To compare means between two groups we used two-way, unpaired Student's t-tests, with p-values of <0.05 considered significant.

Chapter 3

Prodromal metabolic phenotype in MCI cybrids: Implications for Alzheimer´s disease.

3.1 INTRODUCTION

The prevalence of dementia worldwide is becoming a major public health problem. Experts estimate more than 24 millions demented people all over the world and these numbers are expected to double in the next 20 years (Ferri et al., 2005). Alzheimer´s disease (AD) is the most common neurodegenerative disorder with a prevalence of 4,4% for those older than 65 years old and represents at least 60% of all dementia cases (Lobo et al., 2000). The disease has an insidious onset that is usually heralded by a progressive tendency to forget recent day-to-day events and gradually other cognitive skills become compromised leading to loss of autonomy. This impairment in cognitive functions is due to anatomical atrophy of AD brains, which correlates with severe neuronal loss (Mattson, 2004). Moreover, AD brains show increased levels of amyloid beta (Aβ) plaques and tangles composed of hyperphosphorylated tau (Pereira et al., 2005). Mild Cognitive Impairment (MCI) can be described as an intermediate state between normal aging and AD, where 15% of individuals develops dementia per year (Dawe, 1992). Indeed, MCI state is believed to be the earliest stage of the AD for the majority of patients (Butterfield et al., 2010). Although, the molecular mechanisms of AD are still uncovered, there is increasing evidence pointing out the primordial role of mitochondria in this pathology (Swerdlow and Khan, 2004). Interestingly, the metabolic changes observed in AD are at least partially observable in MCI subjects. Studies in MCI subjects revealed elevated levels of mitochondrial DNA (mtDNA) oxidative damage, which may be a major risk for AD development and progression (Hirai et al., 2001; Manczak et al., 2004; Migliore et al., 2005; Swerdlow and Khan, 2004). Further, deficits in mitochondrial electric transport chain (ETC) have been verified, particularly in cytochrome c oxidase (COX) platelets from MCI subjects in agreement with

observations made in platelets from AD patients (Cardoso et al., 2004a; Valla et al., 2006).

The outcome of mitochondrial dysfunction-mediated oxidative stress may have an important contribution to AD development. When an imbalance occurs between free radical generation and antioxidant capacity, oxidative stress is responsible can damage a variety of biomolecules, such as lipids, proteins, RNA and DNA(Lovell and Markesbery, 2007). Human *postmortem* brain samples from MCI and AD subjects showed elevated levels of protein carbonyls and lipid peroxides as compared to controls (Keller et al., 2005). This increment in oxidative stress markers was specific for superior and middle temporal gyri, which indicates specificity for brain regions more affected by the disease and related with cognitive decline. In accordance, peripheral oxidative damage has been described in AD and MCI individuals (Baldeiras et al., 2008, 2010; Migliore et al., 2005). Studies in lymphocytes showed significantly higher levels of oxidative mtDNA damage in AD and MCI compared with control subjects (Migliore et al., 2005).

Since it is now generally accepted that mitochondrial metabolic alterations begin years before the manifestation of the disease, this time window needs to be the basis for research to find more effective therapeutic targets and, in consequence, disease modifying therapies, to slow or stop the disease progression(Ferri et al., 2005).

In this work we used the cytoplasmic hybrid (cybrid) model, first described by King and Attardi (King and Attardi, 1989), to generate a disease-specific *ex-vivo* model of mitochondrial dysfunction. Together with abnormalities in mitochondrial structure and morphology we found that mitochondrial deficits and increased oxidative stress where transversal to AD and MCI group, which we attributed to inherited mtDNA (Swerdlow and Khan, 2004). Indeed, mitochondrial dysfunction and oxidative stress precede the

increase in mitochondrial Aβ oligomers content. We propose that mitochondrial impairments trigger AD sporadic pathology, since these defects are already present in MCI individuals and MCI itself can be considered a pre-stage for dementia.

3.2 RESULTS

3.2.1 Mitochondrial metabolism alterations

Specific mitochondrial COX activity decreased in MCI and AD cybrids (data not shown). Moreover, COX/citrate synthase activities ratio also decreased in MCI and AD cybrids as compared to CT cybrids (Fig. 1A). We corrected COX activity with citrate synthase (CS) activity to overcome possible variation of mitochondrial enrichment between groups. IN AD, MCI and CT cybrids CS activity were equivalent (Fig. 2A). COX/CS activities ratio in MCI cybrids had intermediate values between CT and AD cybrids (Fig. 2A).

Table I
Demographic characteristics of patient population

	CTR (n=3)	MCI (n=5)	AD (n=5)
Gender	F	F	F
Age, years	81 ± 3.6	76 ± 3.4	81 ± 2.6

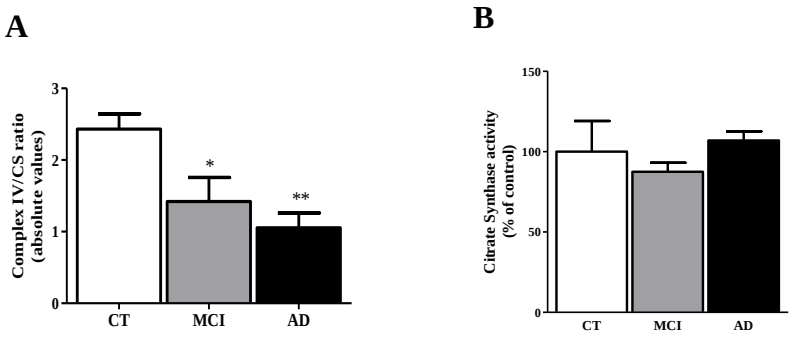

Figure 1. Mitochondrial function. (A) Activity of mitochondrial respiratory chain complex IV corrected for citrate synthase activity. The results are the means ± S.E.M. derived from five independent experiments and are expressed as absolute values. (B) Citrate synthase activity. Data represent the mean ± SEM derived from five independent experiments and are expressed as percentage relatively to control cybrids. . *p < 0.05, **p < 0.01; significantly different as compared to control CT cybrids.

The amount of rhodamine 123 taken up and retained by mitochondria is proportional to the magnitude of the mitochondrial membrane potential. Under basal conditions rhodamine 123 levels were lower in AD cybrids when compared with CT cybrids. Further, MCI cybrids have rhodamine 123 retention levels in-between AD and CT cybrids (Fig. 2A). Mitochondrial fractions prepared from AD and MCI cybrids contained less cytochrome *c* than mitochondrial fractions prepared from CT cybrids (Fig. 2B, C). Mitochondrial fractions purity was previously established by us (Cardoso et al., 2004a) and find to be over 80%.

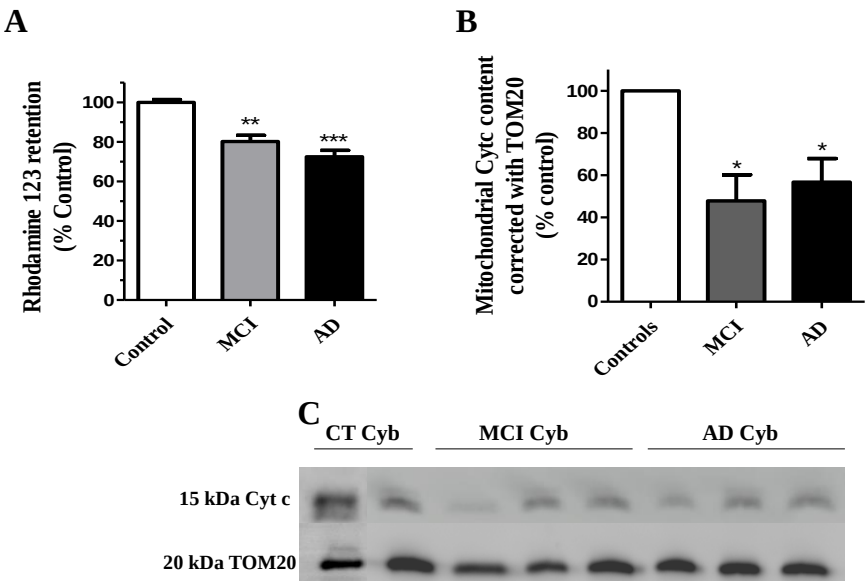

Figure 2. (A) Mitochondrial membrane potential was expressed as the percentage of CT cybrids rhodamine 123 retention, with the mean ± SEM derived from five independent experiments. Data are expressed as percentage relatively to control cybrids. (B) Basal mitochondrial cytochrome *c* levels were reduced in MCI and AD cybrids. Data represent the mean ± SEM derived from five independent experiments and are expressed as percentage relatively to control cybrids. (C) A representative western blot experiment showing mitochondrial cytochrome c content. *$p < 0.05$, **$p < 0.01$; ***$p < 0.001$, significantly different as compared to control CT cybrids.

3.2.2 Mitochondria: ultrastructure and distribution.

At an ultrastructural level, CT cybrids have a eukaryotic nucleus and exhibit dark, oval mitochondria (Fig. 3A). However, AD cybrids contained pale and enlarged shaped mitochondria with disrupted cristae (Fig. 3A), which is in accordance with the alterations observed in mitochondrial function.

To assess mitochondrial distribution and morphology we used Tom20 staining and determined mitochondrial interconnectivity and elongation. Mitochondrial interconnectivity determines the degree of mitochondrial branching, namely the connectivity/dynamics between mitochondria. A higher mitochondrial interconnectivity

means a higher access and communication between mitochondria. We have found that in AD cybrids mitochondrial distribution was more perinuclear than in CT cybrids (Fig. 3B). Moreover, AD cybrids showed a decrease in mitochondria elongation and interconnectivity, both features correlating with increased mitochondrial fragmentation. In fact, in AD cybrids mitochondria appears as small dots instead of a mitochondrial interconnected net. The above mentioned alteration in AD cybrid biochemical features are in agreement with an altered mitochondrial ultrastructure and may account for the clinical phenotype of the patients included in this study. Under basal conditions MCI cybrids showed an intermediated state between CT and AD cybrids. FCCP, a mitochondrial uncoupler, induced mitochondrial network disruption in CT cybrids; more pronounced perinuclear mitochondria localization in CT and MCI cybrids, but failed to induce additive changes in AD cybrids due their basal injure (Fig. 3B).

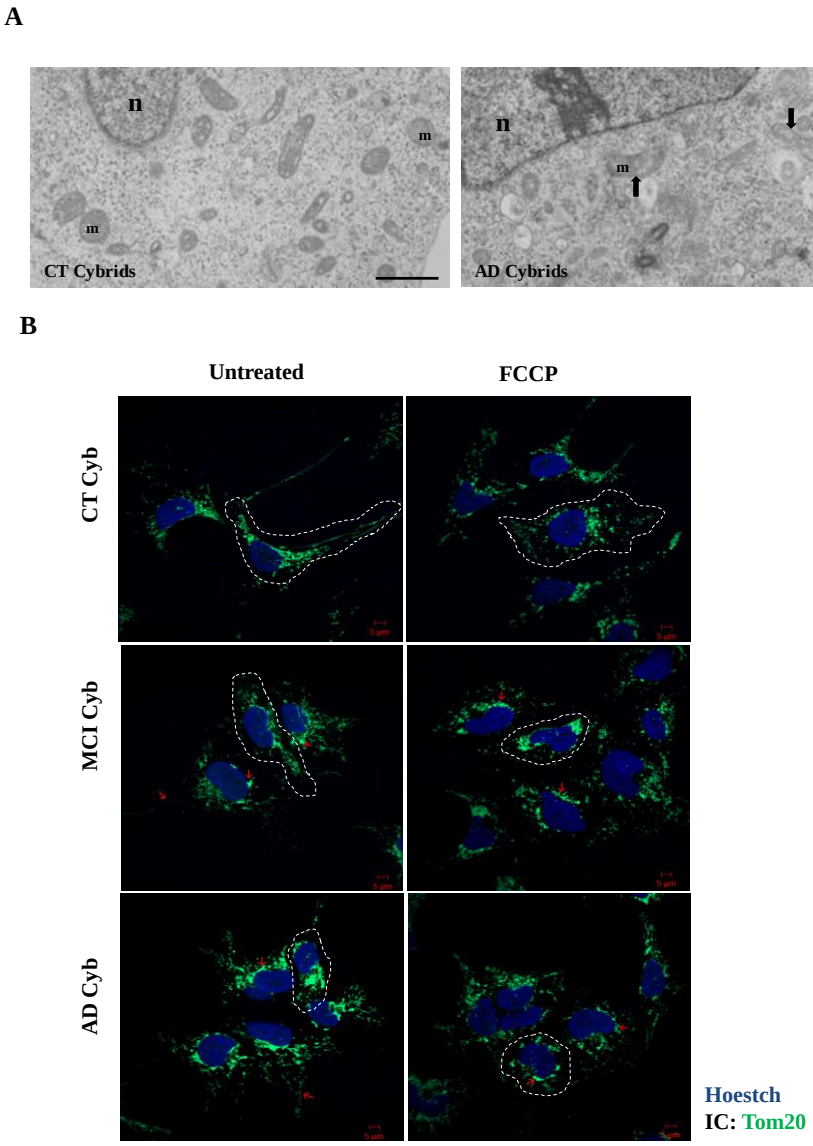

Figure 3. Mitochondrial ultrastructure, morphology and distribution. (A) Electron microscopy of an AD and a CT cybrid cell. CT cybrid have a euchromatic nucleus (n) and rod-shaped mitochondria (m) with a dark matrix. AD cybrids have also a euchromatic nucleus (n) and oval mitochondria (m) with pale matrix. AD cybrids mitochondria are enlarged and with disrupted cristae (arrows). Bars, 10 µm. (B) Tom20 immunostaining (green) of CT, MCI and AD cybrids showing alterations in mitochondria distribution, elongation and interconnectivity. AD cybrids show increased mitochondrial perinuclear distribution and were non-responsive to FCCP treatment. Cell nuclei were labeled with Hoechst. The images are representative of 3 independent experiments. Mitochondrial network outline (white) shows the shift of mitochondria localization to the perinuclear region and the arrows indicate an alteration of mitochondrial morphology to a more fragmented network. Bars, 5 µm.

3.2.3 Oxidative stress markers are increased in AD, MCI cybrids and patients plasma.

Inefficient electron transport through the mitochondrial respiratory complexes can lead to the generation of ROS as a byproduct. Increased levels of ROS can directly damage various macromolecules, which lead to their loss of function and culminate in cell demise. Under basal conditions MCI cybrids have a slight increase in superoxide radical production whereas AD cybrids have significant increment in superoxide radical levels (Fig. 4A). When challenged with rotenone, a complex I inhibitor, CT, MCI and AD cybrids increase significantly superoxide radical production. MCI cybrids show intermediate values of superoxide radical production between AD and CT cybrids.

Carbonyls and lipid hydroperoxides are oxidatively post-translational modifications in protein and lipids due to increases in oxidative stress. Indeed, we found higher levels of protein carbonyls and lipid peroxidation by-products in AD and MCI cybrids (Fig. 4B and 4C). Moreover, MCI cybrids increment of both lipid peroxides and protein carbonyls levels was smaller than what was observed in AD. In plasma of the studied subjects we found no significant changes in concentration of Vitamin E, although there was a slight tendency, not significant, for higher levels of protein carbonyls and of lipid peroxidation marker malondialdehyde (MDA) in MCI and AD groups (Table II).

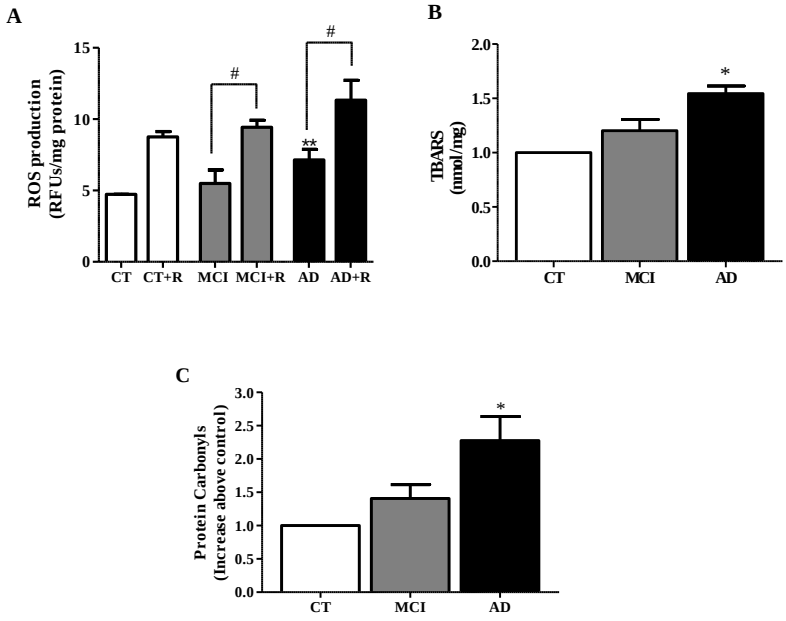

Table II
Oxidative markers in patients plasma

	CTR (n=3)	MCI (n=5)	AD (n=5)
Vitamin E (μM)	26.30 ± 5.3	26.73 ± 3.4	30.96 ± 10.3
MDA (μM)	1.5 ± 0.8	1.86 ± 0.2	1.98 ± 0.2
Carbonyl groups (μM)	184.1 ± 22.6	221.1 ± 0.1	195.6 ± 3.3

Figure 4. Oxidative stress markers. (A) Superoxide production in basal conditions and after challenging cells with rotenone. Data are expressed as the increasing slope per milligram of protein (RFU/mg), and as the mean ±S.E.M. for 5 independent experiments. (B) Lipid peroxidation products (TBARS) content was measured using thiobarbituric acid and was expressed as nmol of TBARS per milligram of protein (nmol/mg). Data are the mean ± S.E.M. for 5 independent experiments. (C) Protein carbonyl groups were determined using DNPH. Data are expressed as the mean ± S.E.M, for 5 independent experiments. *$p < 0.05$, **$p < 0.01$, significantly different as compared to control CT cybrids. $^{\#}p < 0.05$, significantly different compared with untreated cells.

3.2.4 Mitochondrial Aβ monomers/oligomers content.

Cybrid cells showed basal intracellular production of Aβ peptide, which can be correlated with increases of this peptide in the mitochondrial pool (Fig. 5).

Although, is not yet clear how increases in Aβ oligomers correlate with mitochondrial dysfunction in sporadic AD, it is interesting to notice that mitochondrial Aβ oligomeric content increases in AD cybrids as compared MCI or to aged-match controls (Fig. 5).

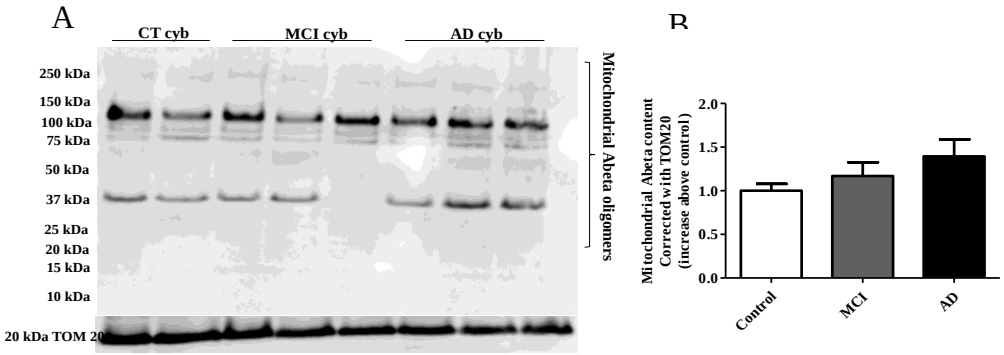

Figure 5. Mitochondrial Aβ oligomers content. (A) Western Blot analysis and (B) densitometry of mitochondrial Aβ content, showing an increase of mitochondrial Aβ oligomeric content in AD cybrids. Aβ oligomers were quantified from 37 kDa to 100 kDa. Mitochondrial fractions were reprobed for Tom20 in order to correct Aβ levels to mitochondrial mass. Blots are representative of 3 different experiments. Data is reported as the fold increase over untreated CT cybrids. *$p<0.05$, significantly different when compared to CT cybrid.

3.3 DISCUSSION

Mitochondrial dysfunction has been widely implicated in AD etiology as a primordial event (Moreira et al., 2006; Silva et al., 2011b; Swerdlow and Khan, 2009). Our data confirm prior studies showing that COX activity is decreased in AD cybrids (Cardoso et

al., 2004b), and show for the first time that this mitochondrial defect is also present in MCI cybrids. In accordance, experiments performed with platelets shown that COX activity is decreased in subjects with MCI and AD (Cardoso et al., 2004b; Valla et al., 2006). Our findings corroborate the hypothesis that mitochondrial threshold effect, due to the synergy between inherited polymorphic variations of mtDNA and age-related changes, accounts for systemic alterations of mitochondrial function that ultimately induces sporadic AD pathology (Swerdlow et al., 2010). Since AD and MCI cybrids perpetuate the defects found in the brains and peripheral tissues, it is reasonable to argue that mtDNA could entail the responsibility for MCI progression into AD. Indeed, our results show that MCI cybrids have reduced mitochondrial membrane potential and mitochondrial cytochrome *c* content suggesting mitochondrial-dependent apoptotic activation, similarly to what we observed in AD cybrids (Cardoso et al., 2004a). This is further supported by ultrastrutural images showing that AD cybrids mitochondria are enlarged or swollen and have a pale matrix with few remaining cristae as compared with CT cybrids. These ultrastrutural mitochondrial changes, also demonstrated by Trimmer and colleagues (Trimmer et al., 2000), sustain the altered mitochondrial distribution and pattern observed in AD cybrids. Mitochondrial distribution is also strikingly different in cells that overexpress APP, Tg APP mice and Aβ-treated neurons (Du et al., 2010; Wang et al., 2008b). More significantly, we show for the first time that MCI cybrids exhibit a shift of mitochondrial network to the perinuclear region with an increase in fragmentation. Mitochondrial perinuclear clustering and fragmentation can be triggered by depolarization, that in turn potentiates mitophagy (Cardoso et al., 2010), or by impaired mitochondrial transport along microtubules. Indeed, it was previously described in different AD models that microtubule-dependent mitochondrial intracellular traffic is compromised (Brunden et al., 2011; Silva et al., 2011a; Silva et

al., 2011b). In support of this point of view, CT cybrids treated with a mitochondrial uncoupler exhibited fragmentation of mitochondrial network accompanied by a more pronounced perinuclear localization of mitochondria. Importantly, MCI cybrids challenged with the mitochondrial uncoupler are still responsive, whereas AD cybrids are not. This data indicates that mitochondrial compromise occurs in a progressive manner during the course of pathology.

Mitochondrial metabolism also regulates cellular oxidative stress (Moreira et al., 2006). Moreover, it has been described that oxidative stress is an early event in the pathogenesis of AD (Smith et al., 2010). Accordingly the majority of oxidative stress markers are altered in MCI, which may occur decades before the disease manifestation (Perrin et al., 2011). We observed that mtDNA-driven COX dysfunction leads to increased ROS formation (superoxide radical). Furthermore, it was found that ROS generation by mitochondria, namely hydroxyl radicals, is enhanced in ETC-inhibited and mtDNA-deleted cells (Cardoso and Oliveira, 2003; Indo et al., 2007). In fact, redox proteomics analysis of MCI brains revealed higher levels of protein carbonyls similarly to what is observed in AD brains (Aluise et al., 2011). Our results also demonstrate a gradual increase in protein oxidation, since the levels of carbonyl groups in MCI cybrids levels are between AD and CT cybrids values. Increased content in protein carbonyls correlates positively with increased ROS production in both MCI and AD cybrids.

Lipids are molecules commonly attacked by free radicals in a process nominated lipid peroxidation. Lipid peroxidation products have been found augmented in *postmortem* samples of brains from MCI and AD subjects, with significant incidence in regions where Aβ pathology is more prominent (Ansari and Scheff, 2010; Lovell and Markesbery, 2007). In peripheral tissues, Baldeiras and colleagues (Baldeiras et al.,

2008) found increased levels of nitrogen reactive species and markers of lipid peroxidation in both MCI and AD individuals. Other studies detected a positive correlation between the decreased antioxidant defense and increased lipid peroxidation in AD and MCI patients when compared with age-matched controls (Padurariu et al., 2010). In our cybrid cell lines we also observed higher levels of TBARS in both MCI and AD groups. Baldeiras and colleagues (Baldeiras et al., 2010) evaluated the role of peripheral oxidative stress in MCI progression to AD. Significant changes in several oxidative stress markers were found in the MCI group that converted to AD, which lead the authors to propose that antioxidant therapy is indicated for prevention of AD, in pre-symptomatic phases. Our MCI and AD subject's plasma samples also show a tendency to increased levels of protein carbonyls, MDA but no changes in vitamin E levels (Table II).

It was already demonstrated in AD cybrids that mitochondria dysfunction induces Aβ pathology increasing its cellular levels, however the underlying mechanism has not been disclosed (Khan et al., 2000). Previously, in an attempt to address this issue, authors using Aβ-treated cells or Aβ-overproducing cells, showed that Aβ-rich synaptic mitochondria revealed early deficits in mitochondrial function and increased mitochondrial oxidative stress (Du et al., 2010). These results highlight the essential importance of synaptic mitochondrial dysfunction for the development of synaptic degeneration in AD. We now found that Aβ oligomers levels are increased in mitochondrial fractions from AD in comparison with CT cybrids. On the other hand, the increase of theses Aβ species in MCI cybrids did not reach statistical significance. Therefore, we can argue that Aβ mitochondrial enrichment is downstream of mitochondrial impairment and may aggravate the defect even further. Our results clearly indicate that Aβ mitochondrial accumulation increases as mitochondrial function

declines. Moreover, it was shown that mitochondria are a privileged site for Aβ accumulation (Manczak et al., 2006; Pagani and Eckert, 2011; Silva et al., 2011a). Pavlov and colleagues (Pavlov et al., 2011) recently showed that mitochondrial-associated amyloid precursor protein (APP) is cleaved by mitochondrial secretases contributing to increase Aβ content within the mitochondria, which exacerbates mitochondrial dysfunction.

In conclusion, our results point out to the primordial role of mtDNA, and consequently, mitochondrial dysfunction, in the pathogenesis of AD. Features of mitochondrial dysfunction and oxidative stress are found in both MCI and AD cybrids. Furthermore, the alterations in MCI cybrids are often intermediate between CT and AD, indicating that the molecular and biochemical events occurring in MCI cells can disclosure the molecular mechanisms underlying AD etiopathogenesis. So, we propose that MCI may be an important stage for developing new therapeutic approaches, not only targeting oxidative stress but also mitochondrial dysfunction, in order to avoid MCI progression to aged-related AD.

Although, not all cases of MCI will progress to AD, this nosologic entity does show alterations in mitochondrial function, which are no doubt interrelated with AD degenerative pathway. An early identification of individuals in this preclinical period that are not yet demented is imperative, in order to potentiate the effect of disease-modifying agents.

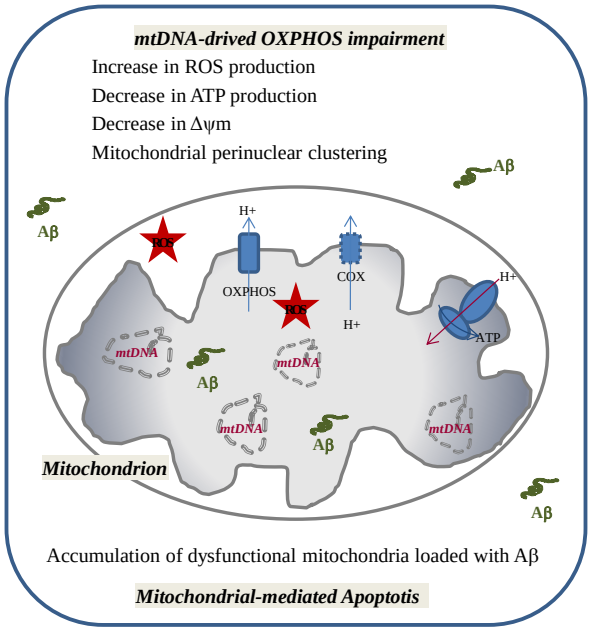

Figure 6. Integrative diagram of mtDNA-drived OXPHOS impairment. The model proposes that inherited mtDNA is responsible for aged-related dysfunctional mitochondrial oxidative phosphorylation (OXPHOS), which contributes to the appearance of Aβ aggregates, a major histopathological hallmark of AD.

Chapter 4

Bioenergetic Flux, Mitochondrial Mass, and Mitochondrial Morphology Dynamics in AD and MCI Cybrid Cell Lines

4.1 INTRODUCTION

Perturbed bioenergetic function, and especially mitochondrial dysfunction, is observed in brains and peripheral tissues of subjects with Alzheimer's disease (AD) and mild cognitive impairment (MCI) (Swerdlow, 2012b; Valla et al., 2006), a clinical syndrome that frequently represents a transition between normal cognition and AD dementia (Petersen, 2011). Neurons are vulnerable to mitochondrial dysfunction due to their high energy demands and dependence on respiration to generate ATP (Pellerin and Magistretti, 2003). Mitochondrial dysfunction may, therefore, drive or mediate various AD pathologies (Swerdlow et al., 2010).

While AD hippocampal neurons have reduced numbers of morphologically preserved mitochondria (Hirai et al., 2001), other changes in overall neuron mitochondrial mass are less straightforward. Dystrophic neurites concentrate mitochondria within autophagic vesicles, a phenomenon that could reflect defective retrograde transport (Henriques et al., 2010; Nixon, 2007; Silva et al., 2011a). While PCR-amplifiable mitochondrial DNA (mtDNA) levels are reduced (de la Monte et al., 2000), approaches that detect mtDNA within autophagosomes in addition to mtDNA within intact mitochondria suggest hippocampal neuron mtDNA levels may actually increase (Hirai et al., 2001). Other studies report mitochondrial mass increases in healthy-appearing neurons while markedly declining in tangle-bearing neurons from AD subject hippocampi (Nagy et al., 1999).

Mitochondrial fission-fusion dynamics are also altered in AD and could impact organelle proliferation, movement, and distribution (Hoppins et al., 2007; Santos et al., 2010; Su et al., 2010). Biopsies from AD patient hippocampi show increased Fis1 as well as reduced Drp1, Opa1, Mfn1, and Mfn2. These proteins further redistribute away

from neuron processes and towards cell bodies (Wang et al., 2009). In AD subject frontal cortex, expression of the pro-fission Drp1 and Fis1 genes increases, while Mfn1, Mnf2, and Opa1 pro-fusion gene expression decreases (Manczak et al., 2011b). In AD fibroblasts, H_2O_2 and Aβ (amyloid beta) treatment reduces Drp1 and disrupts mitochondrial networks (Wang et al., 2008b). Perturbed mitochondrial fission-fusion in AD may relate to increased mitochondrial autophagy (mitophagy), since altering fusion and fission protein levels induces mitophagy (Twig and Shirihai, 2011).

In order to study AD and MCI bioenergetic fluxes, intermediates and proteins that relate to those fluxes, and mitochondrial mass/morphology-related phenomena, we generated cytoplasmic hybrid (cybrid) cell lines using platelet mitochondria from AD, MCI, and age-matched control subjects. We found that bioenergetic flux and flux-associated parameters were altered in MCI and AD cybrid lines. Many of the changes we observed either mediate or represent retrograde responses that are probably compensatory in nature. These compensatory changes, though, may have mal-adaptive as well as adaptive consequences.

4.2 RESULTS

4.2.1 COX Vmax activities

Numerous studies have found that following a 6 week selection process, relative to control cybrid cell lines AD cybrid cell lines have reduced COX Vmax activities (Swerdlow, 2012b). One previous study reported MCI cybrid COX Vmax activities are also reduced relative to that of control cybrids (Silva et al., 2012a), and another study found that after correcting for mtDNA synthesis rates AD cybrid COX Vmax activity reductions persist for at least 1-2 months after the 6-week cybrid selection process is complete (Trimmer et al., 2004). Our COX Vmax data, which come from cybrid cell

lines maintained in continuous culture for 2 additional months after the 6 week selection process was completed, are for the most part consistent with the existing literature. Although reporting whole cell COX Vmax activities only as pseudo-first order rate constants normalized to mg protein (sec^{-1}/mg protein) did not reveal differences (Figure 1A), further normalizing to a marker of COX quantity, in this case COX4I1 protein, found that the COX activity mean per COX subunit protein was lower in the AD cybrid lines than it was in the control cybrid lines (Figure 1B). The MCI cybrid COX Vmax activity mean was intermediate, as it was not statistically different from either the control or AD group means (Figure 1B). The possibility that COX function is perturbed in MCI cybrids is further supported by an analysis in which the MCI and AD cybrids were combined to create a single group. In this case, the AD+MCI cybrid COX Vmax mean, when normalized to COX4I1 protein levels, was lower than that of the control cybrids (Figure 1C). Conversely, adding the MCI and control cybrids together created a group whose COX Vmax mean was statistically comparable to that of the AD cybrids (data not shown).

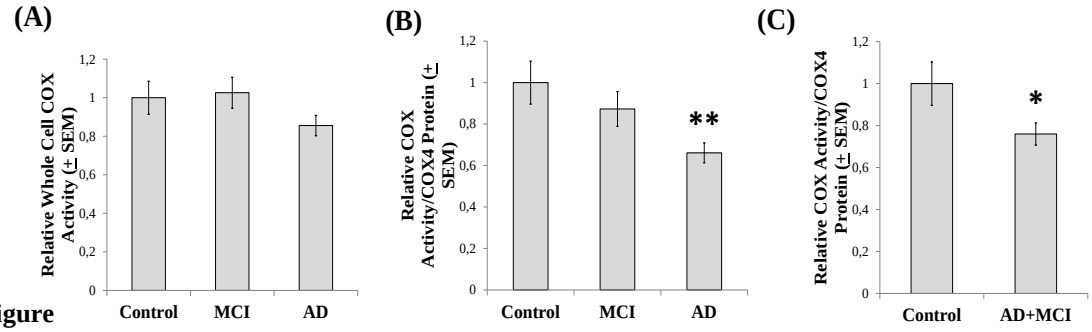

Figure 1. COX Vmax activities. The pseudo-first order rate constant in sec^{-1} was spectrophotometrically determined by following the conversion of reduced cytochrome c to oxidized cytochrome c. In (A), each cybrid line's rate constant was normalized to the amount of whole cell protein in its assay cuvette to provide a rate in sec^{-1}/mg protein (A). As immunochemical measurements of COX4I1 protein revealed the amount of COX4I1 protein differed between the groups (see Figure 8), we also normalized the sec-

^{1}/mg protein rate for each line to its relative amount of COX4I1 protein (B and C). * indicates a $p<0.05$ difference from the control group; ** indicates a $p<0.01$ difference from the control group.

4.2.2 Oxygen and glucose fluxes

We used a Seahorse XF24 Analyzer to assess cybrid line respiration-related fluxes. To quantify mitochondrial OCRs under unstressed conditions, the total OCR for each cell line was determined in the presence of 25 mM glucose before and after the addition of rotenone and antimycin A to the cells. Rotenone (a complex I inhibitor) and antimycin A (a complex III inhibitor) blocks mitochondrial respiration, and reveals the cell non-mitochondrial OCR contribution. Subtracting the non-mitochondrial OCR from the total OCR yields the mitochondrial OCR. The mitochondrial OCRs were then normalized to the amount of total protein that was present in the well that was being read. In the presence of 25 mM glucose, the MCI group OCR mean was lower than the control group OCR mean (Figure 2A). On post-hoc testing the AD group was statistically comparable to both groups ($p=0.07$ compared to the control group, and $p=0.42$ compared to the MCI group). Combining the MCI and AD cybrids generated a single group whose OCR was lower than that of the controls (Figure 2B), while a group formed by combining the MCI with the control group was not statistically different from the AD group (data not shown). Glucose deprivation prevents glycolysis, which renders cells increasingly dependent on oxidative phosphorylation to make energy. This manifests as an increased OCR. Relative to total cell OCR measurements taken under 25 mM glucose conditions, under glucose deprivation conditions the control group OCR increased by 67%, the MCI group OCR increased by 74%, and the AD group OCR increased by 61%. When no glucose was present in the assay medium the mitochondrial OCR rate was lower in the MCI and AD groups than it was in the control group (Figure

2C). Combining the MCI and AD cybrids generated a single group whose glucose-deprived OCR was lower than that of the controls (Figure 2D), while a group formed by combining the MCI with the control group was not statistically different from the AD group (data not shown).

To evaluate the mitochondrial proton leak rate, we determined each cell line's OCR following oligomycin treatment. Oligomycin inhibits the mitochondrial ATP synthase, at which point all mitochondrial oxygen consumption is due to the ATP synthase-independent leakage of protons from the intermembrane space to the mitochondrial matrix. The respiratory leak rate was higher in the AD cybrids than it was in the control cybrids. The MCI leak rate was intermediate, as its value was not significantly different from the other two groups (Figure 2E). Combining the MCI and AD groups in order to increase statistical power yielded a group whose leak rate exceeded that of the control group (Figure 2F). Combining the control and MCI groups yielded a group whose leak rate did not differ from the AD group (data not shown). In addition to measuring medium oxygen levels and calculating the rate at which oxygen is consumed by cultured cells, Seahorse Analyzers also measure medium pH and calculate the rate at which cells acidify their surrounding medium. Since cell lactic acid excretion is primarily responsible for medium acidification, and lactic acid is produced by anaerobic glycolysis, ECARs can be used to estimate glycolysis fluxes. We initially placed cells from each of our cybrid lines in a glucose-free medium, at which point ECARs were quite low and equivalent between the groups; at the conclusion of each experiment 2-deoxyglucose was added to each well, and revealed baseline ECAR measurements were stable throughout. The post-2-deoxyglucose ECARs were used to provide non-glycolysis acidification rates. An initial injection introduced 10 mM glucose to the cells. The non-glycolysis, baseline ECAR for each line was subtracted from the rate in 10 mM

glucose to yield a true glycolysis-dependent ECAR. The glucose injection was followed by an injection of oligomycin, which eliminates mitochondrial ATP production by inhibiting the mitochondrial ATP synthase and forces a compensatory increase in glycolysis-related ATP production. The difference between the post-oligomycin ECAR and the post-2-deoxyglucose baseline ECAR indicates the glycolysis capacity. The difference between the post-glucose, pre-oligomycin ECAR and the post-glucose, post-oligomycin ECAR indicates the glycolysis spare reserve capacity. The ECARs from each line were normalized to cell protein, organized by groups, and further normalized to the control group mean.

The post-glucose, pre-oligomycin ECARs in the MCI and AD cybrids, as a group, were lower than the control cybrid ECARs (Figure 2G). This suggests that glycolysis rates were lower in the MCI and AD cybrids. The post-glucose, post-oligomycin ECARs were also lower in the MCI and AD cybrids, suggesting their glycolysis capacity was also lower than that of the control cybrid lines (Figure 2H). The calculated glycolysis spare capacities were lower in the MCI and AD cybrid groups (data not shown).

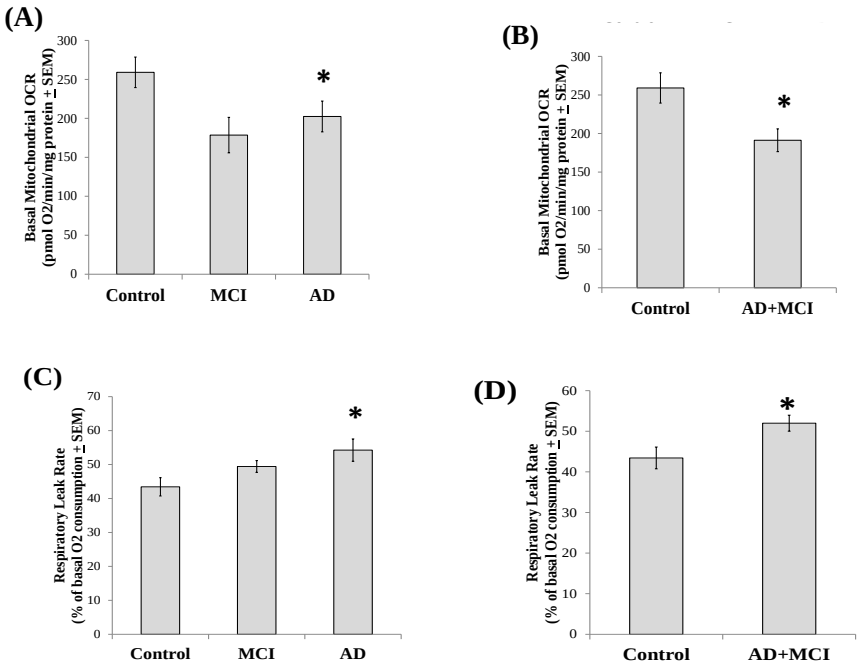

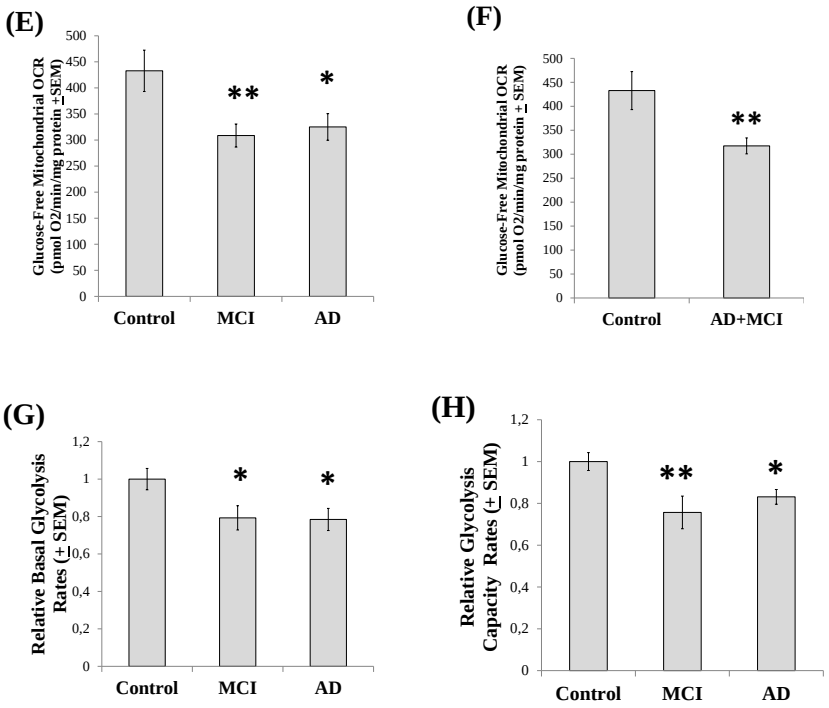

Figure 2. Mitochondrial respiration and ECAR values. Mitochondrial OCR values in the presence of non-limiting amounts of glucose (A and B) and in the absence of glucose (C and D) were determined for each separate cybrid group and for the combined AD+MCI group. Mitochondrial OCR values for each cybrid group (E) and for the AD+MCI group (F) were determined following exposure to oligomycin. The basal glycolysis rate for each cybrid line was estimated by determining its ECAR in the presence of non-limiting amounts of glucose (G). The maximal glycolysis rate (the glycolysis capacity) for each cybrid line was estimated by determining the ECAR in the presence of glucose and oligomycin (H). * indicates a $p<0.05$ difference from the control group; ** indicates a $p<0.01$ difference from the control group.

4.2.3 Energy and redox intermediates

Similar to what was found in a prior study of AD and control cybrid cell lines prepared on an NT2 cell nuclear background (Cardoso et al., 2004b), inter-group differences in energy substrate levels were observed. These differences were subtle but distinct. Mean ADP levels between AD, MCI, and control cybrid lines were comparable on ANOVA,

although a post-hoc test suggested a potential increase in the AD cybrid ADP mean as compared to the control cybrid ADP mean ($p<0.05$ on LSD test) (Figure 3A). ATP levels were comparable between the three groups (Figure 3B). The ADP/ATP ratio, though, was elevated in the AD group as compared to the control group, while the MCI group ADP/ATP ratio was intermediate between the AD and control groups as it did not differ from either of those groups (Figure 3C). Since MCI is often an AD precursor state, we attempted to increase power by generating a combined AD+MCI group. In this analysis, the AD+MCI group ADP concentration and ADP/ATP ratio exceeded the control ADP concentration and ADP/ATP ratio (Figure 3D, E). No differences were seen when the MCI and control cybrid values were combined and compared to the AD cybrid values (data not shown).MCI and AD cybrid whole cell NAD^+/NADH ratios were lower than the control cybrid NAD^+/NADH ratio (Figure 3F). This difference was driven by statistically significant reductions in MCI and AD cybrid NAD^+ concentrations (Figure 3G). Increases in MCI and AD cybrid NADH concentrations may also have accentuated the inter-group ratio differences (see Figure 3H), although NADH levels were statistically equivalent between the groups. Combining the MCI and AD cell lines into a single group did not alter this analysis; the combined group showed decreased NAD^+, statistically unchanged NADH, and a decreased NAD^+/NADH ratio (Figure 3 I-K). Combining the MCI and control groups to form a single group, which was then compared to the AD group, also revealed no quantitative differences in NAD^+ concentration (data not shown).

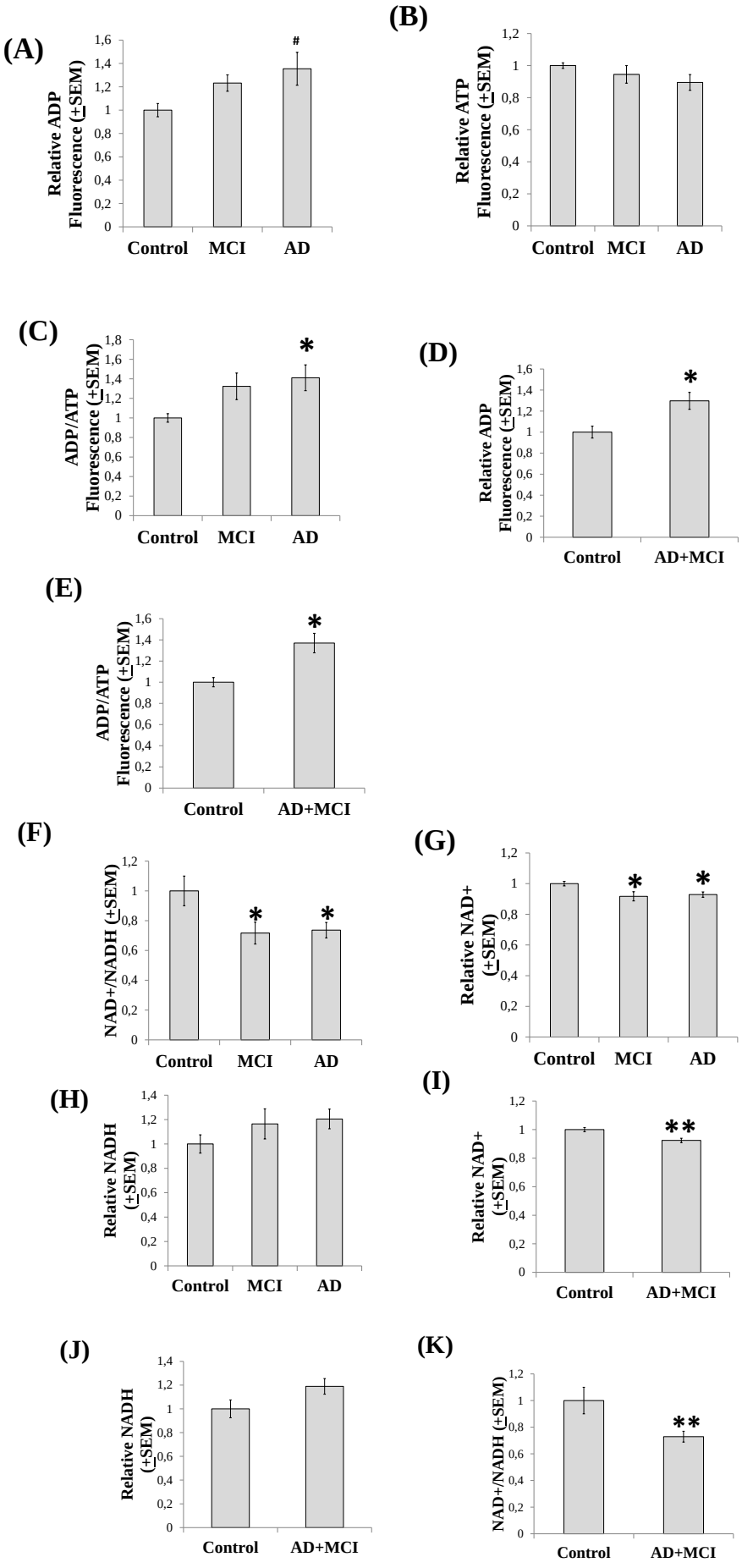
(A)
Relative ADP Fluorescence (±SEM)
#
Control
MCI
AD
(B)
Relative ATP Fluorescence (±SEM)
Control
MCI
AD
(C)
ADP/ATP Fluorescence (±SEM)
*
Control
MCI
AD
(D)
Relative ADP Fluorescence (±SEM)
*
Control
AD+MCI
(E)
ADP/ATP Fluorescence (±SEM)
*
Control
AD+MCI
(F)
NAD+/NADH (±SEM)
*
*
Control
MCI
AD
(G)
Relative NAD+ (±SEM)
*
*
Control
MCI
AD
(H)
Relative NADH (±SEM)
Control
MCI
AD
(I)
Relative NAD+ (±SEM)
**
Control
AD+MCI
(J)
Relative NADH (±SEM)
Control
AD+MCI
(K)
NAD+/NADH (±SEM)
**
Control
AD+MCI

Figure 3. Energy and redox intermediates. Relative ADP levels, ATP levels, and ADP/ATP ratios for each separate group are shown in (A), (B), and (C). Relative ADP levels and ADP/ATP ratios are shown for the combined AD+MCI group in (D), (E). Relative NAD^+ levels, NADH levels, and NAD^+/NADH ratios for each separate group are shown in (F), (G), and (H). Relative NAD^+ levels, NADH levels, and NAD^+/NADH ratios are shown for the combined AD+MCI group in (I), (J), and (K). * indicates a $p<0.05$ difference from the control group; ** indicates a $p<0.01$ difference from the control group; # indicates the ANOVA calculation itself was not statistically significant, but the LSD post-hoc comparison with the control group showed a p value of <0.05.

4.2.4 Flux modifying genes and proteins

We assessed the status of genes and proteins that regulate or are regulated by bioenergetic fluxes. HIF1α, a protein that senses and responds to cell oxygenation status (Semenza, 2012), was lower in MCI and AD cybrids than it was in control cybrids (Figure 4A). HIF1α mRNA expression levels were comparable between the groups ($p=0.054$ on ANOVA), although a post-hoc analysis suggested HIF1α mRNA levels in the AD cybrid group could have exceeded that of the MCI and control cybrid groups ($p<0.05$ on LSD) (Figure 4B). Peroxisome proliferator-activated receptor γ coactivator α (PGC1α) mediates changes in mitochondrial mass and coupling efficiency (Handschin and Spiegelman, 2006). Total cell PGC1α protein levels were lower in MCI and AD cybrids than they were in control cybrids (Figure 4C). No differences in PGC1α mRNA expression were observed, perhaps because of an unexpectedly large variation in individual cell line values (Figure 4D). We also assessed the mRNA levels of two other PGC family members, peroxisome proliferator-activated receptor γ coactivator β (PGC1β) and PGC1α-related coactivator (PRC). PGC1β expression was comparable between the groups, while PRC expression was higher in the AD cybrid group than it was in the control and MCI groups (Figure 4E, F). It was recently shown that PGC1α

expression is also regulated by PARIS, a protein that binds the PGC1α promoter and blocks PGC1α gene transcription (Shin et al., 2011). While ANOVA between the control, MCI, and AD cybrids showed no intergroup differences in whole cell PARIS, whole cell PARIS levels in the combined AD+MCI group were reduced relative to the control group level (Figure 4G). When just nuclear PARIS was considered, protein levels were lower in the AD group than they were in the control group and also in the combined AD+MCI group (Figure 4H).

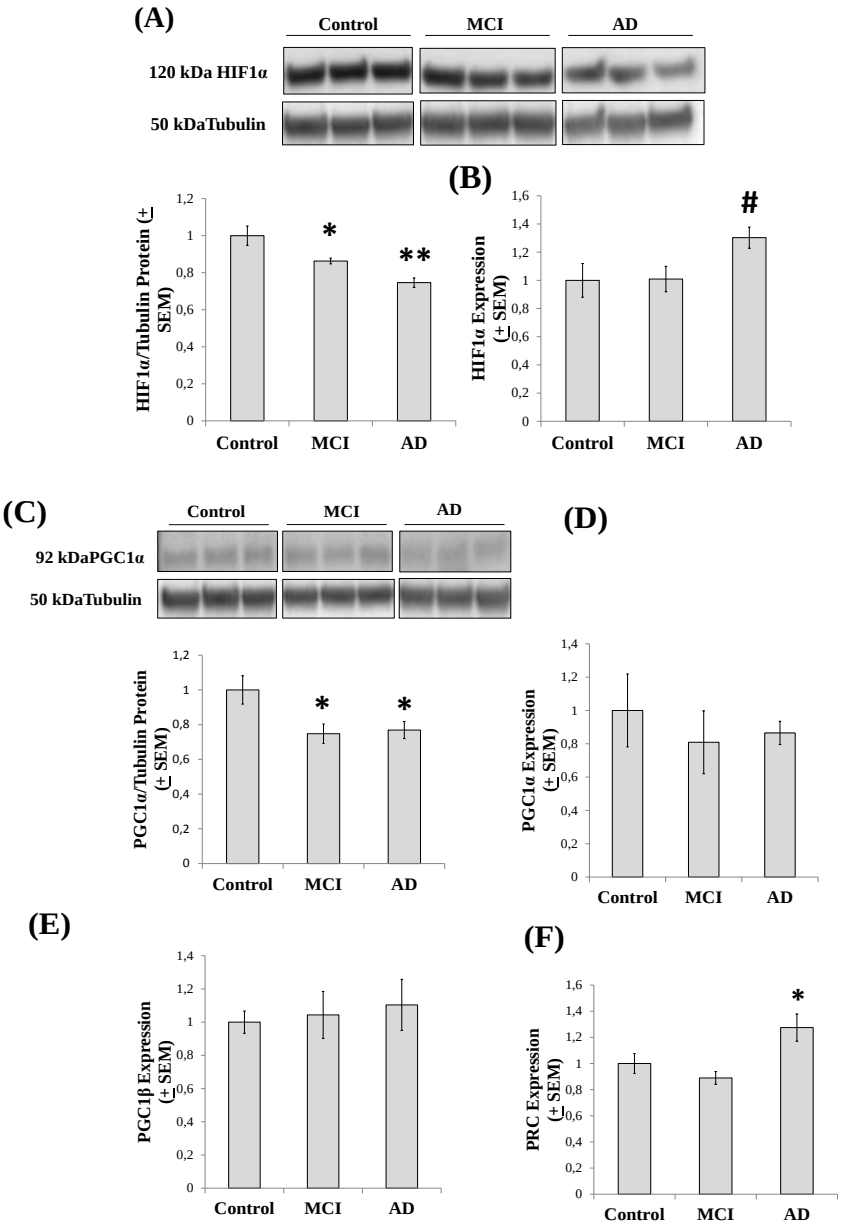

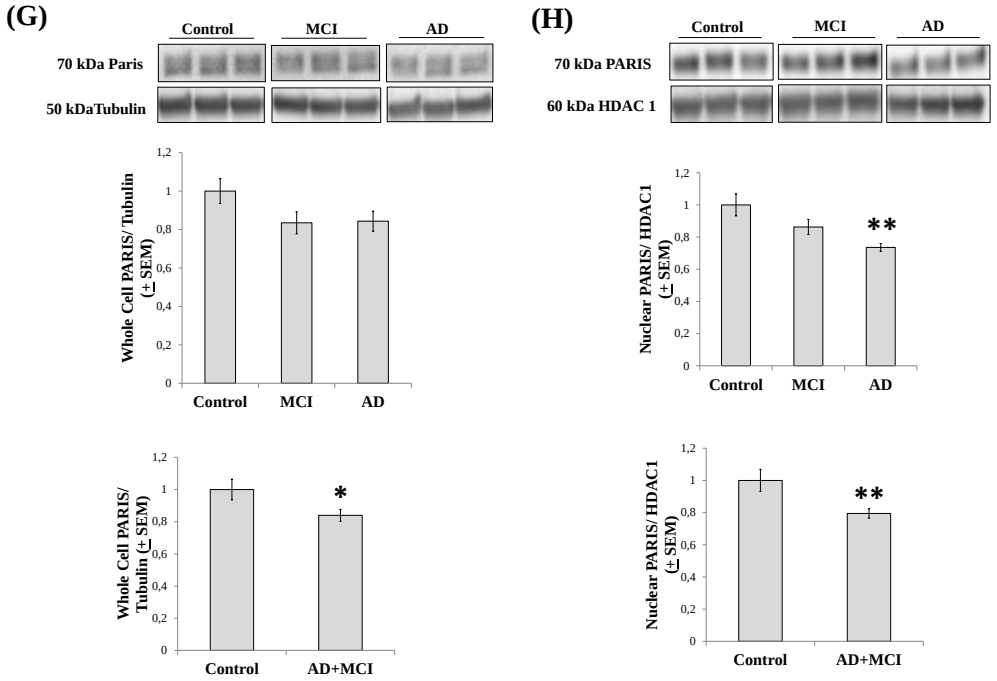

Figure 4. Flux regulatory pathways. Relative HIF1α protein levels are shown in (A). Relative HIF1α mRNA levels are shown in (B). Relative PGC1α protein levels are shown in (C) and relative PGC1α mRNA levels are shown in (D). Relative PGC1β (E) and PRC (F) mRNA levels were also determined. Relative whole cell PARIS protein levels are shown for all three groups and for the combined AD+MCI group (G). Relative nuclear PARIS protein levels are shown for all three groups and for the combined AD+MCI group (H). * indicates a $p<0.05$ difference from the control group; ** indicates a $p<0.01$ difference from the control group; # indicates the ANOVA calculation itself was not statistically significant, but the LSD post-hoc comparison with the control group showed a p value of <0.05.

PGC1α activity is post-translationally regulated. Acetylation reduces its activity while de-acetylation, which is SIRT1-mediated, increases activity (Canto and Auwerx, 2009; Nemoto et al., 2005). Whole-cell SIRT1 protein and expression levels were comparable between the groups (Figure 5A, B). SIRT1 compartmentalization, though, changed and this manifested as a decrease in the protein's nucleus to cytoplasm ratio (Figure 5C). Compared to the control group, on a post-hoc analysis nuclear SIRT1 trended towards a

lower level, and in the combined AD+MCI group nuclear SIRT1 levels were significantly lower (Figure 5D). Cytosolic SIRT1 protein levels were increased in both the MCI and AD groups, as well as in the combined AD+MCI group (Figure 5E). The ratio of phosphorylated to total SIRT1 was also reduced in the AD and AD+MCI groups (Figure 5F).

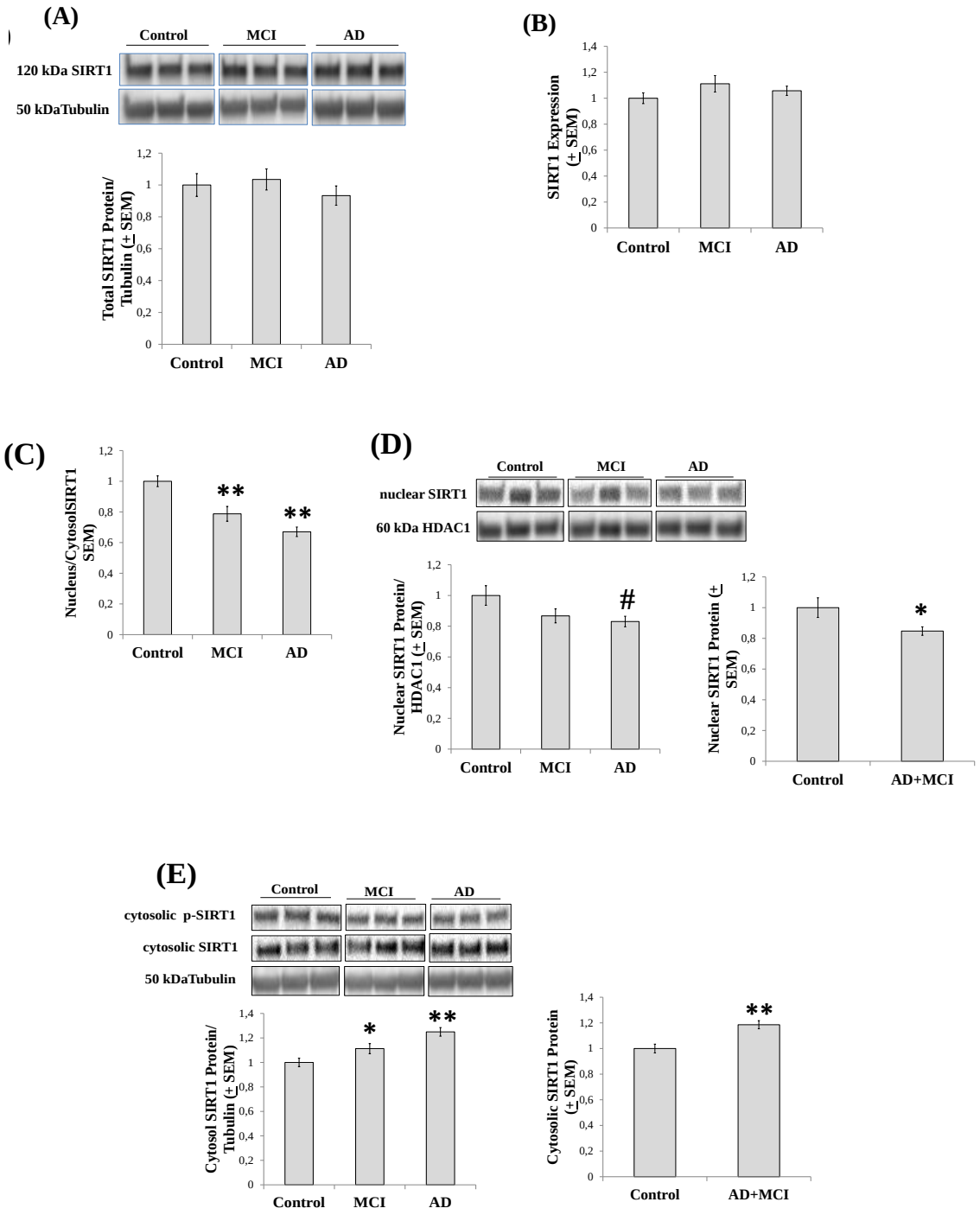

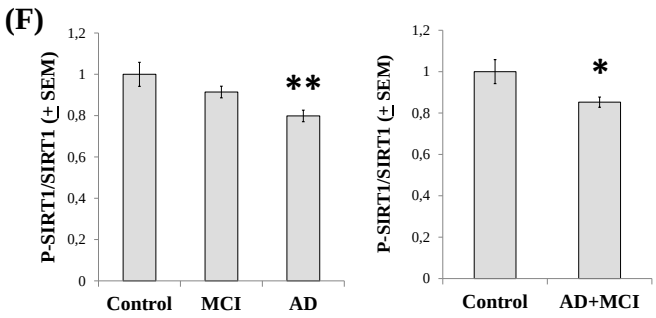

Figure 5. SIRT1 analyses. Relative SIRT1 and whole cell protein levels (A) and mRNA levels (B) were similar between groups. However, the AD and MCI cybrid nucleus/cytosolic SIRT1 protein ratio decreased (C). This was due to a decrease in nuclear SIRT1 protein in the AD+MCI group and perhaps the AD group (D), as well as increased amounts of cytosolic SIRT1 protein in the AD, MCI, and AD+MCI groups (E). SIRT1 phosphorylation was reduced in the AD and AD+MCI groups (F). * indicates a $p<0.05$ difference from the control group; ** indicates a $p<0.01$ difference from the control group; # indicates the ANOVA calculation itself was not statistically significant, but the LSD post-hoc comparison with the control group showed a p value of <0.05.

Phosphorylation provides another layer of PGC1α post-translational modification; increased phosphorylation associates with increased activity (Canto and Auwerx, 2009). AMPK is one enzyme that phosphorylates PGC1α (Jager et al., 2007). While total AMPK protein levels were comparable between groups, relative to the control group AMPK phosphorylation increased in the AD and AD+MCI groups (Figure 6A). We measured levels of a second PGC1α-phosphorylating enzyme, the p38 mitogen associated protein kinase (Feige and Auwerx, 2007), and found that relative to the control group total p38 protein levels were decreased in the AD group. Similar to what was previously found in other studies of AD cybrids (Onyango et al., 2010; Onyango et al., 2005), though, the ratio of phosphorylated to non-phosphorylated p38 was increased in the AD cybrids and this ratio was also increased in the AD+MCI group (Figure 6B).

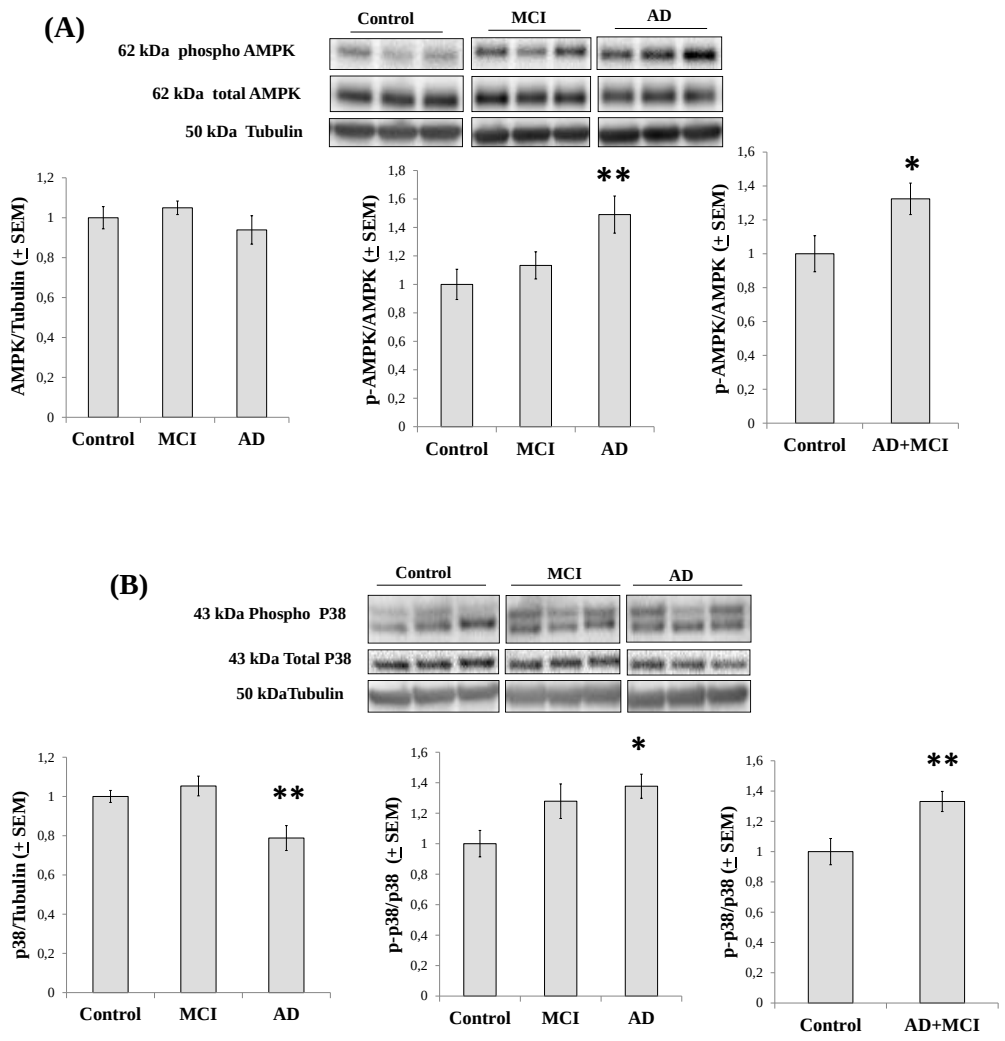

Figure 6. AMPK and p38 analyses. (A) Total cell AMPK protein levels were equivalent between the groups, while AMPK phosphorylation was increased in the AD and AD+MCI groups. (B) Total cell p38 protein levels decreased in the AD group, while p38 phosphorylation increased in the AD and AD+MCI groups. * indicates a $p<0.05$ difference from the control group; ** indicates a $p<0.01$ difference from the control group.

As various results were consistent with either increased or decreased PGC1α activation, we measured COX4I1 mRNA levels since COX4I1 expression is induced by PGC1α-nuclear respiratory factor (NRF) complexes (Scarpulla, 2008). COX4I1 expression was higher in the AD group than it was in the control group, although the control and AD+MCI groups were comparable (Figure 7A). We further assessed mRNA and protein levels of transcription factor A of the mitochondria (TFAM), which is also induced by

PGC1α-NRF complexes (Scarpulla, 2008). Although TFAM mRNA levels were comparable between groups (Figure 7B), relative to the control group TFAM protein was increased in the MCI, AD, and AD+MCI groups (Figure 7C). Cytochrome C is transcribed from a nuclear gene, translated in the cytoplasm, and mostly resides in the mitochondrial intermembrane space. We did not measure cytochrome c protein levels in this study, but relative to the control group cytochrome C expression was increased in the AD and AD+MCI groups (Figure 7D).

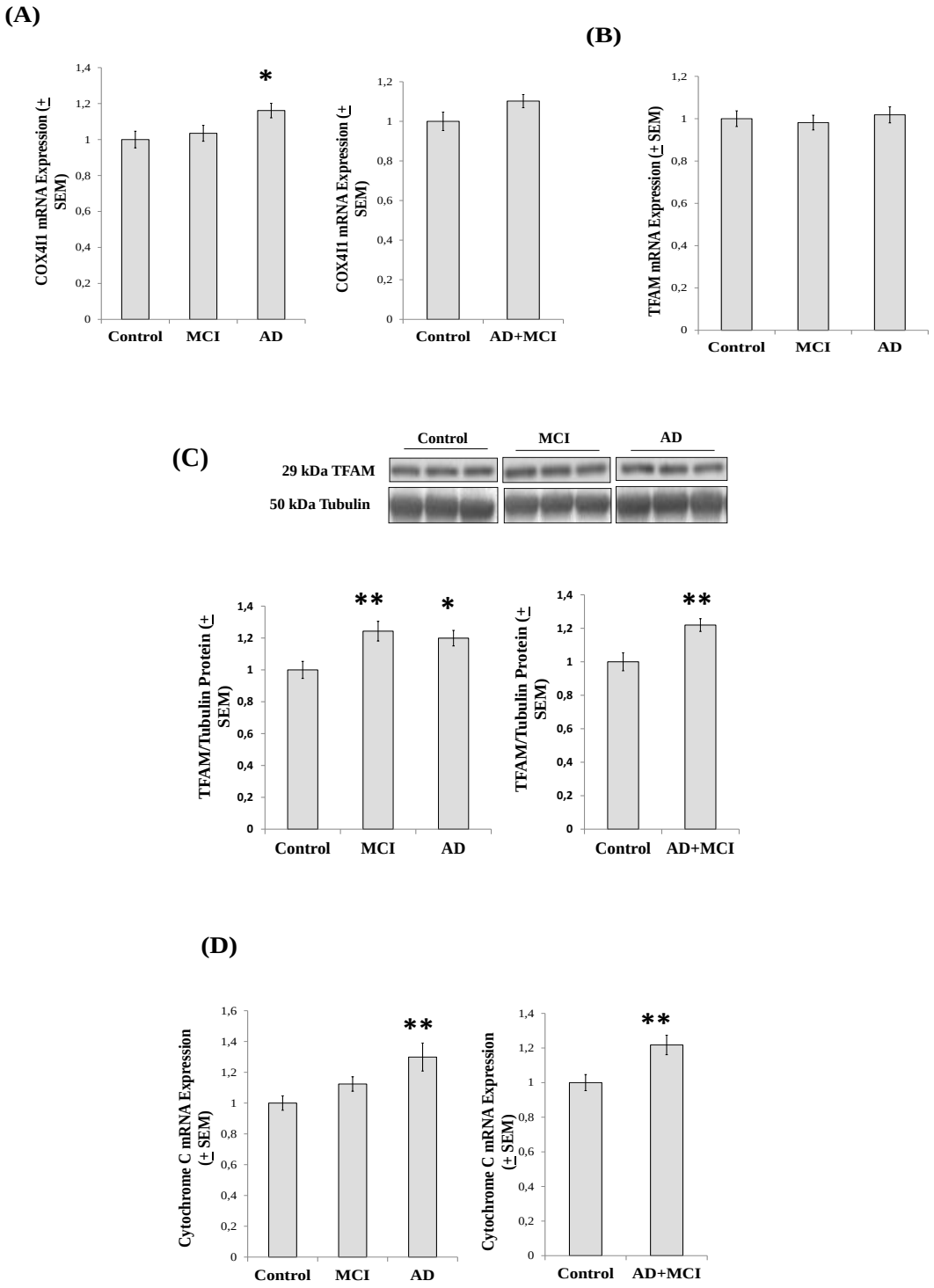

Figure 7. Expression of PGC1α-coactivated genes. COX4I1 mRNA levels were increased in the AD group but not the AD+MCI group (A). TFAM mRNA levels were equivalent between groups (B), while TFAM protein levels were increased in the MCI, AD, and AD+MCI groups (C). Cytochrome C mRNA levels were increased in the AD and AD+MCI groups (D). * indicates a $p<0.05$ difference from the control group; ** indicates a $p<0.01$ difference from the control group.

4.2.5 Mitochondrial mass and morphology

We evaluated several markers of mitochondrial mass. COX4I1, a COX subunit, is encoded by a nuclear gene and translocates to the inner mitochondrial membrane. On the ANOVA comparison, COX4I1 protein was higher in the AD group than it was in the control group. COX4I1 protein levels were not statistically different between the control and MCI groups, with the p value being 0.067 (Figure 8A). COX4I1 protein levels were greater in the AD+MCI group than they were in the control group (Figure 8A). COX2, another COX subunit, is encoded by an mtDNA gene and localizes to the inner mitochondrial membrane. On the ANOVA comparison, COX2 protein was higher in the AD group than it was in either the control or MCI group (Figure 8B); the control and AD+MCI group COX2 protein levels were comparable (data not shown). Lastly, we determined relative mtDNA to nDNA ratios in our cybrid cell lines. When we normalized the copy number of an mtDNA gene, ND1, to the copy number of a nuclear gene, the 18S RNA, the ratio was higher in the AD and AD+MCI groups than it was in the control group (Figure 8C). When the amount of the 16S RNA mtDNA gene was normalized to the amount of the 18S gene no statistically significant quantitative differences were seen between the groups, although qualitatively the 16S:18S data resembled the ND1:18S data (Figure 8D).

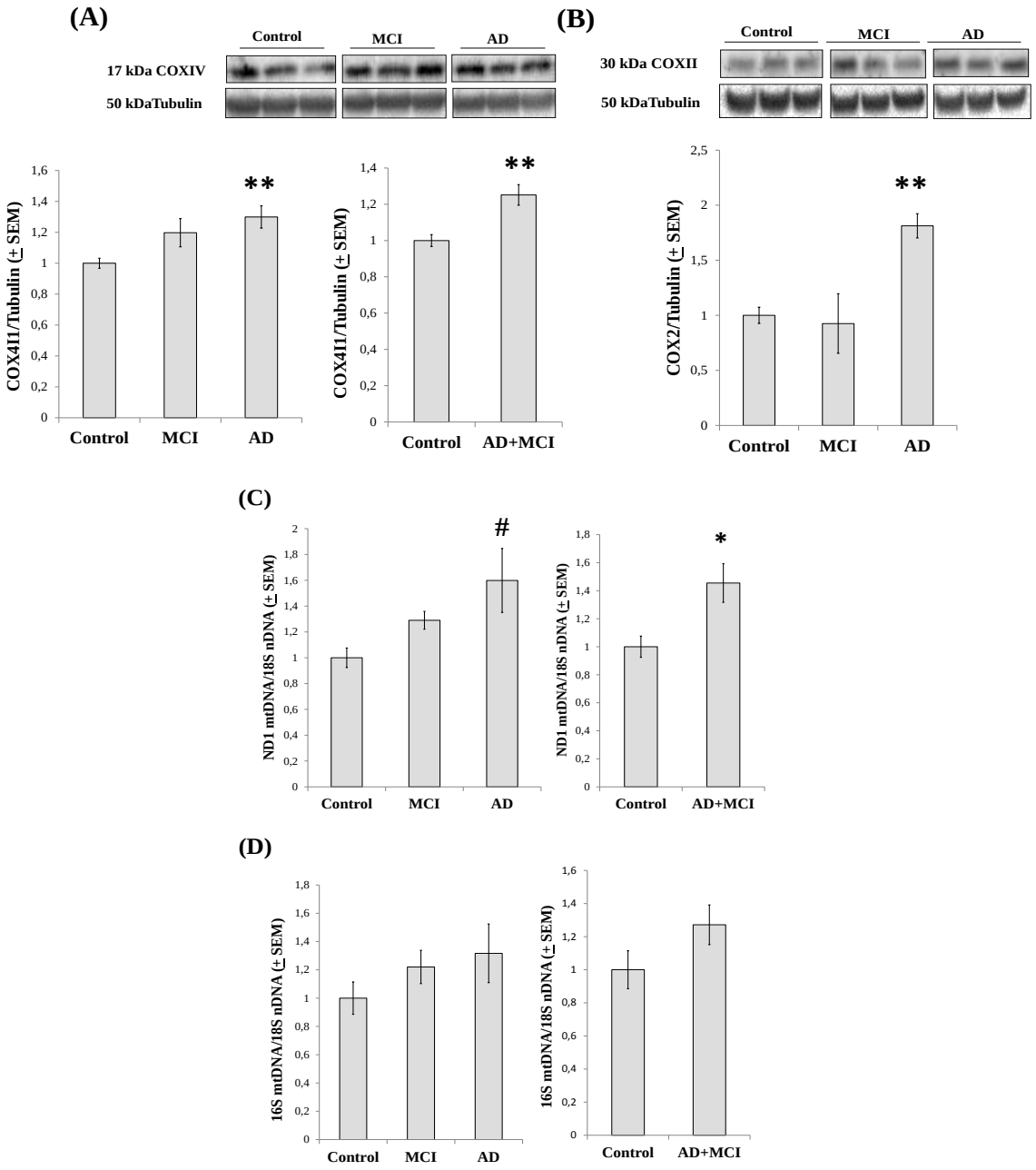

Figure 8. Mitochondrial mass markers. COX4I1 protein levels were increased in the AD and MCI+AD groups (A). COX2 protein was increased in the AD group (B). When relative mtDNA levels were determined using primers to the mtDNA ND1 gene, mtDNA levels trended higher in the AD group and were elevated in the AD+MCI group (C). When relative mtDNA levels were determined using primers to the mtDNA 16S gene, no inter-group differences were seen although qualitatively results obtained with the 16s primers resembled those obtained with the ND1 primers (D). * indicates a $p<0.05$ difference from the control group; ** indicates a $p<0.01$ difference from the control group; # indicates the ANOVA

calculation itself was not statistically significant, but the LSD post-hoc comparison with the control group showed a p value of <0.05.

Mitochondrial morphology is partly determined by fission-fusion dynamics (Chan, 2006b; Chen and Chan, 2009). Mitochondrial fission and fusion are enzyme-mediated processes that facilitate bioenergetic adaptation. In purified mitochondrial fractions, no differences in Opa1, a protein that drives mitochondrial fusion, were observed between our cybrid groups (Figure 9A). Levels of Drp1 protein, which drives mitochondrial fission, were comparable on ANOVA (p=0.076) but a post-hoc analysis suggested Drp1 trended higher in the MCI and AD groups (both less than p<0.05 on LSD comparison) than it was in the control group (Figure 9B). Drp1 was higher in the combined AD+MCI group than it was in the control group (Figure 9B). Drp1 activity is also controlled through post-translational modification, and Drp1 phosphorylation at serine 637 inversely correlates with Drp1 activity (Cereghetti et al., 2010; Cereghetti et al., 2008; Cho et al., 2010). We found that Drp1 phosphorylation, when normalized to total mitochondrial Drp1 protein, was lower in the MCI and AD groups than it was in the control group (Figure 9C). Since the pro-apoptotic protein Bax reportedly enhances mitochondrial fission and fragmentation we quantified Bax expression (Autret and Martin, 2010; Sheridan et al., 2008). The inter-group ANOVA was negative (p=0.099), although on post-hoc analysis there was a trend for higher expression in the AD group as compared to the control group (p=0.036 on LSD) (Figure 9D). Bax expression was higher in the combined AD+MCI group than it was in the control group (Figure 9D). Finally, we quantified cell mTOR protein levels, as mTOR is sensitive to bioenergetic states and counters autophagy, a process that might predictably increase under conditions that favor increased mitochondrial fission (Cunningham et al., 2007; Schieke

et al., 2006). Relative to the control group, mTOR levels were reduced in the AD group and in the AD+MCI groups (Figure 9E).

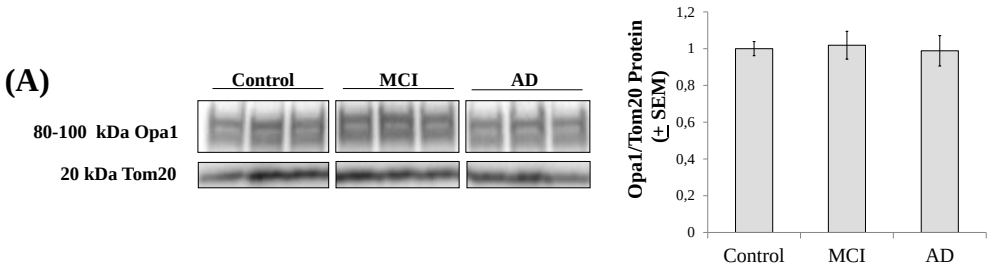
(A)
Control
MCI
AD
80-100 kDa Opa1
20 kDa Tom20
Opa1/Tom20 Protein (± SEM)
1,2
1
0,8
0,6
0,4
0,2
0
Control
MCI
AD

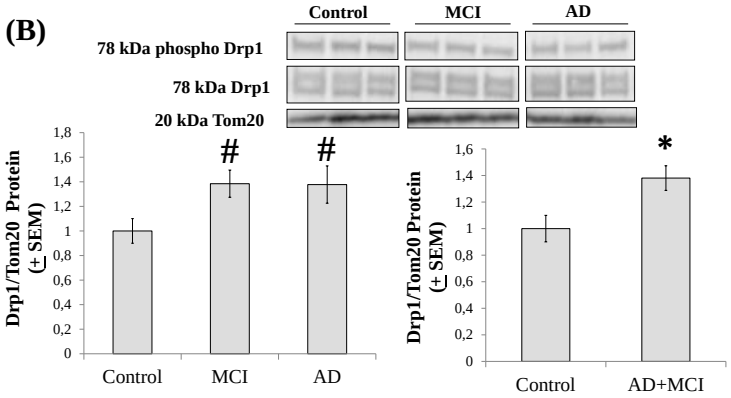
(B)
Control
MCI
AD
78 kDa phospho Drp1
78 kDa Drp1
20 kDa Tom20
Drp1/Tom20 Protein (± SEM)
1,8
1,6
1,4
1,2
1
0,8
0,6
0,4
0,2
0
#
#
Control
MCI
AD
Drp1/Tom20 Protein (± SEM)
1,6
1,4
1,2
1
0,8
0,6
0,4
0,2
0
*
Control
AD+MCI

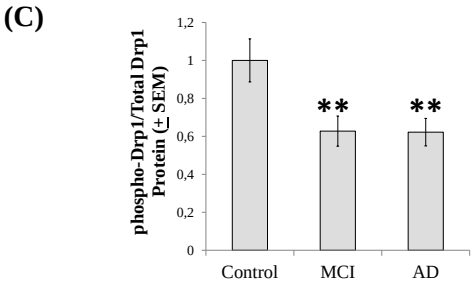
(C)
phospho-Drp1/Total Drp1 Protein (± SEM)
1,2
1
0,8
0,6
0,4
0,2
0
**
**
Control
MCI
AD

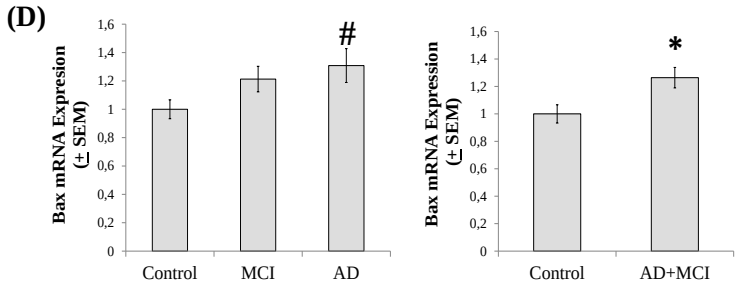
(D)
Bax mRNA Expresion (± SEM)
1,6
1,4
1,2
1
0,8
0,6
0,4
0,2
0
#
Control
MCI
AD
Bax mRNA Expression (± SEM)
1,6
1,4
1,2
1
0,8
0,6
0,4
0,2
0
*
Control
AD+MCI

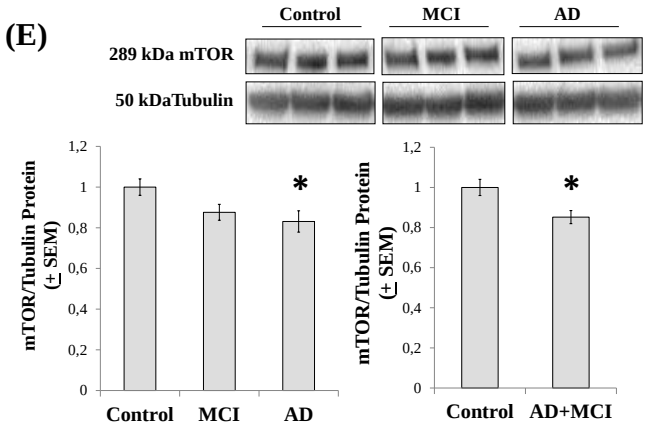
(E)
Control
MCI
AD
289 kDa mTOR
50 kDaTubulin
mTOR/Tubulin Protein (± SEM)
1,2
1
0,8
0,6
0,4
0,2
0
*
Control
MCI
AD
mTOR/Tubulin Protein (± SEM)
1,2
1
0,8
0,6
0,4
0,2
0
*
Control
AD+MCI

Figure 9. Mitochondrial fission, mitochondrial fusion, and mTOR analyses. Opa1 protein levels were equivalent between groups (A), while Drp1 protein levels trended higher in the MCI and AD groups and were higher in the AD+MCI group (B). Drp1 serine 637 phosphorylation was reduced in the MCI and AD groups (C). Bax expression trended higher in the AD group, and was higher in the AD+MCI group (D). mTOR protein levels were reduced in the AD and AD+MCI groups (E). * indicates a $p<0.05$ difference from the control group; ** indicates a $p<0.01$ difference from the control group; # indicates the ANOVA calculation itself was not statistically significant, but the LSD post-hoc comparison with the control group showed a p value of <0.05.

4.3 DISCUSSION

Cybrid cell lines created through transfer of AD and MCI subject mitochondria show altered bioenergetic function and bioenergetics-associated infrastructures. COX holoenzyme function and respiratory fluxes are less efficient, glucose utilization is less robust, and these changes impact cell energy and redox states. Proteins that sense, respond to, and regulate bioenergetic fluxes are altered. While the majority of these retrograde responses are certainly compensatory, they appear to represent a mix of adaptive and mal-adaptive changes.

COX activity in AD or MCI groups is lower than it is in age-matched control groups (Parker et al., 1990; Stephan et al., 2012; Swerdlow, 2012b; Valla et al., 2006). Initial studies reported COX activity is also lower in AD and MCI cybrid cell lines than it is in control cybrid lines (Silva et al., 2012a; Swerdlow, 2012b; Swerdlow et al., 1997), despite apparent attempts by AD cybrids to increase their mitochondrial mass (Trimmer et al., 2004). We again found COX in AD and, to a lesser extent, MCI cybrid cell lines is less efficient than it is in control cybrid lines despite the presence of seemingly adaptive compensations.

In AD and MCI cybrid cell lines mitochondrial oxygen consumption is altered under non-stress conditions. Respiration differences are accentuated when cells are forced to increase their mitochondrial ATP production. Decreased respiratory coupling in AD and, to a lesser extent, MCI cybrids further suggests respiration in AD and MCI cybrids is less efficient than it is in control cybrids.

Despite this, glycolysis fluxes are reduced, rather than enhanced, in AD and MCI cybrids. Glycolysis flux is partly determined by NAD^+/NADH ratios and NAD^+ availability. We found AD and MCI cybrids have less NAD^+ and lower NAD^+/NADH ratios than control cybrids. Such changes would predictably reduce glycolysis flux. While activities of some glycolysis enzymes are increased in AD brain neurons (Soucek et al., 2003), glucose utilization is reduced in brains from AD and MCI subjects (Matsuda, 2007; Silverman et al., 2001). Cybrid modeling recapitulates this well-recognized bioenergetic phenomenon.

Reduced glucose utilization would constitute a mal-adaptive retrograde response because it predictably exacerbates rather than alleviates an energy shortfall. In AD and MCI cybrids this manifests as an elevated ADP/ATP ratio. Addressing respiration-induced glycolysis flux reductions in AD and MCI cybrids and, ideally, subjects might favorably influence cell energy stores.

HIF1α protein was reduced in AD and MCI cybrids. HIF1α enhances glycolysis by promoting glycolysis enzyme gene expression (Semenza, 1999, 2012). Reduced HIF1α levels would seem to represent an ultimately mal-adaptive compensation (Soucek et al., 2003). One study previously reported HIF1α protein levels are reduced in AD brains (Liu et al., 2008). Our cybrid data support the view that increasing HIF1α protein levels is a justifiable AD therapeutic strategy (Soucek et al., 2003).

While HIF1α protein decreases in AD cybrids, HIF1expression increases. HIF1α is regulated more by protein degradation rates than gene expression rates, so dissociations should be possible. Interestingly, one study found HIF1α gene expression was increased in AD subject brain microvessels (Grammas et al., 2006).

PGC1α expression is reduced in AD brains (Qin et al., 2009; Sheng et al., 2012). We did not replicate this finding in our AD and MCI cybrids. Levels of PARIS, a protein that blocks PGC1α expression (Shin et al., 2011), were low in AD and MCI cybrids and this also would tend to favor increased rather than decreased PGC1α expression. Expression of a related gene, PRC (Vercauteren et al., 2006), increased in AD cybrids. The status of PRC in AD brains is unknown.

AD subject brains, AD cybrid cell lines, and MCI cybrid cell lines all show reduced PGC1α protein levels (Sheng et al., 2012; Swerdlow, 2012a). If this exacerbates a respiratory chain defect, then PGC1α protein reduction constitutes a mal-adaptive compensation. Alternatively, reducing PGC1α protein levels could conceivably benefit AD and MCI cybrid cells by limiting exposure to impaired mitochondria.

Reductions in nuclear SIRT1 and SIRT1 phosphorylation, in conjunction with or perhaps due to low NAD^+, would predictably increase PGC1α acetylation and decrease PGC1α activity (Jin et al., 2007; Piantadosi and Suliman, 2012). On the other hand, increased AMPK and p38 phosphorylation, which we presume occurred in response to energy compromise and oxidative stress, should increase PGC1α phosphorylation and increase PGC1α activity (Canto and Auwerx, 2009; Feige and Auwerx, 2007; Jager et al., 2007). These results indicate respiratory chain dysfunction alters cell milieus in ways that permit the coincident presence of contradictory responses. Similar contradictory profiles are also seen in AD brains, where SIRT1 protein is reportedly

reduced while AMPK and p38 are reportedly activated (Hensley et al., 1999; Julien et al., 2009; Salminen et al., 2011; Sun et al., 2003; Vingtdeux et al., 2011).

COX4I1 expression, which is co-activated by PGC1α (Scarpulla, 2008), and COX4I1 protein levels were increased in AD and, to a lesser extent, MCI cybrids. TFAM expression, which is also co-activated by PGC1α (Scarpulla, 2008), was unchanged in AD and MCI cybrids but TFAM protein levels were increased. Cytochrome C, a gene co-activated by both PGC1α and PRC (Scarpulla, 2008), showed increased expression in AD and MCI cybrids. Therefore, despite the fact that PGC1α protein levels are reduced in AD and MCI cybrids, we cannot conclude overall PGC1α activity is reduced. Whether it occurs due to PGC1α activation or despite reduced PGC1a protein, mitochondrial mass markers increase in AD and MCI cybrids. AD cybrids have more COX2 protein, COX4I1 protein, COX4I1 expression, cytochrome c expression, TFAM protein, and mtDNA than control cybrids. If we combine the AD and MCI cybrids to form one group, then the MCI cybrids also showed evidence of increased mitochondrial mass.

Less mTOR protein was present in the AD and AD+MCI groups. Since mTOR counters autophagy (Hands et al., 2009; Ravikumar et al., 2004), decreased mTOR should predict increased autophagy. While total mTOR levels were unchanged in one study of AD brains (Li et al., 2005), autophagy markers do increase in AD (Boland et al., 2008; Mizushima et al., 2008; Nixon, 2007; Nixon et al., 2005). AMPK, which was activated in our AD and MCI cybrids, also inhibits mTOR and through this action promotes autophagy (Salminen et al., 2011).

For our mitochondrial fission-fusion protein analysis, in order to more directly test protein-mitochondria relationships we measured Opa1 and Drp1 in mitochondrial fractions rather than whole cell lysates. Data obtained via this approach are consistent

with our mTOR and AMPK data, in that AD and MCI cybrids show enhanced mitochondrial fission infrastructure. An increase in fission infrastructure, which is seen in AD subject brains (Manczak et al., 2011b; Su et al., 2010; Wang et al., 2009), would predictably facilitate mitochondrial autophagy (Twig et al., 2008; Twig and Shirihai, 2011).

Autophagy differences may complicate mtDNA copy number measurements. While levels of PCR-amplifiable mtDNA are consistently reduced in AD brain (Brown et al., 2001; Coskun et al., 2004; de la Monte et al., 2000; Hirai et al., 2001; Rodriguez-Santiago et al., 2001) one study found, using an immunochemical rather than PCR approach, large amounts of mtDNA within an expanded autophagosome pool (Hirai et al., 2001). Since less mtDNA amplification was seen in AD brains in that study, this autophagosome-localized mtDNA may have eluded amplification (Hirai et al., 2001).

While overall numbers of normal-appearing mitochondria are reduced in AD (Baloyannis, 2006, 2011; de la Monte et al., 2000; Hirai et al., 2001), between individual neurons mitochondrial mass estimations range from markedly increased to profoundly decreased (de la Monte et al., 2000; Manczak et al., 2004; Nagy et al., 1999). The balance between mitochondrial biogenesis and mitochondrial autophagy may, therefore, vary between different neurons at any particular time, and vary over time within a single neuron.

Several factors may explain the small magnitude of most inter-group changes observed in this study. Differences could truly be subtle, cybrids may minimize differences, or diagnostic inaccuracy could converge means and inflate variations. Increasing statistical power would address such limitations. We accomplished this by treating the AD and MCI groups as a single group. We believe this was justified because in most cases the

MCI clinical syndrome occurs in association with, or is due to, AD (Morris et al., 2001; Stephan et al., 2012).

Our data suggest AD-specific bioenergetic profiles are present when clinical symptoms manifest and longitudinally evolve. This chronology is consistent with the mitochondrial cascade hypothesis, which postulates AD histopathology in sporadic, late-onset AD is initiated when an individual's mitochondrial function declines below a critical threshold (Swerdlow et al., 2010; Swerdlow and Khan, 2004, 2009). If, as has previously been assumed, mtDNA accounts for differences between cybrid lines created from cytoplasts of different origins (Swerdlow, 2007a), then mtDNA differences are already present in subjects when clinical changes begin (Lu et al., 2010).

In this cybrid study, correlative inference was occasionally used to deduce functional and, in particular cases, causal relationships. Some interpretive points, therefore, should be considered within that context. For example, we assumed changes observed in cytosolic or nuclear compartments arise due to changes in mitochondrial function. While this seems reasonable given our understanding of cybrid cell lines, the degree to which cytosolic or nuclear compartment changes in turn alter mitochondrial function is difficult to quantify. We further assumed bioenergetic flux changes impact cell signaling pathways more than cell signaling pathways impact bioenergetics fluxes. In a study like ours ascertaining the effect, and especially the magnitude of effect, of one parameter on another is certainly challenging since many of the parameters we studied are exceedingly intertwined. Future experiments designed to address this issue are indicated.

In summary (Figure 10), our data suggest respiratory chain changes affect respiratory fluxes and cell redox states. Redox changes, in turn, reduce glycolysis flux and further stress cell energy supplies. Mitochondrial biogenesis and autophagy are up-regulated, at

least initially, but contradictions within pathways that regulate mitochondrial mass occur. The balance between mitochondrial biogenesis and mitochondrial autophagy is lost, and over time the functional mitochondrial pool shrinks. In AD, reversing potentially mal-adaptive compensations, such as a decline in glycolysis flux or the drive to maintain mitochondrial mass (Swerdlow, 2011b), would seem to represent logical therapeutic goals.

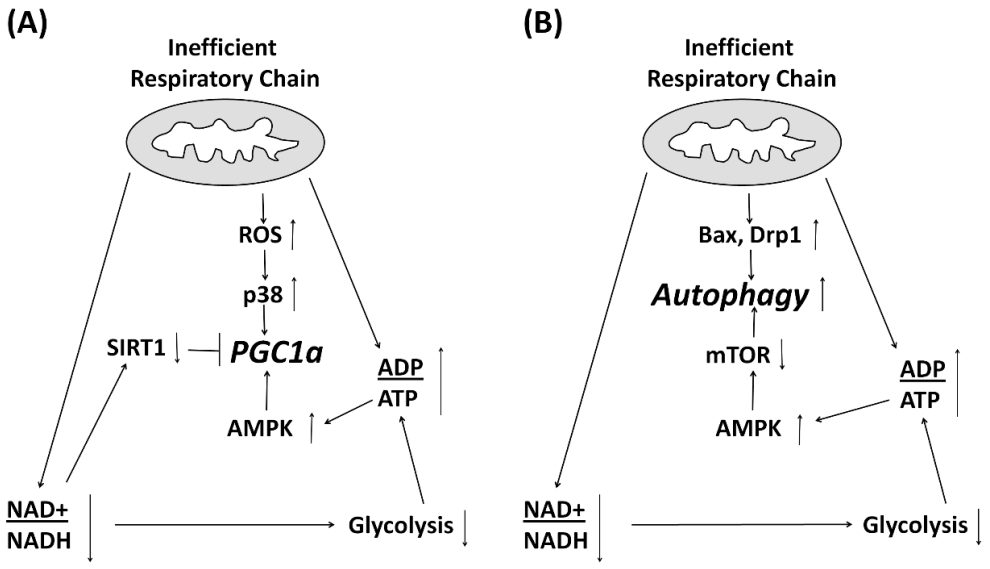

Figure 10. Suggested regulation of mitochondrial biogenesis and autophagy in AD and MCI cybrids. (A) Respiratory chain inefficiency induces oxidative stress, energy stress, and a decreased NAD^+/NADH ratio. The lowered NAD^+/NADH ratio reduces glycolysis, which adds to the energy stress. AMPK and p38 are activated, while SIRT1 input falls. Depending on the balance of these signals, PGC1α activity can increase or decrease. (B) Energy stress activates AMPK, reduces mTOR activity, and initiates autophagy. Enhanced fission of dysfunctional mitochondria also contributes to an increase in autophagy markers. ROS=reactive oxygen species.

Chapter 5

Sirtuin 2-dependent mechanism of microtubule network disruption and autophagic-lysosomal pathway failure in Alzheimer´s disease

5.1 INTRODUCTION

Sirtuins, an evolutionary conserved family of proteins deacetylases, which activity is dependent on NAD^+ availability, have been related with important biological functions such as aging and longevity control and, as a consequently, age-associated pathologies (Satoh and Imai, 2014), such as Parkinson´s and Alzheimer´s disease (AD). Among the seven mammalian sirtuins (Sirt1-7) Sirt1, 6 and 7 are nuclear, Sirt3-5 are mitochondrial and SIRT2 is mainly cytoplasmic but has been found to associate with nuclear proteins in dividing cells (Sebastian et al., 2012). SIRT2 cellular functions remain the most elusive among all sirtuins. SIRT2 has been reported to regulate several cellular pathways, such as cell cycle progression (Inoue et al., 2007), cell differentiation, oxidative stress (Inoue et al., 2014). Additionally SIRT2 was found to be the most abundant in the brain (Pandithage et al., 2008) and, is uniformly expressed in neurites and growth cones exclusively in the cytoplasm of post-mitotic cells (Harting and Knoll, 2010), which may attribute to SIRT2 a key role in neuronal motility and maintenance of axons and dendrites. Indeed, SIRT2 was shown to deacetylate tubulin (North et al., 2003). Since neurons are polarized cells that strongly rely on cytoskeletal tracks for the movement of cargos along the cell (Stokin and Goldstein, 2006), SIRT2 is a strong candidate for neurodegeneration-induction in AD. Microtubule damage is long recognized to occur in AD brains (Cash et al., 2003; Nathan et al., 1995), either by reduction of total content and length of microtubules (Cash et al., 2003) or by reduction of tubulin acetylation, a marker for microtubule stability (Hempen and Brion, 1996). One possible mechanism for the contribution of SIRT2 to the neurodegenerative process is that its activation will impair microtubule network and, due to transport impairment, autophagosomes will accumulate within dystrophic neurites which culminates in cell

death (Silva et al., 2011b). Herein, we sought to demonstrate that inherent mitochondrial dysfunction, present in AD cybrids (Cardoso et al., 2004b; Silva et al., 2013a; Silva et al., 2013b; Trimmer et al., 2000), is the unifying event that sets off a number of metabolic changes that activates SIRT2, driving microtubule network breakdown and, consequently, autophagic-lysosomal pathway impairment. Dysfunctional mitochondria and protein aggregates, such as Abeta oligomers, will not be eliminated, exerting further toxicity. We describe that mitochondrial dysfunction is present in AD and Mild Cognitive Impairment (MCI) cybrids, an intermediate state between normal aging and AD. Then we investigated the causal effect of mitochondrial dysfunction on SIRT2 activation, microtubule network disruption and accumulation of autophagosomes and the relation of these events with the appearance of the hallmarks of AD, the phosphorylation of Tau and Abeta oligomers accumulation. Further, we used a specific inhibitor of SIRT2, AK1, and showed that the inhibition of SIRT2 increases microtubule acetylation and rescues autophagosome clearance in AD cells harboring mtDNA from patients. Overall we demonstrate that microtubule disruption, through the activation of SIRT2, is responsible for the accumulation of autophagosomes in AD, rather than an increment in autophagy induction, which will result in the well documented neuritic dystrophy in AD brains (Nixon et al., 2005).

5.2 RESULTS

5.2.1 Loss of mitochondral potential correlates with mitochondria network alterations in MCI and sAD cybrids.

Mitochondrial dysfunction is a striking feature of AD. Firstly described in AD brains (Gibson et al., 1988; Saraiva et al., 1985; Sorbi et al., 1983), early in the 90s

mitochondrial dysfunction was also described in platelets from AD patients (Parker et al., 1990), allowing the emergence of new viewpoints for AD etiology and the creation of AD cybrids, that results from the fusion of mtDNA depleted cells (ρ0 cells) with platelets isolated from AD and control subjects (Swerdlow et al., 1997). The cybrid technique presupposes that all cell lines have the same nuclear backgroud and differ only on the mtDNA. Mitochondrial cascade hypothesis was then proposed (Swerdlow and Khan, 2004) asserting that for sporadic AD the decline in mitochondrial function increases with age, reaching a threshold where the pathological hallmarks of AD - hyperphosphorylation of Tau and Abeta oligomers enriched senil plaques appear. Also, in MCI subjects mitochondrial dysfunction has been widely characterized (Silva et al., 2013a; Silva et al., 2013b; Valla et al., 2006). Mitochondrial dysfunction in AD models is detected in a number of different parameters. We found decreased mitochondrial membrane potential in sAD cybrids, and the usual patern of MCI group, that normally have intermediate values between Controls and AD, is maintained (Figure 1A). Also, we observed fragmented mitochondrial networks in both sAD and MCI groups, where mitochondria are less elongated and lost their interconectivity (Figure 1B).

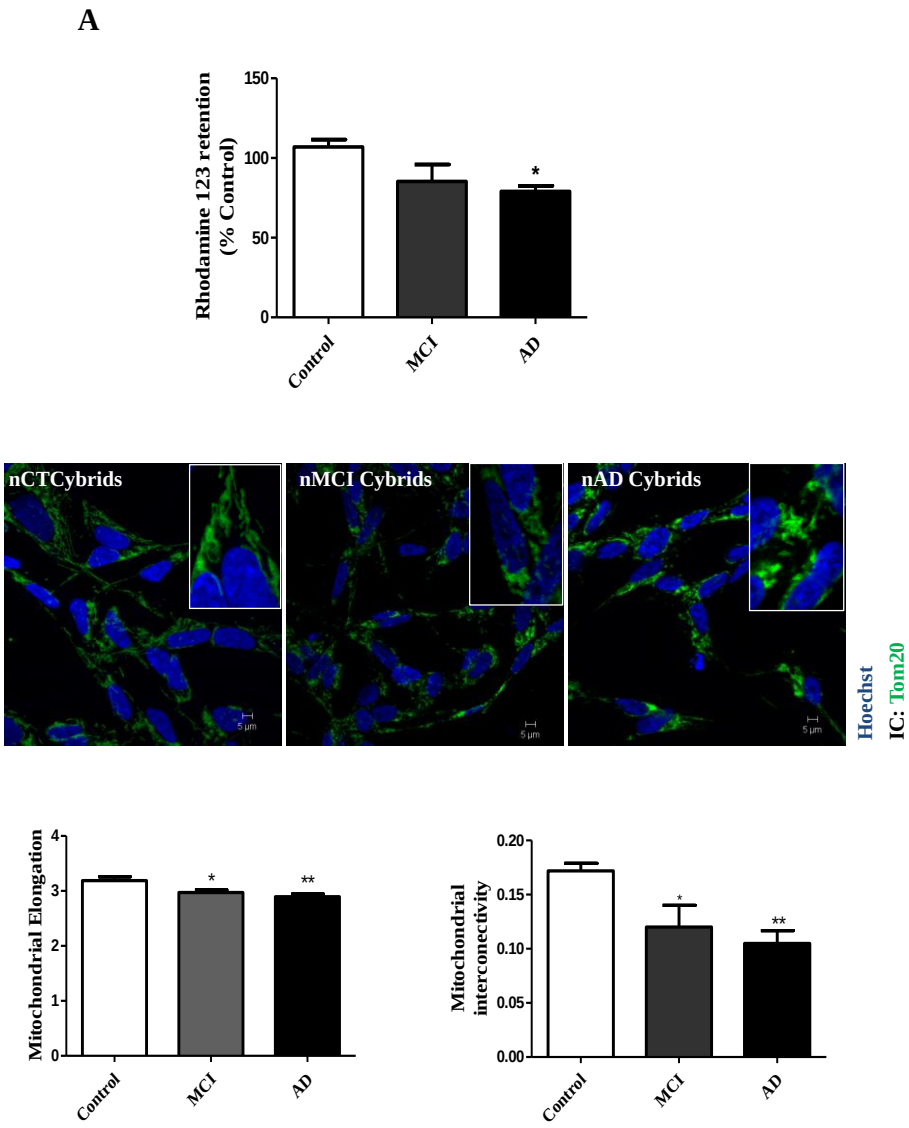

Figure 1. Depolarization of mitochondria results in reduced mitochondrial interconnectivity, elongation and induces a perinuclear localization. (A) Mitochondrial membrane potential (ΔΨmit). Data represent the mean ± SEM derived from four independent experiments and are expressed as percentage relatively to control cybrids (*p<0.05, versus nCT cybrids). (B) Tom20 immunostaining (green) of nCT, nMCI and nAD cybrids showing alterations in mitochondria distribution, elongation and interconnectivity. Both nAD and nMCI cybrids show increased mitochondrial perinuclear distribution (n= 3, *p<0.05, ** p<0.01 versus nCT cybrids). Cell nuclei were labeled with Hoechst 33342. Scale bars: 5 µm.

While the origin for mitochondrial dysfunction in AD remains elusive, it is now recognized that mtDNA have a determinant role in AD pathogenesis. From AD models to patients, the early alterations on mitochondrial metabolism either due to DNA damage, disturbed energy metabolism or synaptic dysfunction, makes of mitochondria a interesting starting point to study AD (Wirz et al., 2014).

5.2.2 Mitochondrial dynamics is altered in sAD cells harboting patient mitochondria.

Compeling evidence have shown that the normally strict regulation of mitochondria morphology, by fusion and fission processes, is impaired in AD, either in cellular models and AD brains. Mitochondrial dynamics are critical for mitochondrial integrity in eukaryotic cells (Zhu et al., 2013). For once, mitochondrial fusion permits the exchanges of critical mitochondrial components within mitochondrial network such as lipid membranes, oxidative phosphorylation complexes, and mitochondrial DNA (mtDNA) allowing the exclusion of defective mitochondria and maintenance of a healthy mitochondrial pool (Detmer and Chan, 2007). Complementarily, mitochondrial fission enables the sequestration and subsequent elimination through autophagy of irreversibly damaged mitochondria and mitochondrial content (Twig et al., 2008). Despite some contradictory data, it is generally accepted that mitochondrial shape is abnormal in AD, where broken cristae are evident (Zhu et al., 2013). Transcripts and proteins responsible for fusion process are generally decreased in opposition to fission proteins that were reported to be increased. Indeed, in brain tissue from AD subjects mitochondrial fusion proteins are decreased namely OPA1, Mfn1 and Mfn2 whereas the levels of mitochondrial fission protein Fis1 are increased (Manczak et al., 2004; Wang et al., 2009). In peripheral samples, an increase in the levels of DRP1 and alterations in

mitochondrial length were found in AD fibroblasts (Wang et al., 2008a). We have previously demonstrated that in mitochondrial-dysfunction bearing AD and MCI cybrids, mitochondrial DRP1 protein levels are increased and also there is an increase in its phosphorylation at Serine 637 that inversely correlates with its activity, whereas no alteration was found in OPA1 levels (Silva et al., 2013b). Here we show that in differentiated cybrids the tendency is maintained and we observe no alterations in fusion proteins (Figure 2 A-F) and, in opposition, Fis1 and DRP1 are significantly increased in mitochondrial fractions of AD cybrids (Figure 2 G-J). Also increased phosphorylation of DRP1 at serine 616 is observed, which has been correlated with increased translocation of DRP1 to mitochondria and fission stimulation (Zhu et al., 2013)

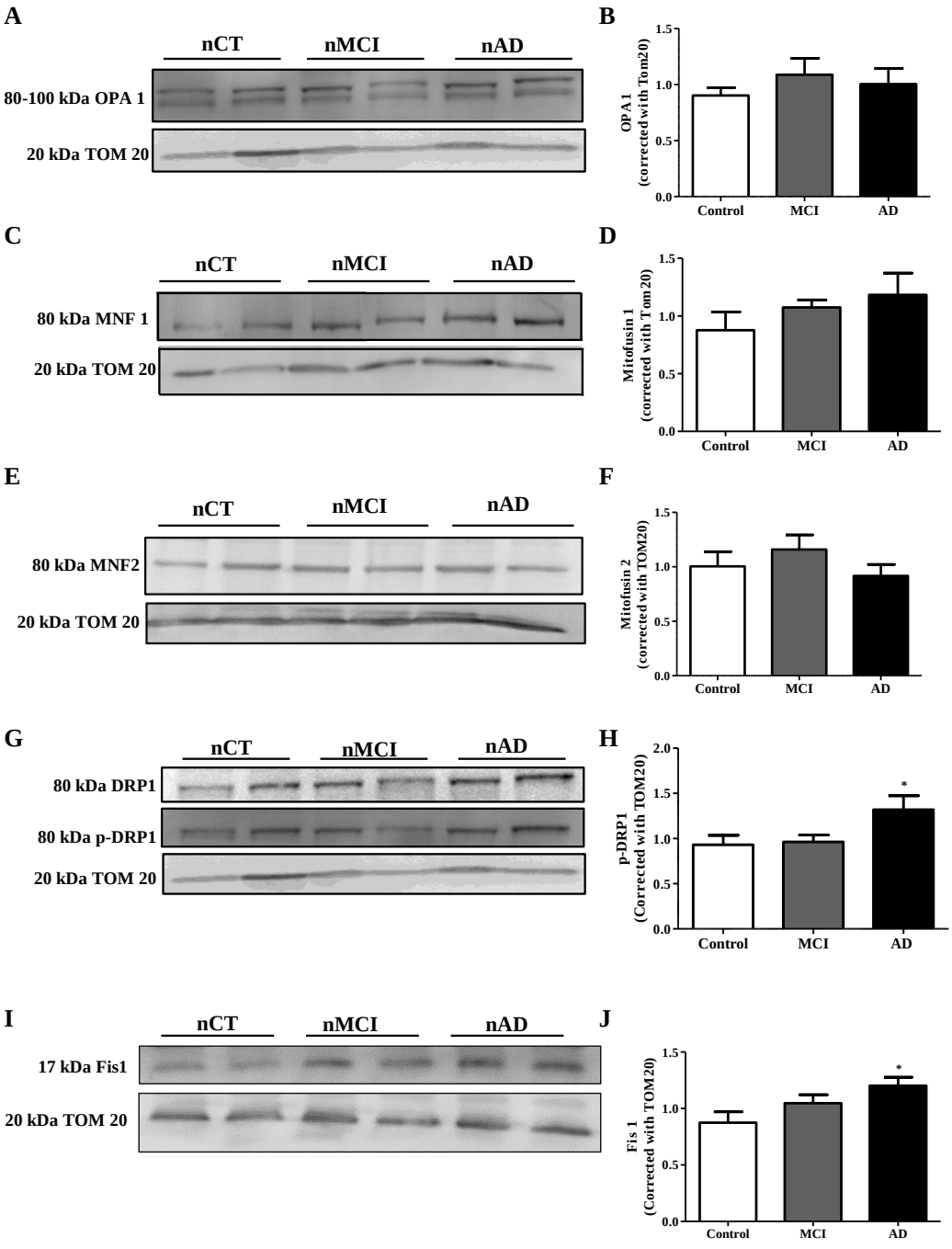

Figure 2. Mitochondrial distribution relates to increased mitochondrial fragmentation. (A) Immunoblot for mitochondrial OPA1. (B) Densitometric analysis of OPA1 (n=3). (C), (E) Immunoblot for mitochondrial MFN1 and 2. (D) (F) Densitometric analysis of MFN1and 2 (n=4). (G) Immunoblot for total and phospho mitochondrial DRP1. (H) Densitometric analysis of total and phospho mitochondrial DRP1 (n=3, *p<0.05 versus nCT cybrids). (I) Immunoblot for mitochondrial Fis1. (J) Densitometric analysis for mitochondrial Fis1 (n=5, *p<0.05 versus nCT cybrids).

5.2.3 SIRT2 activation induce microtubule network deficits.

Although SIRT2 is described to be activated due to an increase in NAD^+ levels, we found no alteration in nicotinamide phosphoribosiyltransferase (NAMPT) (Figure 3 A and B) and decreased levels of total cellular NAD^+ (nuclear plus mitochondrial and cytosolic pools; see Chapter 4). In RA-differentiated cybrids SIRT2 is located only in the cytoplasm (Figure 3 C and D) corroborating previous observations (Li et al., 2007b; Pandithage et al., 2008) and its levels are increased in AD. Indeed, SIRT2 was found to accumulate with age in brain and spinal cord from mouse (Maxwell et al., 2011). We hypothesize that the exclusive cytoplasmic localization and the increase in protein levels of SIRT2 are sufficient to result in increased activation of this protein in AD cells. It is described that SIRT2 primary cellular localization is the cytoplasm, where co-localizes with microtubules and deacetylates α-tubulin at lysine 40 (North et al., 2003). SIRT2 transiently migrates to the nucleus during G_2/M transition and regulates chromatin condensation during metaphase (Vaquero et al., 2006), in mitotic cells (North and Verdin, 2007). During neuronal differentiation, cell migration is crucial for neurons to acquire specific localization and to build polarity by differentiation into the axons and dendrites (Harting and Knoll, 2010). SIRT2 is described to block cell migration of non-neuronal cells in wound-healing assay. In hippocampal neurons overexpression of SIRT2 inhibited neurite elongation whereas SIRT2 knockdown rescued the phenotype (Pandithage et al., 2008). These observations support our results, where we found decreased α-tubulin acetylation in AD cybrids (Figure 3E bottom pannel and F). In opposition, MCI group have increased α-tubulin acetylation, which suggests that the damage in these cells have not yet reached the threshold that leads to system failure, like in AD cells (Figure 3E bottom pannel and F). Although the relation between microtubule acetylation and microtubule depolymerization is poorly understood, it has

been hypothesized that depolymerization occurs dependently on acetylation (Suzuki and Koike, 2007). Anomalies in microtubule network were described in neurophatological studies of AD brain biopsies (Cash et al., 2003; Terry, 1998), where there was a decrease in microtubule length and number. We show that both MCI and AD groups have decreased α-tubulin fibers organization (Figure 3E, top panel) but concerning microtubule polymerization these groups follow different directions. MCI cybrids have decreased free tubulin in opposition to AD cybrids that present, although not statistically significant, increased free tubulin (Figure 3G), which is in accordance with α-tubulin acetylation levels (Figure 3 E bottom panel, H and I), supporting Suzuki and Koike hypothesis. These authors found that SIRT2 overexpression abolished the resistance to axonal degeneration in Wallerian degeneration mice granule cells (Wlds) and SIRT2 silencing enhanced axonal degeneration resistance in WT granule cells. We hypothesize that SIRT2 activation in the cytosol leads to microtubule loss of stability and depolymerization which facilitates Tau dissociation and consequent phosphorylation. The rational that microtubule damage precedes Tau phosphorylation was address by Miyasaka and colleagues (Miyasaka et al., 2010). It is well described that Tau is a microtubule-associated protein, acts in the stabilization of neuronal cytoskeleton and the phosphorylation state of Tau correlates with microtubule damage in AD (Hanger et al., 2014). Our results point to an increase in Tau phosphorylation in serine 396 residue but not in threonine 181, in AD cybrids (Figure 3 J-M). In AD brains was found that Tau phosphorylation at serine 396 is significantly increased when compared with other phosphorylation sites and constitutes an early site of Tau phosphorylation, occurring prior to the appearance of fibrillary tangles (Mondragon-Rodriguez et al., 2014). Further, experiments show that phosphorylation at serine 396 residue enhances Tau aggregation, affecting the binding and stabilization of

microtubules (Ding et al., 2006). Tau abnormal phosphorylation has been described to correlate with Braak and CERAD staging systems, constituting a valid biochemical assessment to complement other evaluations in AD diagnosis (Zhou et al., 2006).

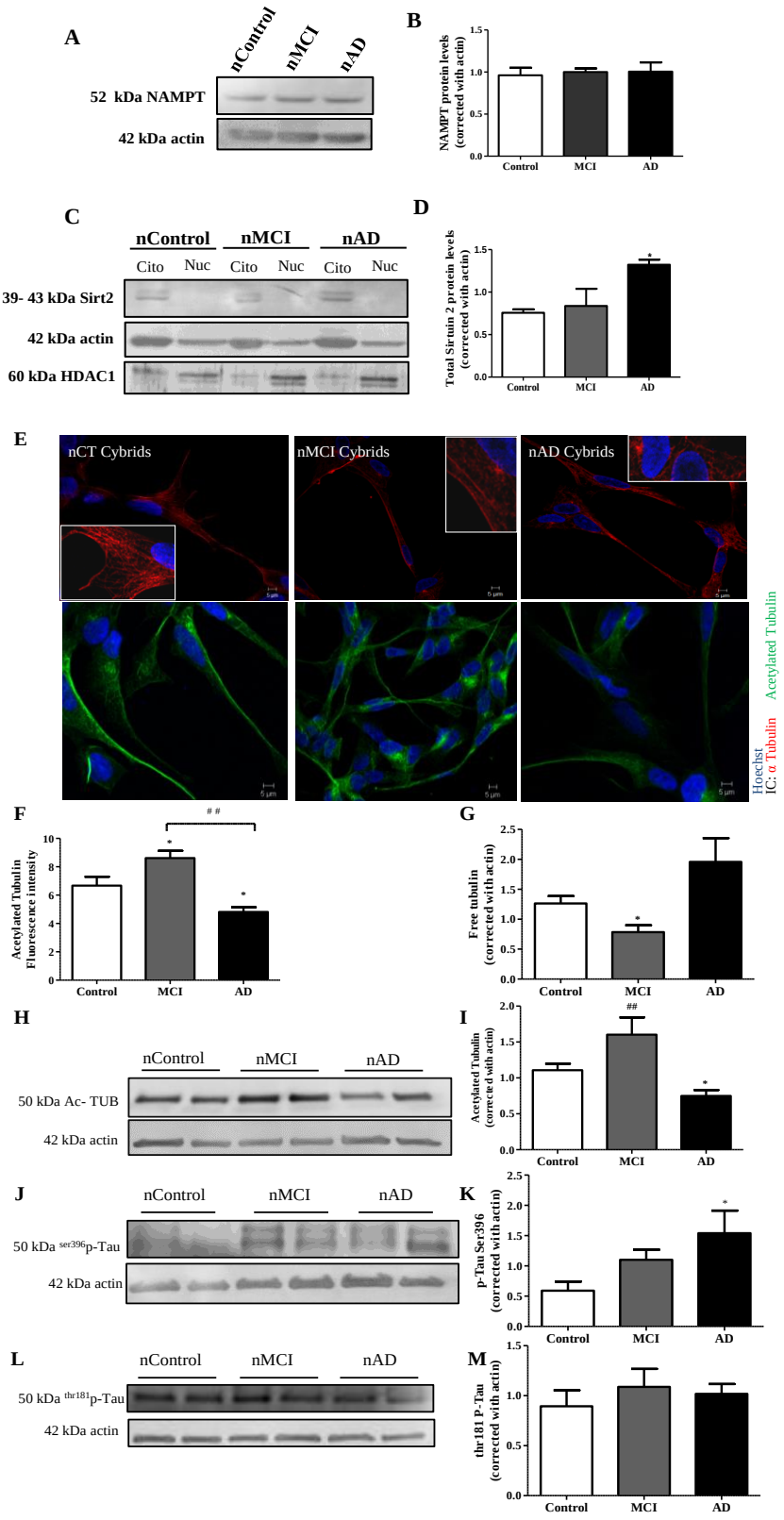

Figure 3. Microtubule network disruption in sAD cells. (A) Immunoblot for cytosolic NAMPT protein levels. (B) Densitometric analysis of NAMPT protein levels (n=3). (C) Immunoblot for cytosolic and nuclear Sirtuin2 levels. (D) Densitometry for cytosolic Sirtuin2 levels (n=3, **p*<0.05 versus nCT

cybrids). (E) α-Tubulin (red) and Ac-Tub (green) immunostaining. Hoechst 33342-stained nuclei are in blue. Scale bars: 5 µm. (F) Mean fluorescence intensity for Acetylated-tubulin (n=4, *$p<0.05$ versus nCT cybrids; $^{\#\#}$ $p<0.01$ nMCI versus nAD cybrids). (G) Densitometry for Free Tubulin analysis (n=4, *$p<0.05$ versus nCT cybrids). (H) Immunoblot for Acetylated-tubulin. (I) Densitometric analysis of Ac-Tub (n=8, *$p<0.05$ versus nCT cybrids; $^{\#\#}$ $p<0.01$ nMCI versus nAD cybrids). (J), (K) Immuniblot for phosphor Tau, at serine 396 and threonine 181, respectively. (L), (M) Densitometric analysis of p-Tau serine 396 and thr 181, respectively (n=4, *$p<0.05$ versus nCT cybrids).

5.2.4 Microtubule breakdown impairs autophagy completion.

Due the high polarization of neurons, axonal transport is crucial because it assures that proteins, vesicles, mRNAs, signaling molecules and organelles, such as mitochondria, are supplied from the cell body to synaptic terminals (Encalada and Goldstein, 2014). Compelling evidence suggests a preponderant involvement of axonal transport failure in AD and other neurodegenerative disorders (Goldstein, 2012; Millecamps and Julien, 2013). Since axonal transport relies on microtubule tracks, axonal swelling and dystrophic neurites have been found to accumulate mitochondria, vesicles and a number of other cellular components indicating transports defects (Coleman, 2005; Millecamps and Julien, 2013). In our differentiated cybrids containing mitochondria from AD patients we found decreased velocity of transport of autophagosomes (Figure 4 A and B), corroborating previous results (Trimmer and Borland, 2005). Because axonal transport is compromised, autophagosomes will not reach lysosomes for degradation of their contents and autophagic flux is compromised (Figure 4 C-F). In opposition MCI cybrids are able to maintain autophagic rates, most probably eliminating dysfunctional mitochondria and other toxic cell waste, in accordance with increased microtubule stability given by increased tubulin acetylation (see Figure 3). Macroautophagy was found to be constitutively active in neurons and when microtubules are disrupted with

vinblastine, large number of double membrane AVs accumulate (Boland et al., 2008). Extensive autophagy involvement in AD was described by Nixon (Nixon et al., 2005), showing massive accumulation of AVs in neurons of affected brain regions. Other studies showed that in transgenic AD mice models the accumulation of AVs in hippocampal dystrophic neurites correlated cytoskeletal defects early in AD phenotype progression (Sanchez-Varo et al., 2012).

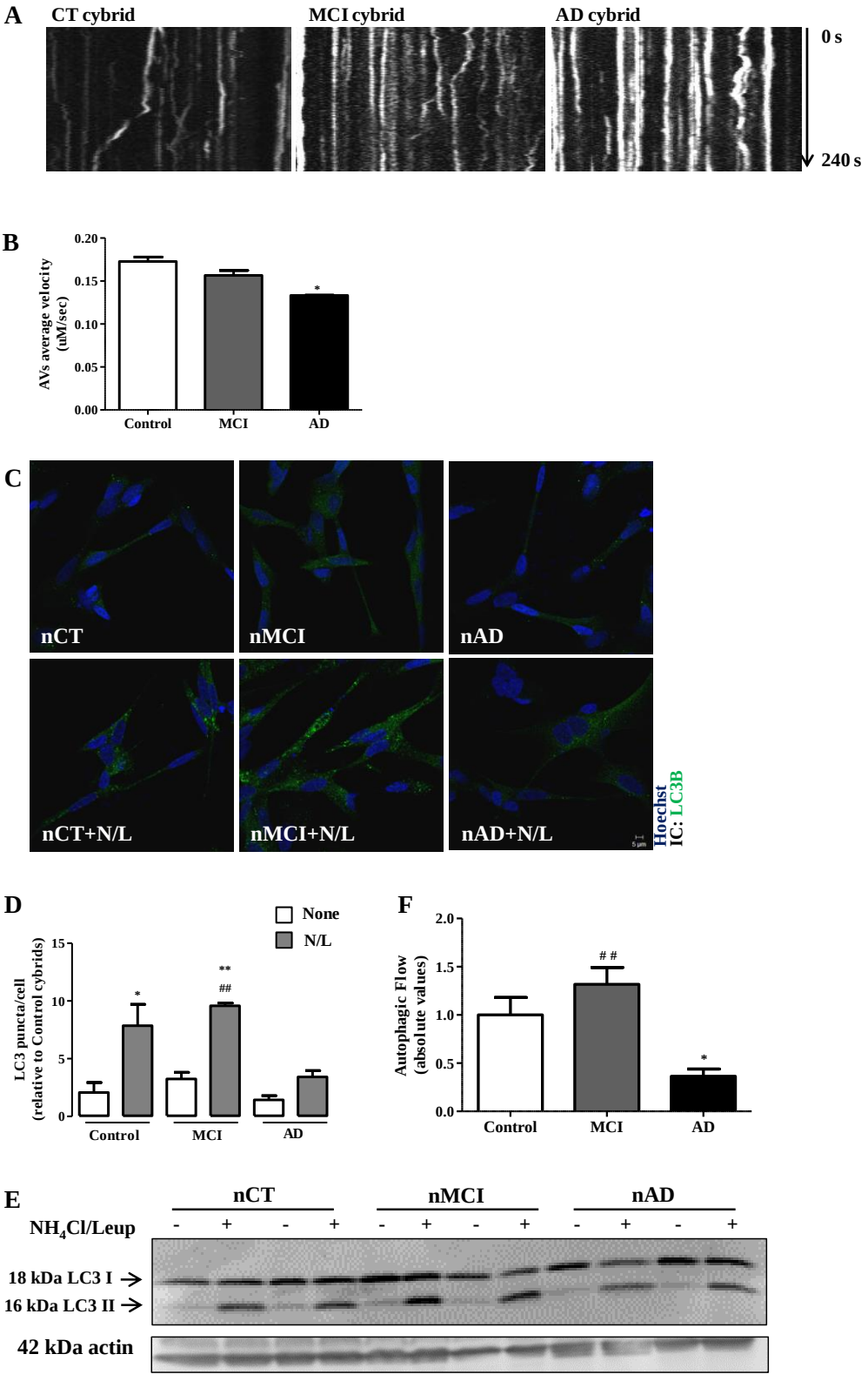

Figure 4. Disruption of microtubule network results in reduced autophagic vesicle movements and deficient autophagic turnover in sAD cybrid cells. (A) Representative kymograph images (out of three

experiments) of AVs movemenst in nCT and sAD cybrid cells treated. (B) Average transport velocity of AVs (µm/s) (n=3, *p<0.05 versus nCT cybrids). (C) Immunostaining for LC3B (green) in cells maintained in the presence or absence of inhibitors of lysososmal proteolysis (N/L). Hoechst 33342-stained nuclei are in blue. (D) Mean number of LC3B-positive vesicles per cell profile (n=3, *p<0.05, ** p<0.01 versus nCT cybrids; $^{\#\#}$ p<0.01 nMCI versus nAD cybrids). Scale bars: 5 µm. (E) Immunoblot for endogenous LC3B from cells untreated or after treatment with N/L. (F) Densitometric analysis of endogenous levels of LC3B (n=6, *p<0.05, 01 versus nCT cybrids; $^{\#\#}$ p<0.01 nMCI versus nAD cybrids).

5.2.5 Autophagic deficits in sAD cells.

Beclin 1 is a molecular anchor that assembles an interactome, which regulates the initiation and nucleation of the autophagosome formation (Salminen et al., 2013). In samples from AD brains, Beclin1 expression is significantly reduced, when compared with age-matched controls (Jaeger et al., 2010; Pickford et al., 2008). Also Jaeger and colleagues (Jaeger et al., 2010) showed that deficiency in Beclin 1 expression impaired the degradation of autophagosomes in cultured cells. The inhibition of autophagosome fusion with lysosomes with bafilomycin A caused the accumulation of vesicles and further reduction in Beclin 1 levels, which implies that a mechanism of negative feedback may be occurring blocking the formation of autophagosomes when fusion with lysosomes is impaired. This was the case with our cybrid model, where Beclin1 protein levels are reduced in AD cybrids, and further reduced when fusion is blocked with ammonium chloride and leupetine, while MCI group shows no changes (Figure 5 A and B). A number os studies have shown that enhancing the number of lysosomes is benefficial in terms of protein agregate degradation, namely Aβ degradation, in various AD models (Butler et al., 2011; Xiao et al., 2014). Nontheless we claim that due to defficient axonal transport and consequent impaired autophagosomes fusion with lysosomes, increasing lysosomal biogenesis may not be the most adequante approach.

In fact, both MCI and AD cybrids show increased Lamp1 protein levels (Figure 5 C and D), which we consider to be a compensatory response where cells are trying to eliminate autophagosomal contents. At leat for AD cybrids this increment in lysosomal biogenesis does not seem to improve autophagosomes fusion with lysosomes, as autophagic flux is impaired (see Figure 5) and p62 is accumulating in both MCI and AD groups (Figure 5 E and F). p62 is a multifunctional protein that is described to play a role in protein aggregation and protein degradation, targeting protein aggregates for autophagic or proteasomal degradation (Salminen et al., 2012). Interestingly p62 levels are decreased in AD brain tissue (Du et al., 2009) and this is associated with increased protein aggregation and deposition.

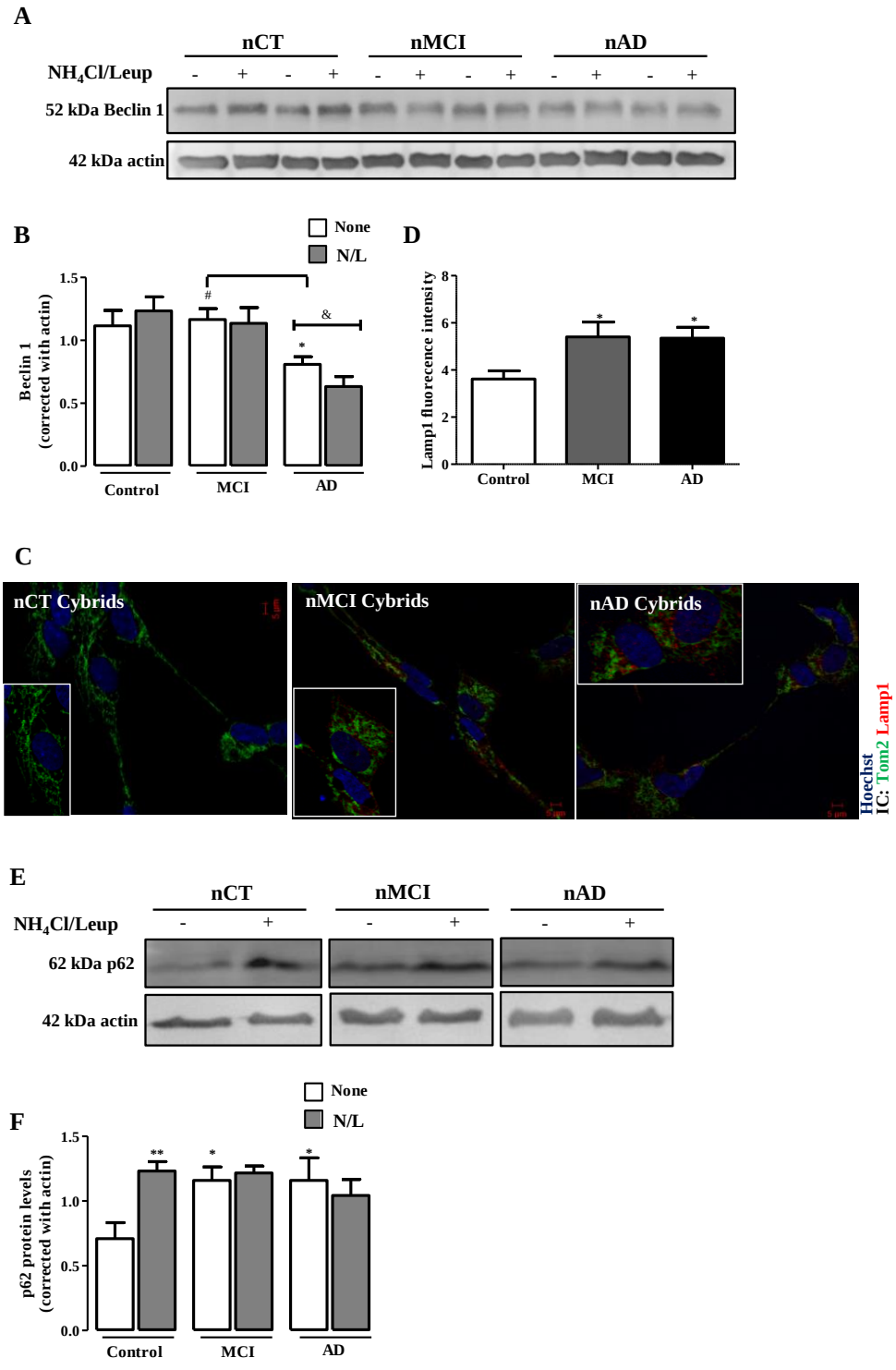

Figure 5. Autophagy is compromised in sAD cybrids. (A) Immnunoblot for Beclin1 protein levels from cells untreated or after treatment with N/L. (B) Densitometric analysis of Beclin1 levels (n=6, *p<0.05, 01 versus untreated nCT cybrids, $^{\#}p$<0.05 untreated nMCI versus nAD cybrids, $^{\&}p$<0.05 untreated versus N/L treated sAD cells). (C) Immunostaining for Lamp1 (red). Hoechst 33342-stained

nuclei are in blue. Scale bars: 5 μm. (D) Mean fluorescence intensity for Lamp1 (n=8, *p<0.05 versus nCT cybrids). (E) Immunobloting for p62 from cells untreated or after treatment with N/L. (F) Densitometric analysis of p62 (n=7, *p<0.05, ** p<0.01 versus nCT cybrids).

5.2.6 Mitophagy alterations in MCI and sAD cells.

The elimination of dysfunctional mitochodria, through mitophagy, occurs via an elegantly regulated process. Following a decrease in mitochondrial membrane potential, PINK1 is autophosphorylated (Okatsu et al., 2012) and sequestered within the mitochondria (Meissner et al., 2011) triggering Parkin translocation to mitochondrial outer membrane. Parkin ubiquitinates several mitochondrial proteins that control mitochondrial dynamics, such as Mfn1 and 2 and ultimatly activates mitochondrial removal by mitophagy. PINK1 was demonstrated to interact with Beclin 1 in mitochondria and its overexpression enhanced autophagy mediated by Beclin 1 (Michiorri et al., 2010). In aggrement with loss of mitochondrial membrane potential (see Figure 1), mitochondrial PINK1 protein levels are increased in AD cybrids while MCI cybrids only show a tendency for an increase (Figure 6 A and B). Also Parkin whole cell protein levels are increased in AD cybrids, suggesting that although autophagy process is impaired in AD cells, dysfunctional mitochondria are recognized and targeted for degradation. Given that dysfunctional mitochondria and protein aggregates are tageted for degradation and the completion of this process is comprimised, ubiquitinated proteins will accumulate within the cytoplasm of MCI and AD groups (Figure 6 E and F). Early accumulation of ubiquitin and its co-localization within neurofribrillary tangles and senile plaques in hippocampus of AD subjects occur (Perry et al., 1989). Further, since dysfunctional mitochondria accumulate within autophagosomes favouring Aβ production (Nixon, 2007) it is expected that Aβ levels

rise in AD group, as our results show (Figure 6 G and H). In agreement with our data, TgCRND8 mice overexpressing human APP with two FAD mutations, show incomplete autophagy digestion with accumulation of LC3II, ubiquitinated proteins and Aβ peptides in autophagosomes (Yang et al., 2011).

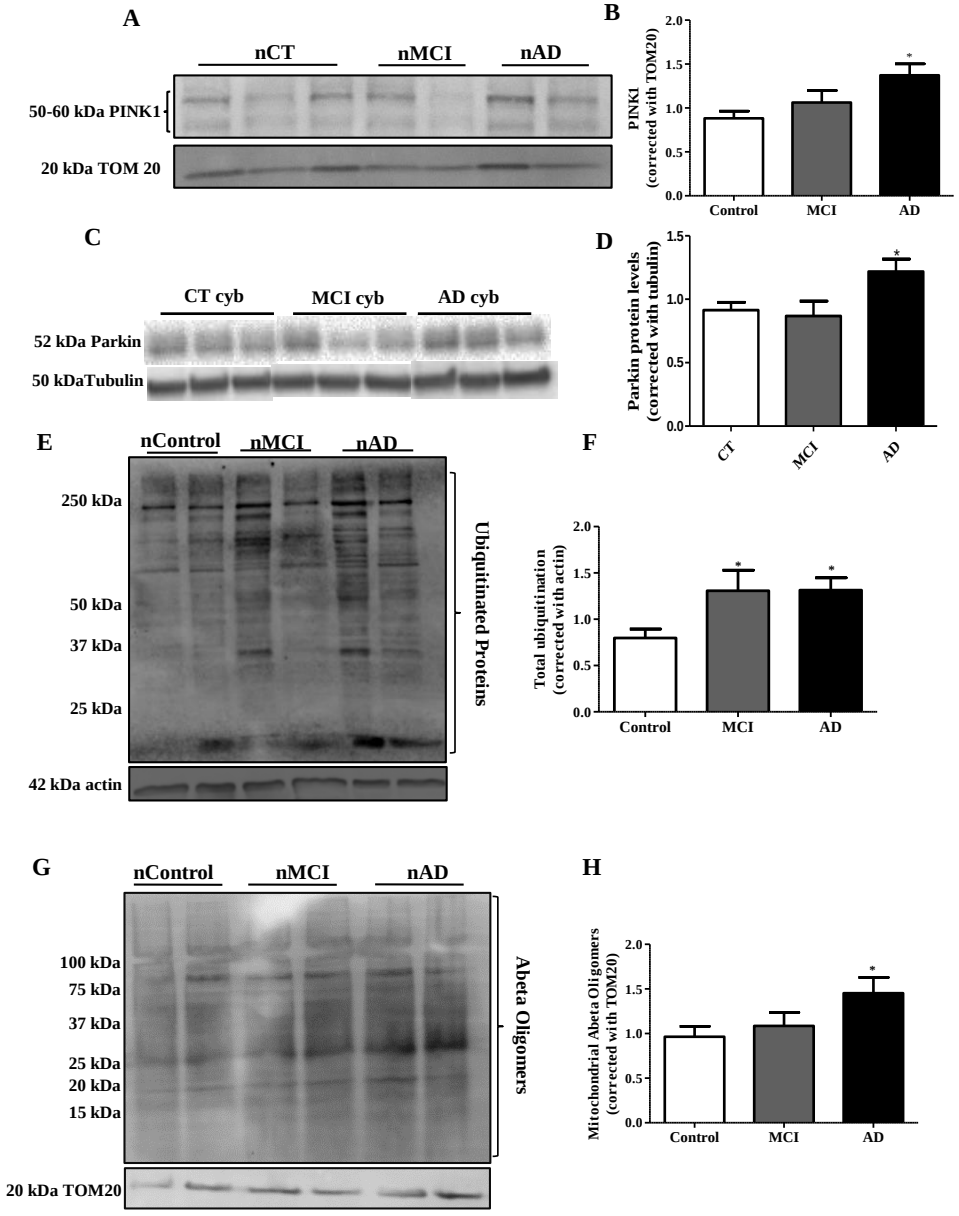

Figure 6. Mitophagy is impaired in nMCI and nAD cells. (A) Immunobloting for mitochondrial PINK1 levels. (B) Densitometric analysis of mitochondrial PINK1 (n=4, *p<0.05 versus nCT cybrids). (C) Immunobloting for total Parkin levels. (D) Densitometric analysis of total Parkin (n= 3, *p<0.05

versus CT cybrids). (E) Immunobloting for total ubiquitination levels. (F) Densitometric analysis of total ubiquitinated proteins (n=8, *p<0.05 versus nCT cybrids). (G) Immunobloting for mitochondrial Aβ oligomers. (H) Densitometric analysis of mitochondrial Aβ oligomers content (n=6, *p<0.05 versus nCT cybrids).

5.2.7 Lysosomal inhibition induces AD related features

After characterizing microtubule and autophagy related features in the differentiated cybrid cell lines the next step was to evaluate wether this alterations were recapitulated when lysosomal function is blocked. In parental SHSY5Y cells treated with NH_4Cl, a weak base that becomes concentrated in acidic compartments, such as lysosomes, cause pH to increase and, consequently, the inhibition of lysosomal hydrolases, and leupeptine, we show that mitochondrial membrane potential decreased after 12h of exposure (Figure 7A). We attribute this fact to the accumulation of dysfunctional mitochondria within the cells, which account for the reduction in membrane potential. Reports on Lysosomal Storage Diseases (LSD) demonstated that dysfunctional lysosomes leads to the accumulation of ubiquitinated proteins, dysfunctional mitochondria, which culminates in the activation of apoptotic cell death mechanisms, in this sense sharing common pathways with neurodegenerative disease such as AD (Settembre et al., 2008). In line with this rational, if the number of dysfunctional mitochondria is rising and their elimination is blocked, microtubule dynamics may get compromised and loose stability by decrease tubulin acetylation (Figure 7 B and C). When microtubule network is disassembled Tau dissociates and becomes susceptible of kinase action, increasing its phosphorylation (Figure 7 D and E). Also, it was described that lysosomal protease inhibition induces defective axonal transport and causes axonal accumulation of AVs in dystrophic neurites in AD (Lee et al., 2011). Finally, as predicted total levels of protein ubiquitination increase and, interestingly, also

mitochondrial Aβ oligomers (Figure 7 F-I). This results allows us to infer that mitochondria are definetly a priviledged site for Aβ targeting and when mitopahgy becomes impaired, Aβ production is favoured within accumulated AVs. These results corroborate others that observed that increased Aβ metabolism is strongly associated with macroautophagy impairment for both for Aβ production and secretion, enhancing neurodegeneration (Nilsson et al., 2013; Nilsson and Saido, 2014; Nixon, 2007).

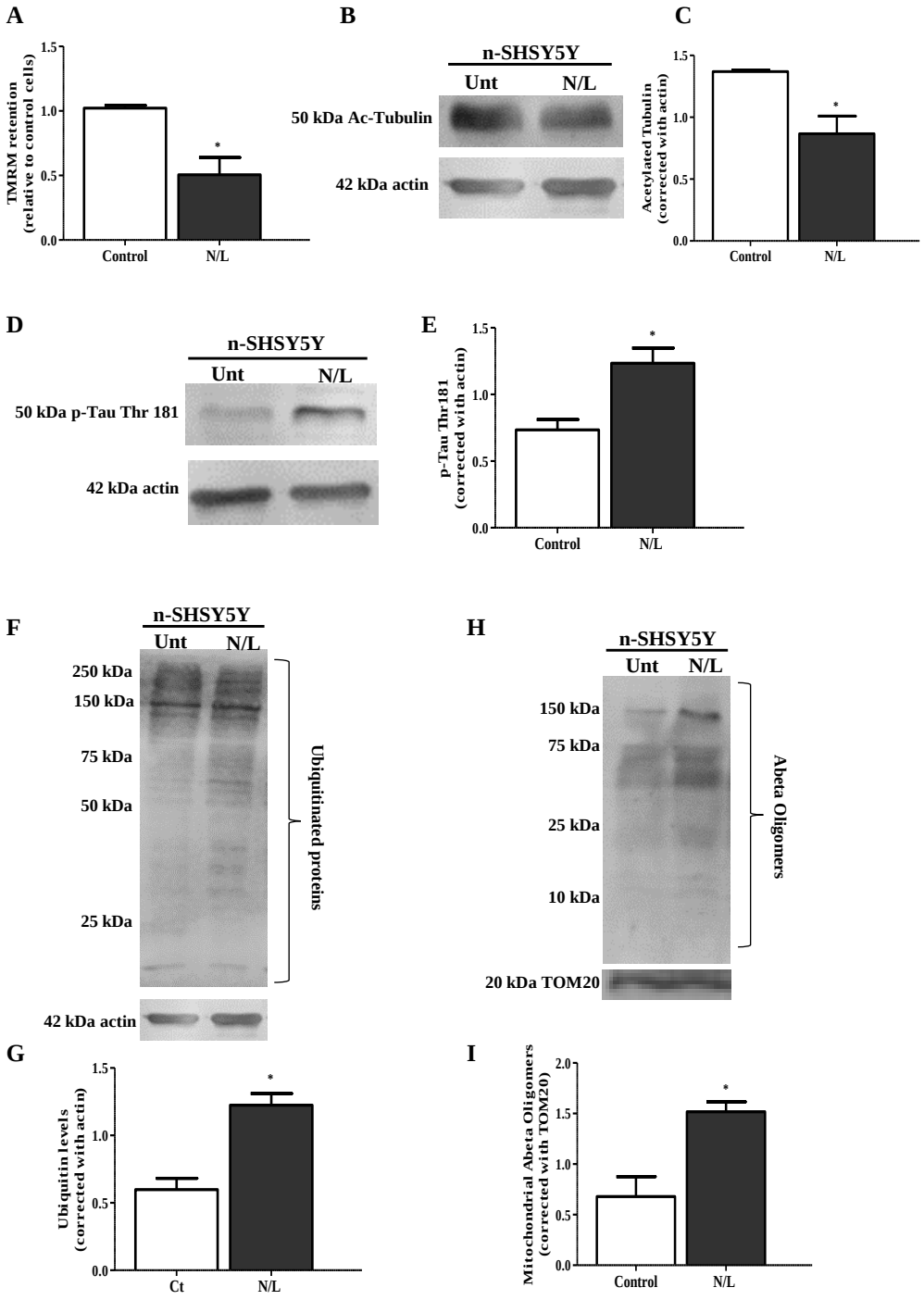

Figure 7. Inhibiting lysosomal degradation recapitulates AD-related features. (A) Mitochondrial membrane potential. Data represent the mean ± SEM derived from three independent experiments and are expressed relatively to untreated cells versus N/L treated cells (*p<0.05, versus untreated cells). (B) Immunobloting for Ac-Tub levels. (C) Densitometric analysis of Ac-Tub (n=3, *p<0.05 versus untreated cells). (D) Immunobloting for phospho Tau, Thr 181. (E) Densitometric analysis of phospho Tau, Thr 181 (n=3, *p<0.05 versus untreated cells). (F) Immunoloting for total ubiquitination. (G) Densitometry

analysis of total ubiquitination (n=3, *p<0.05 versus untreated cells). (H) Immunobloting for mitochondrial Aβ oligomers. (I) Densitometric analysis of mitochondrial Aβ oligomers (n=3, *p<0.05 versus untreated cells).

5.2.8 Sirtuin 2 loss of function prevents ALP dysfunction through the restoration of tubulin acetylation.

Beneficial effects of SIRT2 inhibition were described in a variety of neurodegenerative diseases models. In one study, the inhibition of SIRT2 has been proved to be beneficial in the attenuation of α-synuclein-mediated toxicity in PD and multiple system atrophy (MSA) models (Hasegawa et al., 2010; Outeiro et al., 2007). Others have shown that either genetic as well as pharmacological inhibition of SIRT2 exerts neuroprotection through sterol biosynthesis in Huntington´s disease (HD) models (Luthi-Carter et al., 2010). Our preliminary data shows that SIRT2 knock-out (KO) mice neurons are protected against the toxicity of soluble $A\beta_{1-42}$, displaying no effect in decreasing microtubule acetylation levels (Figure 8A). Further, mitochondrial membrane potential and autophagic flux are maintained in SIRT2 KO mice (Figure 8 B-D). Given these encouraging results, we hypothesized that specific SIRT2 inhibition rescue AD cybrids in terms of loss of microtubule acetylation and impairment in ALP. SIRT2 specific inhibitor AK1 was proven to prevent neuronal loss in rTg4510 mice when injected directly in the hippocampus while having no toxic effects (Spires-Jones et al., 2012). Our results show an increase in acetylated tubulin leves in AD cybrids treated with 10μM of AK1 (Figure 8 E and F). In control cells lines we have the same trend but, interestingly, MCI group fails to further increase the acetylation of tubulin with AK1. As a positive control cells were also treated with HDAC6 inhibitor, Tubastatin A. In this case it is evident the large increase in tubulin acetylation levels, nevertheless, it seems that AD cybrids have a chronic inability to increase tubulin acetylation levels

above a certain point, as its values are lower that control and MCI groups (Figure 8 F). Since microtubule network is restored, ALP should be recovered since axonal transport can be effectuated and fusion of autophagosomes and lysosomes can occur. Indeed our first data shows that AK1 treatment can successfully increase autophagic flux in AD cybrids (Figure 8 G and H). In the remaining groups AK1 does not seem to have an effect, which may be due to control and MCI cybrids having autophagic degradation at their optimal rates. Recent evidence suggest that SIRT2 play an important role in autophagy since SIRT2 overexpression is able to inhibit autophagic flux and cause the accumulation of autophagosomes components given by as LC3II and p62 proteins (Gal et al., 2012).

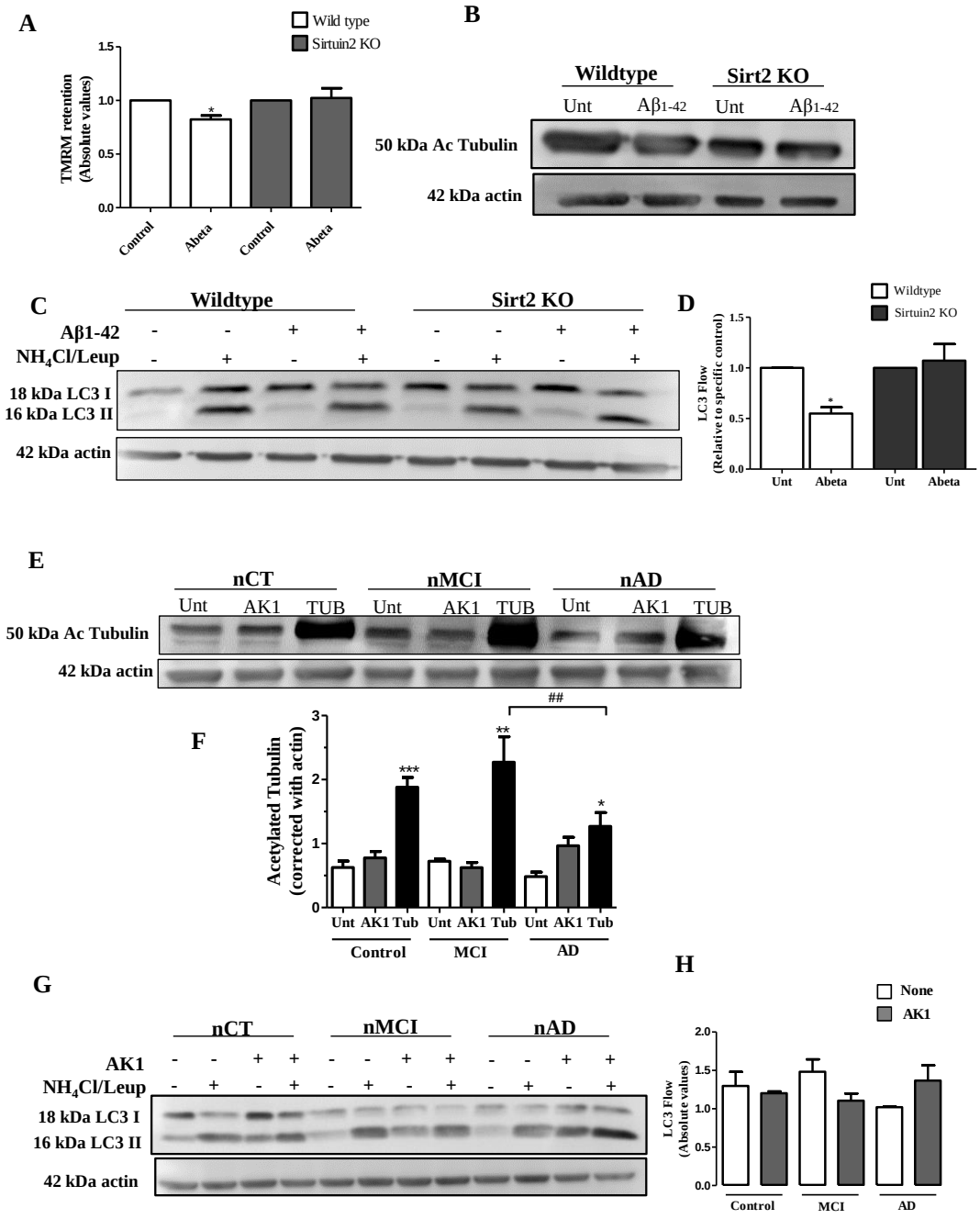

Figure 8. SIRT2 inhibition with AK1 and ablation in SIRT2 KO mice rescues ALP malfunction through microtubule network restoration. (A) Mitochondrial membrane potential. Data represent the mean ± SEM derived from three or five independent experiments, for WT or SIRT2 KO primary neurons respectively, and are expressed relatively to untreated cells (*p<0.05, versus untreated cells) (B) Immunobloting for Ac-Tub levels in WT and Sirt KO mice from primary cortical neurons treated with $A\beta_{1-42}$ for 24h.. (C) Immunobloting for endogenous LC3B from primary cortical neurons treated with $A\beta_{1-42}$ for 24h. Where indicated, cells were co-treated with N/L, in the last 4h. (D) Densitometric analysis

of LC3B endogenous levels (n=4, *p<0.05 versus untreated wildtype cortical neurons). (E) Immunobloting for Ac-Tub from Control, MCI and AD cybrids, untreated or exposed to 10μM of AK1 and 5μM of Tubastatin A for 24 h. (F) Densitometric analysis of Ac-Tub (n=3, *p<0.05; **p<0.01 or *** p<0.001 versus respective control; ## p<0.01 Tubastatin A treated MCI versus AD) . (G) Immunobloting for endogenous LC3B from Control, MCI and AD cybrids untreated or exposed 10μM of AK1 for 24h. (H) Densitometric analysis of endogenous LC3B.

5.3 DISCUSSION

AD has long been associated with mitochondrial dysfunction, observed in many pathways govern by mitochondria and measurable in various cellular models from AD subject brains to the periphery (Swerdlow et al., 2014). Many mitochondrial-derived pathogenic processes have been described but to date no effective mechanism or target was described that enabled an effective therapeutic. Here we propose a mechanism that unifies many well described pathways affected in AD: mitochondrial dysfunction, microtubule disassembly and axonal transport impairment. First we evaluated mitochondrial dynamics and metabolism in RA differentiated control, MCI and AD cybrids and found depolarized and fragmented mitochondria. A body of evidence points to mitochondrial dynamics proteins to be suitable targets for AD pathology rescue, namely mitochondrial fission protein DRP1 (Reddy, 2014). In one study using AD cybrids, the expression of dominant negative DRP1 attenuated mitochondrial functional defects observed in AD cybrid cell lines (Gan et al., 2014). Microtubule damage jeopardizes axonal transport hampering the fusion of AVs and lysosomes in the autophagic pathway. One aspect of microtubule disassembly, the loss of acetylation, was proven to be crucial for the completion of autophagy. When microtubule acetylation is lost there is no fusion of autophagosomes and lysosomes, into autolysosomes (Xie et al., 2010). Further, tubulin acetylation is required for motor

protein, responsible for axonal transport, to bind to microtubules (Reed et al., 2006). Some microtubule targeted drugs were shown to prevent protein accumulation and synaptic loss (Butler et al., 2007) and have a beneficial effect on Aβ peptides production (Ashur-Fabian et al., 2003). These compounds often have brain accessibility issues and may become toxic. On the other hand SIRT2 is abundant and preferentially expressed in mammalian CNS and in a much lower extend in peripheral tissues (Maxwell et al., 2011). It is detected exclusively in the cytosol of neuronal cells and although the exact role of SIRT2 in the cytosol is still elusive, the tubulin deacetylase activity and microtubule damage in AD makes of SIRT2 a desirable candidate for therapeutic intervention. We showed that SIRT2 inhibition with AK1 rescued microtubule acetylation in AD and our preliminary data point to a recovery of autophagic flux. Further studies are needed to address the efficacy of AK1 in ameliorating other AD-related neurophatological hallmarks such as Tau phosphorylation and Aβ oligomers. We hypothesize that targeting microtubule network through SIRT2 manipulation in adult brain may be a more brain-specific approach, and holds a great promise in future AD therapeutics.

Chapter 6

Concluding Remarks

CONCLUDING REMARKS

AD, first described by Alois Alzheimer in the early 1900s, is the most common form of dementia with no effective therapeutic available that could slow or stop the disease progression, despite the efforts made by clinicians and scientist around the world , (Silva et al., 2012b). The fact that Aβ-based therapies failed on both familial and sporadic AD forms (Iqbal et al., 2014), the multifactorial nature of AD and the suggested, although not well understood, relationship between brain aging and this disease, lead to mitochondria being a strong candidate for AD´s initiation. The recognition of mitochondrial metabolism failure in very early AD stages within the brain and the periphery, namely complex IV of ETC, and the involvement of mitochondria in a wide range of cellular functions, namely those who dictate cell death or survival, suggests that mitochondria play a key role in AD pathogenesis. We believe that mitochondria unifies both familial and sporadic AD forms by linking Tau and Aβ pathologies, in a way that mitochondria may be the missing link between mitochondrial and Aβ cascade hypothesis (Silva et al., 2011b). The use of the *ex-vivo* model of cybrids from AD, MCI subjects and age-matched controls, allowed us to show that mitochondrial dysfunction sets off the pathological mechanisms described for MCI and AD cybrids. We showed that mitochondrial dysfunction is inherent to AD group and, in a minor extension, is also present in MCI cybrids. In Chapter 3 we showed that mitochondrial dysfunction, namely reduced Complex IV activity, drives the increase of oxidative damage within the AD cybrids, whereas MCI group present intermediate values. AD cybrids also present intrinsic higher levels of Aβ oligomeric forms when compared to control or MCI groups. We further explored this mitochondrial dysfunction state and found that both AD and MCI cybrids have compromised mitochondria which

results in decreased ATP and a shift of whole cell NAD^+/NADH ratio towards a more oxidized state (Chapter 4). Moreover we were able to show that mitochondria from MCI and AD have decreased respiration accompanied by decreased levels of PGC1α and decreased activation of SIRT1. Nevertheless, we found increased mitochondrial mass markers in MCI and AD cybrids. At this point we had clear evidence that AD and MCI cybrids bearing mitochondrial dysfunction have decreased mitochondrial biogenesis, which lead us to investigate cellular quality control pathways, namely ALP (Chapter 5). We then used RA-differentiated cybrids into neurons and found depolarized and fragmented mitochondria, in accordance with increased mitochondrial fission proteins, in MCI and AD cybrids. We found that SIRT2, a tubulin deacetylase, is only located in the cytoplasm of differentiated cybrids and its levels are increased in AD cybrids. This increment in SIRT2 expression induces microtubule disassembly decreasing significantly the APH trafficking to lysosomes. In accordance AD cells have decreased autophagic flux resulting in the accumulation of dysfunctional mitochondria loaded with Abeta oligomers and protein aggregates that will cause further toxicity. Interestingly, MCI group is able to increase autophagic flux as well as tubulin acetylation. We hypothesize that this is a compensatory response by which these cells are attempting to degrade dysfunctional mitochondria and protein aggregates that are accumulating within their cytoplasm. Further, we present evidence that SIRT2 chemical inhibition with AK1 protects AD cells against deleterious effects resulting from loss of tubulin acetylation, a known marker for microtubule stability, inherent for AD cybrids. Once we restored microtubule acetylation by SIRT2 inhibition, we are able to restore proper ALP function and future studies will be performed in order to access the effects of AK1 dependent SIRT2 inhibition on other neurophatolgical hallmarks of AD, such as Tau phosphorylation and Abeta production.

Overall we show evidence that mitochondrial dysfunction is widely present in AD cybrids, occupies an upstream position in the pathogenesis of AD and starts a sequence of events converging in increased oxidative stress, impairment of ALP and, ultimately, the activation of SIRT2 and consequent microtubule disruption. Targeting mitochondrial function directly or improve microtubule stabilization, namely through SIRT2 inhibition, seem to represent a valid approaches to prevent ALP dysfunction and consequent toxicity through the accumulation of damaged, dysfunctional mitochondria and Aβ protein aggregates.

Chapter 7

REFERENCES

References

(1994). American Psychiatric Association, Diagnostic and Statistical Manual of Mental Disorders, 4th ed edn (Washington, D.C: American Psychiatric Association).

Agostinho, P., and Oliveira, C.R. (2003). Involvement of calcineurin in the neurotoxic effects induced by amyloid-beta and prion peptides. The European journal of neuroscience *17*, 1189-1196.

Aksenov, M.Y., Tucker, H.M., Nair, P., Aksenova, M.V., Butterfield, D.A., Estus, S., and Markesbery, W.R. (1999). The expression of several mitochondrial and nuclear genes encoding the subunits of electron transport chain enzyme complexes, cytochrome c oxidase, and NADH dehydrogenase, in different brain regions in Alzheimer's disease. Neurochem Res *24*, 767-774.

Albrecht, S., Bourdeau, M., Bennett, D., Mufson, E.J., Bhattacharjee, M., and LeBlanc, A.C. (2007). Activation of caspase-6 in aging and mild cognitive impairment. Am J Pathol *170*, 1200-1209.

Aliev, G., Palacios, H.H., Walrafen, B., Lipsitt, A.E., Obrenovich, M.E., and Morales, L. (2009). Brain mitochondria as a primary target in the development of treatment strategies for Alzheimer disease. The international journal of biochemistry & cell biology *41*, 1989-2004.

Aluise, C.D., Robinson, R.A., Cai, J., Pierce, W.M., Markesbery, W.R., and Butterfield, D.A. (2011). Redox proteomics analysis of brains from subjects with amnestic mild cognitive impairment compared to brains from subjects with preclinical Alzheimer's disease: insights into memory loss in MCI. J Alzheimers Dis *23*, 257-269.

Alzheimer, A. (1907). Uber eine eigenartige Erkrankung der Hirnrinde. Allg Z Psychiat Psych-Gerichtl Med *64*, 146-148.

Alzheimer, A. (1911). Uber eigenartige Krankheitsfalle des spateren Alters. Z die Gesamte Neurologie Pscyhiatrie *4*, 456-485.

Alzheimer, A., Stelzmann, R.A., Schnitzlein, H.N., and Murtagh, F.R. (1995). An English translation of Alzheimer's 1907 paper, "Uber eine eigenartige Erkankung der Hirnrinde". Clin Anat *8*, 429-431.

Ames, B.N., Shigenaga, M.K., and Hagen, T.M. (1995). Mitochondrial decay in aging. Biochim Biophys Acta *1271*, 165-170.

Anderson, A.J., Su, J.H., and Cotman, C.W. (1996). DNA damage and apoptosis in Alzheimer's disease: colocalization with c-Jun immunoreactivity, relationship to brain area, and effect of postmortem delay. J Neurosci *16*, 1710-1719.

Anekonda, T.S., and Reddy, P.H. (2006). Neuronal protection by sirtuins in Alzheimer's disease. J Neurochem *96*, 305-313.

Ansari, M.A., and Scheff, S.W. (2010). Oxidative stress in the progression of Alzheimer disease in the frontal cortex. J Neuropathol Exp Neurol *69*, 155-167.

Arduino, D.M., Esteves, A.R., and Cardoso, S.M. (2011). Mitochondrial fusion/fission, transport and autophagy in Parkinson's disease: when mitochondria get nasty. Parkinsons Dis *2011*, 767230.

Arduino, D.M., Esteves, A.R., Cortes, L., Silva, D.F., Patel, B., Grazina, M., Swerdlow, R.H., Oliveira, C.R., and Cardoso, S.M. (2012). Mitochondrial metabolism in Parkinson's disease impairs quality control autophagy by hampering microtubule-dependent traffic. Human molecular genetics *21*, 4680-4702.

Ashur-Fabian, O., Segal-Ruder, Y., Skutelsky, E., Brenneman, D.E., Steingart, R.A., Giladi, E., and Gozes, I. (2003). The neuroprotective peptide NAP inhibits the aggregation of the beta-amyloid peptide. Peptides *24*, 1413-1423.

Autret, A., and Martin, S.J. (2010). Bcl-2 family proteins and mitochondrial fission/fusion dynamics. Cell Mol Life Sci *67*, 1599-1606.

Avila, J. (2010). Alzheimer disease: caspases first. Nat Rev Neurol *6*, 587-588.

Ayala-Grosso, C., Tam, J., Roy, S., Xanthoudakis, S., Da Costa, D., Nicholson, D.W., and Robertson, G.S. (2006). Caspase-3 cleaved spectrin colocalizes with neurofilament-immunoreactive neurons in Alzheimer's disease. Neuroscience *141*, 863-874.

Baar, K., Wende, A.R., Jones, T.E., Marison, M., Nolte, L.A., Chen, M., Kelly, D.P., and Holloszy, J.O. (2002). Adaptations of skeletal muscle to exercise: rapid increase in the transcriptional coactivator PGC-1. FASEB J *16*, 1879-1886.

Baldeiras, I., Santana, I., Proenca, M.T., Garrucho, M.H., Pascoal, R., Rodrigues, A., Duro, D., and Oliveira, C.R. (2008). Peripheral oxidative damage in mild cognitive impairment and mild Alzheimer's disease. J Alzheimers Dis *15*, 117-128.

Baldeiras, I., Santana, I., Proenca, M.T., Garrucho, M.H., Pascoal, R., Rodrigues, A., Duro, D., and Oliveira, C.R. (2010). Oxidative damage and progression to Alzheimer's disease in patients with mild cognitive impairment. J Alzheimers Dis *21*, 1165-1177.

Baloyannis, S.J. (2006). Mitochondrial alterations in Alzheimer's disease. J Alzheimers Dis *9*, 119-126.

Baloyannis, S.J. (2011). Mitochondria are related to synaptic pathology in Alzheimer's disease. Int J Alzheimers Dis *2011*, 305395.

Barinaga, M. (1998). Is apoptosis key in Alzheimer's disease? Science *281*, 1303-1304.

Barrett, M.J., Alones, V., Wang, K.X., Phan, L., and Swerdlow, R.H. (2004). Mitochondria-derived oxidative stress induces a heat shock protein response. J Neurosci Res *78*, 420-429.

Barsoum, M.J., Yuan, H., Gerencser, A.A., Liot, G., Kushnareva, Y., Graber, S., Kovacs, I., Lee, W.D., Waggoner, J., Cui, J., *et al.* (2006). Nitric oxide-induced mitochondrial fission is regulated by dynamin-related GTPases in neurons. The EMBO journal *25*, 3900-3911.

Baur, J.A. (2010). Biochemical effects of SIRT1 activators. Biochim Biophys Acta *1804*, 1626-1634.

Beal, M.F. (2005). Mitochondria take center stage in aging and neurodegeneration. Annals of neurology *58*, 495-505.

Belinson, H., and Michaelson, D.M. (2009). ApoE4-dependent Abeta-mediated neurodegeneration is associated with inflammatory activation in the hippocampus but not the septum. Journal of neural transmission *116*, 1427-1434.

Berg, L. (1988). Clinical Dementia Rating (CDR). Psychopharmacol Bull *24*, 637-639.

Bermejo, P., Martin-Aragon, S., Benedi, J., Susin, C., Felici, E., Gil, P., Ribera, J.M., and Villar, A.M. (2008). Peripheral levels of glutathione and protein oxidation as markers in the development of Alzheimer's disease from Mild Cognitive Impairment. Free Radic Res *42*, 162-170.

Berti, V., Mosconi, L., Glodzik, L., Li, Y., Murray, J., De Santi, S., Pupi, A., Tsui, W., and De Leon, M.J. (2011). Structural brain changes in normal individuals with a maternal history of Alzheimer's. Neurobiol Aging, Epub ahead of print.

Bettens, K., Sleegers, K., and Van Broeckhoven, C. (2013). Genetic insights in Alzheimer's disease. Lancet neurology *12*, 92-104.

Bicalho, M.A., Pimenta, F.A., Bastos-Rodrigues, L., de Oliveira Hansen, E., Neves, S.C., Melo, M., Rosa, D.V., Pedra de Souza, R., Marques de Miranda, D., Nunes de Moraes, E., *et al.* (2013). Sociodemographic characteristics, clinical factors, and genetic polymorphisms associated with Alzheimer's disease. International journal of geriatric psychiatry *28*, 640-646.

Bindokas, V.P., Jordan, J., Lee, C.C., and Miller, R.J. (1996). Superoxide production in rat hippocampal neurons: selective imaging with hydroethidine. J Neurosci *16*, 1324-1336.

Boland, B., Kumar, A., Lee, S., Platt, F.M., Wegiel, J., Yu, W.H., and Nixon, R.A. (2008). Autophagy induction and autophagosome clearance in neurons: relationship to autophagic pathology in Alzheimer's disease. The Journal of neuroscience : the official journal of the Society for Neuroscience *28*, 6926-6937.

Bonda, D.J., Wang, X., Perry, G., Nunomura, A., Tabaton, M., Zhu, X., and Smith, M.A. (2010). Oxidative stress in Alzheimer disease: a possibility for prevention. Neuropharmacology *59*, 290-294.

Boumezbeur, F., Mason, G.F., de Graaf, R.A., Behar, K.L., Cline, G.W., Shulman, G.I., Rothman, D.L., and Petersen, K.F. (2010). Altered brain mitochondrial metabolism in healthy aging as assessed by in vivo magnetic resonance spectroscopy. Journal of cerebral blood flow and metabolism : official journal of the International Society of Cerebral Blood Flow and Metabolism *30*, 211-221.

Breitenbach, M., Rinnerthaler, M., Hartl, J., Stincone, A., Vowinckel, J., Breitenbach-Koller, H., and Ralser, M. (2013). Mitochondria in ageing: there is metabolism beyond the ROS. FEMS yeast research.

Broe, M., Shepherd, C.E., Milward, E.A., and Halliday, G.M. (2001). Relationship between DNA fragmentation, morphological changes and neuronal loss in Alzheimer's disease and dementia with Lewy bodies. Acta Neuropathol *101*, 616-624.

Brown, A.M., Sheu, R.K., Mohs, R., Haroutunian, V., and Blass, J.P. (2001). Correlation of the clinical severity of Alzheimer's disease with an aberration in mitochondrial DNA (mtDNA). J Mol Neurosci *16*, 41-48.

Brunden, K.R., Yao, Y., Potuzak, J.S., Ferrer, N.I., Ballatore, C., James, M.J., Hogan, A.M., Trojanowski, J.Q., Smith, A.B., 3rd, and Lee, V.M. (2011). The characterization of microtubule-stabilizing drugs as possible therapeutic agents for Alzheimer's disease and related tauopathies. Pharmacol Res *63*, 341-351.

Bubber, P., Haroutunian, V., Fisch, G., Blass, J.P., and Gibson, G.E. (2005). Mitochondrial abnormalities in Alzheimer brain: mechanistic implications. Ann Neurol *57*, 695-703.

Burns, D.H., Rosendahl, S., Bandilla, D., Maes, O.C., Chertkow, H.M., and Schipper, H.M. (2009). Near-infrared spectroscopy of blood plasma for diagnosis of sporadic Alzheimer's disease. J Alzheimers Dis *17*, 391-397.

Butler, D., Bendiske, J., Michaelis, M.L., Karanian, D.A., and Bahr, B.A. (2007). Microtubule-stabilizing agent prevents protein accumulation-induced loss of synaptic markers. European journal of pharmacology *562*, 20-27.

Butler, D., Hwang, J., Estick, C., Nishiyama, A., Kumar, S.S., Baveghems, C., Young-Oxendine, H.B., Wisniewski, M.L., Charalambides, A., and Bahr, B.A. (2011). Protective effects of positive lysosomal modulation in Alzheimer's disease transgenic mouse models. PloS one *6*, e20501.

Butterfield, D.A., Bader Lange, M.L., and Sultana, R. (2010). Involvements of the lipid peroxidation product, HNE, in the pathogenesis and progression of Alzheimer's disease. Biochim Biophys Acta *1801*, 924-929.

Butterfield, D.A., Hensley, K., Cole, P., Subramaniam, R., Aksenov, M., Aksenova, M., Bummer, P.M., Haley, B.E., and Carney, J.M. (1997). Oxidatively induced structural alteration of glutamine synthetase assessed by analysis of spin label incorporation kinetics: relevance to Alzheimer's disease. J Neurochem *68*, 2451-2457.

Butterfield, D.A., and Lange, M.L. (2009). Multifunctional roles of enolase in Alzheimer's disease brain: beyond altered glucose metabolism. J Neurochem *111*, 915-933.

Butterfield, D.A., Poon, H.F., St Clair, D., Keller, J.N., Pierce, W.M., Klein, J.B., and Markesbery, W.R. (2006a). Redox proteomics identification of oxidatively modified hippocampal proteins in mild cognitive impairment: insights into the development of Alzheimer's disease. Neurobiol Dis *22*, 223-232.

Butterfield, D.A., Reed, T., Perluigi, M., De Marco, C., Coccia, R., Cini, C., and Sultana, R. (2006b). Elevated protein-bound levels of the lipid peroxidation product, 4-hydroxy-2-nonenal, in brain from persons with mild cognitive impairment. Neurosci Lett *397*, 170-173.

Butterfield, D.A., Reed, T.T., Perluigi, M., De Marco, C., Coccia, R., Keller, J.N., Markesbery, W.R., and Sultana, R. (2007). Elevated levels of 3-nitrotyrosine in brain from subjects with amnestic mild cognitive impairment: implications for the role of nitration in the progression of Alzheimer's disease. Brain Res *1148*, 243-248.

Buttke, T.M., and Sandstrom, P.A. (1994). Oxidative stress as a mediator of apoptosis. Immunol Today *15*, 7-10.

Cacabelos, R. (2007). Molecular pathology and pharmacogenomics in Alzheimer's disease: polygenic-related effects of multifactorial treatments on cognition, anxiety and

depression. Methods and findings in experimental and clinical pharmacology *29 Suppl A*, 1-91.

Cacabelos, R., Fernandez-Novoa, L., Lombardi, V., Kubota, Y., and Takeda, M. (2005). Molecular genetics of Alzheimer's disease and aging. Methods and findings in experimental and clinical pharmacology *27 Suppl A*, 1-573.

Calkins, M.J., Manczak, M., Mao, P., Shirendeb, U., and Reddy, P.H. (2011). Impaired mitochondrial biogenesis, defective axonal transport of mitochondria, abnormal mitochondrial dynamics and synaptic degeneration in a mouse model of Alzheimer's disease. Human molecular genetics *20*, 4515-4529.

Calkins, M.J., and Reddy, P.H. (2011). Amyloid beta impairs mitochondrial anterograde transport and degenerates synapses in Alzheimer's disease neurons. Biochim Biophys Acta *1812*, 507-513.

Campion, D., Dumanchin, C., Hannequin, D., Dubois, B., Belliard, S., Puel, M., Thomas-Anterion, C., Michon, A., Martin, C., Charbonnier, F., *et al.* (1999). Early-onset autosomal dominant Alzheimer disease: prevalence, genetic heterogeneity, and mutation spectrum. American journal of human genetics *65*, 664-670.

Canto, C., and Auwerx, J. (2009). PGC-1alpha, SIRT1 and AMPK, an energy sensing network that controls energy expenditure. Curr Opin Lipidol *20*, 98-105.

Cappelletti, G., Surrey, T., and Maci, R. (2005). The parkinsonism producing neurotoxin MPP+ affects microtubule dynamics by acting as a destabilising factor. FEBS letters *579*, 4781-4786.

Cardoso, S.M., and Oliveira, C.R. (2003). Glutathione cycle impairment mediates A beta-induced cell toxicity. Free Radic Res *37*, 241-250.

Cardoso, S.M., Pereira, C.F., Moreira, P.I., Arduino, D.M., Esteves, A.R., and Oliveira, C.R. (2010). Mitochondrial control of autophagic lysosomal pathway in Alzheimer's disease. Experimental neurology *223*, 294-298.

Cardoso, S.M., Proenca, M.T., Santos, S., Santana, I., and Oliveira, C.R. (2004a). Cytochrome c oxidase is decreased in Alzheimer's disease platelets. Neurobiology of aging *25*, 105-110.

Cardoso, S.M., Santana, I., Swerdlow, R.H., and Oliveira, C.R. (2004b). Mitochondria dysfunction of Alzheimer's disease cybrids enhances Abeta toxicity. Journal of neurochemistry *89*, 1417-1426.

Cardoso, S.M., Santos, S., Swerdlow, R.H., and Oliveira, C.R. (2001). Functional mitochondria are required for amyloid beta-mediated neurotoxicity. FASEB journal :

official publication of the Federation of American Societies for Experimental Biology *15*, 1439-1441.

Cash, A.D., Aliev, G., Siedlak, S.L., Nunomura, A., Fujioka, H., Zhu, X., Raina, A.K., Vinters, H.V., Tabaton, M., Johnson, A.B., *et al.* (2003). Microtubule reduction in Alzheimer's disease and aging is independent of tau filament formation. The American journal of pathology *162*, 1623-1627.

Casley, C.S., Canevari, L., Land, J.M., Clark, J.B., and Sharpe, M.A. (2002). Beta-amyloid inhibits integrated mitochondrial respiration and key enzyme activities. Journal of neurochemistry *80*, 91-100.

Caspersen, C., Wang, N., Yao, J., Sosunov, A., Chen, X., Lustbader, J.W., Xu, H.W., Stern, D., McKhann, G., and Yan, S.D. (2005). Mitochondrial Abeta: a potential focal point for neuronal metabolic dysfunction in Alzheimer's disease. FASEB journal : official publication of the Federation of American Societies for Experimental Biology *19*, 2040-2041.

Castegna, A., Aksenov, M., Aksenova, M., Thongboonkerd, V., Klein, J.B., Pierce, W.M., Booze, R., Markesbery, W.R., and Butterfield, D.A. (2002a). Proteomic identification of oxidatively modified proteins in Alzheimer's disease brain. Part I: creatine kinase BB, glutamine synthase, and ubiquitin carboxy-terminal hydrolase L-1. Free radical biology & medicine *33*, 562-571.

Castegna, A., Aksenov, M., Thongboonkerd, V., Klein, J.B., Pierce, W.M., Booze, R., Markesbery, W.R., and Butterfield, D.A. (2002b). Proteomic identification of oxidatively modified proteins in Alzheimer's disease brain. Part II: dihydropyrimidinase-related protein 2, alpha-enolase and heat shock cognate 71. J Neurochem *82*, 1524-1532.

Castello, M.A., and Soriano, S. (2013). On the origin of Alzheimer's disease. Trials and tribulations of the amyloid hypothesis. Ageing research reviews *13C*, 10-12.

Cataldo, A.M., Hamilton, D.J., Barnett, J.L., Paskevich, P.A., and Nixon, R.A. (1996). Abnormalities of the endosomal-lysosomal system in Alzheimer's disease: relationship to disease pathogenesis. Advances in experimental medicine and biology *389*, 271-280.

Cereghetti, G.M., Costa, V., and Scorrano, L. (2010). Inhibition of Drp1-dependent mitochondrial fragmentation and apoptosis by a polypeptide antagonist of calcineurin. Cell Death Differ *17*, 1785-1794.

Cereghetti, G.M., Stangherlin, A., Martins de Brito, O., Chang, C.R., Blackstone, C., Bernardi, P., and Scorrano, L. (2008). Dephosphorylation by calcineurin regulates translocation of Drp1 to mitochondria. Proc Natl Acad Sci U S A *105*, 15803-15808.

Chan, D.C. (2006a). Mitochondria: dynamic organelles in disease, aging, and development. Cell *125*, 1241-1252.

Chan, D.C. (2006b). Mitochondrial fusion and fission in mammals. Annu Rev Cell Dev Biol *22*, 79-99.

Chandrasekaran, K., Giordano, T., Brady, D.R., Stoll, J., Martin, L.J., and Rapoport, S.I. (1994). Impairment in mitochondrial cytochrome oxidase gene expression in Alzheimer disease. Brain Res Mol Brain Res *24*, 336-340.

Chang, S.W., Zhang, D., Chung, H.D., and Zassenhaus, H.P. (2000). The frequency of point mutations in mitochondrial DNA is elevated in the Alzheimer's brain. Biochem Biophys Res Commun *273*, 203-208.

Chang, Y.L., Fennema-Notestine, C., Holland, D., McEvoy, L.K., Stricker, N.H., Salmon, D.P., Dale, A.M., Bondi, M.W., and for the Alzheimer's Disease Neuroimaging, I. (2013). APOE interacts with age to modify rate of decline in cognitive and brain changes in Alzheimer's disease. Alzheimer's & dementia : the journal of the Alzheimer's Association.

Chen, H., and Chan, D.C. (2009). Mitochondrial dynamics--fusion, fission, movement, and mitophagy--in neurodegenerative diseases. Hum Mol Genet *18*, R169-176.

Cho, D.H., Nakamura, T., Fang, J., Cieplak, P., Godzik, A., Gu, Z., and Lipton, S.A. (2009). S-nitrosylation of Drp1 mediates beta-amyloid-related mitochondrial fission and neuronal injury. Science *324*, 102-105.

Cho, S.G., Du, Q., Huang, S., and Dong, Z. (2010). Drp1 dephosphorylation in ATP depletion-induced mitochondrial injury and tubular cell apoptosis. American journal of physiology. Renal physiology *299*, F199-206.

Chong, Z.Z., Lin, S.H., Li, F., and Maiese, K. (2005). The sirtuin inhibitor nicotinamide enhances neuronal cell survival during acute anoxic injury through AKT, BAD, PARP, and mitochondrial associated "anti-apoptotic" pathways. Current neurovascular research *2*, 271-285.

Civitarese, A.E., Smith, S.R., and Ravussin, E. (2007). Diet, energy metabolism and mitochondrial biogenesis. Curr Opin Clin Nutr Metab Care *10*, 679-687.

Coleman, M. (2005). Axon degeneration mechanisms: commonality amid diversity. Nature reviews. Neuroscience *6*, 889-898.

Colurso, G.J., Nilson, J.E., and Vervoort, L.G. (2003). Quantitative assessment of DNA fragmentation and beta-amyloid deposition in insular cortex and midfrontal gyrus from patients with Alzheimer's disease. Life Sci *73*, 1795-1803.

Coore, H.G., Denton, R.M., Martin, B.R., and Randle, P.J. (1971). Regulation of adipose tissue pyruvate dehydrogenase by insulin and other hormones. Biochem J *125*, 115-127.

Corral-Debrinski, M., Horton, T., Lott, M.T., Shoffner, J.M., McKee, A.C., Beal, M.F., Graham, B.H., and Wallace, D.C. (1994). Marked changes in mitochondrial DNA deletion levels in Alzheimer brains. Genomics *23*, 471-476.

Coskun, P.E., Beal, M.F., and Wallace, D.C. (2004). Alzheimer's brains harbor somatic mtDNA control-region mutations that suppress mitochondrial transcription and replication. Proc Natl Acad Sci U S A *101*, 10726-10731.

Coskun, P.E., Wyrembak, J., Derbereva, O., Melkonian, G., Doran, E., Lott, I.T., Head, E., Cotman, C.W., and Wallace, D.C. (2010). Systemic mitochondrial dysfunction and the etiology of Alzheimer's disease and down syndrome dementia. J Alzheimers Dis *20 Suppl 2*, S293-310.

Cottrell, D.A., Blakely, E.L., Johnson, M.A., Ince, P.G., and Turnbull, D.M. (2001). Mitochondrial enzyme-deficient hippocampal neurons and choroidal cells in AD. Neurology *57*, 260-264.

Cribbs, D.H., Poon, W.W., Rissman, R.A., and Blurton-Jones, M. (2004). Caspase-mediated degeneration in Alzheimer's disease. Am J Pathol *165*, 353-355.

Cuervo, A.M. (2004). Autophagy: many paths to the same end. Molecular and cellular biochemistry *263*, 55-72.

Cunningham, J.T., Rodgers, J.T., Arlow, D.H., Vazquez, F., Mootha, V.K., and Puigserver, P. (2007). mTOR controls mitochondrial oxidative function through a YY1-PGC-1alpha transcriptional complex. Nature *450*, 736-740.

Da, X., Toledo, J.B., Zee, J., Wolk, D.A., Xie, S.X., Ou, Y., Shacklett, A., Parmpi, P., Shaw, L., Trojanowski, J.Q., *et al.* (2013). Integration and relative value of biomarkers for prediction of MCI to AD progression: Spatial patterns of brain atrophy, cognitive scores, APOE genotype and CSF biomarkers. NeuroImage. Clinical *4*, 164-173.

Dagda, R.K., Cherra, S.J., 3rd, Kulich, S.M., Tandon, A., Park, D., and Chu, C.T. (2009). Loss of PINK1 function promotes mitophagy through effects on oxidative stress and mitochondrial fission. The Journal of biological chemistry *284*, 13843-13855.

Dai, J., Buijs, R.M., Kamphorst, W., and Swaab, D.F. (2002). Impaired axonal transport of cortical neurons in Alzheimer's disease is associated with neuropathological changes. Brain Res *948*, 138-144.

Dawe, B., Procter, A, Philpot, M, (1992). Concepts of mild cognitive impairment in the elderly and their relationship to dementia: a review. Int. J. Geriatr. Psychiatry *7*, 473-479.

de la Monte, S.M., Luong, T., Neely, T.R., Robinson, D., and Wands, J.R. (2000). Mitochondrial DNA damage as a mechanism of cell loss in Alzheimer's disease. Lab Invest *80*, 1323-1335.

De Leenheer, A.P., De Bevere, V.O., and Claeys, A.E. (1979). Measurement of alpha-, beta-, and gamma tocopherol in serum by liquid chromatography. Clin Chem *25*, 425-428.

De Vos, K.J., Chapman, A.L., Tennant, M.E., Manser, C., Tudor, E.L., Lau, K.F., Brownlees, J., Ackerley, S., Shaw, P.J., McLoughlin, D.M., *et al.* (2007). Familial amyotrophic lateral sclerosis-linked SOD1 mutants perturb fast axonal transport to reduce axonal mitochondria content. Hum Mol Genet *16*, 2720-2728.

Denu, J.M. (2005). The Sir 2 family of protein deacetylases. Current opinion in chemical biology *9*, 431-440.

Detmer, S.A., and Chan, D.C. (2007). Functions and dysfunctions of mitochondrial dynamics. Nature reviews. Molecular cell biology *8*, 870-879.

Devi, L., Prabhu, B.M., Galati, D.F., Avadhani, N.G., and Anandatheerthavarada, H.K. (2006). Accumulation of amyloid precursor protein in the mitochondrial import channels of human Alzheimer's disease brain is associated with mitochondrial dysfunction. The Journal of neuroscience : the official journal of the Society for Neuroscience *26*, 9057-9068.

Ding, H., Matthews, T.A., and Johnson, G.V. (2006). Site-specific phosphorylation and caspase cleavage differentially impact tau-microtubule interactions and tau aggregation. The Journal of biological chemistry *281*, 19107-19114.

Divinski, I., Mittelman, L., and Gozes, I. (2004). A femtomolar acting octapeptide interacts with tubulin and protects astrocytes against zinc intoxication. J Biol Chem *279*, 28531-28538.

Draper, H.H., and Hadley, M. (1990). Malondialdehyde determination as index of lipid peroxidation. Methods Enzymol *186*, 421-431.

Du, H., Guo, L., Yan, S., Sosunov, A.A., McKhann, G.M., and Yan, S.S. (2010). Early deficits in synaptic mitochondria in an Alzheimer's disease mouse model. Proceedings of the National Academy of Sciences of the United States of America *107*, 18670-18675.

Du, Y., Wooten, M.C., Gearing, M., and Wooten, M.W. (2009). Age-associated oxidative damage to the p62 promoter: implications for Alzheimer disease. Free radical biology & medicine *46*, 492-501.

Ebneth, A., Godemann, R., Stamer, K., Illenberger, S., Trinczek, B., and Mandelkow, E. (1998). Overexpression of tau protein inhibits kinesin-dependent trafficking of vesicles, mitochondria, and endoplasmic reticulum: implications for Alzheimer's disease. The Journal of cell biology *143*, 777-794.

Eckert, A., Oster, M., Zerfass, R., Hennerici, M., and Muller, W.E. (2001). Elevated levels of fragmented DNA nucleosomes in native and activated lymphocytes indicate an enhanced sensitivity to apoptosis in sporadic Alzheimer's disease. Specific differences to vascular dementia. Dement Geriatr Cogn Disord *12*, 98-105.

Encalada, S.E., and Goldstein, L.S. (2014). Biophysical challenges to axonal transport: motor-cargo deficiencies and neurodegeneration. Annual review of biophysics *43*, 141-169.

Ernster L, N.K. (1967). Microsomal lipid peroxidation. Methods Enzymol *10*, 574-580.

Evin, G., Zhu, A., Holsinger, R.M., Masters, C.L., and Li, Q.X. (2003). Proteolytic processing of the Alzheimer's disease amyloid precursor protein in brain and platelets. Journal of neuroscience research *74*, 386-392.

Feige, J.N., and Auwerx, J. (2007). Transcriptional coregulators in the control of energy homeostasis. Trends Cell Biol *17*, 292-301.

Feinendegen, L.E. (2002). Reactive oxygen species in cell responses to toxic agents. Hum Exp Toxicol *21*, 85-90.

Ferri, C.P., Prince, M., Brayne, C., Brodaty, H., Fratiglioni, L., Ganguli, M., Hall, K., Hasegawa, K., Hendrie, H., Huang, Y., *et al.* (2005). Global prevalence of dementia: a Delphi consensus study. Lancet *366*, 2112-2117.

Folstein, M.F., Folstein, S.E., and McHugh, P.R. (1975). "Mini-mental state". A practical method for grading the cognitive state of patients for the clinician. J Psychiatr Res *12*, 189-198.

Gabbita, S.P., Lovell, M.A., and Markesbery, W.R. (1998). Increased nuclear DNA oxidation in the brain in Alzheimer's disease. J Neurochem *71*, 2034-2040.

Gal, J., Bang, Y., and Choi, H.J. (2012). SIRT2 interferes with autophagy-mediated degradation of protein aggregates in neuronal cells under proteasome inhibition. Neurochemistry international *61*, 992-1000.

Gan, X., Huang, S., Wu, L., Wang, Y., Hu, G., Li, G., Zhang, H., Yu, H., Swerdlow, R.H., Chen, J.X., *et al.* (2014). Inhibition of ERK-DLP1 signaling and mitochondrial division alleviates mitochondrial dysfunction in Alzheimer's disease cybrid cell. Biochimica et biophysica acta *1842*, 220-231.

Geldmacher, D.S., Fritsch, T., McClendon, M.J., and Landreth, G. (2011). A randomized pilot clinical trial of the safety of pioglitazone in treatment of patients with Alzheimer disease. Arch Neurol *68*, 45-50.

Ghavami, S., Shojaei, S., Yeganeh, B., Ande, S.R., Jangamreddy, J.R., Mehrpour, M., Christoffersson, J., Chaabane, W., Moghadam, A.R., Kashani, H.H., *et al.* (2014). Autophagy and apoptosis dysfunction in neurodegenerative disorders. Progress in neurobiology *112*, 24-49.

Ghosh, S., Patel, N., Rahn, D., McAllister, J., Sadeghi, S., Horwitz, G., Berry, D., Wang, K.X., and Swerdlow, R.H. (2007). The thiazolidinedione pioglitazone alters mitochondrial function in human neuron-like cells. Mol Pharmacol *71*, 1695-1702.

Gibson, G.E., Sheu, K.F., and Blass, J.P. (1998). Abnormalities of mitochondrial enzymes in Alzheimer disease. J Neural Transm *105*, 855-870.

Gibson, G.E., Sheu, K.F., Blass, J.P., Baker, A., Carlson, K.C., Harding, B., and Perrino, P. (1988). Reduced activities of thiamine-dependent enzymes in the brains and peripheral tissues of patients with Alzheimer's disease. Archives of neurology *45*, 836-840.

Gibson, G.E., Starkov, A., Blass, J.P., Ratan, R.R., and Beal, M.F. (2010). Cause and consequence: mitochondrial dysfunction initiates and propagates neuronal dysfunction, neuronal death and behavioral abnormalities in age-associated neurodegenerative diseases. Biochim Biophys Acta *1802*, 122-134.

Gold, M., Alderton, C., Zvartau-Hind, M., Egginton, S., Saunders, A.M., Irizarry, M., Craft, S., Landreth, G., Linnamagi, U., and Sawchak, S. (2010). Rosiglitazone monotherapy in mild-to-moderate Alzheimer's disease: results from a randomized, double-blind, placebo-controlled phase III study. Dement Geriatr Cogn Disord *30*, 131-146.

Goldstein, L.S. (2012). Axonal transport and neurodegenerative disease: can we see the elephant? Progress in neurobiology *99*, 186-190.

Gomes, A.P., Price, N.L., Ling, A.J., Moslehi, J.J., Montgomery, M.K., Rajman, L., White, J.P., Teodoro, J.S., Wrann, C.D., Hubbard, B.P., *et al.* (2013). Declining NAD(+) Induces a Pseudohypoxic State Disrupting Nuclear-Mitochondrial Communication during Aging. Cell *155*, 1624-1638.

Gong, C.X., and Iqbal, K. (2008). Hyperphosphorylation of microtubule-associated protein tau: a promising therapeutic target for Alzheimer disease. Current medicinal chemistry *15*, 2321-2328.

Gotz, J., Ittner, L.M., Schonrock, N., and Cappai, R. (2008). An update on the toxicity of Abeta in Alzheimer's disease. Neuropsychiatric disease and treatment *4*, 1033-1042.

Gotz, J., Schild, A., Hoerndli, F., and Pennanen, L. (2004). Amyloid-induced neurofibrillary tangle formation in Alzheimer's disease: insight from transgenic mouse and tissue-culture models. International journal of developmental neuroscience : the official journal of the International Society for Developmental Neuroscience *22*, 453-465.

Gozes, I., and Divinski, I. (2004). The femtomolar-acting NAP interacts with microtubules: Novel aspects of astrocyte protection. J Alzheimers Dis *6*, S37-41.

Gozes, I., and Divinski, I. (2007). NAP, a neuroprotective drug candidate in clinical trials, stimulates microtubule assembly in the living cell. Curr Alzheimer Res *4*, 507-509.

Gozes, I., Morimoto, B.H., Tiong, J., Fox, A., Sutherland, K., Dangoor, D., Holser-Cochav, M., Vered, K., Newton, P., Aisen, P.S., *et al.* (2005). NAP: research and development of a peptide derived from activity-dependent neuroprotective protein (ADNP). CNS Drug Rev *11*, 353-368.

Gozes, I., Stewart, A., Morimoto, B., Fox, A., Sutherland, K., and Schmeche, D. (2009). Addressing Alzheimer's disease tangles: from NAP to AL-108. Curr Alzheimer Res *6*, 455-460.

Grammas, P., Samany, P.G., and Thirumangalakudi, L. (2006). Thrombin and inflammatory proteins are elevated in Alzheimer's disease microvessels: implications for disease pathogenesis. Journal of Alzheimer's disease : JAD *9*, 51-58.

Green, K.N., Steffan, J.S., Martinez-Coria, H., Sun, X., Schreiber, S.S., Thompson, L.M., and LaFerla, F.M. (2008). Nicotinamide restores cognition in Alzheimer's disease transgenic mice via a mechanism involving sirtuin inhibition and selective reduction of Thr231-phosphotau. The Journal of neuroscience : the official journal of the Society for Neuroscience *28*, 11500-11510.

Greggio, S., de Paula, S., de Oliveira, I.M., Trindade, C., Rosa, R.M., Henriques, J.A., and DaCosta, J.C. (2011). NAP prevents acute cerebral oxidative stress and protects against long-term brain injury and cognitive impairment in a model of neonatal hypoxia-ischemia. Neurobiol Dis *44*, 152-159.

Guarente, L. (2007). Sirtuins in aging and disease. Cold Spring Harb Symp Quant Biol *72*, 483-488.

Guerreiro, M. (1998). Contribution of Neuropsychology to the Study of Dementias. Ph.D. thesis In Faculty of Medicine of Lisbon, (Lisbon, Portugal).

Guerreiro M, F.S., Barreto J, (2003a). Escalas e Testes na Demência. Grupo de Estudos de Envelhecimento Cerebral e Demência. pp 33-49.

Guerreiro M, S.A., Botelho MA, (2003b). Avaliação Breve do Estado Mental: Escalas e Testes na Demência Grupo de Estudos de Envelhecimento Cerebral e Demência *pp 27-32*.

Guo, H., Albrecht, S., Bourdeau, M., Petzke, T., Bergeron, C., and LeBlanc, A.C. (2004). Active caspase-6 and caspase-6-cleaved tau in neuropil threads, neuritic plaques, and neurofibrillary tangles of Alzheimer's disease. Am J Pathol *165*, 523-531.

Haigis, M.C., and Guarente, L.P. (2006). Mammalian sirtuins--emerging roles in physiology, aging, and calorie restriction. Genes Dev *20*, 2913-2921.

Hamblet, N.S., and Castora, F.J. (1997). Elevated levels of the Kearns-Sayre syndrome mitochondrial DNA deletion in temporal cortex of Alzheimer's patients. Mutat Res *379*, 253-262.

Han, S.H. (2009). Potential role of sirtuin as a therapeutic target for neurodegenerative diseases. Journal of clinical neurology *5*, 120-125.

Hands, S.L., Proud, C.G., and Wyttenbach, A. (2009). mTOR's role in ageing: protein synthesis or autophagy? Aging *1*, 586-597.

Handschin, C., and Spiegelman, B.M. (2006). Peroxisome proliferator-activated receptor gamma coactivator 1 coactivators, energy homeostasis, and metabolism. Endocr Rev *27*, 728-735.

Hanger, D.P., Lau, D.H., Phillips, E.C., Bondulich, M.K., Guo, T., Woodward, B.W., Pooler, A.M., and Noble, W. (2014). Intracellular and extracellular roles for tau in neurodegenerative disease. Journal of Alzheimer's disease : JAD *40 Suppl 1*, S37-45.

Hansford, R.G., Hogue, B.A., and Mildaziene, V. (1997). Dependence of H2O2 formation by rat heart mitochondria on substrate availability and donor age. J Bioenerg Biomembr *29*, 89-95.

Hansson Petersen, C.A., Alikhani, N., Behbahani, H., Wiehager, B., Pavlov, P.F., Alafuzoff, I., Leinonen, V., Ito, A., Winblad, B., Glaser, E., *et al.* (2008). The amyloid beta-peptide is imported into mitochondria via the TOM import machinery and localized to mitochondrial cristae. Proceedings of the National Academy of Sciences of the United States of America *105*, 13145-13150.

Hardy, J., and Selkoe, D.J. (2002). The amyloid hypothesis of Alzheimer's disease: progress and problems on the road to therapeutics. Science *297*, 353-356.

Harting, K., and Knoll, B. (2010). SIRT2-mediated protein deacetylation: An emerging key regulator in brain physiology and pathology. European journal of cell biology *89*, 262-269.

Hasegawa, T., Baba, T., Kobayashi, M., Konno, M., Sugeno, N., Kikuchi, A., Itoyama, Y., and Takeda, A. (2010). Role of TPPP/p25 on alpha-synuclein-mediated oligodendroglial degeneration and the protective effect of SIRT2 inhibition in a cellular model of multiple system atrophy. Neurochemistry international *57*, 857-866.

Hempen, B., and Brion, J.P. (1996). Reduction of acetylated alpha-tubulin immunoreactivity in neurofibrillary tangle-bearing neurons in Alzheimer's disease. Journal of neuropathology and experimental neurology *55*, 964-972.

Henriques, A.G., Vieira, S.I., da Cruz, E.S.E.F., and da Cruz, E.S.O.A. (2010). Abeta promotes Alzheimer's disease-like cytoskeleton abnormalities with consequences to APP processing in neurons. Journal of neurochemistry *113*, 761-771.

Hensley, K., Floyd, R.A., Zheng, N.Y., Nael, R., Robinson, K.A., Nguyen, X., Pye, Q.N., Stewart, C.A., Geddes, J., Markesbery, W.R., *et al.* (1999). p38 kinase is activated in the Alzheimer's disease brain. J Neurochem *72*, 2053-2058.

Hirai, K., Aliev, G., Nunomura, A., Fujioka, H., Russell, R.L., Atwood, C.S., Johnson, A.B., Kress, Y., Vinters, H.V., Tabaton, M., *et al.* (2001). Mitochondrial abnormalities in Alzheimer's disease. The Journal of neuroscience : the official journal of the Society for Neuroscience *21*, 3017-3023.

Hollenbeck, P.J., and Saxton, W.M. (2005). The axonal transport of mitochondria. J Cell Sci *118*, 5411-5419.

Holloszy, J.O., and Coyle, E.F. (1984). Adaptations of skeletal muscle to endurance exercise and their metabolic consequences. J Appl Physiol *56*, 831-838.

Honea, R.A., Swerdlow, R.H., Vidoni, E., and Burns, J.M. (2011). Progressive regional atrophy in normaladults with a maternal history of Alzheimer disease. Neurology *76*, 822-829.

Honea, R.A., Swerdlow, R.H., Vidoni, E.D., Goodwin, J., and Burns, J.M. (2010). Reduced gray matter volume in normal adults with a maternal family history of Alzheimer disease. Neurology *74*, 113-120.

Hood, D.A. (2009). Mechanisms of exercise-induced mitochondrial biogenesis in skeletal muscle. Appl Physiol Nutr Metab *34*, 465-472.

Hoppins, S., Lackner, L., and Nunnari, J. (2007). The machines that divide and fuse mitochondria. Annu Rev Biochem *76*, 751-780.

Hunter, S., and Brayne, C. (2013). Integrating the molecular and the population approaches to dementia research to help guide the future development of appropriate therapeutics. Biochemical pharmacology.

Idan-Feldman, A., Schirer, Y., Polyzoidou, E., Touloumi, O., Lagoudaki, R., Grigoriadis, N.C., and Gozes, I. (2011). Davunetide (NAP) as a preventative treatment for central nervous system complications in a diabetes rat model. Neurobiol Dis *44*, 327-339.

Indo, H.P., Davidson, M., Yen, H.C., Suenaga, S., Tomita, K., Nishii, T., Higuchi, M., Koga, Y., Ozawa, T., and Majima, H.J. (2007). Evidence of ROS generation by mitochondria in cells with impaired electron transport chain and mitochondrial DNA damage. Mitochondrion *7*, 106-118.

Inoue, M., Sato, E.F., Nishikawa, M., Park, A.M., Kira, Y., Imada, I., and Utsumi, K. (2003). Mitochondrial generation of reactive oxygen species and its role in aerobic life. Curr Med Chem *10*, 2495-2505.

Inoue, T., Hiratsuka, M., Osaki, M., Yamada, H., Kishimoto, I., Yamaguchi, S., Nakano, S., Katoh, M., Ito, H., and Oshimura, M. (2007). SIRT2, a tubulin deacetylase, acts to block the entry to chromosome condensation in response to mitotic stress. Oncogene *26*, 945-957.

Inoue, T., Nakayama, Y., Li, Y., Matsumori, H., Takahashi, H., Kojima, H., Wanibuchi, H., Katoh, M., and Oshimura, M. (2014). SIRT2 knockdown increases basal autophagy and prevents postslippage death by abnormally prolonging the mitotic arrest that is induced by microtubule inhibitors. The FEBS journal *281*, 2623-2637.

Iqbal, K., and Grundke-Iqbal, I. (2008). Alzheimer neurofibrillary degeneration: significance, etiopathogenesis, therapeutics and prevention. Journal of cellular and molecular medicine *12*, 38-55.

Iqbal, K., Liu, F., and Gong, C.X. (2014). Alzheimer disease therapeutics: Focus on the disease and not just plaques and tangles. Biochemical pharmacology.

Ishihara, N., Nomura, M., Jofuku, A., Kato, H., Suzuki, S.O., Masuda, K., Otera, H., Nakanishi, Y., Nonaka, I., Goto, Y., *et al.* (2009). Mitochondrial fission factor Drp1 is essential for embryonic development and synapse formation in mice. Nat Cell Biol *11*, 958-966.

Jaeger, P.A., Pickford, F., Sun, C.H., Lucin, K.M., Masliah, E., and Wyss-Coray, T. (2010). Regulation of amyloid precursor protein processing by the Beclin 1 complex. PloS one *5*, e11102.

Jager, S., Handschin, C., St-Pierre, J., and Spiegelman, B.M. (2007). AMP-activated protein kinase (AMPK) action in skeletal muscle via direct phosphorylation of PGC-1alpha. Proc Natl Acad Sci U S A *104*, 12017-12022.

Javitt, D.C., Buchanan, R.W., Keefe, R.S., Kern, R., McMahon, R.P., Green, M.F., Lieberman, J., Goff, D.C., Csernansky, J.G., McEvoy, J.P., *et al.* (2011). Effect of the neuroprotective peptide davunetide (AL-108) on cognition and functional capacity in schizophrenia. Schizophr Res.

Ji, L.L. (1999). Antioxidants and oxidative stress in exercise. Proc Soc Exp Biol Med *222*, 283-292.

Jin, Q., Yan, T., Ge, X., Sun, C., Shi, X., and Zhai, Q. (2007). Cytoplasm-localized SIRT1 enhances apoptosis. J Cell Physiol *213*, 88-97.

Julien, C., Tremblay, C., Emond, V., Lebbadi, M., Salem, N., Jr., Bennett, D.A., and Calon, F. (2009). Sirtuin 1 reduction parallels the accumulation of tau in Alzheimer disease. Journal of neuropathology and experimental neurology *68*, 48-58.

Kawamoto, E.M., Munhoz, C.D., Glezer, I., Bahia, V.S., Caramelli, P., Nitrini, R., Gorjao, R., Curi, R., Scavone, C., and Marcourakis, T. (2005). Oxidative state in platelets and erythrocytes in aging and Alzheimer's disease. Neurobiol Aging *26*, 857-864.

Keil, U., Bonert, A., Marques, C.A., Scherping, I., Weyermann, J., Strosznajder, J.B., Muller-Spahn, F., Haass, C., Czech, C., Pradier, L., *et al.* (2004). Amyloid beta-induced changes in nitric oxide production and mitochondrial activity lead to apoptosis. The Journal of biological chemistry *279*, 50310-50320.

Keller, J.N., Schmitt, F.A., Scheff, S.W., Ding, Q., Chen, Q., Butterfield, D.A., and Markesbery, W.R. (2005). Evidence of increased oxidative damage in subjects with mild cognitive impairment. Neurology *64*, 1152-1156.

Khan, S.M., Cassarino, D.S., Abramova, N.N., Keeney, P.M., Borland, M.K., Trimmer, P.A., Krebs, C.T., Bennett, J.C., Parks, J.K., Swerdlow, R.H., *et al.* (2000). Alzheimer's

disease cybrids replicate beta-amyloid abnormalities through cell death pathways. Ann Neurol *48*, 148-155.

King, M.P., and Attardi, G. (1989). Human cells lacking mtDNA: repopulation with exogenous mitochondria by complementation. Science *246*, 500-503.

Kish, S.J., Mastrogiacomo, F., Guttman, M., Furukawa, Y., Taanman, J.W., Dozic, S., Pandolfo, M., Lamarche, J., DiStefano, L., and Chang, L.J. (1999). Decreased brain protein levels of cytochrome oxidase subunits in Alzheimer's disease and in hereditary spinocerebellar ataxia disorders: a nonspecific change? J Neurochem *72*, 700-707.

Kitamura, Y., Shimohama, S., Kamoshima, W., Ota, T., Matsuoka, Y., Nomura, Y., Smith, M.A., Perry, G., Whitehouse, P.J., and Taniguchi, T. (1998). Alteration of proteins regulating apoptosis, Bcl-2, Bcl-x, Bax, Bak, Bad, ICH-1 and CPP32, in Alzheimer's disease. Brain Res *780*, 260-269.

Klionsky, D.J., Elazar, Z., Seglen, P.O., and Rubinsztein, D.C. (2008). Does bafilomycin A1 block the fusion of autophagosomes with lysosomes? Autophagy *4*, 849-850.

Kochl, R., Hu, X.W., Chan, E.Y., and Tooze, S.A. (2006). Microtubules facilitate autophagosome formation and fusion of autophagosomes with endosomes. Traffic *7*, 129-145.

Lagouge, M., Argmann, C., Gerhart-Hines, Z., Meziane, H., Lerin, C., Daussin, F., Messadeq, N., Milne, J., Lambert, P., Elliott, P., *et al.* (2006). Resveratrol improves mitochondrial function and protects against metabolic disease by activating SIRT1 and PGC-1alpha. Cell *127*, 1109-1122.

Lambert, A.J., Wang, B., Yardley, J., Edwards, J., and Merry, B.J. (2004). The effect of aging and caloric restriction on mitochondrial protein density and oxygen consumption. Exp Gerontol *39*, 289-295.

Lassmann, H., Bancher, C., Breitschopf, H., Wegiel, J., Bobinski, M., Jellinger, K., and Wisniewski, H.M. (1995). Cell death in Alzheimer's disease evaluated by DNA fragmentation in situ. Acta Neuropathol *89*, 35-41.

Lauderback, C.M., Hackett, J.M., Huang, F.F., Keller, J.N., Szweda, L.I., Markesbery, W.R., and Butterfield, D.A. (2001). The glial glutamate transporter, GLT-1, is oxidatively modified by 4-hydroxy-2-nonenal in the Alzheimer's disease brain: the role of Abeta1-42. J Neurochem *78*, 413-416.

Laws, S.M., Hone, E., Gandy, S., and Martins, R.N. (2003). Expanding the association between the APOE gene and the risk of Alzheimer's disease: possible roles for APOE

promoter polymorphisms and alterations in APOE transcription. Journal of neurochemistry *84*, 1215-1236.

Lee, J.A., and Gao, F.B. (2008). Regulation of Abeta pathology by beclin 1: a protective role for autophagy? The Journal of clinical investigation *118*, 2015-2018.

Lee, S., Sato, Y., and Nixon, R.A. (2011). Primary lysosomal dysfunction causes cargo-specific deficits of axonal transport leading to Alzheimer-like neuritic dystrophy. Autophagy *7*, 1562-1563.

Lee, V.M., Daughenbaugh, R., and Trojanowski, J.Q. (1994). Microtubule stabilizing drugs for the treatment of Alzheimer's disease. Neurobiol Aging *15 Suppl 2*, S87-89.

Levine, B., and Kroemer, G. (2008). Autophagy in the pathogenesis of disease. Cell *132*, 27-42.

Levine, R.L., Williams, J.A., Stadtman, E.R., and Shacter, E. (1994). Carbonyl assays for determination of oxidatively modified proteins. Methods Enzymol *233*, 346-357.

Li, B., Chohan, M.O., Grundke-Iqbal, I., and Iqbal, K. (2007a). Disruption of microtubule network by Alzheimer abnormally hyperphosphorylated tau. Acta neuropathologica *113*, 501-511.

Li, G., Faibushevich, A., Turunen, B.J., Yoon, S.O., Georg, G., Michaelis, M.L., and Dobrowsky, R.T. (2003). Stabilization of the cyclin-dependent kinase 5 activator, p35, by paclitaxel decreases beta-amyloid toxicity in cortical neurons. J Neurochem *84*, 347-362.

Li, W., Zhang, B., Tang, J., Cao, Q., Wu, Y., Wu, C., Guo, J., Ling, E.A., and Liang, F. (2007b). Sirtuin 2, a mammalian homolog of yeast silent information regulator-2 longevity regulator, is an oligodendroglial protein that decelerates cell differentiation through deacetylating alpha-tubulin. The Journal of neuroscience : the official journal of the Society for Neuroscience *27*, 2606-2616.

Li, W.P., Chan, W.Y., Lai, H.W., and Yew, D.T. (1997). Terminal dUTP nick end labeling (TUNEL) positive cells in the different regions of the brain in normal aging and Alzheimer patients. J Mol Neurosci *8*, 75-82.

Li, X., Alafuzoff, I., Soininen, H., Winblad, B., and Pei, J.J. (2005). Levels of mTOR and its downstream targets 4E-BP1, eEF2, and eEF2 kinase in relationships with tau in Alzheimer's disease brain. The FEBS journal *272*, 4211-4220.

Li, Z., Okamoto, K., Hayashi, Y., and Sheng, M. (2004). The importance of dendritic mitochondria in the morphogenesis and plasticity of spines and synapses. Cell *119*, 873-887.

Liang, W.S., Reiman, E.M., Valla, J., Dunckley, T., Beach, T.G., Grover, A., Niedzielko, T.L., Schneider, L.E., Mastroeni, D., Caselli, R., *et al.* (2008). Alzheimer's disease is associated with reduced expression of energy metabolism genes in posterior cingulate neurons. Proc Natl Acad Sci U S A *105*, 4441-4446.

Lin, M.T., and Beal, M.F. (2006). Mitochondrial dysfunction and oxidative stress in neurodegenerative diseases. Nature *443*, 787-795.

Lin, M.T., Simon, D.K., Ahn, C.H., Kim, L.M., and Beal, M.F. (2002). High aggregate burden of somatic mtDNA point mutations in aging and Alzheimer's disease brain. Hum Mol Genet *11*, 133-145.

Liu, Y., Ali, S.M., Boge, T.C., Georg, G.I., Victory, S., Zygmunt, J., Marquez, R.T., and Himes, R.H. (2002). A systematic SAR study of C10 modified paclitaxel analogues using a combinatorial approach. Comb Chem High Throughput Screen *5*, 39-48.

Liu, Y., Liu, F., Iqbal, K., Grundke-Iqbal, I., and Gong, C.X. (2008). Decreased glucose transporters correlate to abnormal hyperphosphorylation of tau in Alzheimer disease. FEBS Lett *582*, 359-364.

Lobo, A., Launer, L.J., Fratiglioni, L., Andersen, K., Di Carlo, A., Breteler, M.M., Copeland, J.R., Dartigues, J.F., Jagger, C., Martinez-Lage, J., *et al.* (2000). Prevalence of dementia and major subtypes in Europe: A collaborative study of population-based cohorts. Neurologic Diseases in the Elderly Research Group. Neurology *54*, S4-9.

Lopez-Lluch, G., Hunt, N., Jones, B., Zhu, M., Jamieson, H., Hilmer, S., Cascajo, M.V., Allard, J., Ingram, D.K., Navas, P., *et al.* (2006). Calorie restriction induces mitochondrial biogenesis and bioenergetic efficiency. Proc Natl Acad Sci U S A *103*, 1768-1773.

Lovell, M.A., and Markesbery, W.R. (2007). Oxidative DNA damage in mild cognitive impairment and late-stage Alzheimer's disease. Nucleic Acids Res *35*, 7497-7504.

Lovell, M.A., and Markesbery, W.R. (2008). Oxidatively modified RNA in mild cognitive impairment. Neurobiol Dis *29*, 169-175.

Lu, J., Wang, K., Rodova, M., Esteves, R., Berry, D., E, L., Crafter, A., Barrett, M., Cardoso, S.M., Onyango, I., *et al.* (2010). Polymorphic variation in cytochrome oxidase subunit genes. Journal of Alzheimer's disease : JAD *21*, 141-154.

Luthi-Carter, R., Taylor, D.M., Pallos, J., Lambert, E., Amore, A., Parker, A., Moffitt, H., Smith, D.L., Runne, H., Gokce, O., *et al.* (2010). SIRT2 inhibition achieves neuroprotection by decreasing sterol biosynthesis. Proceedings of the National Academy of Sciences of the United States of America *107*, 7927-7932.

Maas, T., Eidenmuller, J., and Brandt, R. (2000). Interaction of tau with the neural membrane cortex is regulated by phosphorylation at sites that are modified in paired helical filaments. The Journal of biological chemistry *275*, 15733-15740.

MacAskill, A.F., Atkin, T.A., and Kittler, J.T. (2010). Mitochondrial trafficking and the provision of energy and calcium buffering at excitatory synapses. Eur J Neurosci *32*, 231-240.

Manczak, M., Anekonda, T.S., Henson, E., Park, B.S., Quinn, J., and Reddy, P.H. (2006). Mitochondria are a direct site of A beta accumulation in Alzheimer's disease neurons: implications for free radical generation and oxidative damage in disease progression. Human molecular genetics *15*, 1437-1449.

Manczak, M., Calkins, M.J., and Reddy, P.H. (2011a). Impaired mitochondrial dynamics and abnormal interaction of amyloid beta with mitochondrial protein Drp1 in neurons from patients with Alzheimer's disease: implications for neuronal damage. Hum Mol Genet.

Manczak, M., Calkins, M.J., and Reddy, P.H. (2011b). Impaired mitochondrial dynamics and abnormal interaction of amyloid beta with mitochondrial protein Drp1 in neurons from patients with Alzheimer's disease: implications for neuronal damage. Human molecular genetics *20*, 2495-2509.

Manczak, M., Park, B.S., Jung, Y., and Reddy, P.H. (2004). Differential expression of oxidative phosphorylation genes in patients with Alzheimer's disease: implications for early mitochondrial dysfunction and oxidative damage. Neuromolecular medicine *5*, 147-162.

Markesbery, W.R., and Lovell, M.A. (1998). Four-hydroxynonenal, a product of lipid peroxidation, is increased in the brain in Alzheimer's disease. Neurobiol Aging *19*, 33-36.

Markesbery, W.R., and Lovell, M.A. (2007). Damage to lipids, proteins, DNA, and RNA in mild cognitive impairment. Arch Neurol *64*, 954-956.

Marlow, L., Cain, M., Pappolla, M.A., and Sambamurti, K. (2003). Beta-secretase processing of the Alzheimer's amyloid protein precursor (APP). Journal of molecular neuroscience : MN *20*, 233-239.

Masliah, E., Hansen, L., Mallory, M., Albright, T., and Terry, R.D. (1991). Abnormal brain spectrin immunoreactivity in sprouting neurons in Alzheimer disease. Neurosci Lett *129*, 1-5.

Masliah, E., Iimoto, D.S., Saitoh, T., Hansen, L.A., and Terry, R.D. (1990). Increased immunoreactivity of brain spectrin in Alzheimer disease: a marker for synapse loss? Brain Res *531*, 36-44.

Masliah, E., Mallory, M., Alford, M., Tanaka, S., and Hansen, L.A. (1998). Caspase dependent DNA fragmentation might be associated with excitotoxicity in Alzheimer disease. J Neuropathol Exp Neurol *57*, 1041-1052.

Massaad, C.A., Amin, S.K., Hu, L., Mei, Y., Klann, E., and Pautler, R.G. (2010). Mitochondrial superoxide contributes to blood flow and axonal transport deficits in the Tg2576 mouse model of Alzheimer's disease. PLoS One *5*, e10561.

Matsuda, H. (2007). The role of neuroimaging in mild cognitive impairment. Neuropathology : official journal of the Japanese Society of Neuropathology *27*, 570-577.

Matsuoka, Y., Gray, A.J., Hirata-Fukae, C., Minami, S.S., Waterhouse, E.G., Mattson, M.P., LaFerla, F.M., Gozes, I., and Aisen, P.S. (2007). Intranasal NAP administration reduces accumulation of amyloid peptide and tau hyperphosphorylation in a transgenic mouse model of Alzheimer's disease at early pathological stage. J Mol Neurosci *31*, 165-170.

Matsuoka, Y., Jouroukhin, Y., Gray, A.J., Ma, L., Hirata-Fukae, C., Li, H.F., Feng, L., Lecanu, L., Walker, B.R., Planel, E., *et al.* (2008). A neuronal microtubule-interacting agent, NAPVSIPQ, reduces tau pathology and enhances cognitive function in a mouse model of Alzheimer's disease. The Journal of pharmacology and experimental therapeutics *325*, 146-153.

Mattson, M.P. (2004). Pathways towards and away from Alzheimer's disease. Nature *430*, 631-639.

Mattson, M.P., Gleichmann, M., and Cheng, A. (2008). Mitochondria in neuroplasticity and neurological disorders. Neuron *60*, 748-766.

Maxwell, M.M., Tomkinson, E.M., Nobles, J., Wizeman, J.W., Amore, A.M., Quinti, L., Chopra, V., Hersch, S.M., and Kazantsev, A.G. (2011). The Sirtuin 2 microtubule deacetylase is an abundant neuronal protein that accumulates in the aging CNS. Human molecular genetics *20*, 3986-3996.

McKhann, G., Drachman, D., Folstein, M., Katzman, R., Price, D., and Stadlan, E.M. (1984). Clinical diagnosis of Alzheimer's disease: report of the NINCDS-ADRDA Work Group under the auspices of Department of Health and Human Services Task Force on Alzheimer's Disease. Neurology *34*, 939-944.

Mecocci, P., MacGarvey, U., and Beal, M.F. (1994). Oxidative damage to mitochondrial DNA is increased in Alzheimer's disease. Ann Neurol *36*, 747-751.

Mecocci, P., Polidori, M.C., Cherubini, A., Ingegni, T., Mattioli, P., Catani, M., Rinaldi, P., Cecchetti, R., Stahl, W., Senin, U., *et al.* (2002). Lymphocyte oxidative DNA damage and plasma antioxidants in Alzheimer disease. Arch Neurol *59*, 794-798.

Mecocci, P., Polidori, M.C., Ingegni, T., Cherubini, A., Chionne, F., Cecchetti, R., and Senin, U. (1998). Oxidative damage to DNA in lymphocytes from AD patients. Neurology *51*, 1014-1017.

Meissner, C., Lorenz, H., Weihofen, A., Selkoe, D.J., and Lemberg, M.K. (2011). The mitochondrial intramembrane protease PARL cleaves human Pink1 to regulate Pink1 trafficking. Journal of neurochemistry *117*, 856-867.

Meng, X., and D'Arcy, C. (2013). Apolipoprotein E gene, environmental risk factors, and their interactions in dementia among seniors. International journal of geriatric psychiatry *28*, 1005-1014.

Michaelis, M.L., Dobrowsky, R.T., and Li, G. (2002). Tau neurofibrillary pathology and microtubule stability. J Mol Neurosci *19*, 289-293.

Michan, S., and Sinclair, D. (2007). Sirtuins in mammals: insights into their biological function. The Biochemical journal *404*, 1-13.

Michiorri, S., Gelmetti, V., Giarda, E., Lombardi, F., Romano, F., Marongiu, R., Nerini-Molteni, S., Sale, P., Vago, R., Arena, G., *et al.* (2010). The Parkinson-associated protein PINK1 interacts with Beclin1 and promotes autophagy. Cell death and differentiation *17*, 962-974.

Migliore, L., Fontana, I., Trippi, F., Colognato, R., Coppede, F., Tognoni, G., Nucciarone, B., and Siciliano, G. (2005). Oxidative DNA damage in peripheral leukocytes of mild cognitive impairment and AD patients. Neurobiology of aging *26*, 567-573.

Millecamps, S., and Julien, J.P. (2013). Axonal transport deficits and neurodegenerative diseases. Nature reviews. Neuroscience *14*, 161-176.

Miller, S.W., Trimmer, P.A., Parker, W.D., Jr., and Davis, R.E. (1996). Creation and characterization of mitochondrial DNA-depleted cell lines with "neuronal-like" properties. J Neurochem *67*, 1897-1907.

Miyasaka, T., Sato, S., Tatebayashi, Y., and Takashima, A. (2010). Microtubule destruction induces tau liberation and its subsequent phosphorylation. FEBS letters *584*, 3227-3232.

Mizushima, N. (2005). A(beta) generation in autophagic vacuoles. The Journal of cell biology *171*, 15-17.

Mizushima, N., Levine, B., Cuervo, A.M., and Klionsky, D.J. (2008). Autophagy fights disease through cellular self-digestion. Nature *451*, 1069-1075.

Mohs, R.C., Rosen, W.G., and Davis, K.L. (1983). The Alzheimer's disease assessment scale: an instrument for assessing treatment efficacy. Psychopharmacol Bull *19*, 448-450.

Mondragon-Rodriguez, S., Perry, G., Luna-Munoz, J., Acevedo-Aquino, M.C., and Williams, S. (2014). Phosphorylation of tau protein at sites Ser(396-404) is one of the earliest events in Alzheimer's disease and Down syndrome. Neuropathology and applied neurobiology *40*, 121-135.

Moniot, S., Weyand, M., and Steegborn, C. (2012). Structures, substrates, and regulators of Mammalian sirtuins - opportunities and challenges for drug development. Frontiers in pharmacology *3*, 16.

Moreira, P.I., Cardoso, S.M., Santos, M.S., and Oliveira, C.R. (2006). The key role of mitochondria in Alzheimer's disease. J Alzheimers Dis *9*, 101-110.

Moreira, P.I., Siedlak, S.L., Wang, X., Santos, M.S., Oliveira, C.R., Tabaton, M., Nunomura, A., Szweda, L.I., Aliev, G., Smith, M.A., *et al.* (2007). Autophagocytosis of mitochondria is prominent in Alzheimer disease. Journal of neuropathology and experimental neurology *66*, 525-532.

Morocz, M., Kalman, J., Juhasz, A., Sinko, I., McGlynn, A.P., Downes, C.S., Janka, Z., and Rasko, I. (2002). Elevated levels of oxidative DNA damage in lymphocytes from patients with Alzheimer's disease. Neurobiol Aging *23*, 47-53.

Morris, J.C., Storandt, M., Miller, J.P., McKeel, D.W., Price, J.L., Rubin, E.H., and Berg, L. (2001). Mild cognitive impairment represents early-stage Alzheimer disease. Archives of neurology *58*, 397-405.

Morten, K.J., Ackrell, B.A., and Melov, S. (2006). Mitochondrial reactive oxygen species in mice lacking superoxide dismutase 2: attenuation via antioxidant treatment. J Biol Chem *281*, 3354-3359.

Mosconi, L., Berti, V., Swerdlow, R.H., Pupi, A., Duara, R., and de Leon, M. (2010a). Maternal transmission of Alzheimer's disease: prodromal metabolic phenotype and the search for genes. Hum Genomics *4*, 170-193.

Mosconi, L., Brys, M., Switalski, R., Mistur, R., Glodzik, L., Pirraglia, E., Tsui, W., De Santi, S., and de Leon, M.J. (2007). Maternal family history of Alzheimer's disease

predisposes to reduced brain glucose metabolism. Proc Natl Acad Sci U S A *104*, 19067-19072.

Mosconi, L., Glodzik, L., Mistur, R., McHugh, P., Rich, K.E., Javier, E., Williams, S., Pirraglia, E., De Santi, S., Mehta, P.D., *et al.* (2010b). Oxidative stress and amyloid-beta pathology in normal individuals with a maternal history of Alzheimer's. Biol Psychiatry *68*, 913-921.

Mosconi, L., Mistur, R., Switalski, R., Brys, M., Glodzik, L., Rich, K., Pirraglia, E., Tsui, W., De Santi, S., and de Leon, M.J. (2009). Declining brain glucose metabolism in normal individuals with a maternal history of Alzheimer disease. Neurology *72*, 513-520.

Mosconi, L., Rinne, J.O., Tsui, W.H., Berti, V., Li, Y., Wang, H., Murray, J., Scheinin, N., Nagren, K., Williams, S., *et al.* (2010c). Increased fibrillar amyloid-{beta} burden in normal individuals with a family history of late-onset Alzheimer's. Proc Natl Acad Sci U S A *107*, 5949-5954.

Nagy, Z., Esiri, M.M., LeGris, M., and Matthews, P.M. (1999). Mitochondrial enzyme expression in the hippocampus in relation to Alzheimer-type pathology. Acta Neuropathol *97*, 346-354.

Nathan, B.P., Chang, K.C., Bellosta, S., Brisch, E., Ge, N., Mahley, R.W., and Pitas, R.E. (1995). The inhibitory effect of apolipoprotein E4 on neurite outgrowth is associated with microtubule depolymerization. The Journal of biological chemistry *270*, 19791-19799.

Nemoto, S., Fergusson, M.M., and Finkel, T. (2005). SIRT1 functionally interacts with the metabolic regulator and transcriptional coactivator PGC-1{alpha}. J Biol Chem *280*, 16456-16460.

Neve, R.L., McPhie, D.L., and Chen, Y. (2000). Alzheimer's disease: a dysfunction of the amyloid precursor protein(1). Brain research *886*, 54-66.

Nilsson, P., Loganathan, K., Sekiguchi, M., Matsuba, Y., Hui, K., Tsubuki, S., Tanaka, M., Iwata, N., Saito, T., and Saido, T.C. (2013). Abeta secretion and plaque formation depend on autophagy. Cell reports *5*, 61-69.

Nilsson, P., and Saido, T.C. (2014). Dual roles for autophagy: degradation and secretion of Alzheimer's disease Abeta peptide. BioEssays : news and reviews in molecular, cellular and developmental biology *36*, 570-578.

Nisoli, E., Tonello, C., Cardile, A., Cozzi, V., Bracale, R., Tedesco, L., Falcone, S., Valerio, A., Cantoni, O., Clementi, E., *et al.* (2005). Calorie restriction promotes mitochondrial biogenesis by inducing the expression of eNOS. Science *310*, 314-317.

Nixon, R.A. (2007). Autophagy, amyloidogenesis and Alzheimer disease. Journal of cell science *120*, 4081-4091.

Nixon, R.A., Wegiel, J., Kumar, A., Yu, W.H., Peterhoff, C., Cataldo, A., and Cuervo, A.M. (2005). Extensive involvement of autophagy in Alzheimer disease: an immuno-electron microscopy study. Journal of neuropathology and experimental neurology *64*, 113-122.

Noble, W., Hanger, D.P., Miller, C.C., and Lovestone, S. (2013). The importance of tau phosphorylation for neurodegenerative diseases. Frontiers in neurology *4*, 83.

North, B.J., Marshall, B.L., Borra, M.T., Denu, J.M., and Verdin, E. (2003). The human Sir2 ortholog, SIRT2, is an NAD+-dependent tubulin deacetylase. Molecular cell *11*, 437-444.

North, B.J., and Verdin, E. (2007). Mitotic regulation of SIRT2 by cyclin-dependent kinase 1-dependent phosphorylation. The Journal of biological chemistry *282*, 19546-19555.

Nunomura, A., Perry, G., Aliev, G., Hirai, K., Takeda, A., Balraj, E.K., Jones, P.K., Ghanbari, H., Wataya, T., Shimohama, S., *et al.* (2001). Oxidative damage is the earliest event in Alzheimer disease. J Neuropathol Exp Neurol *60*, 759-767.

Nunomura, A., Perry, G., Pappolla, M.A., Wade, R., Hirai, K., Chiba, S., and Smith, M.A. (1999). RNA oxidation is a prominent feature of vulnerable neurons in Alzheimer's disease. J Neurosci *19*, 1959-1964.

Okatsu, K., Oka, T., Iguchi, M., Imamura, K., Kosako, H., Tani, N., Kimura, M., Go, E., Koyano, F., Funayama, M., *et al.* (2012). PINK1 autophosphorylation upon membrane potential dissipation is essential for Parkin recruitment to damaged mitochondria. Nature communications *3*, 1016.

Onyango, I.G., Ahn, J.Y., Tuttle, J.B., Bennett, J.P., Jr., and Swerdlow, R.H. (2010). Nerve growth factor attenuates oxidant-induced beta-amyloid neurotoxicity in sporadic Alzheimer's disease cybrids. J Neurochem *114*, 1605-1618.

Onyango, I.G., Tuttle, J.B., and Bennett, J.P., Jr. (2005). Altered intracellular signaling and reduced viability of Alzheimer's disease neuronal cybrids is reproduced by beta-amyloid peptide acting through receptor for advanced glycation end products (RAGE). Molecular and cellular neurosciences *29*, 333-343.

Outeiro, T.F., Kontopoulos, E., Altmann, S.M., Kufareva, I., Strathearn, K.E., Amore, A.M., Volk, C.B., Maxwell, M.M., Rochet, J.C., McLean, P.J., *et al.* (2007). Sirtuin 2 inhibitors rescue alpha-synuclein-mediated toxicity in models of Parkinson's disease. Science *317*, 516-519.

Outeiro, T.F., Marques, O., and Kazantsev, A. (2008). Therapeutic role of sirtuins in neurodegenerative disease. Biochimica et biophysica acta *1782*, 363-369.

Padurariu, M., Ciobica, A., Hritcu, L., Stoica, B., Bild, W., and Stefanescu, C. (2010). Changes of some oxidative stress markers in the serum of patients with mild cognitive impairment and Alzheimer's disease. Neuroscience letters *469*, 6-10.

Pagani, L., and Eckert, A. (2011). Amyloid-Beta interaction with mitochondria. Int J Alzheimers Dis *2011*, 925050.

Pandithage, R., Lilischkis, R., Harting, K., Wolf, A., Jedamzik, B., Luscher-Firzlaff, J., Vervoorts, J., Lasonder, E., Kremmer, E., Knoll, B., *et al.* (2008). The regulation of SIRT2 function by cyclin-dependent kinases affects cell motility. The Journal of cell biology *180*, 915-929.

Panza, F., Solfrizzi, V., Seripa, D., Imbimbo, B.P., Pilotto, A., and Frisardi, V. (2010). Peripheral antioxidant markers in mild cognitive impairment and its progression to dementia. J Alzheimers Dis *21*, 1179-1183.

Parker, W.D., Jr., Filley, C.M., and Parks, J.K. (1990). Cytochrome oxidase deficiency in Alzheimer's disease. Neurology *40*, 1302-1303.

Parker, W.D., Jr., and Parks, J.K. (1995). Cytochrome c oxidase in Alzheimer's disease brain: purification and characterization. Neurology *45*, 482-486.

Pavlov, P.F., Wiehager, B., Sakai, J., Frykman, S., Behbahani, H., Winblad, B., and Ankarcrona, M. (2011). Mitochondrial gamma-secretase participates in the metabolism of mitochondria-associated amyloid precursor protein. FASEB J *25*, 78-88.

Pellerin, L., and Magistretti, P.J. (2003). Food for thought: challenging the dogmas. J Cereb Blood Flow Metab *23*, 1282-1286.

Pereira, C., Agostinho, P., Moreira, P.I., Cardoso, S.M., and Oliveira, C.R. (2005). Alzheimer's disease-associated neurotoxic mechanisms and neuroprotective strategies. Curr Drug Targets CNS Neurol Disord *4*, 383-403.

Pereira, C., Santos, M.S., and Oliveira, C. (1999). Involvement of oxidative stress on the impairment of energy metabolism induced by A beta peptides on PC12 cells: protection by antioxidants. Neurobiology of disease *6*, 209-219.

Perrin, R.J., Craig-Schapiro, R., Malone, J.P., Shah, A.R., Gilmore, P., Davis, A.E., Roe, C.M., Peskind, E.R., Li, G., Galasko, D.R., *et al.* (2011). Identification and validation of novel cerebrospinal fluid biomarkers for staging early Alzheimer's disease. PLoS One *6*, e16032.

Perry, G., Mulvihill, P., Fried, V.A., Smith, H.T., Grundke-Iqbal, I., and Iqbal, K. (1989). Immunochemical properties of ubiquitin conjugates in the paired helical filaments of Alzheimer disease. Journal of neurochemistry *52*, 1523-1528.

Petersen, R.B., Nunomura, A., Lee, H.G., Casadesus, G., Perry, G., Smith, M.A., and Zhu, X. (2007). Signal transduction cascades associated with oxidative stress in Alzheimer's disease. J Alzheimers Dis *11*, 143-152.

Petersen, R.C. (2011). Clinical practice. Mild cognitive impairment. N Engl J Med *364*, 2227-2234.

Petersen, R.C., Stevens, J.C., Ganguli, M., Tangalos, E.G., Cummings, J.L., and DeKosky, S.T. (2001). Practice parameter: early detection of dementia: mild cognitive impairment (an evidence-based review). Report of the Quality Standards Subcommittee of the American Academy of Neurology. Neurology *56*, 1133-1142.

Peterson, C., Vanderklish, P., Seubert, P., Cotman, C., and Lynch, G. (1991). Increased spectrin proteolysis in fibroblasts from aged and Alzheimer donors. Neurosci Lett *121*, 239-243.

Piantadosi, C.A., and Suliman, H.B. (2012). Redox regulation of mitochondrial biogenesis. Free radical biology & medicine *53*, 2043-2053.

Pickford, F., Masliah, E., Britschgi, M., Lucin, K., Narasimhan, R., Jaeger, P.A., Small, S., Spencer, B., Rockenstein, E., Levine, B., *et al.* (2008). The autophagy-related protein beclin 1 shows reduced expression in early Alzheimer disease and regulates amyloid beta accumulation in mice. The Journal of clinical investigation *118*, 2190-2199.

Pigino, G., Morfini, G., Pelsman, A., Mattson, M.P., Brady, S.T., and Busciglio, J. (2003). Alzheimer's presenilin 1 mutations impair kinesin-based axonal transport. J Neurosci *23*, 4499-4508.

Pratico, D. (2005). Peripheral biomarkers of oxidative damage in Alzheimer's disease: the road ahead. Neurobiol Aging *26*, 581-583.

Pratico, D., Clark, C.M., Liun, F., Rokach, J., Lee, V.Y., and Trojanowski, J.Q. (2002). Increase of brain oxidative stress in mild cognitive impairment: a possible predictor of Alzheimer disease. Arch Neurol *59*, 972-976.

Pratico, D., V, M.Y.L., Trojanowski, J.Q., Rokach, J., and Fitzgerald, G.A. (1998). Increased F2-isoprostanes in Alzheimer's disease: evidence for enhanced lipid peroxidation in vivo. FASEB J *12*, 1777-1783.

Qin, W., Haroutunian, V., Katsel, P., Cardozo, C.P., Ho, L., Buxbaum, J.D., and Pasinetti, G.M. (2009). PGC-1alpha expression decreases in the Alzheimer disease brain as a function of dementia. Arch Neurol *66*, 352-361.

Raber, J., Huang, Y., and Ashford, J.W. (2004). ApoE genotype accounts for the vast majority of AD risk and AD pathology. Neurobiology of aging *25*, 641-650.

Ravikumar, B., Vacher, C., Berger, Z., Davies, J.E., Luo, S., Oroz, L.G., Scaravilli, F., Easton, D.F., Duden, R., O'Kane, C.J., *et al.* (2004). Inhibition of mTOR induces autophagy and reduces toxicity of polyglutamine expansions in fly and mouse models of Huntington disease. Nature genetics *36*, 585-595.

Ray, P.D., Huang, B.W., and Tsuji, Y. (2012). Reactive oxygen species (ROS) homeostasis and redox regulation in cellular signaling. Cell Signal.

Reddy, P.H. (2014). Inhibitors of mitochondrial fission as a therapeutic strategy for diseases with oxidative stress and mitochondrial dysfunction. Journal of Alzheimer's disease : JAD *40*, 245-256.

Reddy, P.H., and McWeeney, S. (2006). Mapping cellular transcriptosomes in autopsied Alzheimer's disease subjects and relevant animal models. Neurobiology of aging *27*, 1060-1077.

Reddy, P.H., and Shirendeb, U.P. (2011). Mutant huntingtin, abnormal mitochondrial dynamics, defective axonal transport of mitochondria, and selective synaptic degeneration in Huntington's disease. Biochim Biophys Acta *1822*, 101-110.

Reed, N.A., Cai, D., Blasius, T.L., Jih, G.T., Meyhofer, E., Gaertig, J., and Verhey, K.J. (2006). Microtubule acetylation promotes kinesin-1 binding and transport. Current biology : CB *16*, 2166-2172.

Rhinn, H., Fujita, R., Qiang, L., Cheng, R., Lee, J.H., and Abeliovich, A. (2013). Integrative genomics identifies APOE epsilon4 effectors in Alzheimer's disease. Nature *500*, 45-50.

Risner, M.E., Saunders, A.M., Altman, J.F., Ormandy, G.C., Craft, S., Foley, I.M., Zvartau-Hind, M.E., Hosford, D.A., and Roses, A.D. (2006). Efficacy of rosiglitazone in a genetically defined population with mild-to-moderate Alzheimer's disease. Pharmacogenomics J *6*, 246-254.

Rodriguez-Santiago, B., Casademont, J., and Nunes, V. (2001). Is mitochondrial DNA depletion involved in Alzheimer's disease? Eur J Hum Genet *9*, 279-285.

Rohn, T.T., and Head, E. (2009). Caspases as therapeutic targets in Alzheimer's disease: is it time to "cut" to the chase? Int J Clin Exp Pathol *2*, 108-118.

Rohn, T.T., Head, E., Nesse, W.H., Cotman, C.W., and Cribbs, D.H. (2001a). Activation of caspase-8 in the Alzheimer's disease brain. Neurobiol Dis *8*, 1006-1016.

Rohn, T.T., Head, E., Su, J.H., Anderson, A.J., Bahr, B.A., Cotman, C.W., and Cribbs, D.H. (2001b). Correlation between caspase activation and neurofibrillary tangle formation in Alzheimer's disease. Am J Pathol *158*, 189-198.

Rohn, T.T., Rissman, R.A., Davis, M.C., Kim, Y.E., Cotman, C.W., and Head, E. (2002). Caspase-9 activation and caspase cleavage of tau in the Alzheimer's disease brain. Neurobiol Dis *11*, 341-354.

Rosa, M.I., Perucchi, J., Medeiros, L.R., Fernandes, B., Fernandes Dos Reis, M.E., and Silvae, B.R. (2014). Accuracy of Cerebrospinal Fluid Abeta1-42 for Alzheimer's Disease Diagnosis: A Systematic Review and Meta-Analysis. Journal of Alzheimer's disease : JAD.

Rosen, W.G., Mohs, R.C., and Davis, K.L. (1984). A new rating scale for Alzheimer's disease. Am J Psychiatry *141*, 1356-1364.

Salminen, A., Kaarniranta, K., Haapasalo, A., Hiltunen, M., Soininen, H., and Alafuzoff, I. (2012). Emerging role of p62/sequestosome-1 in the pathogenesis of Alzheimer's disease. Progress in neurobiology *96*, 87-95.

Salminen, A., Kaarniranta, K., Haapasalo, A., Soininen, H., and Hiltunen, M. (2011). AMP-activated protein kinase: a potential player in Alzheimer's disease. J Neurochem *118*, 460-474.

Salminen, A., Kaarniranta, K., Kauppinen, A., Ojala, J., Haapasalo, A., Soininen, H., and Hiltunen, M. (2013). Impaired autophagy and APP processing in Alzheimer's disease: The potential role of Beclin 1 interactome. Progress in neurobiology *106-107*, 33-54.

Sambamurti, K., Greig, N.H., and Lahiri, D.K. (2002). Advances in the cellular and molecular biology of the beta-amyloid protein in Alzheimer's disease. Neuromolecular medicine *1*, 1-31.

Sanchez-Varo, R., Trujillo-Estrada, L., Sanchez-Mejias, E., Torres, M., Baglietto-Vargas, D., Moreno-Gonzalez, I., De Castro, V., Jimenez, S., Ruano, D., Vizuete, M., *et al.* (2012). Abnormal accumulation of autophagic vesicles correlates with axonal and

synaptic pathology in young Alzheimer's mice hippocampus. Acta neuropathologica *123*, 53-70.

Sandstrom, P.A., Tebbey, P.W., Van Cleave, S., and Buttke, T.M. (1994). Lipid hydroperoxides induce apoptosis in T cells displaying a HIV-associated glutathione peroxidase deficiency. J Biol Chem *269*, 798-801.

Santa-Maria, I., Smith, M.A., Perry, G., Hernandez, F., Avila, J., and Moreno, F.J. (2005). Effect of quinones on microtubule polymerization: a link between oxidative stress and cytoskeletal alterations in Alzheimer's disease. Biochimica et biophysica acta *1740*, 472-480.

Santos, R.X., Correia, S.C., Wang, X., Perry, G., Smith, M.A., Moreira, P.I., and Zhu, X. (2010). A synergistic dysfunction of mitochondrial fission/fusion dynamics and mitophagy in Alzheimer's disease. J Alzheimers Dis *20 Suppl 2*, S401-412.

Saraiva, A.A., Borges, M.M., Madeira, M.D., Tavares, M.A., and Paula-Barbosa, M.M. (1985). Mitochondrial abnormalities in cortical dendrites from patients with Alzheimer's disease. Journal of submicroscopic cytology *17*, 459-464.

Satoh, A., and Imai, S. (2014). Systemic regulation of mammalian ageing and longevity by brain sirtuins. Nature communications *5*, 4211.

Sayre, L.M., Zelasko, D.A., Harris, P.L., Perry, G., Salomon, R.G., and Smith, M.A. (1997). 4-Hydroxynonenal-derived advanced lipid peroxidation end products are increased in Alzheimer's disease. J Neurochem *68*, 2092-2097.

Scarpulla, R.C. (2008). Transcriptional paradigms in mammalian mitochondrial biogenesis and function. Physiol Rev *88*, 611-638.

Schieke, S.M., Phillips, D., McCoy, J.P., Jr., Aponte, A.M., Shen, R.F., Balaban, R.S., and Finkel, T. (2006). The mammalian target of rapamycin (mTOR) pathway regulates mitochondrial oxygen consumption and oxidative capacity. J Biol Chem *281*, 27643-27652.

Schwalbe, M., Biernat, J., Bibow, S., Ozenne, V., Jensen, M.R., Kadavath, H., Blackledge, M., Mandelkow, E., and Zweckstetter, M. (2013). Phosphorylation of human tau protein by microtubule affinity-regulating kinase 2. Biochemistry *52*, 9068-9079.

Sebastian, C., Satterstrom, F.K., Haigis, M.C., and Mostoslavsky, R. (2012). From sirtuin biology to human diseases: an update. The Journal of biological chemistry *287*, 42444-42452.

Selkoe, D.J. (2001). Alzheimer's disease: genes, proteins, and therapy. Physiological reviews *81*, 741-766.

Selznick, L.A., Holtzman, D.M., Han, B.H., Gokden, M., Srinivasan, A.N., Johnson, E.M., Jr., and Roth, K.A. (1999). In situ immunodetection of neuronal caspase-3 activation in Alzheimer disease. J Neuropathol Exp Neurol *58*, 1020-1026.

Semenza, G.L. (1999). Regulation of mammalian O2 homeostasis by hypoxia-inducible factor 1. Annu Rev Cell Dev Biol *15*, 551-578.

Semenza, G.L. (2012). Hypoxia-inducible factors in physiology and medicine. Cell *148*, 399-408.

Settembre, C., Fraldi, A., Jahreiss, L., Spampanato, C., Venturi, C., Medina, D., de Pablo, R., Tacchetti, C., Rubinsztein, D.C., and Ballabio, A. (2008). A block of autophagy in lysosomal storage disorders. Human molecular genetics *17*, 119-129.

Sheng, B., Wang, X., Su, B., Lee, H.G., Casadesus, G., Perry, G., and Zhu, X. (2012). Impaired mitochondrial biogenesis contributes to mitochondrial dysfunction in Alzheimer's disease. Journal of neurochemistry *120*, 419-429.

Shepherd, C., McCann, H., and Halliday, G.M. (2009). Variations in the neuropathology of familial Alzheimer's disease. Acta neuropathologica *118*, 37-52.

Sheridan, C., Delivani, P., Cullen, S.P., and Martin, S.J. (2008). Bax- or Bak-induced mitochondrial fission can be uncoupled from cytochrome C release. Mol Cell *31*, 570-585.

Shi, C., Guo, K., Yew, D.T., Yao, Z., Forster, E.L., Wang, H., and Xu, J. (2008). Effects of ageing and Alzheimer's disease on mitochondrial function of human platelets. Experimental gerontology *43*, 589-594.

Shi, Q., Xu, H., Yu, H., Zhang, N., Ye, Y., Estevez, A.G., Deng, H., and Gibson, G.E. (2011). Inactivation and reactivation of the mitochondrial alpha-ketoglutarate dehydrogenase complex. J Biol Chem *286*, 17640-17648.

Shigenaga, M.K., Hagen, T.M., and Ames, B.N. (1994). Oxidative damage and mitochondrial decay in aging. Proceedings of the National Academy of Sciences of the United States of America *91*, 10771-10778.

Shimohama, S. (2000). Apoptosis in Alzheimer's disease--an update. Apoptosis *5*, 9-16.

Shin, J.H., Ko, H.S., Kang, H., Lee, Y., Lee, Y.I., Pletinkova, O., Troconso, J.C., Dawson, V.L., and Dawson, T.M. (2011). PARIS (ZNF746) repression of PGC-1alpha contributes to neurodegeneration in Parkinson's disease. Cell *144*, 689-702.

Shiryaev, N., Jouroukhin, Y., Giladi, E., Polyzoidou, E., Grigoriadis, N.C., Rosenmann, H., and Gozes, I. (2009). NAP protects memory, increases soluble tau and reduces tau hyperphosphorylation in a tauopathy model. Neurobiol Dis *34*, 381-388.

Shiryaev, N., Pikman, R., Giladi, E., and Gozes, I. (2011). Protection Against Tauopathy by the Drug Candidates NAP (Davunetide) and D-SAL: Biochemical, Cellular and Behavioral Aspects. Curr Pharm Des *17*, 2603-2612.

Silva, D.F., Esteves, A.R., Arduino, D.M., Oliveira, C.R., and Cardoso, S.M. (2011a). Amyloid-beta-induced mitochondrial dysfunction impairs the autophagic lysosomal pathway in a tubulin dependent pathway. Journal of Alzheimer's disease : JAD *26*, 565-581.

Silva, D.F., Esteves, A.R., Oliveira, C.R., and Cardoso, S.M. (2011b). Mitochondria: the common upstream driver of amyloid-beta and tau pathology in Alzheimer's disease. Current Alzheimer research *8*, 563-572.

Silva, D.F., Santana, I., Esteves, A.R., Baldeiras, I., Arduino, D.M., Oliveira, C.R., and Cardoso, S.M. (2012a). Prodromal Metabolic Phenotype in MCI Cybrids: Implications for Alzheimers Disease. Curr Alzheimer Res.

Silva, D.F., Santana, I., Esteves, A.R., Baldeiras, I., Arduino, D.M., Oliveira, C.R., and Cardoso, S.M. (2013a). Prodromal metabolic phenotype in MCI cybrids: implications for Alzheimer's disease. Current Alzheimer research *10*, 180-190.

Silva, D.F., Selfridge, J.E., Lu, J., E, L., Cardoso, S.M., and Swerdlow, R.H. (2012b). Mitochondrial abnormalities in Alzheimer's disease: possible targets for therapeutic intervention. Advances in pharmacology *64*, 83-126.

Silva, D.F., Selfridge, J.E., Lu, J., E, L., Roy, N., Hutfles, L., Burns, J.M., Michaelis, E.K., Yan, S., Cardoso, S.M., *et al.* (2013b). Bioenergetic flux, mitochondrial mass and mitochondrial morphology dynamics in AD and MCI cybrid cell lines. Human molecular genetics *22*, 3931-3946.

Silverman, D.H., Small, G.W., Chang, C.Y., Lu, C.S., Kung De Aburto, M.A., Chen, W., Czernin, J., Rapoport, S.I., Pietrini, P., Alexander, G.E., *et al.* (2001). Positron emission tomography in evaluation of dementia: Regional brain metabolism and long-term outcome. JAMA *286*, 2120-2127.

Simonian, N.A., and Hyman, B.T. (1993). Functional alterations in Alzheimer's disease: diminution of cytochrome oxidase in the hippocampal formation. J Neuropathol Exp Neurol *52*, 580-585.

Singh, M., Nam, D.T., Arseneault, M., and Ramassamy, C. (2010). Role of by-products of lipid oxidation in Alzheimer's disease brain: a focus on acrolein. J Alzheimers Dis *21*, 741-756.

Skulachev, V.P. (1996). Role of uncoupled and non-coupled oxidations in maintenance of safely low levels of oxygen and its one-electron reductants. Q Rev Biophys *29*, 169-202.

Smale, G., Nichols, N.R., Brady, D.R., Finch, C.E., and Horton, W.E., Jr. (1995). Evidence for apoptotic cell death in Alzheimer's disease. Exp Neurol *133*, 225-230.

Small, S.A., and Duff, K. (2008). Linking Abeta and tau in late-onset Alzheimer's disease: a dual pathway hypothesis. Neuron *60*, 534-542.

Smith, C.D., Carney, J.M., Starke-Reed, P.E., Oliver, C.N., Stadtman, E.R., Floyd, R.A., and Markesbery, W.R. (1991). Excess brain protein oxidation and enzyme dysfunction in normal aging and in Alzheimer disease. Proc Natl Acad Sci U S A *88*, 10540-10543.

Smith, M.A., Rottkamp, C.A., Nunomura, A., Raina, A.K., and Perry, G. (2000). Oxidative stress in Alzheimer's disease. Biochim Biophys Acta *1502*, 139-144.

Smith, M.A., Zhu, X., Tabaton, M., Liu, G., McKeel, D.W., Jr., Cohen, M.L., Wang, X., Siedlak, S.L., Dwyer, B.E., Hayashi, T., *et al.* (2010). Increased iron and free radical generation in preclinical Alzheimer disease and mild cognitive impairment. J Alzheimers Dis *19*, 363-372.

Sorbi, S., Bird, E.D., and Blass, J.P. (1983). Decreased pyruvate dehydrogenase complex activity in Huntington and Alzheimer brain. Annals of neurology *13*, 72-78.

Sorrentino, G., and Bonavita, V. (2007). Neurodegeneration and Alzheimer's disease: the lesson from tauopathies. Neurological sciences : official journal of the Italian Neurological Society and of the Italian Society of Clinical Neurophysiology *28*, 63-71.

Soucek, T., Cumming, R., Dargusch, R., Maher, P., and Schubert, D. (2003). The regulation of glucose metabolism by HIF-1 mediates a neuroprotective response to amyloid beta peptide. Neuron *39*, 43-56.

Spires-Jones, T.L., Fox, L.M., Rozkalne, A., Pitstick, R., Carlson, G.A., and Kazantsev, A.G. (2012). Inhibition of Sirtuin 2 with Sulfobenzoic Acid Derivative AK1 is Non-Toxic and Potentially Neuroprotective in a Mouse Model of Frontotemporal Dementia. Frontiers in pharmacology *3*, 42.

Stadelmann, C., Deckwerth, T.L., Srinivasan, A., Bancher, C., Bruck, W., Jellinger, K., and Lassmann, H. (1999). Activation of caspase-3 in single neurons and autophagic

granules of granulovacuolar degeneration in Alzheimer's disease. Evidence for apoptotic cell death. Am J Pathol *155*, 1459-1466.

Stamer, K., Vogel, R., Thies, E., Mandelkow, E., and Mandelkow, E.M. (2002). Tau blocks traffic of organelles, neurofilaments, and APP vesicles in neurons and enhances oxidative stress. The Journal of cell biology *156*, 1051-1063.

Stephan, B.C., Hunter, S., Harris, D., Llewellyn, D.J., Siervo, M., Matthews, F.E., and Brayne, C. (2012). The neuropathological profile of mild cognitive impairment (MCI): a systematic review. Molecular psychiatry *17*, 1056-1076.

Sterky, F.H., Lee, S., Wibom, R., Olson, L., and Larsson, N.G. (2011). Impaired mitochondrial transport and Parkin-independent degeneration of respiratory chain-deficient dopamine neurons in vivo. Proc Natl Acad Sci U S A *108*, 12937-12942.

Stokin, G.B., and Goldstein, L.S. (2006). Axonal transport and Alzheimer's disease. Annual review of biochemistry *75*, 607-627.

Su, B., Wang, X., Bonda, D., Perry, G., Smith, M., and Zhu, X. (2010). Abnormal mitochondrial dynamics--a novel therapeutic target for Alzheimer's disease? Mol Neurobiol *41*, 87-96.

Su, J.H., Anderson, A.J., Cummings, B.J., and Cotman, C.W. (1994). Immunohistochemical evidence for apoptosis in Alzheimer's disease. Neuroreport *5*, 2529-2533.

Su, J.H., Deng, G., and Cotman, C.W. (1997). Bax protein expression is increased in Alzheimer's brain: correlations with DNA damage, Bcl-2 expression, and brain pathology. J Neuropathol Exp Neurol *56*, 86-93.

Subramaniam, R., Roediger, F., Jordan, B., Mattson, M.P., Keller, J.N., Waeg, G., and Butterfield, D.A. (1997). The lipid peroxidation product, 4-hydroxy-2-trans-nonenal, alters the conformation of cortical synaptosomal membrane proteins. J Neurochem *69*, 1161-1169.

Sullivan, P.G., and Brown, M.R. (2005). Mitochondrial aging and dysfunction in Alzheimer's disease. Prog Neuropsychopharmacol Biol Psychiatry *29*, 407-410.

Sullivan, P.G., Rippy, N.A., Dorenbos, K., Concepcion, R.C., Agarwal, A.K., and Rho, J.M. (2004). The ketogenic diet increases mitochondrial uncoupling protein levels and activity. Ann Neurol *55*, 576-580.

Sultana, R., and Butterfield, D.A. (2009). Oxidatively modified, mitochondria-relevant brain proteins in subjects with Alzheimer disease and mild cognitive impairment. J Bioenerg Biomembr *41*, 441-446.

Sultana, R., Perluigi, M., Newman, S.F., Pierce, W.M., Cini, C., Coccia, R., and Butterfield, D.A. (2010). Redox proteomic analysis of carbonylated brain proteins in mild cognitive impairment and early Alzheimer's disease. Antioxid Redox Signal *12*, 327-336.

Sun, A., Liu, M., Nguyen, X.V., and Bing, G. (2003). P38 MAP kinase is activated at early stages in Alzheimer's disease brain. Exp Neurol *183*, 394-405.

Suzuki, K., and Koike, T. (2007). Mammalian Sir2-related protein (SIRT) 2-mediated modulation of resistance to axonal degeneration in slow Wallerian degeneration mice: a crucial role of tubulin deacetylation. Neuroscience *147*, 599-612.

Swerdlow, R.H. (2007a). Mitochondria in cybrids containing mtDNA from persons with mitochondriopathies. J Neurosci Res *85*, 3416-3428.

Swerdlow, R.H. (2007b). Pathogenesis of Alzheimer's disease. Clinical interventions in aging *2*, 347-359.

Swerdlow, R.H. (2007c). Treating neurodegeneration by modifying mitochondria: potential solutions to a "complex" problem. Antioxid Redox Signal *9*, 1591-1603.

Swerdlow, R.H. (2011a). Mitochondria and Cell Bioenergetics: Increasingly Recognized Components and a Possible Etiologic Cause of Alzheimer's Disease. Antioxid Redox Signal.

Swerdlow, R.H. (2011b). Role and treatment of mitochondrial DNA-related mitochondrial dysfunction in sporadic neurodegenerative diseases. Curr Pharm Des *17*, 3356-3373.

Swerdlow, R.H. (2012a). beta-Apptists and Tauists, it is time for a sermon from the book of biogenesis. J Neurochem *120*, 347-349.

Swerdlow, R.H. (2012b). Mitochondria and cell bioenergetics: increasingly recognized components and a possible etiologic cause of Alzheimer's disease. Antioxidants & redox signaling *16*, 1434-1455.

Swerdlow, R.H., Burns, J.M., and Khan, S.M. (2010). The Alzheimer's disease mitochondrial cascade hypothesis. Journal of Alzheimer's disease : JAD *20 Suppl 2*, S265-279.

Swerdlow, R.H., Burns, J.M., and Khan, S.M. (2013). The Alzheimer's disease mitochondrial cascade hypothesis: Progress and perspectives. Biochimica et biophysica acta.

Swerdlow, R.H., Burns, J.M., and Khan, S.M. (2014). The Alzheimer's disease mitochondrial cascade hypothesis: progress and perspectives. Biochimica et biophysica acta *1842*, 1219-1231.

Swerdlow, R.H., and Khan, S.M. (2004). A "mitochondrial cascade hypothesis" for sporadic Alzheimer's disease. Medical hypotheses *63*, 8-20.

Swerdlow, R.H., and Khan, S.M. (2009). The Alzheimer's disease mitochondrial cascade hypothesis: an update. Experimental neurology *218*, 308-315.

Swerdlow, R.H., and Kish, S.J. (2002). Mitochondria in Alzheimer's disease. Int Rev Neurobiol *53*, 341-385.

Swerdlow, R.H., Parks, J.K., Cassarino, D.S., Maguire, D.J., Maguire, R.S., Bennett, J.P., Jr., Davis, R.E., and Parker, W.D., Jr. (1997). Cybrids in Alzheimer's disease: a cellular model of the disease? Neurology *49*, 918-925.

Swerdlow, R.H., Parks, J.K., Miller, S.W., Tuttle, J.B., Trimmer, P.A., Sheehan, J.P., Bennett, J.P., Jr., Davis, R.E., and Parker, W.D., Jr. (1996). Origin and functional consequences of the complex I defect in Parkinson's disease. Ann Neurol *40*, 663-671.

Terman, A., Gustafsson, B., and Brunk, U.T. (2006). Mitochondrial damage and intralysosomal degradation in cellular aging. Molecular aspects of medicine *27*, 471-482.

Terry, R.D. (1998). The cytoskeleton in Alzheimer disease. Journal of neural transmission. Supplementum *53*, 141-145.

Terry, R.D., Masliah, E., Salmon, D.P., Butters, N., DeTeresa, R., Hill, R., Hansen, L.A., and Katzman, R. (1991). Physical basis of cognitive alterations in Alzheimer's disease: synapse loss is the major correlate of cognitive impairment. Ann Neurol *30*, 572-580.

Torres, L.L., Quaglio, N.B., de Souza, G.T., Garcia, R.T., Dati, L.M., Moreira, W.L., Loureiro, A.P., de Souza-Talarico, J.N., Smid, J., Porto, C.S., *et al.* (2011). Peripheral oxidative stress biomarkers in mild cognitive impairment and Alzheimer's disease. J Alzheimers Dis *26*, 59-68.

Trimmer, P.A., and Borland, M.K. (2005). Differentiated Alzheimer's disease transmitochondrial cybrid cell lines exhibit reduced organelle movement. Antioxidants & redox signaling *7*, 1101-1109.

Trimmer, P.A., Keeney, P.M., Borland, M.K., Simon, F.A., Almeida, J., Swerdlow, R.H., Parks, J.P., Parker, W.D., Jr., and Bennett, J.P., Jr. (2004). Mitochondrial

abnormalities in cybrid cell models of sporadic Alzheimer's disease worsen with passage in culture. Neurobiology of disease *15*, 29-39.

Trimmer, P.A., Swerdlow, R.H., Parks, J.K., Keeney, P., Bennett, J.P., Jr., Miller, S.W., Davis, R.E., and Parker, W.D., Jr. (2000). Abnormal mitochondrial morphology in sporadic Parkinson's and Alzheimer's disease cybrid cell lines. Experimental neurology *162*, 37-50.

Troncoso, J.C., Sukhov, R.R., Kawas, C.H., and Koliatsos, V.E. (1996). In situ labeling of dying cortical neurons in normal aging and in Alzheimer's disease: correlations with senile plaques and disease progression. J Neuropathol Exp Neurol *55*, 1134-1142.

Turrens, J.F., and Boveris, A. (1980). Generation of superoxide anion by the NADH dehydrogenase of bovine heart mitochondria. Biochem J *191*, 421-427.

Twig, G., Elorza, A., Molina, A.J., Mohamed, H., Wikstrom, J.D., Walzer, G., Stiles, L., Haigh, S.E., Katz, S., Las, G., *et al.* (2008). Fission and selective fusion govern mitochondrial segregation and elimination by autophagy. The EMBO journal *27*, 433-446.

Twig, G., and Shirihai, O.S. (2011). The interplay between mitochondrial dynamics and mitophagy. Antioxid Redox Signal *14*, 1939-1951.

Valla, J., Schneider, L., Niedzielko, T., Coon, K.D., Caselli, R., Sabbagh, M.N., Ahern, G.L., Baxter, L., Alexander, G., Walker, D.G., *et al.* (2006). Impaired platelet mitochondrial activity in Alzheimer's disease and mild cognitive impairment. Mitochondrion *6*, 323-330.

Vaquero, A., Scher, M.B., Lee, D.H., Sutton, A., Cheng, H.L., Alt, F.W., Serrano, L., Sternglanz, R., and Reinberg, D. (2006). SirT2 is a histone deacetylase with preference for histone H4 Lys 16 during mitosis. Genes & development *20*, 1256-1261.

Varadi, A., Johnson-Cadwell, L.I., Cirulli, V., Yoon, Y., Allan, V.J., and Rutter, G.A. (2004). Cytoplasmic dynein regulates the subcellular distribution of mitochondria by controlling the recruitment of the fission factor dynamin-related protein-1. J Cell Sci *117*, 4389-4400.

Vatassery, G.M.U., Hagen DF (1978). Highperformance liquid chromatography of various tocopherols. J. Chromatogr *161*, 299-302.

Vercauteren, K., Pasko, R.A., Gleyzer, N., Marino, V.M., and Scarpulla, R.C. (2006). PGC-1-related coactivator: immediate early expression and characterization of a CREB/NRF-1 binding domain associated with cytochrome c promoter occupancy and respiratory growth. Mol Cell Biol *26*, 7409-7419.

Vieira, S.I., Rebelo, S., Esselmann, H., Wiltfang, J., Lah, J., Lane, R., Small, S.A., Gandy, S., da Cruz, E.S.E.F., and da Cruz, E.S.O.A. (2010). Retrieval of the Alzheimer's amyloid precursor protein from the endosome to the TGN is S655 phosphorylation state-dependent and retromer-mediated. Molecular neurodegeneration *5*, 40.

Vingtdeux, V., Davies, P., Dickson, D.W., and Marambaud, P. (2011). AMPK is abnormally activated in tangle- and pre-tangle-bearing neurons in Alzheimer's disease and other tauopathies. Acta neuropathologica *121*, 337-349.

Vitte, J., Michel, B.F., Bongrand, P., and Gastaut, J.L. (2004). Oxidative stress level in circulating neutrophils is linked to neurodegenerative diseases. J Clin Immunol *24*, 683-692.

Vulih-Shultzman, I., Pinhasov, A., Mandel, S., Grigoriadis, N., Touloumi, O., Pittel, Z., and Gozes, I. (2007). Activity-dependent neuroprotective protein snippet NAP reduces tau hyperphosphorylation and enhances learning in a novel transgenic mouse model. J Pharmacol Exp Ther *323*, 438-449.

Wang, X., Su, B., Fujioka, H., and Zhu, X. (2008a). Dynamin-like protein 1 reduction underlies mitochondrial morphology and distribution abnormalities in fibroblasts from sporadic Alzheimer's disease patients. The American journal of pathology *173*, 470-482.

Wang, X., Su, B., Lee, H.G., Li, X., Perry, G., Smith, M.A., and Zhu, X. (2009). Impaired balance of mitochondrial fission and fusion in Alzheimer's disease. The Journal of neuroscience : the official journal of the Society for Neuroscience *29*, 9090-9103.

Wang, X., Su, B., Siedlak, S.L., Moreira, P.I., Fujioka, H., Wang, Y., Casadesus, G., and Zhu, X. (2008b). Amyloid-beta overproduction causes abnormal mitochondrial dynamics via differential modulation of mitochondrial fission/fusion proteins. Proceedings of the National Academy of Sciences of the United States of America *105*, 19318-19323.

Wang, X., Wang, W., Li, L., Perry, G., Lee, H.G., and Zhu, X. (2013). Oxidative stress and mitochondrial dysfunction in Alzheimer's disease. Biochimica et biophysica acta.

Westermann, B. (2009). Nitric oxide links mitochondrial fission to Alzheimer's disease. Science signaling *2*, pe29.

Wharton DC, T.A. (1967). Cytochrome oxidase from beef heart mitochondria. Methods Enzymol *10*, 245–250.

Wirz, K.T., Keitel, S., Swaab, D.F., Verhaagen, J., and Bossers, K. (2014). Early molecular changes in Alzheimer disease: can we catch the disease in its presymptomatic phase? Journal of Alzheimer's disease : JAD *38*, 719-740.

Wu, F., Schweizer, C., Rudinskiy, N., Taylor, D.M., Kazantsev, A., Luthi-Carter, R., and Fraering, P.C. (2010). Novel gamma-secretase inhibitors uncover a common nucleotide-binding site in JAK3, SIRT2, and PS1. FASEB journal : official publication of the Federation of American Societies for Experimental Biology *24*, 2464-2474.

Xiao, Q., Yan, P., Ma, X., Liu, H., Perez, R., Zhu, A., Gonzales, E., Burchett, J.M., Schuler, D.R., Cirrito, J.R., *et al.* (2014). Enhancing astrocytic lysosome biogenesis facilitates Abeta clearance and attenuates amyloid plaque pathogenesis. The Journal of neuroscience : the official journal of the Society for Neuroscience *34*, 9607-9620.

Xie, R., Nguyen, S., McKeehan, W.L., and Liu, L. (2010). Acetylated microtubules are required for fusion of autophagosomes with lysosomes. BMC cell biology *11*, 89.

Yang, D.S., Kumar, A., Stavrides, P., Peterson, J., Peterhoff, C.M., Pawlik, M., Levy, E., Cataldo, A.M., and Nixon, R.A. (2008). Neuronal apoptosis and autophagy cross talk in aging PS/APP mice, a model of Alzheimer's disease. The American journal of pathology *173*, 665-681.

Yang, D.S., Stavrides, P., Mohan, P.S., Kaushik, S., Kumar, A., Ohno, M., Schmidt, S.D., Wesson, D., Bandyopadhyay, U., Jiang, Y., *et al.* (2011). Reversal of autophagy dysfunction in the TgCRND8 mouse model of Alzheimer's disease ameliorates amyloid pathologies and memory deficits. Brain : a journal of neurology *134*, 258-277.

Yates, C.M., Butterworth, J., Tennant, M.C., and Gordon, A. (1990). Enzyme activities in relation to pH and lactate in postmortem brain in Alzheimer-type and other dementias. J Neurochem *55*, 1624-1630.

Yoon, Y., Krueger, E.W., Oswald, B.J., and McNiven, M.A. (2003). The mitochondrial protein hFis1 regulates mitochondrial fission in mammalian cells through an interaction with the dynamin-like protein DLP1. Mol Cell Biol *23*, 5409-5420.

Yu, J., and Auwerx, J. (2009). The role of sirtuins in the control of metabolic homeostasis. Annals of the New York Academy of Sciences *1173 Suppl 1*, E10-19.

Yu, W.H., Cuervo, A.M., Kumar, A., Peterhoff, C.M., Schmidt, S.D., Lee, J.H., Mohan, P.S., Mercken, M., Farmery, M.R., Tjernberg, L.O., *et al.* (2005). Macroautophagy--a novel Beta-amyloid peptide-generating pathway activated in Alzheimer's disease. J Cell Biol *171*, 87-98.

Yu, W.H., Kumar, A., Peterhoff, C., Shapiro Kulnane, L., Uchiyama, Y., Lamb, B.T., Cuervo, A.M., and Nixon, R.A. (2004). Autophagic vacuoles are enriched in amyloid precursor protein-secretase activities: implications for beta-amyloid peptide over-production and localization in Alzheimer's disease. The international journal of biochemistry & cell biology *36*, 2531-2540.

Zhang, Y., Tian, Q., Zhang, Q., Zhou, X., Liu, S., and Wang, J.Z. (2009). Hyperphosphorylation of microtubule-associated tau protein plays dual role in neurodegeneration and neuroprotection. Pathophysiology : the official journal of the International Society for Pathophysiology / ISP *16*, 311-316.

Zheng, L., Marcusson, J., and Terman, A. (2006). Oxidative stress and Alzheimer disease: the autophagy connection? Autophagy *2*, 143-145.

Zhou, X.W., Li, X., Bjorkdahl, C., Sjogren, M.J., Alafuzoff, I., Soininen, H., Grundke-Iqbal, I., Iqbal, K., Winblad, B., and Pei, J.J. (2006). Assessments of the accumulation severities of amyloid beta-protein and hyperphosphorylated tau in the medial temporal cortex of control and Alzheimer's brains. Neurobiology of disease *22*, 657-668.

Zhu, X., Perry, G., Smith, M.A., and Wang, X. (2013). Abnormal mitochondrial dynamics in the pathogenesis of Alzheimer's disease. Journal of Alzheimer's disease : JAD *33 Suppl 1*, S253-262.

Zhu, X., Raina, A.K., Perry, G., and Smith, M.A. (2004). Alzheimer's disease: the two-hit hypothesis. Lancet Neurol *3*, 219-226.